Landscape genomics and adaptive resilience to climate change of the tropical rainbowfish (*Melanotaenia splendida splendida*)

Katie Gates

Thesis

Submitted to Flinders University for the degree of

Doctor of Philosophy

College of Science and Engineering

Primary supervisor: Professor Luciano Beheregaray

Secondary supervisor: Associate Professor Luciana Möller

Adjunct supervisor: Professor Louis Bernatchez, C.Q.

17th March 2022

Contents

List of figures

Figure 2.3. Genomic differentiation and population structuring among nine rainforest sampling localities for the eastern rainbowfish *Melanotaenia splendida splendida*, represented by **(A)** Heatmap of pairwise F_{ST} based on 14,478 putatively neutral SNPs; **(B)** Correlation map for BAYPASS core model scaled covariance matrix Ω based on allele frequencies of the full dataset of 14,540 SNPs; and **(C)** Cluster plot based on FASTSTRUCTURE analysis of 14,478 putatively neutral SNPs, where colours represent inferred ancestral populations of individuals based on an optimal *K* of five. Large type refers to drainage systems, which are separated by thicker black lines. Small type refers to sampling localities, separated by thinner black lines. Locality abbreviations follow Table 1.   43

Figure 2.4. Wireframe graphical representation of significant principal components of body shape variation based on 18 landmarks for 207 *Melanotaenia splendida splendida* individuals sampled across nine rainforest sampling localities in the Wet Tropics of Queensland. Dark and light blue frames respectively represent body shape at high and low extremes of each significant axis (scale factor = 0.75).   45

Figure 2.5. Ordination plots summarising the first two axes of partial redundancy analyses (pRDAs) for *Melanotaenia splendida splendida* individuals sampled across nine rainforest sampling localities in the Wet Tropics of Queensland. **(A)** Genomic variation (based on 14,540 SNPs) explained by five associated environmental variables, after partialing out the locality-specific effect of Ω (allelic covariance). Environmental predictors accounted for 16.6% of total variation (p = <0.001). **(B)** Body shape variation (based on 18 morphometric landmarks) explained by four associated environmental variables, after partialing out the locality-specific effect of Ω (allelic covariance) and the individual effect of body size (log centroid). Environmental predictors accounted for 14% of total variation (p = <0.001). **(C)** Genomic variation (based on 864 putative climate-adaptive alleles) explained by four associated principal components of body shape, after partialing out the individual effect of body size (log centroid). Body shape accounted for 6.5% of climate-associated genetic variation (p = <0.001). For all plots, large points represent individual-level responses, and are coloured by drainage system of origin. Small purple points represent SNP-level responses. Vectors represent the magnitude and direction of relationships with explanatory variables.   47

List of tables

Summary

As ecosystems are exposed to rapidly changing climates, impacts may depend not only on magnitudes of change, but on organisms' existing physiologies, plastic capacities, and their potential for evolutionary adaptation. These factors are likely to vary among environments, and in accordance with local or regional biogeographic influences. Tropical regions, and particularly freshwater environments, remain understudied relative to their temperate counterparts, and disputes exist about evolutionary mechanisms in these hyper-diverse landscapes. We therefore aimed to clarify how hydroclimatic selection and landscape structure shape intraspecies adaptive diversity and evolution of an Australian tropical-endemic rainbowfish, *Melanotaenia splendida splendida*, as well as resilience under rapid climatic change.

Our first two data chapters employed a comparative riverscape-based approach, integrating genomic, phenotypic, and environmental datasets (14,540 filtered SNPs, 18 morphometric landmarks, and eight hydrological attributes, respectively) for 381 individuals from 17 sampling sites across rainforest and savannah biomes. Environmental associations both within and among these contrasting and heterogeneous habitats allowed us to test contributions of adaptive and non-adaptive influences on intraspecies diversity. Strong ecotype-specific environmental associations provided evidence for divergent adaptations to hydroclimate. Moreover, environment was a better predictor of genetic and morphological variation than neutral or spatial factors. This was particularly evident for body shape, which was relatively poorly explained by neutral population structure. Given that similar trait divergence has been associated with heritable hydrodynamic-related variation in congeneric species, this may reflect important functional consequences of body shape variation. Additional combined associations between genotype, phenotype, and environment supported the tentative inference of evolved adaptive differences. Weaker adaptive signals in the more connected savannah ecotype were consistent with a homogenising effect of gene flow on local adaptation.

In our third data chapter, we used experiments to compare short-term responses to climate warming among rainforest and savannah ecotypes, as well as in relation to previously studied temperate, desert, and subtropical rainbowfish ecotypes. Specifically, we assessed rapid acclimation capacity via tests of critical thermal maxima, as well as transcriptional responses to projected 2070 summer temperatures using differential expression analysis. We identified 189 DE genes as candidates for future thermal responses, including hub genes related to heat shock and lipid metabolism. We found a strong positive relationship between induced transcriptional responses and upper thermal tolerance, both of which were greater in the savannah ecotype. Meanwhile, the rainforest ecotype's more limited plastic capacity may reflect greater specialisation of thermal responses suited to its more temporally stable native environment.

Our work suggests that both contemporary hydroclimatic variation and drainage connectivity have shaped regional diversity in this species, with possible trade-offs between system-wide and locally specialised adaptations among rainforest and savannah ecotypes. We expect that alteration of current climates will necessitate substantial evolutionary responses for *in situ* population persistence, and that these may be more constrained in the climatically stable rainforest biome. Overall, the findings contribute to broader discussions about mechanisms promoting and maintaining patterns of tropical diversity, and highlight the utility of integrating diverse biological datasets to better disentangle complex evolutionary processes.

Declaration

I certify that this thesis does not incorporate without acknowledgment any material previously submitted for a degree or diploma in any university; and that to the best of my knowledge and belief it does not contain any material previously published or written by another person except where due reference is made in the text.

Signed

Acknowledgements

And thanks to Yuma. I can't even think of a part of this journey you haven't been with me on. Thanks for you love, your belief in me, your advice, your debate, and for keeping me going when I thought I couldn't do it. Thanks for your contribution to the work, for the long hours spent looking at scripts, and well, thanks for teaching me how to use a pipette.

Finally, I would like to acknowledge the traditional owners of country, who have been involved in conservation management of biodiversity in Australian for millenia, and remain active in this role today. Our study region includes country of the Kuku Yalanji, Kokomini, Kokowarra, Kunjen, Djabuganjdji, and Yidinjdji peoples. The thesis was written on the lands of the Kaurna and Peramangk nations.

Chapter 1: Introduction

Adaptation and persistence in changing climates

Ecological structure and function are unequivocally influenced by the surrounding environment, and in an era of global change, understanding the dynamics of these relationships is necessary for effective biodiversity management. Evolutionary pressures may influence not only organisms' capacity to respond to existing environmental conditions, but their adaptive potential in the face of novel challenges (Somero 2010, Chen et al. 2018c, Buckley and Kingsolver 2021). In tropical regions, relatively stable long-term climatic conditions have been linked to high richness, endemism, and specialisation of inhabitant species (Fjeldsaå et al. 1997, Weir and Schluter 2007, Salisbury et al. 2012, Furness et al. 2021). However, it has also been suggested that this same stability could predispose vulnerability to disturbance from anthropogenic climate change (Addo-Bediako et al. 2000, Kellermann et al. 2009, Brown et al. 2020). Therefore, contextualising both adaptive and non-adaptive evolutionary processes across tropical landscapes is a prerequisite to identifying patterns of vulnerability and resilience to future change (Moritz 2002, Moritz and McDonald 2005).

If magnitudes of environmental change exceed organisms' physiological tolerance, possible outcomes include range shifts, adaptation via genetic changes, persistence via phenotypic plasticity, or local extinction (Parmesan 2006, Bernatchez 2016). Dispersal is often limited by the fragmented nature of modern landscapes, particularly in constrained habitats such as freshwater (Fuller et al. 2015, Grummer et al. 2019). Because of this, adaptive and plastic capacities may be last lines of defence against extinction, making them key areas of research interest (Fensham et al. 2011, Erős et al. 2015). While there are still many challenges to identifying climatic adaptation in natural populations, correlations between biological and climatic gradients are an integral first line of evidence (Endler 1982, Sork et al. 2016). Moreover, DNA sequencing techniques and analytical methods are developing rapidly, with analytical integration of next generation sequencing (NGS) with physiological and environmental data

offering unprecedented power for studying evolutionary divergence across landscapes (Stapley et al. 2010, Andrew et al. 2013, Joost et al. 2013, Balkenhol et al. 2017, Li et al. 2017).

A Tropical context for adaptation research

Climate change and habitat fragmentation represent major risks for tropical ecosystems (Hilbert 2008, Gibson et al. 2013, Barlow et al. 2018). These biomes are the most diverse and species rich in the world, with rainforests alone estimated to contain around two thirds of all vascular plant species and perhaps more than half of total species (Turner 2001, Primack and Corlett 2005, Barlow et al. 2018). Despite predicted magnitudes of temperature change being less than that of temperate regions (Solomon 2007), tropical ecosystems may be vulnerable due to the narrower tolerance ranges of their biotas, and smaller resulting thermal safety margins (Deutsch et al. 2008, Huey et al. 2009, Eguiguren-Velepucha et al. 2016). Tropical regions are also likely to be subjected to some of the most extreme weather events, such as more frequent and intense tropical cyclones (Knutson et al. 2010). This high level of diversity combined with high projected extinction risks makes tropical ecosystems an urgent research priority (Myers et al. 2000, Wilson et al. 2016). Yet, publication rates in conservation and ecological diversification are comparatively sparse in tropical regions (Beheregaray et al. 2015, Wilson et al. 2016, Clarke et al. 2017).

Relevant to both conservation and theoretical developments, there is ongoing debate about the contribution of ecological and vicariant processes in explaining biodiversity in the terrestrial tropics (Endler 1982, Mayr and O'Hara 1986, Haffer 1997, Smith et al. 1997, Moritz et al. 2000). Many pioneering studies in tropical diversification have emphasised the role of physical and genetic isolation on patterns of divergence (Wallace 1854, Haffer 1969, Vuilleumier 1971, Mayr and O'Hara 1986, Ayres and Clutton-Brock 1992, Dias et al. 2013). Indeed, differentiation via both neutral and adaptive mechanisms may be expediated by barries to gene flow (Nosil and Funk 2008). However, adaptive processes have classically been difficult to differentiate from confounding influences of demography,

and this has likely contributed to downplaying and even scepticism towards the importance of ecology in tropical diversification (Schluter 2001, Nosil and Funk 2008, Nosil 2012, Beheregaray et al. 2015). Moreover, a growing number of tropical studies that explicitly assessed neutral and adaptive processes found that both mechanisms are important for explaining genetic and physiological trait diversity (Freedman et al. 2010, Smith et al. 2011, Cooke et al. 2014, Brousseau et al. 2015, Benham and Witt 2016, Maestri et al. 2016, Termignoni-García et al. 2017, Zhen et al. 2017, Gallego-García et al. 2019, Morgan et al. 2020), highlighting the need for nuanced assessments of tropical diversification.

Transitions between contrasting biomes provide a very useful spatial context for studying climatic adaptation and resilience (Smith et al. 1997). Rainforest and savannah are major biomes in the terrestrial tropics, and their ubiquity and stark variation in a range of climatic variables (Andersen et al. 2008, Murphy and Bowman 2012, Oliveras and Malhi 2016) provides opportunities for exploring associations with environmental heterogeneity. Tropical rainforests are typically characterised by high rainfall, dense tree cover, and low seasonality (Murphy and Bowman 2012). Meanwhile, savannahs often maintain open tree layers, grassy groundcover, highly seasonal climates, and frequent fire activity (Grace et al. 2006, Murphy and Bowman 2012). Their relative distributions are thought to be influenced by precipitation feedback loops; these have been related to disturbance, with incidences of fire or tree felling likely to promote savannah cover; and to topographic complexity, with greater complexity and rugosity promoting rainforest cover (Ash 1988, Murphy and Bowman 2012, Ondei et al. 2017). Adaptive differences between rainforest and savannah are therefore not only likely to have been influenced by magnitudinal differences in relevant environmental variables, but also by differences in stability and complexity, potentially influencing specialisation and resilience to climate (Hau 2001, Cadena et al. 2012, Ciemer et al. 2019).

These features offer the opportunity for testing hypotheses of geographical variation in adaptive resilience, based on assumptions that organisms are adapted to, or have the ability to acclimate to, the

conditions normally encountered in their habitat range (Ghalambor et al. 2006). For instance, the 'climatic variability hypothesis' predicts a greater range of thermal tolerance and acclimation capacity for organisms that evolved in variable climates compared to those adapted to more stable climates (Janzen 1967, Ghalambor et al. 2006, Aguilar-Kirigin and Naya 2013). Under this premise, it is expected that savannah-adapted organisms will be more resilient to climatic changes than those adapted to rainforest environments. Evidence for habitat-specific physiological adaptation are available for several studies of rainforest-ecotone and rainforest-savannah transitions, for example in birds (*Andropadus virens*, Smith et al. (2005); *Cyanomitra olivacea*, Smith et al. (2011)), lizards (Scincidae, Moritz et al. (2012); *Kentropyx calcarata*, (Pontes-da-Silva et al. 2018)), insects (*Bicyclus dorothea*, Dongmo et al. (2021); Termitidae, Woon et al. (2021)), and mammals (*Praomys misonnei*, Morgan et al. (2020)). However, assessments that integrate data from ecological traits and genome-wide signals of selection remain rare in non-model tropical organisms, and are only beginning to address implications for resilience (Miller et al. 2020, Morgan et al. 2020).

Integrated approaches for detecting adaptation across landscapes

Molecular technologies, from genomics to transcriptomics, are revolutionising the study of landscape ecology (Andrew et al. 2013). Landscape genomics has arisen as a framework to identify associations between genomic variation and the environment, candidate genes under natural selection, and geographic variables shaping biological variation (Schwartz et al. 2010, Balkenhol et al. 2017, Li et al. 2017, Luikart et al. 2018). The approach stems from earlier studies of landscape genetics (*sensu* Manel et al. (2003)), but takes advantage of many thousands of markers along genomes, such as single nucleotide polymorphisms (SNPs) (Salojärvi 2018). This not only increases statistical power, but also provides a sample of both neutral and adaptive genetic variation to enable explicit tests of how landscape heterogeneity influences patterns of gene flow and natural selection (Storfer et al. 2007, Holderegger and Wagner 2008, Bragg et al. 2015).

Prevalent analytical methods include those that identify extreme allele frequency divergence among populations, for example outlier tests (Lewontin and Krakauer 1973, Luikart et al. 2003, Foll and Gaggiotti 2008), and those that identify associations between allele frequencies and environmental gradients, for example genotype environment associations (GEAs) (Joost et al. 2007, Coop et al. 2010, Fitzpatrick and Keller 2015, Rellstab et al. 2015). Both work under the premise that genetic differentiation between populations is not equal across the genome, and that greater differentiation between populations generally accumulates at regions of the genome that are under selection (Nosil 2012). GEAs are in their relative infancy, but provide great sensitivity for detecting polygenic adaptation, a process by which adaptive traits are controlled by many genes of individual low effect size (Orr 2005). Moreover, methods currently exist to accommodate a range of association types and sampling strategies, and can often incorporate and control for confounding variables such as neutral genetic structure or spatial proxies (reviewed by Rellstab et al. (2015), Forester et al. (2018), Balkenhol et al. (2017)).

Landscape genomics does not explicitly require the inclusion of phenotypic data about the adaptive traits of interest (Manel et al. 2010). Rather, identifying even indirect genotypic associations with climate can inform about sources of adaptive variation (Blois et al. 2013). However, without an understanding of physiological or fitness-related traits, the relevance of specific environmental factors and organismal responses can remain murky (Rellstab et al. 2015). Association analyses linking phenotype with either spatial or allelic variation may therefore strengthen inferences of selection, and inform about the likely adaptive relevance of candidate adaptive genotypes (Rellstab et al. 2015, Talbot et al. 2017). Traits such as body shape, physiological capability, or behaviour are useful inclusions. This is particularly relevant where ecological relevance has already been demonstrated, such as in the relationship between habitat type and fin position of Australian rainbowfishes (McGuigan et al. 2003, McGuigan et al. 2005, Smith et al. 2020), topical to this thesis. Multivariate morphological datasets can be created by identifying homologous landmarks on an animal's body to extract geometric morphometric coordinates (Claude 2008, Zelditch et al. 2012). Similar to GEA methods, phenotype-

environment associations (PEAs) can identify ecologically adaptive phenotypes, and can also include controls for confounding influences such as demographic history (Zelditch et al. 2012, Maestri et al. 2016). Moreover, although uncommon, even clearer interpretations can be drawn from integrative genotype-phenotype-environment (GxPxE) associations (Talbot et al. 2017). In these types of approaches, associations between candidate adaptive genotypes and significant phenotypic polymorphisms can help clarify the role of environment, as well as putative genetic functions underlying ecological adaptations (Talbot et al. 2017, Hu et al. 2020, Smith et al. 2020, Carvalho et al. 2021).

Another phenotypic angle for studying adaptation and resilience to environmental change is the regulation of gene expression. For many genes, expression regulation occurs primarily at the level of transcription, whether through quantitative changes in expression levels, or through processes such as alternative splicing (Marden 2008, De Wit et al. 2012). This makes studies of transcriptional variation, using methods such as RNA-seq (i.e. RNA sequencing via NGS), extremely useful for understanding both the potential for and mechanistic basis of short- and long-term adaptive responses (Wellband and Heath 2017). Studies of expression in experimental conditions can inform about the regions and pathways responsible for physiological responses to specific environmental variables (De Wit et al. 2012). Expression regulation may also represent an important adaptive mechanism, enabling genotypes to express different phenotypes under different environmental challenges (Merilä 2015, Xu et al. 2016). The resulting phenotypic plasticity can act as both a buffer against selective pressures such as climatic variation, and may even facilitate diversification at the genetic level (Pfennig et al. 2010, Wund 2012, Bailey et al. 2021). For example, it has been found that populations with high levels of phenotypic plasticity may be more likely to colonise new areas, with the plasticity providing a broader basis for adaptive radiation (Muschick et al. 2011, Stein and Bell 2019). Finally, there is increasing evidence that greater tolerance to challenges such as thermal stress may be reflected by responses in a greater number of relevant genes and with greater magnitudes of expression difference (Garvin et al. 2015, Narum and Campbell 2015, Sandoval-Castillo et al. 2020, Komoroske et al. 2021). Although mechanistic links are

not yet established, such measures of plasticity may improve predictions of resilience to environmental change, and help to explain the physiological basis for performance differences.

Australian rainbowfish study system

In this thesis, we focus on the eastern rainbowfish *Melanotaenia splendida splendida* (Teleostei: Melanotaeniidae; Peters 1866), a tropical member of the "Australis" clade of small-bodied Australian rainbowfishes (Unmack et al. 2013). The group is currently of great interest in climatic adaptation research in freshwater ecosystems (Smith et al. 2013, McCairns et al. 2016, Gates et al. 2017, Brauer et al. 2018, Sandoval-Castillo et al. 2020, Smith et al. 2020). Not only do species ranges correspond closely to the boundaries of major Australian climatic ecoregions (McGuigan et al. 2000, Unmack et al. 2013), but previous studies of the congeneric *M. duboulayi*, *M. eachamensis, M. fluviatilis*, and *M. s. tatei* have identified genotypic and phenotypic traits of adaptive significance for both thermal and hydrological responses (McGuigan et al. 2003, McGuigan et al. 2005, Smith et al. 2013, McCairns et al. 2016, Sandoval-Castillo et al. 2020, Smith et al. 2020). Early morphological work on rainbowfishes found evidence of environmentally driven, heritable body shape divergence in relation to hydrodynamics (McGuigan et al. 2003, McGuigan et al. 2005). In these studies, divergence in fin position was associated with contrasting flow regimes, a key attribute in the context of climate change (Döll and Zhang 2010). More recent landscape genomics approaches in the Molecular Ecology Lab at Flinders University (MELFU) have inferred GEA signals in response to seasonal hydroclimatic variation (Brauer et al. 2018, Smith et al. 2020), and linked morphological differences to climate-associated genes (Smith et al. 2020). Additionally, experimental work testing gene expression responses to projected changes in climate has described highly plastic thermal responses (Smith et al. 2013), heritability of plastic response capacities (McCairns et al. 2016), and evidence for adaptive divergence of plastic capacities among divergent climatic ecotypes (Sandoval-Castillo et al. 2020). Together, these studies indicate that physiological variation in rainbowfishes has been strongly influenced by hydroclimate, and suggests the importance of both genomic adaptation and phenotypic plasticity for

responses to future changes. However, such studies are yet to include a tropical representative species of rainbowfish.

Melanotaenia splendida splendida (Peters 1866) are endemic to tropical north-eastern Australia (Figure 1.1) (McGuigan et al. 2000, Unmack et al. 2013). They are distributed among river systems of bordering rainforest and savannah biomes, which include the Wet Tropics of Queensland UNESCO World Heritage Area, as well as drier central regions of Cape York Peninsula (ALA 2020). Like many Australian rainbowfishes, *M. s. splendida* exhibit extensive phenotypic variation across their range; morphological, meristic, and colour variations have been observed between populations, drainages, and even contrasting habitats within drainages (Pusey et al. 2004). This has led to suggestions of locally divergent genetic variation or highly plastic phenotypes in the species (Pusey et al. 2004). However, the contribution of these influences, and any associated adaptive benefits, are yet to be explored through genomic studies. Topographic heterogeneity across *M. s. splendida*'s distribution also includes variation in the size and connectivity of river drainages, providing a further avenue of exploration in relation to adaptation and divergence. While large rivers are regularly connected by monsoonal flows in lowland savannah areas (Howley et al. 2013), the more mountainous terrain of Queensland's wet tropical rainforests comprise many small but distinct drainages, creating a naturally fragmented freshwater habitat structure (Nott 2005, Pearson et al. 2015). River network architecture is almost invariably associated with population structure in freshwater fishes, and is therefore expected to affect evolutionary dynamics among tropical ecoregions (Jiménez-Cisneros et al. 2014, Thomaz et al. 2016, Davis et al. 2018). The above features, when combined with ease of captive rearing, relative ecological importance, and relative abundance of *M. s. splendida* (up to 7.23 fish per square metre) (Pusey et al. 2004), make the species an ideal target for wild and laboratory studies of adaptation. We suspect that environmental gradients, and climatic gradients in particular, have contributed to their evolutionary diversity across tropical ecosystems.
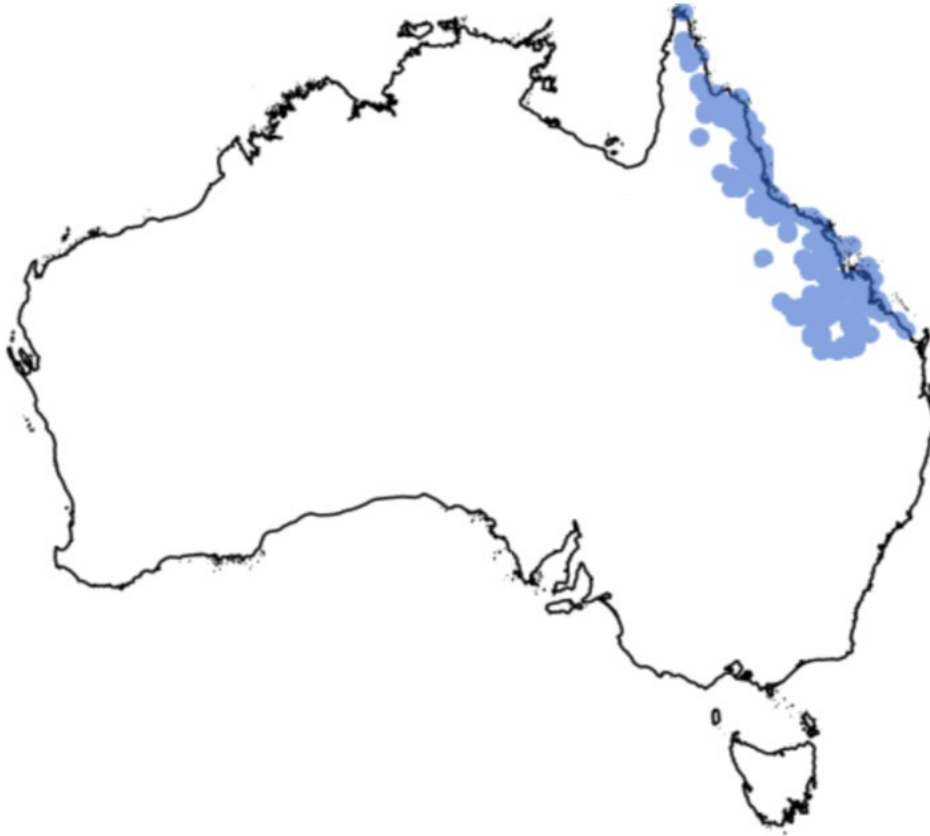
Figure 1.1 *Melanotaenia splendida splendida* species range in tropical north-eastern Australia, based on records from the Atlas of Living Australia (ALA 2020).

Significance and justification

Biodiversity management in the Anthropocene is limited by resource allocation and conflicting political interests (Seddon et al. 2016). Therefore, conservation efforts will be maximised where management is informed by sound knowledge of adaptive patterns affecting vulnerability and resilience in natural populations (Summers et al. 2012, Faleiro et al. 2013, Bernatchez 2016, Seddon et al. 2016). Despite strong theoretical underpinnings, interpreting eco-evolutionary processes in natural systems is complicated by interactions across multiple levels of biological organisation and surrounding abiotic environments (Hansen et al. 2012, Andrew et al. 2013, Merilä and Hendry 2014). Moreover, diverse, and potentially vulnerable ecosystems such as tropical rainforests and savannahs remain understudied compared to temperate systems, remaining an urgent priority for empirical research (Beheregaray et al.

2015, Barlow et al. 2018). This project takes advantage of relatively recent advances in high resolution molecular data generation and prioritises interdisciplinary integration of environmental and biological datasets. We explore intraspecies variation of genotypes, gene expression profiles, morphological phenotypes, and physiological tolerances of an endemic rainbowfish (*Melanotaenia splendida splendida*) across freshwater systems of tropical rainforest and savannah (see framework in Figure 1.2). By assessing evolutionary and plastic signals of divergences across bioregions, we begin to elucidate influences of hydroclimate and catchment structure on adaptive diversity and resilience in tropical riverscapes.

This work forms part of a larger long-term research program on Comparative Evolutionary Genomics of Australian Rainbowfishes within the MELFU (Australian Research Council grants DP110101207 and DP150102903; LB Beheregaray & L Bernatchez), which, as discussed above, has made strides in clarifying climatic and spatial correlates of adaptation in temperate, desert, and subtropical Australian river systems. That broader work has highlighted plastic and evolutionary adaptation in Australian rainbowfishes, and has provided data relevant for conservation planning over large portions of the continent. However, this thesis represents the first tropical component of this growing body of research. Furthermore, the contained chapters will stand alone in informing about adaptive and non-adaptive drivers of evolution in tropical freshwater, as well as factors influencing resilience of rainforest and savannah fish populations in a changing climate.
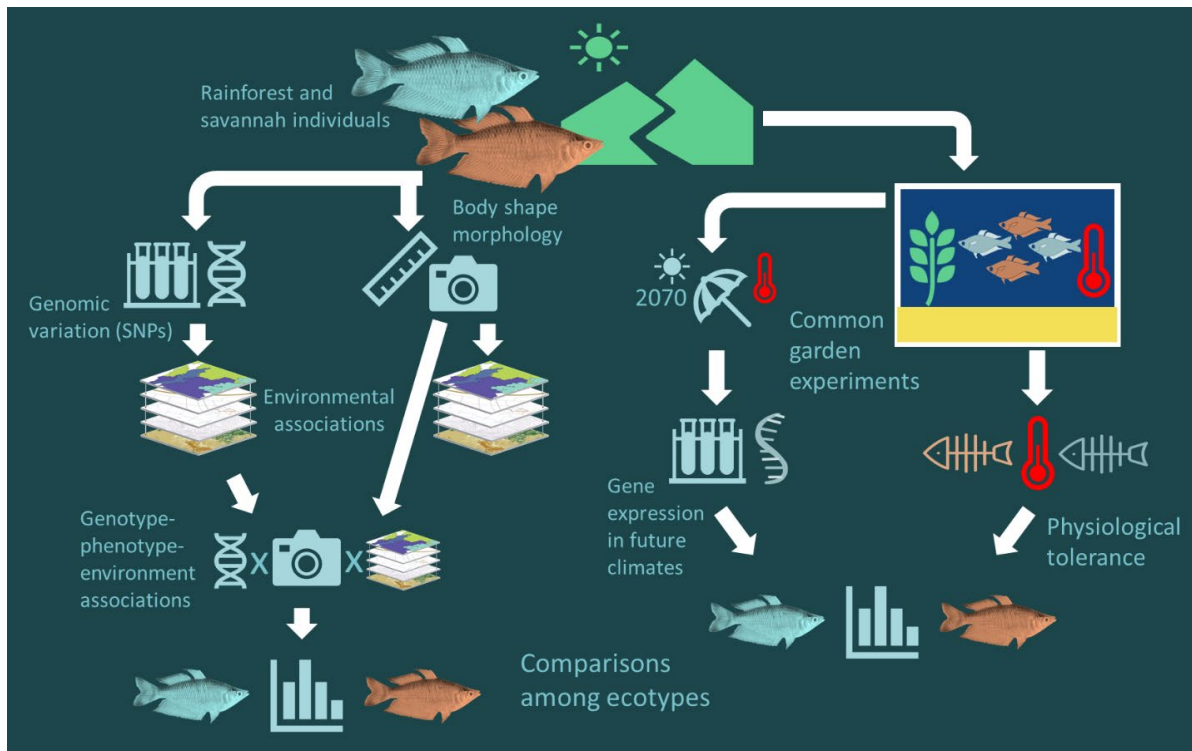
Figure 1.2 The framework implemented in this PhD thesis maps genetic diversity, population structure, signatures of selection and morphological variation of *Melanotaenia splendida splendida* across the climatically heterogeneous landscape of tropical north-eastern Australia (rainforest and savannah ecoregions) to test associations between putative adaptive variation and environment. We also contrast physiological and gene expression responses to thermal stress between rainforest and savannah populations using experimental temperature manipulation to determine potential for the role of phenotypic plasticity in climatic adaptation. We combine the above information to identify genomic regions underlying phenotypic adaptation to climate, and assess differences in adaptive resilience to rapid climatic change between these two key tropical ecotypes.

Thesis outline

This thesis comprises five chapters. Chapter 1 provides a general introduction to the research subject and study system. The chapter is intentionally presented in a concise format to reduce repetition with the data chapters. Chapters 2, 3 and 4 are data chapters, each intended as stand-alone publications. Chapter 5 is a concluding chapter, providing critical discussion of our major results and their broader theoretical and practical implications.

Chapter 2: Environmental selection, rather than neutral processes, best explain patterns of diversity in a tropical rainforest fish

This data chapter investigates ecological influences on intraspecies variation of *M. s. splendida* within its wet tropical rainforest distribution. Integrative landscape genomics methods were combined with morphological (geometric morphometric) phenotyping to identify selection gradients and terrain features contributing to spatial patterns of diversity. We found evidence for adaptive divergence in response to hydrological and thermal gradients. Moreover, ecological variables were better able to predict intraspecies variation than putative neutral structure.

Chapter 3: Divergence among and within tropical biomes: adaptation, specialisation, and resilience

This chapter expands upon the rainforest-specific focus of Chapter 2, to present a comparative assessment of adaptive divergence across rainforest and savannah ecosystems. We tested contributions of environmental and neutral influences among and within ecoregions, using genotype-environment, phenotype-environment, and genotype-phenotype-environment associations. Further, we explored the influence of terrain connectivity on strength and variation of local adaptive signals. In addition to evidence for divergent hydroclimatic adaptation among ecoregions, we found weaker associations among genotype, phenotype, and environment in the highly connected savannah region. We propose a homogenising effect of gene flow on local genomic adaptation, as well as a potentially greater reliance on plasticity for phenotypic variation among savannah localities.

Chapter 4: Comparative transcriptomics and resilience to future climates of rainforest and savannah rainbowfish

We use common-garden experiments to compare short-term adaptive responses to climate warming among rainforest and savannah populations, as well as in relation to temperate, desert, and subtropical

rainbowfishes previously studied at MELFU. We assessed rapid acclimation capacity via tests of critical thermal maximum, and compared plastic responses to projected 2070 summer temperatures using gene expression analyses. We found both the greatest thermal tolerance and the greatest transcriptional flexibility in the savannah ecotype, which may assist plastic responses to the hot and variable conditions of its native environment.

Chapter 4: Conclusion

This chapter concludes the study by summarising our main research findings in relation to our aims. We discuss the contributions of hydroclimatic selection and landscape structure to patterns of genomic and physiological diversity in the tropical rainbowfish *M. s. splendida*. We discuss further implications for resilience between rainforest and savannah biomes in a rapidly changing climate, as well as highlighting limitations and future directions for this work.

During the PhD candidature, I also made a significant contribution to the research and writing of a publication (full version, Appendix 4) which was directly linked to this project but not a part of the PhD:

- Sandoval-Castillo, J., Gates, K., Brauer, C. J., Smith, S., Bernatchez, L., & Beheregaray, L. B. (2020). Adaptation of plasticity to projected maximum temperatures and across climatically defined bioregions. Proceedings of the National Academy of Sciences, 117(29), 17112-17121.

Chapter 2: Environmental selection, rather than neutral processes, best explain patterns of diversity in a tropical rainforest fish

Abstract

To conserve the high functional and genetic variation in hotspots such as tropical rainforests, it is essential to understand the forces driving and maintaining biodiversity. We asked to what extent environmental gradients and terrain structure affect morphological and genomic variation across the wet tropical distribution of an Australian rainbowfish, *Melanotaenia splendida splendida*. We used an integrative riverscape genomics and morphometrics framework to assess the influence of these factors on both putative adaptive and non-adaptive spatial divergence. We found that neutral genetic population structure was largely explainable by restricted gene flow among drainages. However, environmental associations revealed that ecological variables had a similar power to explain overall genetic variation, and greater power to explain body shape variation, than the included neutral covariables. Hydrological and thermal variables were the best environmental predictors and were correlated with traits previously linked to heritable habitat-associated dimorphism in rainbowfishes. Additionally, climate-associated genetic variation was significantly associated with morphology, supporting heritability of shape variation. These results support the inference of evolved functional differences among localities, and the importance of hydroclimate in early stages of diversification. We expect that substantial evolutionary responses will be required in tropical rainforest endemics to mitigate local fitness losses due to changing climates.

Introduction

Empirical studies are fundamental to the advancement of evolutionary theory, and they increase in relevance as we grapple with the novel selective forces of anthropomorphic environmental change. Both adaptive and non-adaptive processes contribute to the proliferation of biodiversity, but there remains much to explore about their relative roles (Bernatchez 2016, Wellenreuther and Hansson 2016, Luikart et al. 2018). At a landscape scale, environment is expected to modulate interactions between evolutionary mechanisms, namely natural selection, genetic drift, and gene flow (Haldane 1948, Slatkin 1987, Manel et al. 2003, Storfer et al. 2007). However, we are only now developing frameworks to untangle coexisting signatures of these processes in natural populations. Such studies are particularly sparse in biodiversity hotspots such as tropical rainforests, where there has not only been substantial debate about diversifying processes (Endler 1982, Mayr and O'Hara 1986, Moritz et al. 2000), but also suggestions of a high risk to adaptive diversity from human influences (Moritz 2002, Barlow et al. 2018, França et al. 2020).

As some of the world's most biodiverse and temporally continuous ecosystems, tropical environments merit a central place in eco-evolutionary research. Tropical rainforests alone may contain more than half the world's species (Turner 2001, Primack and Corlett 2005), and are among the greatest terrestrial providers of ecosystem services (Brandon 2014). Attributes such as localised endemism, high niche specificity and a history of relative stability may increase threats to diversity under environmental change (Reed 1992, Barlow et al. 2018, Hoffmann et al. 2019). However, there is an inherent logistical difficulty of studying such diverse and often remote ecological communities (Beheregaray 2008, Beheregaray et al. 2015, Clarke et al. 2017), and both terrestrial and freshwater tropics remain remarkably understudied relative to temperate ecosystems (Beheregaray et al. 2015, Wilson et al. 2016). There has also been a long history of contention about the processes generating and sustaining tropical rainforest biodiversity (Endler 1982, Mayr and O'Hara 1986, Haffer 1997, Smith et al. 1997). Biogeographic and palaeoecological research has debated factors permitting both the accumulation of species and the preconditions for divergence; while strong evidence suggests that stability of rainforest

refugia through glacial maxima has helped sustain high species richness (Weir and Schluter 2007, Weber et al. 2014, Cattin et al. 2016), the factors precipitating diversification remain less clear. Arguments for vicariant influences such as refugial isolation and landscape breaks (Wallace 1854, Haffer 1969, Vuilleumier 1971, Mayr and O'Hara 1986, Ayres and Clutton-Brock 1992, Dias et al. 2013) have been increasingly contested with evidence for parapatric and sympatric divergence across ecotones (Endler 1982, Smith et al. 1997, Kirschel et al. 2011, Cooke et al. 2012a, Cooke et al. 2012b, Cooke et al. 2014, Morgan et al. 2020).

While providing important geographical context, the polarised nature of early research has sometimes obscured the complexity and continuity of evolutionary processes in rainforest taxa (Butlin et al. 2008, Jardim de Queiroz et al. 2017). For example, the difficulty of inferring adaptation in isolated populations against a neutral 'null hypothesis' may have encouraged the view that allopatric divergences were largely drift-driven, despite evidence that local selection can often be more effective in a low gene flow context (Schluter 2001, Nosil 2012, Beheregaray et al. 2015). Moreover, while species-level diversification has received great emphasis, increased intraspecific research provides a granular approach for identifying evolutionary processes such as drift and adaptation (Moritz et al. 2000, Moritz 2002). In tropical studies explicitly assessing neutral and adaptive patterns, both have been found to contribute to genetic or physiological diversity (Freedman et al. 2010, Smith et al. 2011, Cooke et al. 2014, Brousseau et al. 2015, Benham and Witt 2016, Maestri et al. 2016, Termignoni-García et al. 2017, Zhen et al. 2017, Gallego-García et al. 2019, Morgan et al. 2020). However, only a few tropical studies have so far addressed these questions with the aid of large and integrated datasets, which will be invaluable for more nuanced assessments of evolutionary processes (Moritz et al. 2000, Moritz 2002, Beheregaray et al. 2015).

The field of landscape genomics has exploited rapidly advancing genomic and geospatial toolsets to detect ecological adaptation (Manel and Holderegger 2013, Hoffmann et al. 2015, Li et al. 2017),

including in aquatic ecosystems (Grummer et al. 2019). Genotype-environment association (GEA) analyses have proven to be a powerful means to identify loci under selection by specific environmental factors (Rellstab et al. 2015, Waldvogel et al. 2020), even for relatively weak allele frequency shifts (Bourret et al. 2014, Laporte et al. 2016, Forester et al. 2018). Similarly, phenotype-environment associations (PEAs) can allow identification of ecologically adaptive phenotypes, benefited by multivariate approaches like geometric morphometrics (Zelditch et al. 2012, Maestri et al. 2016). Detection of adaptation is complicated by the expectation of additional random, and potentially neutral, divergences, so statistical methods correcting for shared population history can benefit these approaches (Gautier 2015, Rellstab et al. 2015). For PEAs, it is also important to consider that plastic responses to environement, rather than evolved differences, can produce divergent physical characteristics (Merilä and Hendry 2014). Therefore, clearer interpretations can be made where it is possible to relate ecologically adaptive genotypes to significant phenotypic polymorphisms (Hu et al. 2020). Such integrative genotype-phenotype-environment (GxPxE) associations increase the opportunity for teasing apart eco-evolutionary mechanisms, and may strengthen inferences about candidate genes underlying ecological adaptations (Smith et al. 2020, Carvalho et al. 2021).

Landscape heterogeneity places unique constraints on the biodiversity structure of taxa with restricted niches, including freshwater obligates. In tropical rainforests, high year-round precipitation makes freshwater habitats ubiquitous, and their biotic interactions inextricable from those of the broader forest (Lo et al. 2020). However, available habitats and opportunities for gene flow in freshwater are typically restricted to dendritic, hierarchical, island-like, or ephemeral water features (Lévêque 1997, Grummer et al. 2019). The architecture of river networks and the strength and direction of flows can profoundly influence evolutionary dynamics (Thomaz et al. 2016, Brauer et al. 2018), as well as vulnerability to fragmentation (Jiménez-Cisneros et al. 2014, Davis et al. 2018, Brauer and Beheregaray 2020). These factors make understanding the spatial distribution of aquatic diversity important but complicated, and few riverscape genomic studies have been attempted in tropical freshwater (but see Barreto et al. (2020); Gallego-García et al. (2019)).

We therefore capitalise on growing knowledge of eco-evolutionary processes in Australian rainbowfishes (*Melanotaenia* spp; family Melanotaeniidae) (e.g. McGuigan et al. (2003), McGuigan et al. (2005), Smith et al. (2013), McCairns et al. (2016), Gates et al. (2017), Brauer et al. (2018), Lisney et al. (2020), Sandoval-Castillo et al. (2020), Smith et al. (2020)). In this genus, previous work has indicated not only the likely importance of hydroclimate as a driver of diversity, but the utility of integrative methods for assessing aquatic adaptation. Early work found heritable and potentially convergent body shape variation in association with streamflow (*M. duboulayi; M. eachamensis*) (McGuigan et al. 2003, McGuigan et al. 2005). More recently, experimental assessments of gene expression have detected selection for plasticity of thermal response mechanisms (*M. duboulayi*, *M. fluviatilis*, and *M. s. tatei*) (Smith et al. 2013, McCairns et al. 2016, Sandoval-Castillo et al. 2020). Riverscape GEAs have also supported intraspecies ecological divergence related to hydroclimate for *M. fluviatilis* (Brauer et al. 2018) and *M. duboulayi* (Smith et al. 2020), with the latter including evidence of GxPxE links.

Despite these advances, genome-wide research has not yet been presented for a tropical representative of the clade. Hence, we focus this study on *Melanotaenia splendida splendida* (eastern rainbowfish), endemic to tropical north-eastern Australia. The species is abundant throughout its distribution, including several river systems in the complex rainforest landscape of the Wet Tropics of Queensland World Heritage Area (Pusey et al. 1995, Russell et al. 2003, Hilbert 2008). It inhabits a variety of freshwater environments, and is also known for its high morphological diversity, even within connected drainages (Pusey et al. 2004). Although the ecological relevance of this diversity has not yet been tested, the low to moderate dispersal tendency of *Melanotaenia* spp (Brauer et al. 2018, Smith et al. 2020) makes localised adaptation a plausible contributor. Moreover, the rugged terrain of the Great Dividing Range provides diverse conditions and possible selective influences across the sampled habitat (Nott 2005, Pearson et al. 2015). In that region, temperature, precipitation and streamflow vary with latitude, elevation, terrain structure, and proximity to the coast (Metcalfe and Ford 2009, Stein 2011), and human

impacts according to land use (Pert et al. 2010). This environmental and climatic heterogeneity, combined with the recognised biodiversity values, make the Wet Tropics of Queensland an ideal location for testing hypotheses about evolutionary dynamics in tropical freshwaters.

The broad aims of this study were to develop understanding about the adaptive and non-adaptive drivers of variation in tropical rainforest freshwater ecosystems. This was approached using landscape genomics to characterise spatial patterns of genetic and morphological diversity, identify links between genotype, phenotype and environment, and test the impacts of adaptive and non-adaptive forces on divergence across a variable rainforest hydroclimate. Based on previous evidence for climatic factors promoting adaptive diversity among higher latitude rainbowfishes (Brauer et al. 2018, Sandoval-Castillo et al. 2020, Smith et al. 2020), we tested the hypothesis that hydroclimate would also play a strong role in driving intra-species diversity within a tropical ecotype. The following questions were addressed: First, to what extent does hydroclimate predict genetic and morphological diversity beyond that explained by alternative hypotheses such as neutral genetic structure? Second, if such relationships exist, can further associations be drawn to suggest a genetic (heritable) adaptive component to the relevant morphology? Third, to what extent does catchment structure in this rugged terrain contribute to patterns of divergence? These factors have implications not only for understanding contemporary evolutionary processes in rainforest ecosystems, but also for interpretation of adaptive resilience to environmental change.

Methods

Sample collection

During March 2017, wild *Melanotaenia splendida splendida* (eastern rainbowfish) were sampled from nine rainforest creek sites across five drainages in the Wet Tropics of Queensland, north-eastern Australia (Figure 2.1; Supplementary Table A1). Live fish were captured by seine netting and transported by road in closed containers fitted with battery-running air pumps to a mobile fieldwork

station. Here, 267 fish were euthanised, one at a time, via an overdose of anaesthetic sedative (AQUI-S®: 175mg/L, 20 minutes). Of these, 208 individuals (avg. 23, min. 19 per sampling site; Table A1) were photographed immediately after death for morphometric data collection (details in Supplemental Methods A1). Fin clips from all 267 individuals were preserved in 99% ethanol and stored at -80°, of which 210 high quality samples were selected for the final DNA dataset (avg. 23, min. 20 per site; Table A1). For 180 individuals (avg. 20, min. 15 per site), both genomic and morphometric datasets were of high quality, allowing direct comparisons in later GxPxE analyses.
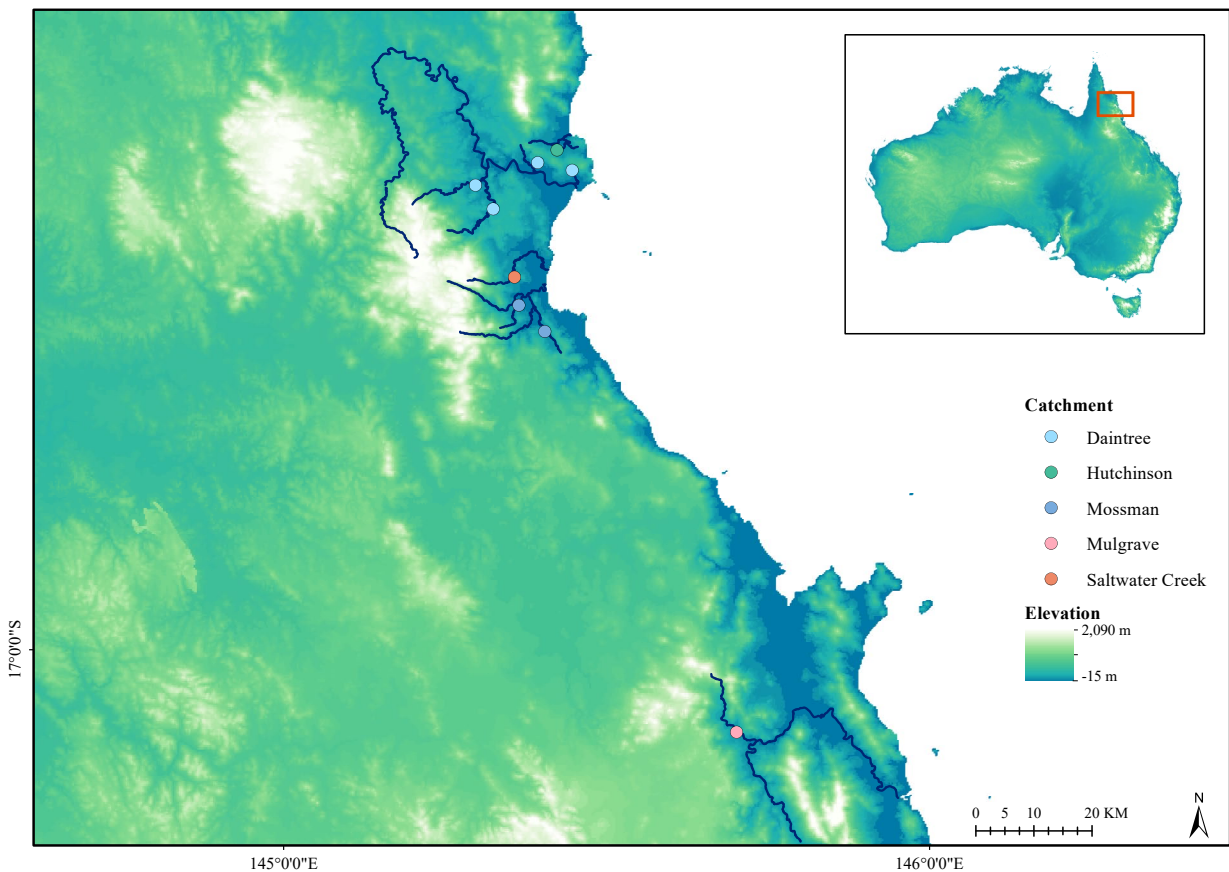
Figure 2.1 Sampling location map of *Melanotaenia splendida splendida* collected from the Wet Tropics of Queensland. Point colours correspond to river drainage of origin. Navy lines highlight only the sampled creeks and major rivers of each represented drainage system. Inset: extent indicator of main map relative to the Australian continent.

DNA extraction, library preparation and sequencing

We extracted DNA from fin clips using a salting-out protocol modified from Sunnucks and Hales (1996) (A2). DNA was assessed for quality using a NanoDrop spectrophotometer (Thermo Scientific), for integrity using gel electrophoresis (agarose, 2%), and for quantity using a Qubit fluorometer (Life Technologies). High-quality samples from 212 individuals were used to produce double-digest restriction site-associated DNA (ddRAD) libraries in-house following Peterson et al. (2012) with modifications according to Sandoval-Castillo et al. (2018) (A3), which have demonstrated efficacy for rainbowfishes (e.g. Brauer et al. (2018)). Samples were randomly assigned across sequencing lanes with an average of six replicates per lane for quality control. Four lanes were sequenced at the South Australian Health and Medical Research Institute Genomics Facility on an Illumina HiSeq25000 (single-ended), and one lane at Novogene Hong Kong on an Illumina HiSeq4000 (paired-ended).

Bioinformatics: read trimming, alignment to genome, variant calling and filtering

We used TRIMMOMATIC 0.39 as part of the DDOCENT 2.2.19 pipeline (Puritz et al. 2014) to demultiplex and trim adaptors from raw sequences, as well as leading and trailing low quality bases (Phred < 20). Individuals with < 700,000 reads were considered poorly sequenced and were removed from the dataset. Sequences were mapped to a reference genome of the closely related *M. duboulayi* (Beheregaray et al. unpublished data; Supplemental Table A4) following the GATK 3.7 pipeline (Van der Auwera and D O'Connor 2020). Briefly, we used BOWTIE 2 2.3.4 (Langmead and Salzberg 2012) to generate a FASTA file reference index and sequence dictionary from the genome and align individual sequences to the reference. After sorting and converting SAM files to BAM format, potential mapping errors and alignment inconsistencies were corrected using a local realignment around indels. Finally, variants were called from the mapped reads using BCFTOOLS 1.9 (Li 2011). To target high quality SNPs, we used VCFTOOLS 0.1.15 (Danecek et al. 2011) to filter poorly sequenced reads, non-biologically informative artefacts (*sensu* O'Leary et al. (2018), variants other than SNPs (e.g. indels), and sites with high likelihood of linkage disequilibrium (full details A4).

Differentiating putatively neutral versus outlier loci

Conformity of loci to neutral expectations was assessed using BAYESCAN 2.1 (Foll and Gaggiotti 2008), which identifies outlier loci under selection based on allele frequency distributions. Because the model relies on F_{ST}, it requires prior specification of population membership. We therefore ran an analysis using FASTSTRUCTURE 1.0 (Raj et al. 2014) for the full filtered dataset (details A5). We then ran BAYESCAN using default settings for all filtered loci, with individuals assigned to putative populations based on the best K selected by FASTSTRUCTURE. A putatively neutral dataset was inferred using a false discovery rate < 0.05. Such an approach is usually considered appropriate for minimally-biased assessments of demographic parameters (Luikart et al. 2003, Luikart et al. 2018). The resulting dataset (14,479 loci, 210 individuals) was used for subsequent analyses of neutral genetic diversity and population structure except where otherwise specified.

Genetic diversity and inference of population structure

We estimated neutral genomic diversity for each sampling site using ARLEQUIN 3.5 (Excoffier and Lischer 2010), including mean expected heterozygosity (H_e), mean nucleotide diversity (π), and proportion of polymorphic loci (*PP*). We also calculated Wright's fixation indices (*F*-statistics) in R (RC Team 2019) using HIERFSTAT 0.04-22 (Goudet 2005) for the entire sampling region. The same package was used to calculate pairwise F_{ST} and site-specific F_{ST} among sampling localities. To produce an overview of phylogenetic relationships among individuals, a Neighbour-Joining tree was constructed in PAUP* 4.0 (Swofford and Sullivan 2003b) using TN93 distances (Tamura and Nei 1993). We also produced a scaled covariance matrix of population allele frequencies (Ω) using BAYPASS 2.2 (Gautier 2015) core model, based on the full SNP dataset rather than the neutral subset. We further interrogated population structure using clustering approaches, including FASTSTRUCTURE, and Discriminant Analysis of Principal Components (DAPC) in R (RC Team 2019) package ADEGENET 2.0.0 (Jombart

2008, Jombart and Ahmed 2011). Full details of above analyses, including preparation of input files, are in Supplemental Methods (A6).

Characterising environmental variation

Environmental variables used to evaluate environmental and morphological variation were obtained from the National Environmental Stream Attributes v1.1.3, a supplementary product of the Australian Hydrological Geospatial Fabric (Geoscience Australia 2011; Stein (2011)). From >400 available attributes, we selected only those which varied among sampling sites, were uncorrelated, were measured at a relevant scale, and were considered to have broad ecological relevance for freshwater organisms (further details A7). The six selected variables were: stream segment aspect (ASPECT), river disturbance index (RDI), average summer mean runoff (RUNSUMMERMEAN), average annual mean rainfall (STRANNRAIN), average annual mean temperature (STRANNTEMP), and total length of upstream segments calculated for the segment pour-point (STRDENSITY) (Figure A7). These were used as a basis for the subsequent analyses of genotype-environment associations (GEA), phenotype environment associations (PEA) and GxPxE associations.

Genotype-environment associations

We used GEAs to assess the effect of environment on genotype of *M. s. splendida* within the climatically heterogeneous Daintree rainforest. We chose to use analytical approaches with different advantages, including a Bayesian hierarchical model (BAYPASS 2.2 auxiliary covariate model (Gautier 2015)), and constrained ordination (redundancy analysis; RDA) performed in R package VEGAN 2.5-6 (Oksanen et al. 2019). For both methods, we tested associations between the full SNP dataset (14,478) and the six scaled, uncorrelated environmental variables (see above) while controlling for putatively neutral genetic variation. The algorithm used by BAYPASS is well suited to study systems involving hierarchical population structure (Gautier 2015), which is particularly common in dendritic habitats such as freshwater (Thomaz et al. 2016). We tested for GEA associations accounting for assumed

population demographic structure (scaled population allelic covariance; Ω), previously identified using the software's core model (details in supplemental methods A8). Meanwhile, RDAs have been shown to have both a low rate of false positives and high rate of true positives under a range of demographic histories, sampling designs, and selection intensities when compared with other popular GEA methods (Forester et al. 2018). We first ran a global RDA using the full SNP dataset as the multivariate response matrix, and the six environmental variables (Figure A7), centred and scaled, as the explanatory matrix. Then, to control for demographic structure, partial RDAs (pRDAs) were used to model relationships between alternative (neutral) explanatory variables and genotypic responses, ordinating only the residual genotypic responses against environmental explanatory variables. To this end, two pRDAs were performed to include different neutral covariable matrices, 1) significant principal components (PCs) of scaled population allelic covariance (Ω), and 2) significant PCs of pairwise F_{ST}. For both, we used the full set of SNP genotypes as a response matrix, and an explanatory matrix containing only environmental variables previously associated with genotype ($p < 0.1$) in the global RDA (full details A8).

Geometric morphometric characterisation and analyses

Eighteen landmarks were positioned on digital images of *M. s. splendida* collected during field sampling using TPSDIG2 2.31 (Rohlf 2017). Landmarks (Figure 2.2) were selected to maximise anatomical homology, repeatability, and representation of potentially ecologically relevant characteristics, based on recommendations by Zelditch et al. (2012) and Farré et al. (2016). The majority represent intersections of fins or other skeletal structures, ensuring homology and providing a thorough representation of overall body shape and fin positioning. The only notable exceptions to homology are the front and rear margins of the maximum eye width (landmarks 3 and 4). However, these were included on the basis that the eye is an important sensory organ and might reflect ecologically relevant differences, and identification is relatively repeatable (Zelditch et al. 2012). The landmarks were also chosen to include those with ecological relevance in previous studies of rainbowfish morphology (McGuigan et al. 2003, McGuigan et al. 2005a).
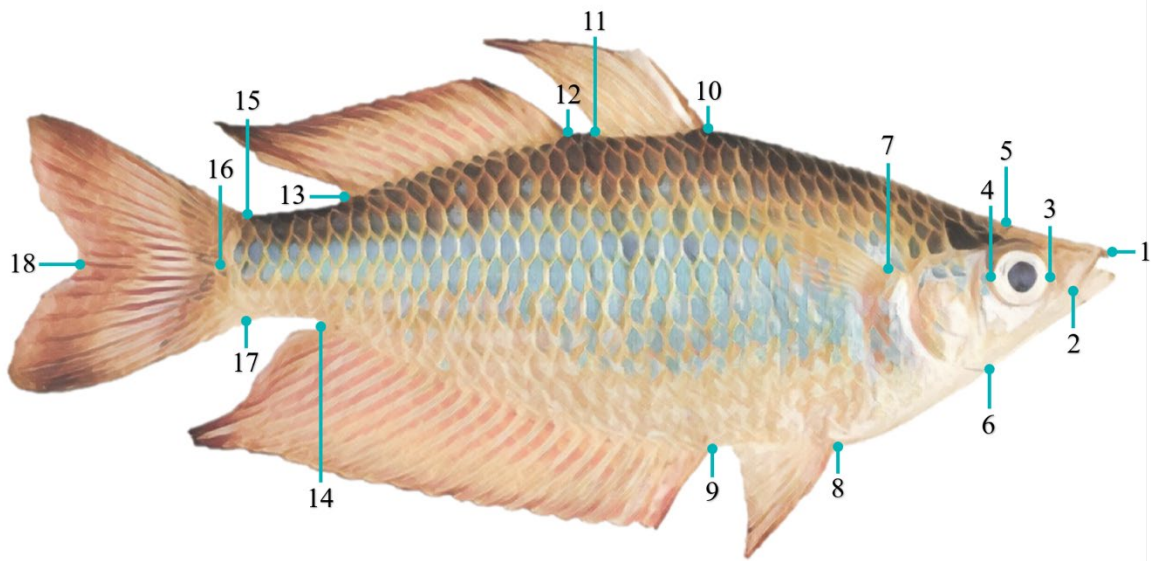
Figure 2.2 The 18 landmarks used for geometric morphometric analysis of the eastern rainbowfish *Melanotaenia splendida splendida*. 1: Anterior tip of head, where premaxillary bones articulate at midline; 2: Posterior tip of maxilla; 3: Anterior margin in maximum eye width; 4: Posterior margin in maximum eye width; 5: Dorsal margin of head at beginning of scales; 6: Ventral margin in the end of the head; 7: Dorsal insertion of pectoral fin; 8: Anterior insertion of the pelvic fin; 9: Anterior insertion of the anal fin; 10: Anterior insertion of the first dorsal fin; 11: Posterior insertion of the first dorsal fin; 12: Anterior insertion of the second dorsal fin; 13: Posterior insertion of the second dorsal fin; 14: Posterior insertion of the anal fin; 15: Dorsal insertion of the caudal fin; 16: Posterior margin of the caudal peduncle (at tip of lateral line); 17: Ventral insertion of the caudal fin; 18: Posterior margin of the caudal fin between dorsal and ventral lobes.

Digitised TPS files were imported into MORPHOJ 1.07a (Klingenberg 2011) for exploratory analyses. Individual landmark configurations were subjected to Procrustes superimposition, that is, a scaling of homologous coordinates by size, rotation and placement in space. The dataset was checked for outliers to ensure correct order and location of landmarks, and a covariance matrix was generated for the full dataset of individual Procrustes fits. To characterise major features of shape variation, a PCA was performed on the resulting covariance matrix. Due to size variation among individuals, an allometric

regression was used to test association between size (log centroid) and shape (Procrustes coordinates), pooled within population-based subgroups earlier identified by neutral genetic analyses. Due to a strong relationship between size and shape (Supplementary Figure A9), residuals from this regression were used for the subsequent canonical variate analyses (CVAs), also performed in MORPHOJ. To test for relationships between body shape and locality of origin, we ran CVAs of Procrustes distances against sampling site and against catchment. This method calculates total of variation among groups, scaling for relative within-group variation. Statistical significance was assessed using 1000 permutation rounds.

Phenotype-environment associations

To assess the effect of environmental gradients on body shape of *M. s. splendida* within the Daintree rainforest, we adapted the RDA approach used for the GEAs (described above) to implement phenotype-environment analyses (PEAs). We used the same set of environmental explanatory variables (above), this time testing body shapes (PCs of individual Procrustes distances determined significant by Broken-Stick method) as response variables. We again controlled for putatively neutral genetic structure (allelic covariance Ω; pairwise F_{ST}), plus the additional covariable of body size (log centroid size). Inputs for the body shape response variable and size covariable were created in R, using functions developed by Claude (2008) (full details in A10).

Genotype-phenotype-environment analysis

If environmental selection for a particular phenotype has promoted evolutionary adaption, then the relevant phenotypic divergence should be accompanied by a genotypic response. We therefore tested whether any of the putative adaptive (environmentally associated) genetic variation could be attributed to environmentally associated morphological variation throughout the study region. This could indicate both a heritable component to the associated body shape traits (as opposed to the alternative hypothesis of phenotypic plasticity), as well as providing further support for their adaptive advantages. In R, we ran a global RDA using the four significant PCs of individual Procrustes distances as explanatory

variables, and 864 putative adaptive alleles (identified in the genotype-environment RDA controlling for Ω) as the multivariate response. The analysis was then repeated as a partial RDA using individual body size (log centroid) as a covariable (details A11), the results of which isolated only the genotype-phenotype interactions best explained by environmental selection.

Results

Genome-wide SNP data, diversity, and population structure

Sequencing produced ~550 million ddRAD reads for 242 *M. s. splendida* individuals (including replicates). After variant filtering and removal of lower quality samples, we retained 14,540 putatively unlinked SNPs (Table B1), of which 14,478 could be considered neutral for the purposes of population genomic analyses (Figure B1). The final dataset comprised 210 high quality individuals across nine sampling sites. Neutral genomic diversity (Table 2.1) was moderately high for most sites, with expected heterozygosity (H_E) ranging from 0.278 to 0.321 (mean = 0.293), and proportion of polymorphic loci (*PP*) ranging from 0.252 to 0.391 (mean = 0.329). Population subdivision accounted for a substantial proportion of the neutral variation, with global $F_{ST} = 0.165$, and $F_{IT} = 0.205$. None of the site-specific F_{IS} values (Table 2.1) were significant. Pairwise F_{ST} comparisons (Figure 2.3a; Table B2) indicated relatively little differentiation between localities within the same drainage (0.017 - 0.029; mean = 0.024) compared with localities in different drainages (0.071 - 0.208; mean = 0.120), consistent with a segregating effect of drainage boundaries. Similarly, greater correlations in allelic covariance (Figure 2.3b) were observed among, rather than within drainages. Both pairwise and site-specific F_{ST} values indicated that the most neutrally divergent sampling localities were the northernmost McClean Creek (Hutchinson Drainage), followed by the centrally located Saltwater Creek (Saltwater Creek Drainage). In addition to being the smallest drainage systems sampled, both are located along the coastal boundary of the species distribution (Figure 2.1).

Table 2.1. Genetic diversity measures for the eastern rainbowfish *Melanotaenia splendida splendida* at nine rainforest localities, based on 14,478 putatively neutral loci (n = sample size for final DNA dataset; H_E = expected heterozygosity; H_O = observed heterozygosity; PP = proportion of polymorphic loci; F_{IS} = site-specific inbreeding coefficient; F_{ST} = site-specific F_{ST} .

Location	Site Code	Drainage system	n	H_E	H_O	PP	F_{IS}	F_{ST}
Little Mulgrave Creek	LM	Mulgrave	23	0.283	0.271	0.323	0.018	0.204
Cassowary Creek	CA	Mossman	23	0.297	0.295	0.314	-0.011	0.177
Marrs Creek	MA	Mossman	20	0.307	0.293	0.305	0.019	0.178
Saltwater Creek	SA	Saltwater Creek	24	0.321	0.307	0.264	0.019	0.261
Stewart Creek	ST	Daintree	25	0.278	0.259	0.391	0.031	0.065
Douglas Creek	DO	Daintree	24	0.289	0.272	0.376	0.038	0.060
Doyle Creek	DY	Daintree	24	0.294	0.280	0.358	0.030	0.095
Forest Creek	AN	Daintree	22	0.289	0.268	0.377	0.054	0.059
McClean Creek	MC	Hutchinson	25	0.279	0.271	0.252	0.009	0.382

Figure 2.3. Genomic differentiation and population structuring among nine rainforest sampling localities for the eastern rainbowfish *Melanotaenia splendida splendida*, represented by **(A)** Heatmap of pairwise F$_{ST}$ based on 14,478 putatively neutral SNPs; **(B)** Correlation map for BAYPASS core model scaled covariance matrix Ω based on allele frequencies of the full dataset of 14,540 SNPs; and **(C)** Cluster plot based on FASTSTRUCTURE analysis of 14,478 putatively neutral SNPs, where colours represent inferred ancestral populations of individuals based on an optimal *K* of five. Large type refers to drainage systems, which are separated by thicker black lines. Small type refers to sampling localities, separated by thinner black lines. Locality abbreviations follow Table 2.1.

Low differentiation within drainages and high differentiation between drainages was also reflected by clustering analyses. Both FASTSTRUCTURE (Figure 2.3c) and DAPC (Figure B3) grouped individuals by their drainage system of origin, resulting in an optimal *K* of five for both analyses. Pairs

of drainages in relatively close geographic proximity (i.e., Daintree and Hutchinson; Saltwater and Mossman) grouped more closely in the DAPC, indicating similarities in genetic variation which may result from a more recent shared history. Consistently, the neighbour-joining tree (Figure B4), representing putative individual-level evolutionary relationships, presented each drainage system as reciprocally monophyletic, and supported a hierarchical pattern of spatial connectivity.

Genotype-environment associations

Without considering neutral influences, global redundancy analyses (RDAs) found six environmental variables associated with 23% of the observed genetic variation among individuals (p = <0.001; Figure B5). After controlling for locality-specific neutral variation, GEAs remained highly significant (p = <0.001). Controlling for scaled allelic covariance Ω (Figure 2.5a; Figure 2.B5), associations with five environmental variables accounted for 16.6% of total SNP variation, from which 864 loci were identified as candidates for environmental selection (p ≤ 0.0027; Figure B7). The environmental explanatory variables STRANNRAIN and STRANNTEMP were the most influential in the model. When controlling for the alternative neutral covariable of pairwise F_{ST} (Figure B8), associations with six environmental variables accounted for 12.1% of total SNP variation, with STRANNRAIN and STRANNTEMP likewise emerging as the most influential. These environmental variables were once again the most important in BAYPASS GEA approach (auxiliary covariate model; Figure B9), which identified a more conservative 176 loci as candidates. Of these, 88 were uniquely associated with STRANNRAIN, 56 with STRANNTEMP, 12 with ASPECT, ten with RDI, nine with STRDESITY, and one with RUNSUMMERMEAN. Twenty percent of these candidates (36 loci) were shared with the pRDA approach.

Morphological variation among localities and environmental gradients

Across the sampled range of rainforest *M. s. splendida*, four PCs of body shape (Figure 2.4; Figure B10) were identified as significant by Broken-Stick modelling. Major shape changes along these axes

included differences in body depth (PCs 1 and 4), dorsal and ventral curvature (PCs 2 and 3), fin length and position (PCs 3 and 4), and upturn of head and mouth (PCs 2 and 3). Despite some overlap of individual variation among localities, CVAs revealed significant differences ($p < 0.05$) in Procrustes distances among most sampling sites, and among all drainages/populations (Figure B11, Table B11). Interestingly, the sites for which shape difference could not be significantly distinguished (Forest Creek, Daintree drainage; and McClean Creek, Hutchinson drainage) were not within the same drainage system (or neutrally inferred population grouping), but were the closest sites in geographical proximity. The most shape-divergent localities were Little Mulgrave (Mulgrave drainage) and Doyle Creek (Daintree drainage).
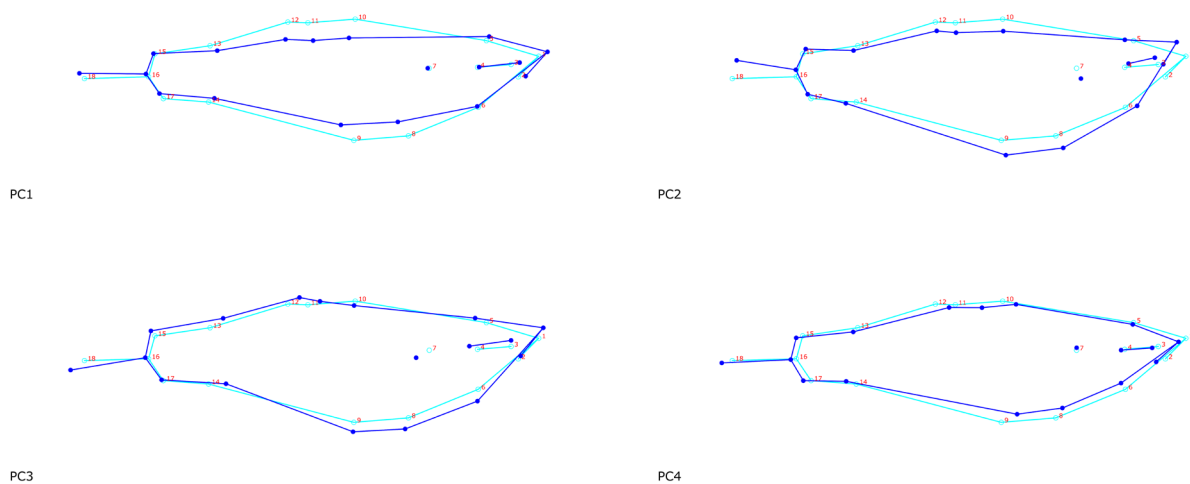
PC1

PC2

PC3

PC4

Figure 2.4. Wireframe graphical representation of significant principal components of body shape variation based on 18 landmarks for 207 *Melanotaenia splendida splendida* individuals sampled across nine rainforest sampling localities in the Wet Tropics of Queensland. Dark and light blue frames respectively represent body shape at high and low extremes of each significant axis (scale factor = 0.75).

Global RDAs found that approximately 24% of body shape variation (based on four significant shape PCs) was associated with environment ($p = <0.001$) (Figure B5). After controlling for possible allometric (log centroid size) and neutral genetic (locality-specific allelic covariance Ω) influences using pRDA, 14% of body shape variation remained significantly associated with four environmental

variables, with STRANNTEMP and STRDENSITY the most influential (p = <0.001; Figure 5b). The body shape components most strongly associated with environment were PC2, relating to dorsal flattening, ventral curvature, and upturn of head; and PC4, relating to width and position of first and second dorsal fins and anal fin, body depth, and length of caudal peduncle (see Figure 2.4 for graphical representation).

Associations among genotype, phenotype and environment

The GxPxE analysis using global RDA revealed that 6.8% of putatively environment-adaptive genetic variation was also associated with the observed morphological variation throughout the study region (p = <0.001). After controlling for possible allometric effects (centroid size) using pRDA, this figure was only slightly reduced to 6.5% (Figure 2.5c). The PCs of body shape that had the strongest influence on the model were PC2, followed by PC4. Based on these associations, we identified 61 candidate loci for climate-adaptive morphological variation with p = <0.0455 (Figure B12). In other words, these loci are predicted to confer a heritable selective advantage under localized environmental conditions based on their association with body shape.

Figure 2.5. Ordination plots summarising the first two axes of partial redundancy analyses (pRDAs) for *Melanotaenia splendida splendida* individuals sampled across nine rainforest sampling localities in the Wet Tropics of Queensland. **(A)** Genomic variation (based on 14,540 SNPs) explained by five associated environmental variables, after partialing out the locality-specific effect of Ω (allelic covariance). Environmental predictors accounted for 16.6% of total variation (p = <0.001). **(B)** Body shape variation (based on 18 morphometric landmarks) explained by four associated environmental variables, after partialing out the locality-specific effect of Ω (allelic covariance) and the individual effect of body size (log centroid). Environmental predictors accounted for 14% of total variation (p = <0.001). **(C)** Genomic variation (based on 864 putative climate-adaptive alleles) explained by four associated principal components of body shape, after partialing out the individual effect of body size (log centroid). Body shape accounted for 6.5% of climate-associated genetic variation (p = <0.001). For all plots, large points represent individual-level responses, and are coloured by drainage system of origin. Small purple points represent SNP-level responses. Vectors represent the magnitude and direction of relationships with explanatory variables.

Discussion

As some of the most diverse, iconic, and potentially vulnerable ecosystems in the world, the tropical rainforests remain remarkably understudied. Their complex and often inaccessible nature has created ongoing challenges to identifying the processes which drive and maintain biodiversity. Here, we contribute insight into these questions on an intraspecies level, by addressing major influences on genetic and morphological variation across the rainforest range of an Australian tropical fish (*Melanotaenia splendida splendida*). A clear association was found between both genetic and morphological variation and the drainage divisions of this mountainous and hierarchically structured catchment system, indicating an important role of gene flow limitations on population divergence. Despite this, a larger component of divergence could be better explained by local environmental conditions, and especially by variables relating to hydroclimate. This pattern was particularly pronounced for the morphological component of diversity, providing further evidence for its functional relevance. Meanwhile, GxPxE associations identified highly significant relationships between major components of body shape divergence and ecologically associated genetic variants. Based on these consistencies, we propose that local evolutionary adaptation is a favourable contributor to the high phenotypic diversity of rainforest *M. s. splendida*. We also infer that hydroclimatic adaptation has been a central mechanism for local divergence in this species, posing future challenges under rapid climatic change.

Environmental selection as a driver of rainforest freshwater diversity

Although there has been substantial historical emphasis on vicariant drivers of tropical rainforest diversity, an increasing number of genomic studies have revealed a dominant influence of contemporary environment (Ntie et al. 2017, Termignoni-García et al. 2017, Zhen et al. 2017, Lam et al. 2018, Jaffé et al. 2019, Miller et al. 2020, Morgan et al. 2020). Most of these works have focussed on terrestrial species, finding strong associations with either temperature or precipitation. In the Wet Tropics of Queensland, local variation dependent on latitude, elevation, terrain, and human impacts (Metcalfe and Ford 2009, Terrain NRM 2016) means that hydroclimatic selection could be expected to contribute to

geographic patterns of diversity in freshwaters. Consistent with this hypothesis, we found strong evidence for the influence of environment on both genetic and body shape divergence of *M. s. splendida*, even after accounting for approximations of neutral demographic structure. We also found tentative support for the role of environmentally modulated genomic variation in shaping the observed morphological diversity. Highly significant genotype-environment associations (GEAs) were supported by both RDA and BAYPASS analytical approaches. Depending on the covariables included, partial RDAs attributed ~12 - 17% of allelic variation to associations with key environmental variables, in contrast to the ~10 - 15% of variation which could be equally well or better explained by neutral conditional variables. Although it is difficult to draw direct comparisons, such strong GEAs support, and even exceed, those previously described for related temperate and subtropical Australian rainbowfishes (*M. fluviatilis*, Brauer et al. (2018); *M. duboulayi*, Smith et al. (2020)).

Large associations with environment were also found between body shape and environment in phenotype-environment associations (PEAs), with greater overlap among sites indicating that morphology may be more conserved than genotype. Environment accounted for ~7 - 14% of body shape variation in partial RDAs after accounting for conditional variables of neutral genetic structure and centroid size. These conditional variables accounted for a much larger 44 - 50% of shape variation, but intriguingly, most of this related to a large effect of size rather than of neutral genetic structure, which could only explain ~4 % of shape variation alone. In contrast to the relatively large contribution of neutral structure in the GEAs, this pattern was surprising, yet plausible, under the premise of greater functional constraints on morphology than on genome-wide variation. While many genomic changes may have little functional functional relevance (e.g. synonymous substitutions, pseudogenes, noncoding sequences), it has been suggested that the effects of random drift on phenotypes, and particularly on morphology, are less likely to be truly neutral ((Ho et al. 2017, Zhang 2018); but see Wideman et al. (2019)). That is, if a physiological trait is subject to strong selection (directional or otherwise), it is unlikely to conform to neutral patterns unless genetic drift is also extremely strong (McKay et al. 2001, Clegg et al. 2002). Considering that body shape variation in teleosts has well-established roles related

to swimming biomechanics, sensory ability, sexual behaviour, and various life history traits (Hanson and Cooke 2009, Langerhans and Reznick 2010, Killen et al. 2016), it is congruous that only a small proportion of variation would be explained by demography.

Few studies in the tropics have so far attempted to link signals of local genetic adaptation with patterns of phenotypic divergence. However, notable overlaps in genetic and morphological associations with environment have been detected by Morgan et al. (2020) for the rodent *Praomys misonnei* in relation to precipitation and vegetation structure, and by Miller et al. (2020) for the frog *Phrynobatrachus auritus* in relation to seasonality of precipitation. Here, we found a strong association among 6.5% of environmentally associated genetic loci and of body shape PCs. While the relationship between these variables remains putative, a plausible explanation is that genes linked to the 61 implicated loci are contributing to body shape differences among sampled sites. Such a scenario would imply a heritable component of the high phenotypic diversity of *M. s. splendida*, which is also congruent with previous evidence for heritability of rainbowfishes' hydrodynamic body morphology (*M. eachamensis*; McGuigan et al. (2003)) and transgenerational heritability of transcriptional plasticity (*M. duboulayi*, McCairns et al. (2016)). In the former example, similar phenotypic differences linked to hydrology were maintained by offspring produced in a common garden environment, providing evidence for evolved functional differences. The association of these signals thus adds an additional layer of support for the influence of local environment on evolutionary trajectories in the Wet Tropics. This level of integration has so far been uncommon in environmental association studies (Smith et al. 2020, Carvalho et al. 2021), and we would therefore recommend a similar strategy where both genomic and phenotypic data are available to improve inferences about candidate genes and potential biological relevance.

In considering which environmental variables may have been the most influential in shaping diversity, repeated associations with thermal and hydrological variables indicated a strong role for hydroclimate. Average annual rainfall, followed by average annual temperature, were the best environmental

predictors of genotype regardless of the GEA software, statistical approach, or neutral covariable used. The PEAs also emphasised the role of hydroclimate, with average annual temperature and stream density explaining the greatest shape variation. As with the GEAs, average annual rainfall was strongly associated with body shape in global RDA modelling. However, its covariation with body size meant effects could not be reliably separated from the alternative hypothesis of allometric shape change. Regardless, both GEA and PEA results accord with globally applicable expectations for climate as a driver of functional diversity (Hawkins et al. 2003, Siepielski et al. 2017), and emerging evidence for its importance in terrestrial tropical adaptation. Their prominence here in a freshwater context supports the broad evolutionary relevance of climatic variance to wet tropical diversity, a key finding in light of the 'ecology vs isolation' debate.

Putative trait adaptation to local environment

Body shape may be one of the best indicators of a fish's inhabited niche (Gatz Jr 1979, Wainwright 1996, Shuai et al. 2018), and shape changes with important associations in this system match several well-described physiological adaptations in other teleosts, including rainbowfishes (McGuigan et al. 2003, McGuigan et al. 2005, Smith et al. 2020). Here, shape PCs 4 and 2 had the strongest relationship with environmentally associated alleles, making them among the most likely to have a heritable adaptive relevance. Interestingly, PC4 was mostly characterised by a change in fin positions, with some striking similarities to those described by McGuigan et al. (2003) and McGuigan et al. (2005) for congeneric *M. duboulayi* and *M. eachamensis*. These studies found that across lineages, streamflow conditions were consistently associated with insertion points of first dorsal and pelvic fins, as well as the width of the second dorsal fin base. Here, changes on PC4 similarly included insertion of the first dorsal fin, and width of the second dorsal fin base. The associated precipitation and stream density variables can be related directly to the stream flow (Carlston 1963), which may therefore be contributing to adaptive diversity of fin position in *M. s. splendida*.

Shape change on PC2 was not only relevant in the GxPxE analyses but was also the most important shape variable directly associated with environment (PEAs). Positive values coincided with a more upturned head, smaller eye, reduced dorsal hump, and distended pelvic region. Much of this divergence appeared latitudinally, with upturned shape extremes more common in the higher rainfall northerly catchments of Hutchinson, Daintree and Saltwater. In a variety of teleost species, an upturned head and flattened dorsal region has been associated with a tendency for surface dwelling and feeding (Wootton 2012), surface breathing in oxygen-deficient waters (Lewis Jr 1970, Kramer and McClure 1982), and predation intensity (Langerhans et al. 2004, Eklöv and Svanbäck 2006). While an arching body shape has also been associated with rigor mortis in fishes (Hooker et al. 2016), the immediate imaging of individuals at the time of death, consistent among sampling sites, is likely to have prevented locality-specific differences in rigor induced shape change. Moreover, *M. s. splendida* are known for an omnivorous feeding strategy, sometimes including floating material such as invertebrates (Pusey et al. 2004). Notably, the surface feeding tendency of the related *M. duboulayi* has been associated with differences in vegetative cover, possibly due to thermoregulatory influences or predator density (Hattori and Warburton 2003). Therefore, while this component of shape variation could be explained by a variety of factors, promising hypotheses include local selective differences due to relative abundance of food sources, predator presence, or vegetation structure. Such examples would involve an indirect role for the measured environmental variables, with thermal and hydrodynamic influences being particularly relevant.

In addition to the described adaptive signals occurring throughout the region, our results suggested an important effect of drainage structure in demographic divergence. Specifically, both neutral genetic clustering and environmental association analyses provided evidence that contemporary drainage boundaries are creating barriers to gene flow, delineating populations and affecting broader patterns of diversity. All clustering methods grouped individuals by their drainage system of origin and provided minimal evidence of recent gene flow, while measures of neutral genetic diversity were more similar within drainages than between. Some additional, shallow substructure was detected among sampling

sites within drainages, possibly resulting from isolation by distance or other resistance within the stream network. Similar hierarchical configurations have been previously described for subtropical and temperate rainbowfishes (*M. fluviatilis*, Brauer et al. (2018); *M. duboulayi*, Smith et al. (2020)), reflecting a recognised pattern of connectivity in lotic environments (Grummer et al. 2019). We therefore propose that, in addition to hydroclimatic factors, the geographic arrangement and relative size of individual watersheds has modulated evolutionary trajectories, with likely implications for genetic variability, rates of divergence and even vulnerability to environmental change (Lévêque 1997). Gene flow barriers such as the drainage divisions in this system not only contribute to neutral genetic structuring, but are also expected to prevent flow of adaptive traits and alleles (Yeaman and Otto 2011). This may increase adaptive divergence among populations in contrasting selective environments, but also prevent the entrance of novel beneficial genotypes (Nosil et al. 2019). Such an effect may promote diversity in robust systems, but detriment small populations or those under novel selective pressures such as a warming climate (Yeaman and Otto 2011, Nosil 2012).

Considerations for the ongoing maintenance of adaptive diversity in tropical rainforests

Both the strong effects of hydroclimate on intraspecies diversity, and the geographical confinement created by catchment structure, indicate that climate warming could place strong selective pressure on rainforest populations of *M. s. splendida*. If a large component of local diversity has developed in either direct or indirect response to climate, we can expect that alteration of current environmental conditions will necessitate an adaptive response (Fitzpatrick and Keller 2015, Bay et al. 2017). It is notable that signals of adaptive divergence were directionally similar for genotype and morphology, and significant overlaps were revealed by GxPxE results. But as previously discussed, there were also some differences among associated environmental variables, their respective contributions, and the relative influences of neutral processes. These factors suggest similar but non-identical ecological dynamics are contributing to genetic and morphological diversity across the studied riverscapes. It therefore seems likely that while management strategies informed by either component of diversity should produce common benefits, a knowledge of both components would benefit more comprehensive management.

Melanotaenia splendida splendida is one of most abundant fishes in the Queensland Wet Tropics (Pusey et al. 2004), and our results indicated relatively high genetic variation in most populations. Moreover, the total species range extends beyond rainforest limits (ALA 2020). Considering these factors, we do not see reason for current concern about the survival of this species and would only anticipate imminent risk for populations confined to the smallest drainages, that is Hutchinson and Saltwater. More concerning are implications for already vulnerable tropical freshwater species, especially those with narrow distributions. Species with small effective population sizes and low genetic diversity are likely to have less standing variation available for selection (Frankham 2015, Ralls et al. 2018), and opportunities for future adaptation have greater chance of being outweighed by random genetic drift (Perrier et al. 2017). While not all tropical rainforests exhibit as structured terrain as the Queensland Wet Tropics, mountainous features are common to most continental tropics. Moreover, rainforests are becoming globally affected by less predictable flow dynamics (Jiménez-Cisneros et al. 2014) and accumulating human modifications (Davis et al. 2018). In the context of dendritic systems, even relatively small structural changes can divide the habitat area over which gene flow can occur (Davis et al. 2018). We therefore suggest that the maintenance of existing connectivity should be prioritised in tropical rainforest river networks, and support a proactive strategy of evolutionary rescue for particularly vulnerable taxa (*sensu* Ralls et al. (2018)). These recommendations should not be limited to tropical regions; however, the empirical evidence for a large climatic influence on intraspecies diversity, combined with documented narrow environmental tolerance ranges of tropical taxa (Deutsch et al. 2008, Huey et al. 2009, Eguiguren-Velepucha et al. 2016) should be considered cause for immediate action.

Conclusion

Our work indicates that interplay between contemporary hydroclimatic variation and drainage connectivity has helped shape regional diversity in the tropical rainforest fish *M. s. splendida*. Thermal and hydrological gradients are inferred to have had a dominant influence on local adaptation, whether

due to direct or indirect effects to the species' selective environment. Moreover, both genomic and morphological divergence appeared to be relevant, including several body shape traits previously found to be both heritable and hydrologically associated in related rainbowfishes. Heritability of adaptive shape variation is also very likely for this species, an idea which was bolstered by three-way associations detected among genotype, phenotype, and environment. Empirical evidence for the role of temperature and precipitation driving phenotypic divergence has been mounting in tropical rainforest research, however this is likely the first freshwater example to benefit from a high-resolution genomic dataset. Given the substantial impacts to freshwater hydroclimates projected under climate warming, this is a critical step towards understanding and mitigating threats to tropical freshwater diversity. This is even more pertinent in complex terrain such as the Queensland Wet Tropics World Heritage Area, which, in addition to dendritic riverine structure, comprises multiple small catchments that limit gene flow and migratory potential. While more than a century of research has progressed our understanding of how biodiversity has been maintained in the tropics, we are only now beginning to uncover the evolutionary mechanisms which continue to diversify these ancient and enigmatic ecosystems. Future work should continue to integrate environmental, genomic and phenotypic datasets to disentangle evolutionary processes applicable to both conservation and theoretical development.

Chapter 3: Evolutionary divergence among and within tropical rainforest and savannah biomes: adaptation, specialisation, and resilience

Abstract

Biodiversity management in a changing climate will rely on an understanding of the factors shaping adaptive diversity and resilience across landscapes. However, untangling interactions between selective and demographic processes is particularly challenging in spatially complex habitats. Here, we integrated landscape-based approaches to investigate adaptive variation and climatic resilience in the freshwater fish *Melanotaenia splendida splendida*. The species range spans tropical biomes of rainforest and savannah, which contrast markedly in both hydroclimate and catchment structure. We tested contributions of environmental and neutral influences among and within ecoregions using genotype-environment, phenotype-environment, and genotype-phenotype-environment associations. Additionally, we compared strength and variation of adaptive signals across terrains with varying connectivity to assess the potential influence of gene flow in homogenising adaptation in tropical lowlands. We found ecoregional differences in environmental associations, suggestive of divergent hydroclimatic adaptation. As in the previous rainforest-specific chapter, environment better predicted intraspecies variation than neutral factors, particularly for morphology. This included environmentally associated body shape variation known to be linked to swimming biomechanics and flow dynamics in teleosts. Finally, we found that genomic associations with environment were weaker and varied less across space in the well-connected savannah habitat, supporting our hypothesis of a homogenising effect of gene flow on local adaptation. Remarkably, this result was not mirrored by morphological patterns, which maintained strong environmental associations in the face of gene flow. Combined with a decoupling of genotypic and phenotypic associations in the savannah region, we hypothesise a greater reliance on phenotypic plasticity when connectivity is high across heterogeneous selective pressures. In contrast, the narrower set of conditions experienced in the more stable and naturally fragmented

rainforest habitat may have permitted more locally specialised evolutionary adaptations. Overall, our results point to trade-offs between system-wide resilience and local hydroclimatic specialisation among rainforest and savannah populations.

Introduction

Understanding relationships between adaptive diversity and environment will be a prerequisite for accurately anticipating and managing ecological responses to climate change in coming decades. The importance of climate as a selective force is becoming well established (Franks and Hoffmann 2012, Anderson and Song 2020), and where migratory opportunities are limited, such as for freshwater organisms, patterns of standing adaptive diversity are likely to be an important determinant of local resilience (Sgrò et al. 2011). Such adaptive patterns are influenced by the selective environment in which a species evolved (Holderegger et al. 2006, Whitlock 2014), and may therefore vary widely in accordance with local or regional conditions (Moritz et al. 2012), in addition to demographic and life history traits (Clarke 1979). Consequently, it is expected that broader patterns of resilience are also likely to vary geographically, influenced by factors such as local and regional climatic variability, and the strength of ecological gradients (Deutsch et al. 2008, Tewksbury et al. 2008). It has been suggested that tropical regions may be more vulnerable to changing climates because of organisms' narrow thermal niches (Huey et al. 2009, Sunday et al. 2011). This may be particularly apparent for ectotherms such as fishes due to their limited internal thermoregulatory capacities (Rohr and Palmer 2013). However, very little is known about the extent that ecological adaptation contributes to tropical diversity or about the adaptive relevance of climatic variation across different tropical habitats.

Transition zones such as the interface between rainforest and savannah are particularly promising arenas for the study of climatic adaptation and resilience (Smith et al. 1997). Rainforest and savannah are the most dominant biomes in the terrestrial tropics, varying not only climatically, but in the structural and functional complexity of their biotic communities (Bond and Parr 2010, Murphy et al. 2016). Although rainforest and savannah often occur adjacently, most species distributions are non-overlapping, reflecting conflicting habitat requirements (Fensham 1995, Azihou et al. 2013). While both are highly biodiverse, rainforests are typically taxonomically richer (Ter Steege et al. 2000, Kier et al. 2005) and include a greater proportion of obligate associations (Fensham 1995, Ibanez et al. 2013). A history of climatic fluctuations and frequent fire activity has contributed to greater temporal variability of

savannah communities (Staver et al. 2011b, Kutt et al. 2012, Vasconcellos et al. 2019). In contrast, many rainforest regions have experienced long-term climatic continuity, maintaining a proliferation of ancient lineages. This stability is one factor thought to have promoted the accumulation of tropical diversity and specialisation (Gaston and Blackburn 1996, Kooyman et al. 2013). However, landscape and environmental heterogeneity must also be considered if we are to adequately explain diversification in tropical bioregions (Moritz and McDonald 2005, Dagallier et al. 2020, Furness et al. 2021).

To formulate hypotheses about likely adaptive influences across rainforest and savannah, we can consider the bioclimatic interactions that are consistently associated with bioregion boundaries. Savannah communities are typically more dominant where annual rainfall is less than ~1,000 mm, and rainforest where more than ~2,000 mm (Hirota et al. 2011, Staver et al. 2011a). Meanwhile, rainfall, fire activity, and substrate may be subsequently influenced by forest density, producing feedback loops which help to sustain distributions (Hirota et al. 2011, Oliveras and Malhi 2016, Wu et al. 2016). These factors have broader implications for organisms' exposure to annual, seasonal, and diurnal climatic extremes, whereby savannah organisms are subjected to more variable but greater intensities of most climatic variables than in the rainforest. Notably, regional bioclimatic dynamics also appear to be influenced by topography, with rainforest biotas more often occurring in rugged and complex terrain (Murphy and Bowman 2012, Ondei et al. 2017). This could in some cases contribute to greater microhabitat structure and less landscape connectivity in rainforests (Svenning 1999), affecting the spatial scale over which both neutral and adaptive divergences may occur (Nosil et al. 2019). It is therefore possible that rainforest and savannah organisms may differ not only in response to regional climatic influences, but in the extent of locally specific adaptation within biomes, both with likely flow-on effects to resilience in changing conditions.

Disentangling environmental influences on adaptive and non-adaptive variation in wild populations is greatly assisted by large genomic datasets, which are expected to encompass loci varying both neutrally

and in response to selective pressures (Holderegger et al. 2006, Schwartz et al. 2010). Moreover, if ecotypic adaptations are a result of heritable evolutionary changes, then relevant associations with environment are likely to be reflected by both genomic and physiological divergence (Santure and Garant 2018). Landscape genomics approaches are increasingly seeking to identify overlap between genotype-environmental associations and divergence in fitness-related traits (Balkenhol et al. 2017). However, a limited number of studies have so far explicitly tested genotype-phenotype-environment associations in natural populations (Vangestel et al. 2018, Smith et al. 2020). This may not only provide a more holistic approach for assessing relevant environmental influences, but also improve inferences about candidate genes underlying environmental and climatic resilience (Carvalho et al. 2021). Additionally, large discrepancies in morphological and genetic patterns may highlight a reliance on plasticity for physiological changes, while strong overlaps can further support evolutionary responses to selection (Merilä and Hendry 2014).

As discussed in previous chapters, Australian rainbowfishes of the genus *Melanotaenia* are currently of great interest in climatic adaptation research in freshwater ecosystems (McCairns et al. 2016, Gates et al. 2017, Brauer et al. 2018, Sandoval-Castillo et al. 2020, Smith et al. 2020). Existing studies suggest that physiological variation has been strongly influenced by hydroclimate, and may be at least partially influenced by genomic adaptation (McGuigan et al. 2003, McGuigan et al. 2005, Sandoval-Castillo et al. 2020). Furthermore, systematics work has suggested relatively recent divergence of species and subspecies across ecological transitions (McGuigan et al. 2000, Hurwood and Hughes 2001, Unmack et al. 2013). In a tropical context, where ancient lineages proliferate, this creates an opportunity for comparative evolutionary studies assessing ongoing mechanisms of divergence (Moritz et al. 2000). Like many Australian rainbowfishes, tropical-endemic *Melanotania splendida splendida* exhibits extensive phenotypic variation across their range, which includes both rainforest and savannah ecoregions. Morphological, meristic and colour variations have been observed between populations, drainages (i.e. river catchments), and even contrasting habitats within drainages (Pusey et al. 2004).

This has led to suggestions of substantial within-species genetic diversity and/or a highly variable and plastic phenotype (Pusey et al. 2004).

In Chapter 2, evidence was provided for hydroclimate-associated genomic and morphological variation within the species' rainforest distribution. Moreover, these environmental influences could account for a greater proportion of biological variation than measures of neutral divergence. This suggests local adaptation has been highly relevant to the intraspecies diversity, with implications for additional adaptation required to withstand climatic changes. The addition of savannah representatives is therefore desirable for assessing broader patterns of trait divergence in tropical landscapes, which is expected to be influenced by both local and regional adaptation. The species' rainforest distribution is relatively rugged and topographically complex, being to a large extent determined by the presence of the highlands of the Great Dividing Range (Nott 2005). Rainforest drainage networks are ancient, densely packed, and mostly perennial (Nott 2005, Pearson 2005, Pearson et al. 2015). In contrast, streams across the lowland drainage systems of Cape York's savannah regions are often ephemeral, but connect at greater spatial scales due to branching between major tributaries during high volume monsoonal runoff (Howley et al. 2013). This comparative scenario provides the opportunity to assess influences of both the hydroclimate and terrain structure on adaptive variation.

To this end, we used a landscape genomics approach to test environmental associations with genotype, phenotype, and genotype-phenotype interactions in *M. s. splendida*, both between and within tropical biomes. Given the striking climatic and ecological differences between ecoregions, we hypothesised that the greatest intraspecies divergence may also occur across the rainforest-savannah interface. Moreover, based on the strong explanatory power of hydroclimatic variation in Chapter 2, we predicted that environmental associations could be better at explaining biological variation than neutral factors, especially for body shape variation which was inferred to have important functional relevance. Within ecoregions, we also interrogated the effects of terrain connectivity on spatial patterns of adaptation,

61

asking whether gene flow may act to strengthen or homogenise local signals of genetic and morphological adaptation, *sensu* Haldane (1930), Fisher (1950), Slatkin (1987) and others. Addressing these questions is important for understanding the dynamics of evolution in tropical freshwaters and may inform prioritisation of management strategies under rapid climatic change.

Methods

Field sampling

We collected wild *Melanotaenia splendida splendida* (eastern rainbowfish) from seventeen sites in tropical north-eastern Australia in March 2017. Localities included nine rainforest creek sites across five drainages, and eight savannah creek sites across one drainage (Figure 3.1; Supplementary Table A1). A total of 510 individuals were captured using seine nets and were euthanised on the day of capture via overdose of anaesthetic sedative (AQUI-S®: 175mg/L, 20 minutes) at mobile fieldwork stations. According to methods described in Chapter 2, this was performed one individual at a time, followed by immediate digital photographing for morphometric data collection (final photographic dataset of 366 individuals, avg. 22, min. 13 per sampling site; Table 3.1). Fin clips from all collected samples were preserved in 99% ethanol and stored at -80°C. Of these, 381 high quality samples were chosen for the final DNA dataset (avg. 22, min. 15 per site; Table 3.1). For 302 individuals (avg. 18, min. 11 per site), final genomic and morphometric datasets overlapped, enabling direct contrasts in later association tests among genotype, phenotype, and environment.
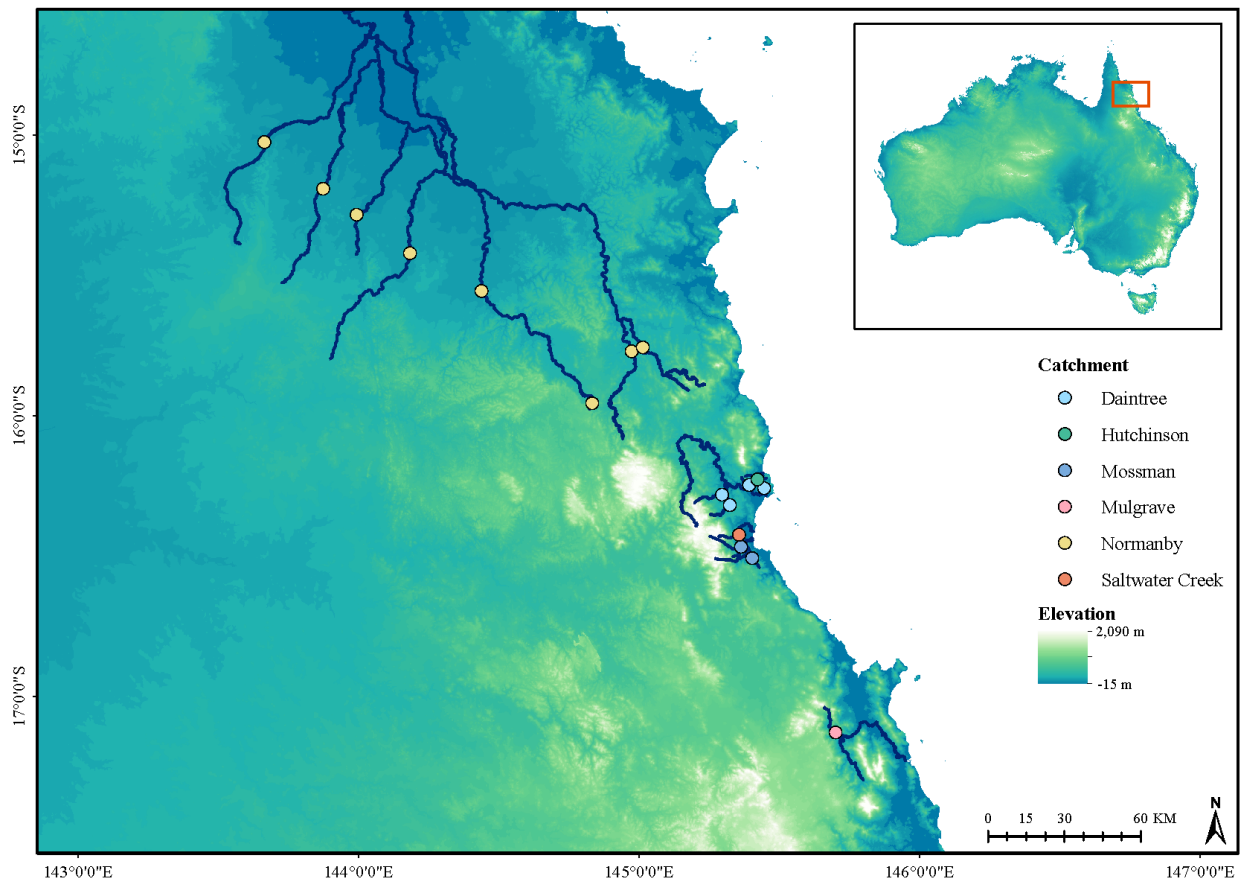
Figure 3.1. Sampling location map of *Melanotaenia splendida splendida* collected from eight savannah (shown in yellow) and nine rainforest locations (other colours) in north-eastern Australia. Point colours correspond to river drainages of origin; all savannah locations were sampled in the Normanby River drainage. Navy lines highlight only the sampled creeks and major river channels of each represented drainage system. Inset: extent indicator of main map relative to the Australian continent.

Table 3.1. Localities and sample sizes (n) of *Melanotaenia splendida splendida* collected from rainforest and savannah biomes of tropical north-eastern Australia for genomic and morphometric data.

Location	Site Code	River Drainage	Latitude	Longitude	Ecotype	Total collected n	Final n (DNA)	Final n (Morpho)	Final n (GxPxE)
Little Mulgrave Creek	LM	Mulgrave	-17.13	145.7	Rainforest	30	23	20	17
Cassowary Creek	CA	Mossman	-16.51	145.41	Rainforest	30	23	30	23
Marrs Creek	MA	Mossman	-16.47	145.36	Rainforest	24	20	19	15
Saltwater Creek	SA	Saltwater Creek	-16.42	145.36	Rainforest	30	24	21	19
Stewart Creek	ST	Daintree	-16.32	145.32	Rainforest	30	25	22	20
Douglas Creek	DO	Daintree	-16.28	145.3	Rainforest	30	24	29	21
Doyle Creek	DY	Daintree	-16.26	145.45	Rainforest	30	24	23	22
Forest Creek	AN	Daintree	-16.25	145.39	Rainforest	31	22	21	18
McClean Creek	MC	Hutchinson	-16.23	145.42	Rainforest	32	25	22	22
Famechon Creek	FA	Normanby	-15.95	144.83	Savannah	30	25	19	17
West Normanby River	WN	Normanby	-15.77	144.97	Savannah	30	21	20	18
East Normanby River	EN	Normanby	-15.76	145.02	Savannah	30	19	13	11
Laura River	LA	Normanby	-15.56	144.44	Savannah	33	23	22	11
Kennedy River	KE	Normanby	-15.42	144.18	Savannah	30	21	20	16
North Kennedy River	NK	Normanby	-15.28	143.99	Savannah	30	15	20	15
Hann River	HA	Normanby	-15.19	143.87	Savannah	30	24	23	18
Morehead River	MO	Normanby	-15.02	143.66	Savannah	30	23	22	19

Genomic data collection

DNA was extracted from fin clips by salting-out, using a protocol modified from Sunnucks and Hales (1996) described in Chapter 2. We then assessed DNA quality, quantity, and integrity using NanoDrop (Thermo Scientific), Qubit (Life Technologies), and gel electrophoresis (agarose, 2%) respectively. We produced double-digest restriction site-associated DNA (ddRAD) libraries in-house following Peterson et al. (2012) with modifications according to Sandoval-Castillo et al. (2018) for 420 individuals (including replicates and those later removed during filtering). We assigned samples randomly over five sequencing lanes (~six replicates per lane), of which four were sequenced by the South Australian Health and Medical Research Institute Genomics Facility (Illumina HiSeq25000; single-ended), and one by Novogene Hong Kong (Illumina HiSeq4000; paired-ended).

Raw sequences were demultiplexed and trimmed of adaptors and leading/trailing low quality bases (Phred < 20) using TRIMMOMATIC 0.39 within the DDOCENT 2.2.19 pipeline (Puritz et al. 2014). Poorly sequenced individuals (< 700,000 reads) were removed from the dataset. Sequences were mapped to a rainbowfish reference genome (*M. duboulayi*; Beheregaray et al. unpublished data; Supplemental Table A4) using the GATK 3.7 pipeline (Van der Auwera and D O'Connor 2020), fully described in Chapter 2. The SNP variants were called from the mapped reads using BCFTOOLS 1.9 (Li 2011), and filtered using VCFTOOLS 0.1.15 (Danecek et al. 2011) to remove poorly sequenced reads, non-biologically informative artefacts (*sensu* O'Leary et al. (2018)), complex variants, and sites with high likelihood of linkage. For the full filtered dataset, we used BAYESCAN 2.1 (Foll and Gaggiotti 2008) to assess locus-specific conformity to neutral expectations based on allele frequency distributions across populations (with population membership first inferred by preliminary FASTSTRUCTURE 1.0 (Raj et al. 2014) analysis detailed in Chapter 2). We used BAYESCAN default settings and a false discovery rate of < 0.05, producing a putatively neutral dataset of 14,479 SNPs for subsequent analyses of neutral genetic diversity and population structure.

Genomic diversity and inferences of population structure

Locality-specific neutral genomic diversity was assessed using ARLEQUIN 3.5 (Excoffier and Lischer 2010) to determine mean expected heterozygosity (H_e), mean nucleotide diversity (π), and proportion of polymorphic loci (*PP*). Pairwise F_{ST}, site-specific F_{ST}, and global *F*-statistics were calculated in R (RC Team 2019) using HIERFSTAT 0.04-22 (Goudet 2005). The latter were calculated for all individuals ('between-systems'), as well as independently within each ecoregion ('savannah-specific' and 'rainforest-specific). Additionally, we produced a scaled covariance matrix of population allele frequencies (Ω) using BAYPASS 2.2 (Gautier 2015) core model, based on all SNPs rather than the neutral subset, which is implicitly estimated. This hierarchical Bayesian model provides an informative basis for demographic inference by accounting for structure resulting from shared history. The method follows from the BayEnv model proposed by (Coop et al. 2010, Günther and Coop 2013), but with several extensions to improve accuracy by estimation of prior distributions. These were plotted in R

using BAYPASS's included utility functions. We further interrogated population structure using a FASTSTRUCTURE clustering approach, also repeated both between and within ecoregions. Full details of above analyses, including preparation of input files, were further described in Chapter 2.

Characterising environmental variation

To characterise environmental heterogeneity across the study region, we accessed National Environmental Stream Attributes v1.1.3 from the Australian Hydrological Geospatial Fabric (Geoscience Australia 2011; Stein (2011). The same six attributes previously used in rainforest-specific analyses were also used here to enable regional comparisons. However, given that covariation among variables differed depending on region and on spatial scale, we were able to include two additional variables in between-systems analyses, and were required to use one fewer in savannah-specific analyses. For between-systems analyses, we included stream segment aspect (ASPECT), river disturbance index (RDI), mean summer runoff (RUNSUMMERMEAN), mean winter runoff (RUNWINTERMEAN), mean annual rainfall (STRANNRAIN), mean annual temperature (STRANNTEMP), total length of upstream segments calculated for the segment pour-point (STRDENSITY), and stream segment slope (VALLEYSLOPE) (Supplemental Figure A1). Rainforest-specific analyses excluded RUNWINTERMEAN and VALLEYSLOPE, while savannah-specific analyses excluded ASPECT, STRANNRAIN and VALLEYSLOPE. Environmental variables were used as a basis for genotype-environment associations (GEA), phenotype-environment associations (PEA) and genotype-phenotype-environment (GxPxE) associations, as described below.

Geometric morphometric characterisation and analyses

We used TPSDIG2 2.31 (Rohlf, 2017) to position eighteen landmarks on the field-collected digital photographs of *M. s. splendida*. These landmarks (Chapter 2; Supplemental Figure A2) were chosen to maximise homology, repeatability, and putative ecological relevance. In MORPHOJ 1.07a (Klingenberg 2011), digitised TPS files were compiled and subjected to Procrustes superimposition,

screened for outliers representing landmarking errors, and used to produce Procrustes covariance matrices for 'between-systems', 'rainforest-specific' and 'savannah-specific' subsets. To characterise major features of shape variation, PCAs were performed on resulting matrices. Allometric regressions, pooled within populations identified in neutral genetic analyses, were used to determine a positive association between size (log centroid) and shape (Procrustes coordinates). Regression residuals were therefore used to test for relationships between body shape and locality. To for test ecoregional differences in the 'between-systems' dataset, we used a discriminant function analysis classifying by rainforest and savannah origin, with 1000 permutation rounds. Additionally, we used a canonical variate analysis (CVA) to determine variation among sampling sites, scaling for relative within-group variation. We again used 1000 permutations to test significance.

Detecting selection between and within ecoregions

To test for environmental adaptation and divergence both between and within rainforest and savannah ecoregions, we used a combination of GEA, PEA, and GxPxE approaches. In all instances, we used highly adaptable constrained ordinations (partial redundancy analyses; pRDAs) performed in the R package VEGAN 2.5-6 (Oksanen et al. 2019). For GEAs only, we also incorporated a Bayesian hierarchical model (BAYPASS 2.2 (Gautier 2015)), which is tailored to genetic analysis and is well suited to study systems with hierarchical population structure (Gautier 2015).

For the GEAs, we first ran a global RDA using the full dataset (14,478 SNPs) for all individuals as a multivariate response matrix, and the eight 'between-systems' environmental variables described above as an explanatory matrix, which was first centred and scaled. Then, using only the environmental explanatory variables found to be associated in the global model ($p = <0.1$), and again using the full set of SNP genotypes as a response matrix, we repeated the analysis using three partial RDAs to control for putative neutral influences. In each, we included a different neutral (or neutral proxy) covariable matrix: 1) significant principal components (PCs) of scaled population allelic covariance (Ω), 2)

significant PCs of pairwise F_{ST}, and 3) scaled river distances. Further details of input file creation for all datasets can be found in Chapter 2, with the exception of the river distances covariable, for which pairwise distances among connected sites were calculated in ARCMAP 10.3 (ESRI 2011), and distances between unconnected sites (i.e. different drainages) were imputed with distances an order of magnitude higher than the average. Starting from the global RDA, these steps were then repeated for 'savannah-specific' and 'rainforest-specific' analyses, including individuals and covariables specific to the region. Finally, we used the alternative method of BAYPASS 2.2 to produce 'savannah-specific', 'rainforest-specific' and 'between-systems' GEA analyses, using the auxiliary covariate model with default settings and the same sets of scaled environmental explanatory variables as for the pRDAs. Here, we accounted for assumed population demographic structure via the scaled covariance matrix of population allele frequencies (Ω) resulting from the core model.

For the PEAs, we adapted the same pRDA approach, with the same environmental explanatory datasets, to test for signals of selection in the observed morphological variation. Here, the response matrix comprised PCs of individual Procrustes distances determined significant by Broken-Stick modelling, again controlled for putatively neutral genetic structure (allelic covariance Ω; pairwise F_{ST}; river distances), plus the additional covariable of body size (log centroid size). Inputs for the body shape response variable and size covariable were created in $_R$, using functions developed by Claude (2008), and further described in Chapter 2. Although sexual dimorphism may produce an additional confounding effect on body shape variation, we found that equal sex ratios were present between sampling regions (11:14 m:f, Chi-Square p value = 0.987) and we therefore did not include sex as a covariable. As with GEAs, PEA analyses were repeated for 'between-systems', 'rainforest-specific' and 'savannah-specific' datasets.

Genotype-phenotype-environment analysis

We used a GxPxE approach to test whether environmentally associated genetic variation could be attributed to morphological adaptation between and within ecoregions. Using R, we ran a global RDA using significant PCs of individual Procrustes distances as explanatory variables, and putative adaptive alleles (candidates combined from genotype-environment RDAs controlling for Ω and BAYPASS 2.2 auxiliary covariate model, described above) as the multivariate responses. The analysis was then repeated as a partial RDA using individual body size (log centroid) as a covariable. This enabled isolation of only the genotype-phenotype associations best explained by environmental selection, and with the potential to underlie heritable body shape variation.

Results

Sequencing, bioinformatics, genetic diversity and population structure

Filtering of genome-mapped sequencing reads from rainforest and savannah individuals produced a high-quality unlinked dataset of 14,540 SNPs, of which 14,478 could be considered neutral for the purposes of population genomic analyses. The full and neutral datasets for this Chapter comprised 381 individuals for population and landscape genomic analyses across nine sampling sites. We found moderately high neutral genomic diversity across the entire study region (Table 3.2) with expected heterozygosity (H_E) among sites ranging from 0.278 to 0.321 (mean = 0.289), and proportion of polymorphic loci (PP) ranging from 0.252 to 0.395 (mean = 0.349). Site-specific averages were similar between rainforest and savannah systems, with H_E slightly higher in the rainforest (rainforest mean = 0.293; savannah mean = 0.284), and PP slightly higher in the savannah (rainforest mean = 0.329; savannah mean = 0.372). However, ranges of variation for all diversity measures were greater among rainforest sites.

Levels of genetic variation were much higher within the rainforest than the savannah, evidenced by differences in global F_{ST} values (rainforest-specific = 0.148; savannah-specific = 0.025; between-systems = 0.173). Site-specific (Table 3.2) and pairwise F_{ST} values (Figure 3.2a; Supplemental Table B1) indicated that much of this divergence could be attributed to inter-drainage rather than intra-drainage differences. This was also reflected by the stronger correlations in allelic covariance within river drainages, detected by BAYPASS (Figure 3.2b). Overall, this equated a pattern of little population differentiation within the savannah (single drainage) in contrast to comparatively strong subdivisions within the rainforest (five drainages), and between rainforest and savannah. Interestingly, global F_{IS} was slightly higher in the savannah (0.0741) than the rainforest (0.0490), however site-specific values were not significant, with the exception of Kennedy River (Table 3.2).

Table 3.2. Genetic diversity measures for the eastern rainbowfish *Melanotaenia splendida splendida* at nine rainforest and eight savannah localities, based on 14,478 putatively neutral loci (n = sample size for final DNA dataset; H_E = expected heterozygosity; H_O = observed heterozygosity; PP = proportion of polymorphic loci; F_{IS} = site-specific inbreeding coefficient (values with $p = < 0.05$ indicated by *); F_{ST} = site-specific F_{ST}).

Location	Ecoregion	Site Code	Drainage system	n	H_E	H_O	PP	F_{IS}	F_{ST}
Morehead River	Savannah	MO	Normanby	23	0.278	0.262	0.395	0.042	0.108
Hann River	Savannah	HA	Normanby	24	0.279	0.258	0.388	0.042	0.118
North Kennedy River	Savannah	NK	Normanby	15	0.295	0.271	0.36	0.045	0.137
Kennedy River	Savannah	KE	Normanby	21	0.283	0.255	0.374	0.062*	0.142
Laura River	Savannah	LA	Normanby	23	0.281	0.261	0.379	0.019	0.136
East Normanby River	Savannah	EN	Normanby	19	0.286	0.268	0.353	0.034	0.179
West Normanby River	Savannah	WN	Normanby	21	0.287	0.269	0.363	0.042	0.156
Famechon Creek	Savannah	FA	Normanby	25	0.283	0.262	0.367	0.045	0.154
McClean Creek	Rainforest	MC	Hutchinson	25	0.279	0.271	0.252	0.009	0.423
Forest Creek	Rainforest	AN	Daintree	22	0.289	0.268	0.377	0.054	0.122
Doyle Creek	Rainforest	DY	Daintree	24	0.294	0.28	0.358	0.03	0.155
Douglas Creek	Rainforest	DO	Daintree	24	0.289	0.272	0.376	0.038	0.123
Stewart Creek	Rainforest	ST	Daintree	25	0.278	0.259	0.391	0.031	0.127
Saltwater Creek	Rainforest	SA	Saltwater Creek	24	0.321	0.307	0.264	0.019	0.31
Marrs Creek	Rainforest	MA	Mossman	20	0.307	0.293	0.305	0.019	0.233
Cassowary Creek	Rainforest	CA	Mossman	23	0.297	0.295	0.314	-0.011	0.232
Little Mulgrave Creek	Rainforest	LM	Mulgrave	23	0.283	0.271	0.323	0.018	0.257
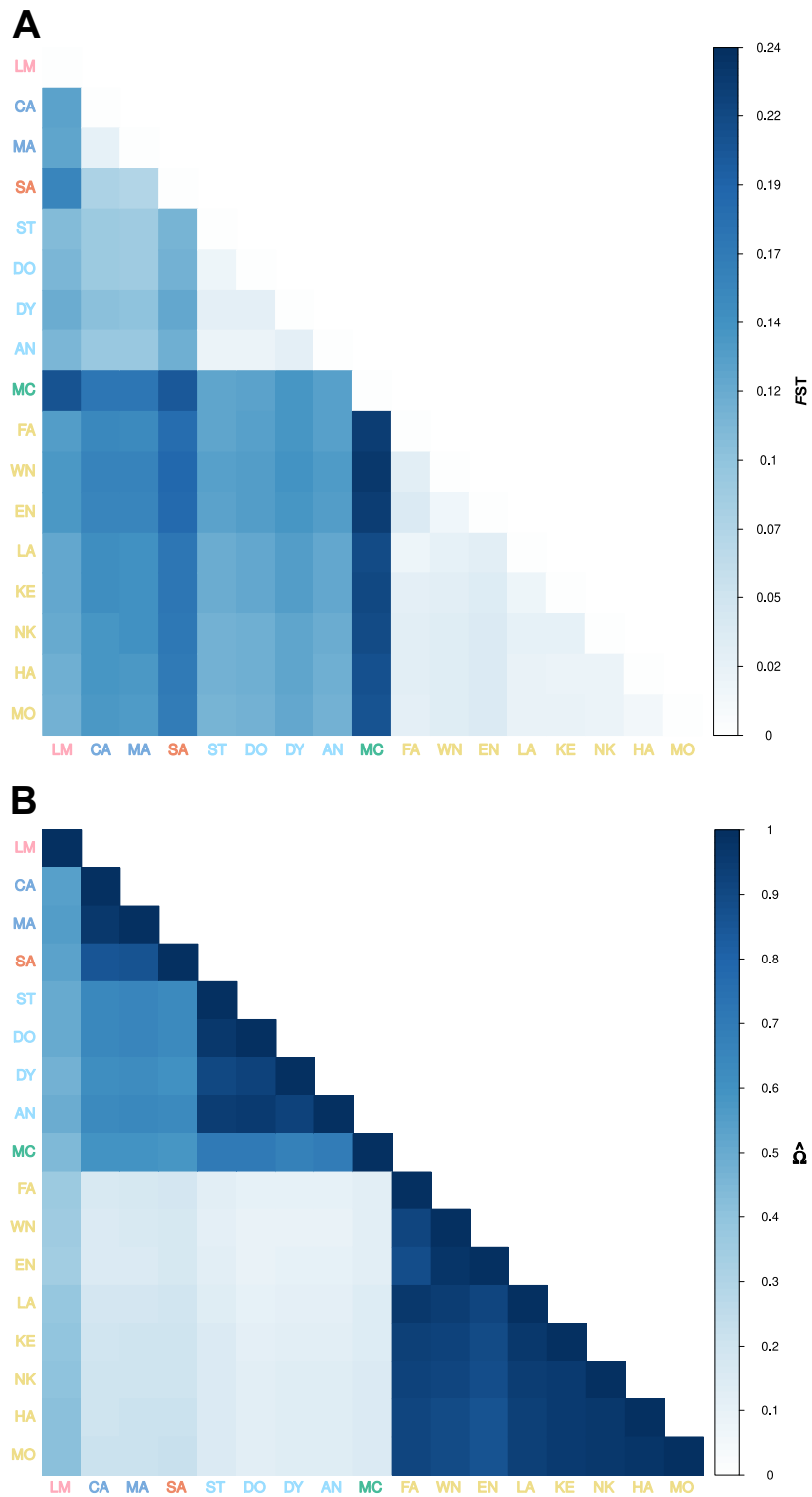
Figure 3.2. Genomic differentiation and population structuring among rainforest and savannah sampling localities for the eastern rainbowfish *Melanotaenia splendida splendida*, represented by **(A)** Heatmap of pairwise F_{ST} based on 14,478 putatively neutral SNPs; **(B)** Correlation map for BAYPASS core model scaled covariance matrix Ω based on allele frequencies of the full dataset of 14,540 SNPs. Locality abbreviations follow Table 3.1, with colouration reflecting drainage of origin as in Figure 3.1.

Clustering analyses also indicated that the main neutral genetic differentiations occurred among river drainages. In between-systems FASTSTRUCTURE analysis (Figure 3.3a), individuals were grouped by drainage with exception of those from Saltwater; these were grouped together with those from the neighbouring Mossman drainage, under a best K of five. However, in ecoregion-specific analyses (Figure 3.3b), rainforest alone was found to have an optimal K of five. Very little admixture was visible between Saltwater and Mossman, indicating hierarchical substructure may have obscured differentiation in the combined-systems analysis. An optimal K of one was found in the savannah-specific analysis of the single Normanby drainage, however Figure 3.3c displays $K = 2$, to demonstrate regional substructure. Overall, despite hierarchical differentiation, contemporary evolutionary processes are likely occurring relatively independently among six drainage-associated subunits, which we will refer to as populations. Locality-based clustering using singular value decompositions of Ω (Supplemental figure B2) also showed strong separation between Saltwater and Mossman, even in combined-systems analysis. Therefore, while delineation of populations may depend on the theoretical or management context at hand, contemporary evolutionary processes are likely occurring relatively independently among six drainage-associated subunits, which we will refer to as populations.
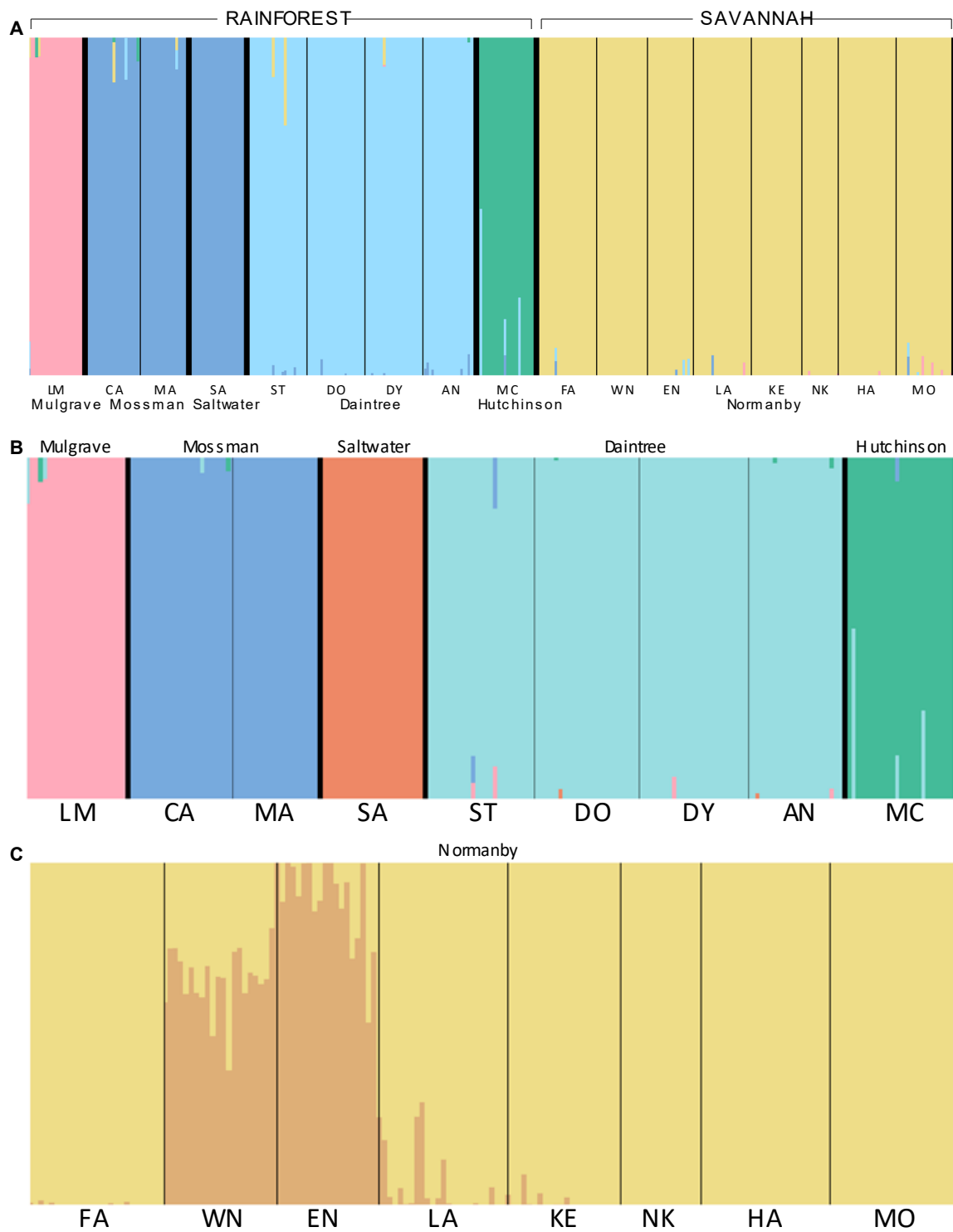
Figure 3.3. Cluster plots based on FASTSTRUCTURE analysis of 14,478 putatively neutral SNPs, where colours represent inferred ancestral populations of individuals based on A) all sampled individuals, showing optimal $K = 5$; B) only rainforest individuals, showing optimal $K = 5$; C) only savannah individuals, showing $K = 2$ to inform about regional substructure within the drainage system (actual inferred optimal $K = 1$). Large type refers to

drainage systems, which are separated by thicker black lines. Small type refers to sampling localities, separated by thinner black lines. Locality abbreviations follow Table 3.1.

Morphological divergence between ecoregions and sampling localities

Principal component analysis of body shape of all *M. s. splendida* individuals produced four significant PCs under broken stick modelling (Supplemental Figure B3). Major aspects of variation included body depth (PC1), dorsal height and head orientation (PC2), length of caudal fork and caudal peduncle (PC3), width and position of fin bases (PCs 3 & 4), and size of eye (PC4). Site-specific CVAs found significant differences in mean body shape among most localities after controlling for size ($p < 0.05$), but with substantial overlap among individuals from different localities (Supplementary Figure B4; Table B). However, strong separation between rainforest and savannah was evident on the first axis. Congruently, discriminant function analysis between rainforest and savannah individuals found that body shape could reliably classify individuals to ecoregion of origin in 96.5% of cases (94.3% in cross-validation; $p = <0.0001$; Supplemental Figure B5; Supplemental Table B3). Rainforest fish were larger on average than savannah fish (mean centroid size 10.20 cm (SD = 2.88 cm) in rainforest versus 6.93 cm (SD = 2.06 cm) in savannah), however they were also dorsoventrally narrower. Even after controlling for allometric differences, body depth was the most notable component of shape divergence between ecoregions (Figure 3.4).
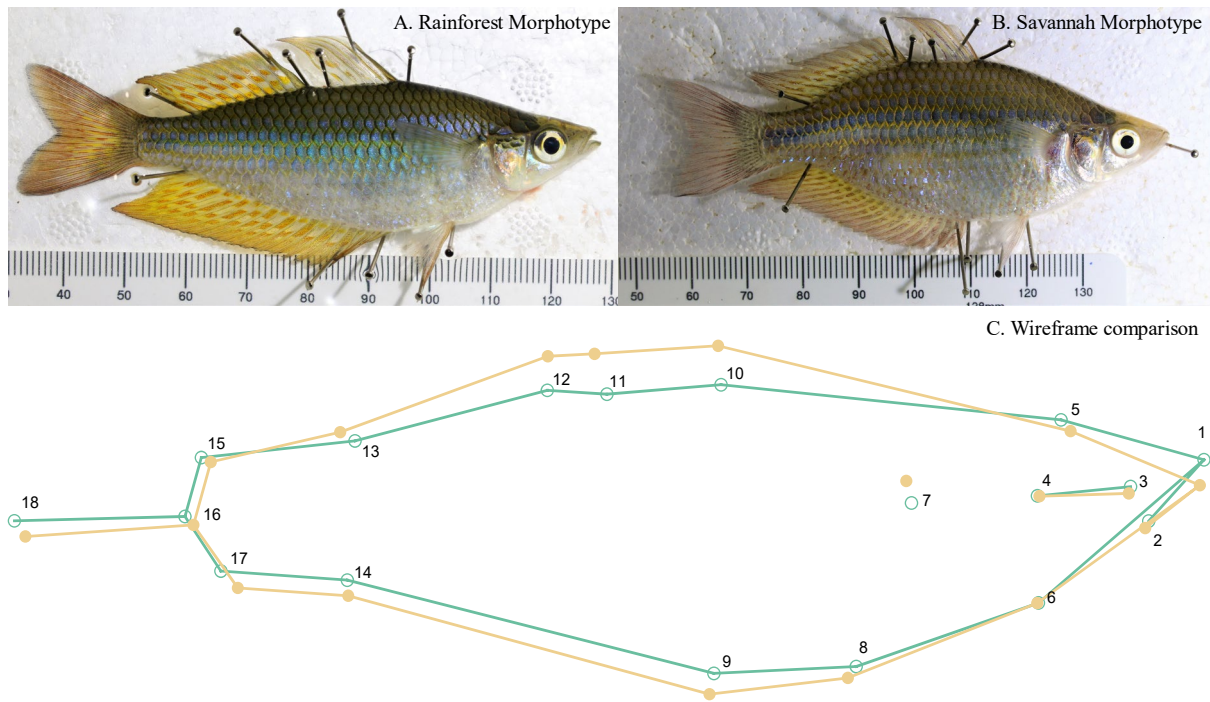
Figure 3.4. Morphological differences between *Melanotaenia splendida splendida* of rainforest and savannah origin. Photographs show examples of similarly sized males collected from rainforest (top left; Saltwater Creek (SA13); centroid size 12.55cm) and savannah (top right; Morehead Creek (MO01); centroid size 12.24 cm) in March, 2017. Wireframe diagram shows group mean shape change between rainforest and savannah individuals, based on discriminant function analysis of size regression residuals (18 landmarks, n = 367). Scale factor = 2. Green = rainforest. Yellow = savannah.

Genomic and morphological associations with environment

The pRDA analyses found strong genomic and morphological associations with environment (Figure 3.5a-f; Supplementary Table B), which consistently explained more of the observed biological variation than neutral or spatial factors (including F_{ST} distance, allelic covariance & river distance; Figure 3.6). On average, environment best explained 3.3 times more genomic variation and 10.5 time more morphological variation than other covariables (Supplemental Table B5). For between-systems analyses, the most important environmental explanatory variables for both genomic and morphological variation were average annual rainfall (STRANNRAIN) and summer mean runoff (RUNSUMMERMEAN). These were also the best explanatory variables identified by the alternative

GEA approach of BAYPASS (auxiliary covariate model; Supplemental Figure B6). In rainforest-specific analyses (described further in Chapter 2), STRANNRAIN and average annual temperature (STRANNTEMP) were the best explanatory variables for both genomic and morphological variation. However, within the savannah, winter mean runoff (RUNWINTERMEAN) and STRANNTEMP best explained genetic variation, in contrast to morphological variation, which was best explained by RUNSUMMERMEAN and stream density (STRDENSITY). Both pRDAs and BAYPASS approaches produced suites of candidate genes for environmental adaptation, totalling 1,284 in between-systems analyses (1,119 pRDA, 233 BAYPASS, 68 shared), 1,004 in rainforest-specific analyses (864 pRDA, 176 BAYPASS, 36 shared), and 987 in savannah-specific analyses (880 pRDA, 145 BAYPASS, 38 shared). Although slightly more candidates were detected by pRDAs in the savannah compared to the rainforest, we found that locus-specific selective signals were weaker, with an average correlation of 0.249 in the savannah compared to 0.371 in the rainforest (Figure 3.7).

Finally, pRDA associations among genotype, phenotype, and environment (Figure 3.5g-i) revealed significant relationships both between and within ecoregions (p = <0.001), even after controlling for size. Between-systems, 7.2% of environment-associated genetic variation could be explained by the first three PCs of body shape variation, revealing 212 SNPs as candidates for climate-adaptive morphological variation. Within the rainforest, 61 candidates were identified in association with the first four body shape PCs, while within the savannah, 72 candidates were identified in association with PCs 1, 2 and 4.
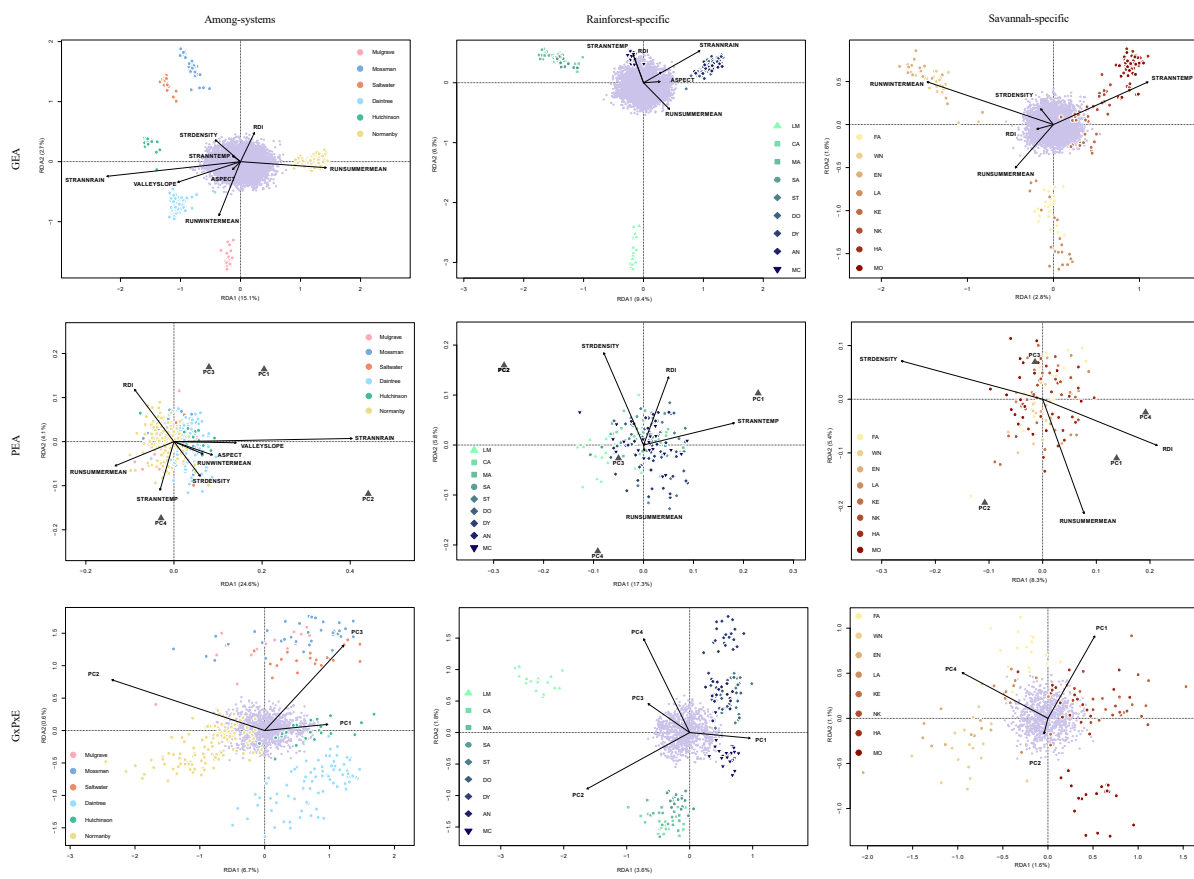
Figure 3.5. Ordination plots summarising the first two axes of partial redundancy analyses (pRDAs) for *Melanotaenia splendida splendida* individuals sampled in tropical north-eastern Australia from 17 sampling localities ('Between-systems'), including nine within the rainforest ('rainforest-specific') and eight within the savannah ('savannah-specific'). Figures a-c represent genotype-environment associations (GEA) controlling for allelic covariance, d-f represent phenotype-environment associations (PEA) controlling for allelic covariance and body size, and g-i represent genotype-phenotype-environement associations (GxPxE) controlling for body size. Large points represent individual-level responses, and are coloured by drainage system of origin in 'Between-systems' plots, and by sampling site in ecoregion-specific plots. Small purple points represent SNP-level responses. Grey triangles represent morphological responses. Vectors represent the magnitude and direction of relationships with explanatory PCs.
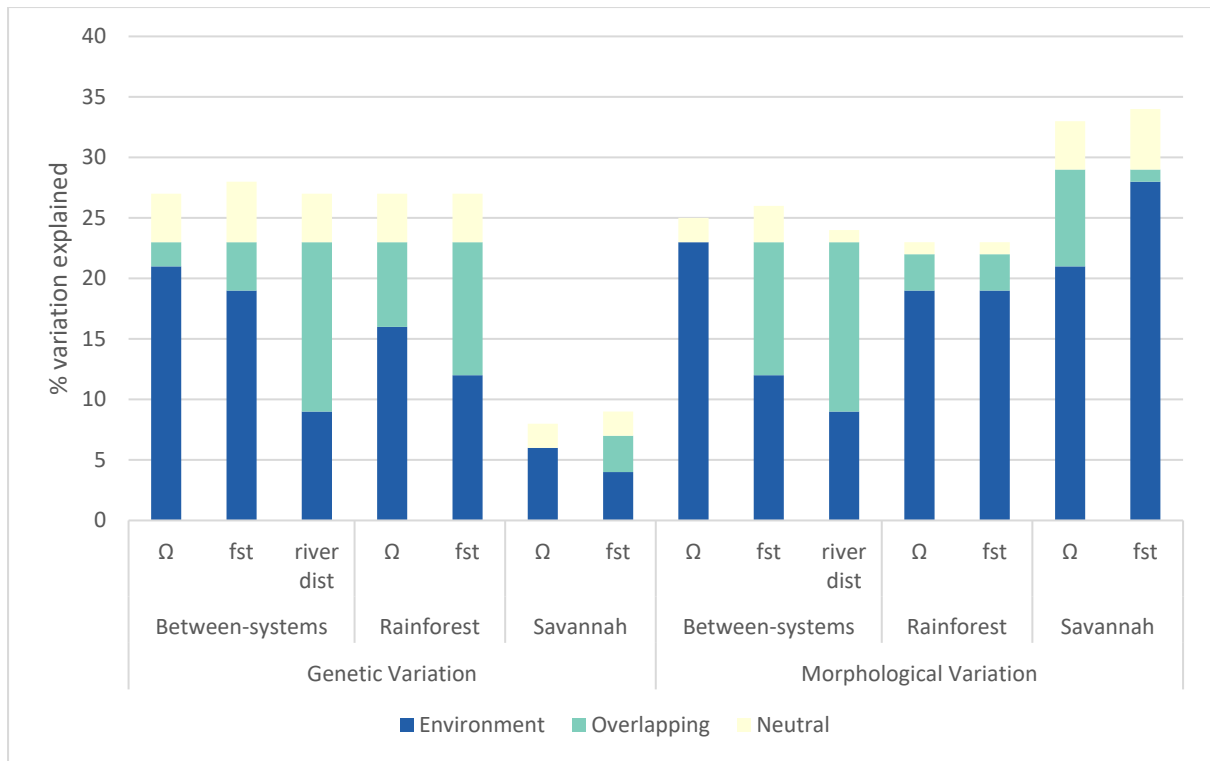
Figure 3.6. Percentage stacked column graph representing variance partitioning of pRDA response variables (genomic variation or morphological variation of *Melanotaenia splendida splendida*) between environmental explanatory variables and neutral covariables (allelic covariance (Ω); F_{ST} distances (*F*ST); river distances (river dist)). Colours correspond to proportion of variation best explained by: environmental variables = "Environment"; by neutral variables = "Neutral"; or by environmental or neutral variables equally = "Overlapping".
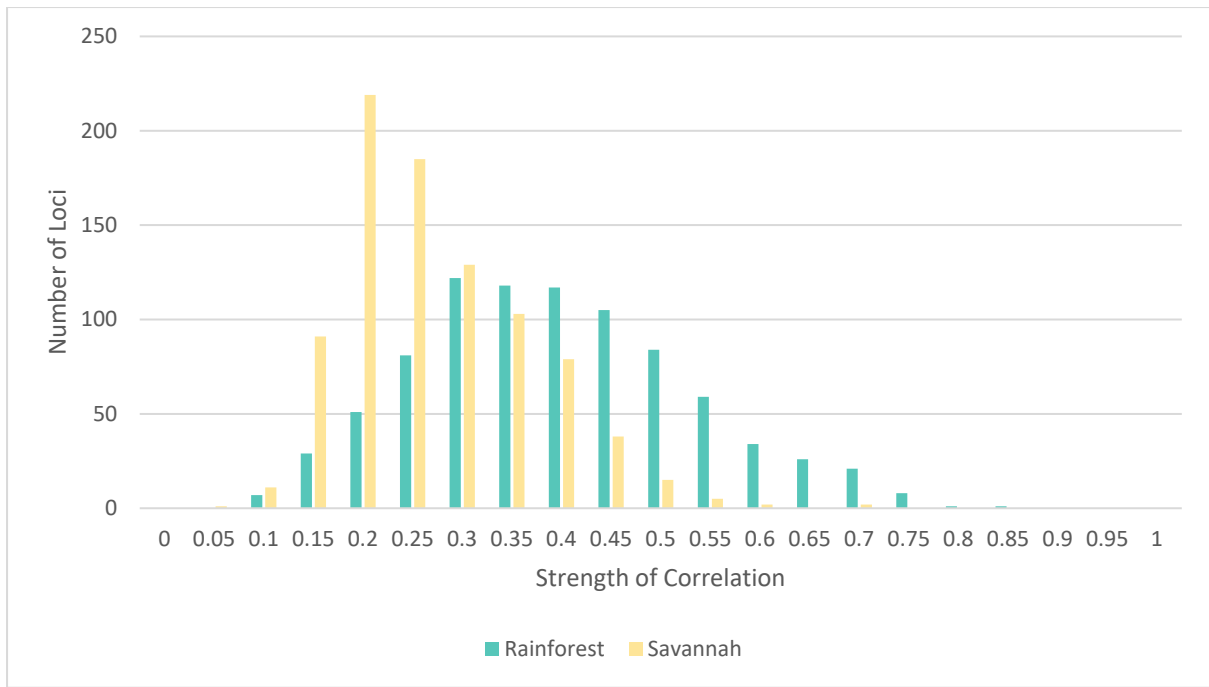
Figure 3.7. Frequency distribution of locus-specific correlations with environment for candidate adaptive SNPs for *Melanotaenia splendida splendida* detected for rainforest (864 SNPs) and savannah (880 SNPs) populations, associated with environment after controlling for putative neutral variation (allelic covariance (Ω)). Data are based on ecoregion-specific pRDAs using a full dataset of 14,540 SNPs.

Discussion

We compared strength and variation of adaptive variation in native rainbowfish ecotypes to understand evolutionary divergence and provide a foundation for further considerations of climatic resilience across contrasting tropical freshwater biomes. Our results support a central role for hydroclimate in driving intraspecies divergence across rainforest and savannah, with terrain connectivity modulating spatial scales of adaptation and resilience. Across systems, we found strong evidence for biome-specific hydroclimatic adaptation, and likely functional relevance of major morphological differences. Within systems, we also found high explanatory power of hydroclimatic variables in shaping local variation. However, regional genomic signals indicated a homogenising effect of gene flow on adaptive variation in the relatively well-connected savannah, fuelling the further hypothesis of compensatory reliance on

phenotypic plasticity. Broadly, this study suggests that differences in habitat variability and complexity can substantially affect evolutionary trajectories of tropical organisms, which we discuss in the context of resilience to a rapidly changing climate.

Environmental and neutral contributions to intraspecies divergence

Despite their proximity, the major biomes of Australia's north-eastern tropics maintain stark bioclimatic differences (Ash 1988). The wet tropical rainforests experience moderate and relatively aseasonal conditions compared to the wet-dry savannah, which is prone to thermal and hydrological extremes (Ash 1988, Bowman et al. 2010). Within the two biomes, climatic gradients are more subtle but still substantial (Supplementary Figure A1). Despite the rainforest's relative stability, a similar amount of environmental variation occurred among the sampled localities, even considering that this sampling covered a narrower geographic range than our sampling region in the savannah (Supplemental Figure A1). Consistent with our first hypothesis, the greatest biological differences among sampled *M. s. splendida* individuals were observed between ecoregions, with both genomic and morphological environmental associations exceeding neutral expectations. Moreover, significant environmental associations were also found within rainforest and savannah, suggesting the relevance of ecological adaptation at both local and regional scales.

Our Chapter 2 results (Gates et al. 2021, under submission) indicated that environmental adaptation may be even more important than neutral factors in explaining patterns of intraspecies diversity within rainforest populations. In this chapter, the results of multiple environmental association analyses supported this finding at a much broader scale. Environmental predictors explained patterns of genomic and morphological variation better than approximations of neutral structure in both rainforest and savannah-specific analyses, as well as those across combined systems. The trend was repeated among pRDAs using a range of neutral covariables, including allelic covariance (Ω), F_{ST}, and river distances. For morphology in particular, the hypothesised adaptive relevance was supported not only by strong

environmental associations, but the extent to which environment exceeded the explanatory power of neutral covariables. Based on average results from all pRDAs, environment best explained approximately ten times more phenotypic variation than did neutral structure, versus only three times more genetic variation. This apparent resistance of phenotypes to neutral influences, especially relative to genomic patterns, is consistent with the hypothesis that body shape has been more constrained by functional requirements than has genomic variation. Finally, the large proportion of variation not explained by any of the included explanatory variables is common to the approach, and may reflect inter-individual variation within sampling localities, in addition to stochastic influences not encompassed by the demographic model.

While we considered that stronger genomic associations with neutral patterns could have been biased by use of the same ddRAD dataset for estimation of both neutral and overall genomic variation, analyses using the independent neutral proxy of river distance produced the same trend, suggesting a genuine difference in relative influences. This result may reflect the fact that, even under divergent selective environments, we generally assume a substantial proportion of genomic loci will vary neutrally, 'nearly-neutrally', or at least with limited detectable influence on physiology and fitness (Ohta 2002, Luikart et al. 2018). The same assumption may not apply to more integrative components of physiology (Ho et al. 2017, Zhang 2018). For instance, it has been hypothesised that the relative prevalence of adaptive changes may depend on hierarchy of biological organisation, with complex organismal traits such as body shape necessarily interacting not just with the surrounding environment, but with lower level components such as cells, tissues and organs (Zhang 2018). Strong selection may therefore be acting to inhibit the effect of drift on morphological adaptation in rainbowfishes which, given the significant GxPxE associations, we propose to be at least partially heritable. In addition, phenotypic plasticity may be responding to environment to further enhance associated variation (e.g. Kelly (2019)).

Many factors are necessary to explain patterns of tropical diversity, not limited to local and regional climates, geographies, biotic interactions, and historical events (Moritz and McDonald 2005, Ricklefs 2005). However, the role of ecological divergence is becoming increasingly recognised (Moritz et al. 2000, Beheregaray et al. 2015). When considering the local and regional environmental divergence observed for *M. s. splendida* alongside broader climatic determinants of tropical transition zones (e.g. Hirota et al. (2011), Oliveras and Malhi (2016), Wu et al. (2016)), we can expect that climate change will have significant repercussions for distributions of tropical diversity. Further, where a large proportion of variation has probably evolved in response to local selection as found here, a large evolutionary turnover may similarly be required to maintain fitness under changing conditions (Fitzpatrick and Keller 2015, Bay et al. 2017).

Putative selective influences and outcomes

Although relatively few studies of natural selection in wild populations have occurred in tropical landscapes (Siepielski et al. 2017), recent publications have highlighted hydrological, thermal, and vegetation gradients as primary selective influences in terrestrial fauna (Ntie et al. 2017, Zhen et al. 2017, Miller et al. 2020, Morgan et al. 2020, Bennett et al. 2021b). Here, and perhaps unsurprisingly for an aquatic obligate (e.g. Cooke et al. (2012a);Cooke et al. (2012b); Cooke et al. (2014)), we found that species-wide adaptive signals were most strongly associated with hydrological variables. For all between-systems environmental association analyses, including pRDA and BAYPASS approaches, the best environmental explanatory variable for both genomic and morphological variation was average annual rainfall, followed in most analyses by summer mean runoff. These variables corresponded closely to the first axes of the pRDA plots, as did the divergences between rainforest and savannah individuals' genetic and morphological variation.

While hydroclimatic variation was similarly important in within-systems association analyses, annual variables (average annual rainfall; average annual temperature) better explained variation among

rainforest sites, while seasonal variables (winter mean runoff; summer mean runoff) were more important among savannah sites. In contrast to the relatively aseasonal conditions of the rainforest sampling sites, this finding may reflect the importance of monsoonal fluctuations to the composition and phenological characteristics of savannah localities (Ma et al. 2013). This is consistent with results of a meta-analysis of climate-predicted selection (Siepielski et al. 2017), which found that precipitation-related variation was one of the most important explanations for global patterns of selection. Moreover, considering that results can sometimes differ among environmental association methods (Forester et al. 2018), the consistency among both RDA and BAYPASS analyses provide support for the reliability of these associations.

The most notable body shape differences between rainforest and savannah individuals were relative depths of body and caudal peduncle. Despite being larger, rainforest fish were comparatively streamlined, with dorsoventral flattening and narrower peduncles. Savannah fish were stouter, with pronounced dorsal humps. Aside from possible sex-specific and allometric influences accounted for in the study design, depth of body and peduncle depth have established relevance to swimming biomechanics in teleost fishes (Gatz 1979). In general, more slender, fusiform shapes in fishes are associated with swimming speed over longer distances (steady locomotion), as well as habitation of higher velocity environments (Gatz 1979, Leavy and Bonner 2009, Langerhans and Reznick 2010). Conversely, deep and compressiform shapes have been associated with manoeuvrability and burst swimming (unsteady locomotion), lower water velocities (Gatz 1979, Leavy and Bonner 2009, Langerhans and Reznick 2010), and in several instances, with greater temporal variability of flows (Scarnecchia 1988, Alexandre et al. 2014, Kern and Langerhans 2018, Pease et al. 2018).

Consistent with hydrological associations in PEAs, the nature of these shape changes suggest that greater interseasonal and interannual flow variability in the savannah could have contributed to selection for deeper bodies, which may provide biomechanical advantages to unsteady locomotion for

foraging and predator evasion (Langerhans et al. 2004, Langerhans 2008), especially during relatively stagnant winter periods. Meanwhile, fusiform body shapes in rainforest fish could help reduce drag and increase thrust propulsion during sustained swimming (Langerhans 2008), a likely advantage in year-round high flows. There has, however, been conflicting evidence for body depth adaptation in congeneric rainbowfishes (McGuigan et al. 2003, Lostrom et al. 2015, Kelley et al. 2017). Although associations have been found among habitat and body depth, trends have been inconsistent among species, sexes, and developmental conditions (McGuigan et al. 2003, Kelley et al. 2017). Therefore, while we expect that the major morphological divergences between rainforest and savannah *M. s. splendida* are accommodating hydrological adaptations, the precise mechanisms at this stage remain putative.

Adaptive dynamics under contrasting terrain structure

In addition to differences in climatic variability across Australia's north-eastern tropical biomes, the rainforest and savannah regions are delineated by contrasting geomorphology, providing the opportunity to assess the effects of connectivity structure on patterns of neutral and adaptive divergence. As reported in Chapter 2, *M. s. splendida* from the five sampled rainforest drainages corresponded to five distinct populations, with some milder intra-drainage structure typical of moderately dispersing fishes (*sensu* Brauer et al. (2018)). While drainage networks in this region may have maintained similar terrain structure for tens of millions of years (Nott 2005), connectivity among the sampled drainages is thought to be more recent, for example via coastal floodplain exposure during glacial periods (Pusey and Kennard 1996, Cook and Hughes 2010). This is likely reflected by the only moderate pairwise F_{ST} values among drainages. However, despite closer clustering among neighbouring systems, there was minimal evidence of recent admixture, as may be expected if substantial gene flow was occurring during cyclonic rainfall events (e.g. Pearson (2005)) or via human translocations. In contrast, all individuals from savannah localities could be attributed to a single population, consistent with expectations of comparatively high gene flow due to river connectivity across the lowland terrain. As in the rainforest,

some intra-drainage substructure was detected, which could result from low winter flows, IBD across the large drainage area, and representation of multiple headwaters.

The connectivity differences between rainforest and savannah regions are likely to have wide-ranging impacts on freshwater inhabitants. In fishes, drainage connectivity is already well established as an influence on species distributions, taxonomic richness, and genetic diversity (Pusey and Kennard 1996, Unmack 2001, Wong et al. 2004, Carvajal-Quintero et al. 2019). Moreover, gene flow across heterogeneous landscapes can have significant effects on adaptive evolution (Garant et al. 2007, Nosil 2012, Tigano and Friesen 2016). Here, we found that signals of locally adaptive genetic divergence were weaker in the savannah for both ecoregion-specific and combined-systems GEAs, despite equivalent magnitudes of regional environmental variation captured by our sampling coverage. This was indicated by the savannah-specific pRDA models' lower overall variance, weaker local clustering of individual adaptive variation, and weaker locus-specific environmental associations than in rainforest-specific analyses. Although the latter effect might alternatively be attributed to selection across a greater number of loci of smaller effect size (e.g., Pritchard and Di Rienzo (2010)), we also found that the combined magnitude of candidate associations remained lower. Moreover, the alternate GEA method of BAYPASS, dependent on Bayesian likelihoods rather than model loadings used in RDAs, detected fewer candidates for local adaptation within savannah. Finally, GxPxE pRDAs similarly explained less variance and displayed weaker local clustering within savannah than within rainforest.

Together, these results support our hypothesis that the greater drainage connectivity in the savannah has promoted homogenisation of adaptive variation, contributing to a pattern of more region-wide, rather than locally specific genomic adaptation. In contrast, natural fragmentation in the rainforest system appears to have permitted relatively independent adaptation of demes in response to local selective pressures. These results are in accordance with what is perhaps a widely held expectation of gene flow's

influence on local adaptation, as theorised by Haldane (1930), Fisher (1950), Slatkin (1987), and others, by which divergence at individual localities is dampened by inflow of genetic variation from neighbouring sites. However, homogenisation is only one of gene flow's several possible effects, which antithetically include facilitation of local adaptation (Tigano and Friesen 2016, Nosil et al. 2019). This can occur through the spread of novel beneficial mutations, and the build-up of standing diversity across landscapes (Haldane 1948, Hendry and Taylor 2004, Nosil et al. 2019). That homogenisation appears to be the dominant effect may indicate that gene flow in the savannah is too high for local selection to completely counteract swamping of adaptive alleles (*sensu* Storfer and Sih (1998)). Alternatively, it is possible that the likely large populations of *M. s. splendida* present in both regions (Pusey et al. 2004) have helped to maintain sufficient standing diversity for efficient adaptation without external input (*sensu* Jensen and Bachtrog (2011)), even among isolated rainforest drainages.

These differences in adaptive dynamics are likely to affect evolutionary trajectories under changing climates, although the nature will be dependent on both spatial and temporal turnover of conditions. For instance, Nosil et al. (2019) has suggested that in well-connected systems such as the savannah, local shifts are likely to be inhibited unless the system as a whole is driven to a selective 'tipping point'. At this point however, gene flow can act to facilitate rapid and widespread adaptive change. Meanwhile, poorly connected systems may produce steadier evolutionary responses to locally-specific selective pressures, with the constraint that new adaptive variation must arise locally and independently within each deme (Tigano and Friesen 2016, Nosil et al. 2019). The later may become particularly problematic under rapid and unprecedented change (e.g. Brauer and Beheregaray (2020)). In the context of these expectations, we propose that trade-offs exist between local specialisation and system-wide resilience between rainforest and savannah populations. Considering the strong evidence for climatic divergence within *M. s. splendia* and a growing number of other tropical species (Ntie et al. 2017, Zhen et al. 2017, Miller et al. 2020, Morgan et al. 2020, Bennett et al. 2021b), such trade-offs are likely to be particularly pertinent to long term persistence.

A possible role for plasticity

Despite evidence for homogenisation of genomic patterns in the savannah, it was intriguing to find that morphological associations with environment were no weaker in this high gene flow system than in the poorly connected rainforest. Rather, PEA models were consistently stronger, suggestive of locally adaptive body shape variation. Although unexpected, this result was not necessarily incongruous with homogenising gene flow, with phenotypic plasticity being a particularly favourable explanation. While the GxPxE associations in this study suggested heritability of at least some body shape variation across both ecoregions, the weaker associations in the savannah support a relative decoupling of genotype and morphology, as could be expected under plastic divergence (Schmid and Guillaume 2017). Moreover, previous common garden experiments with congeneric rainbowfishes found that morphological plasticity could similarly explain a subset of overall shape variation (McGuigan et al. 2003, McGuigan et al. 2005, Kelley et al. 2017). For instance, divergence in *M. australis* was inducible by flow manipulation during development (Kelley et al. 2017), which is particularly relevant given associations in this study with flow-related variables.

Without further experimental work, it cannot be assumed that plastic capacity differs between ecoregions, and alternative factors (e.g., covariance relationships between genotypic and environmental influences (Conover and Schultz 1995)) could account for the observed discrepancies. However, it is notable that theoretical models do predict selection for increased phenotypic plasticity in systems with both high gene flow and environmentally heterogeneous environments (Sultan and Spencer 2002, Crispo 2008). Under such a scenario, the savannah's high connectivity could have promoted system-wide adaptation of greater plasticity to compensate for a relative shortage of locally specialised genetic variation. Analogously, it has been argued that if populations expressing divergent locally adaptive phenotypes become isolated, then these plastic traits may become genetically assimilated via selection for developmental efficiency (Pigliucci et al. 2006, Fitzpatrick 2012). This latter scenario is plausible for populations in the naturally fragmented rainforest, and could have contributed to the stronger associations between genotype, phenotype, and environment in rainforest localities. Finally, it's

possible that selection on plastic capacity could result from not only spatial, but also temporal dynamics. For instance, greater plasticity could provide wider margins of tolerance to accommodate fluctuating environmental conditions (Hendry 2015), as expected under the climatic variability hypothesis (Janzen 1967). In the absence of clear inferences, these results provide seeds for future hypothesis testing, which may be applicable not only to body shape but to other physiological adaptations across rainforest and savannah ecosystems.

Conclusion

The tropical rainforest and savannah ecosystems of north-eastern Australia are marked by conditions of ecological stability and habitat complexity in the former, and of temporal variability and terrain connectivity in the latter. Accordingly, we found that rainforest and savannah fish diverged not only in their responses to regional hydroclimatic variation, but in the extent of locally specific adaptation within biomes. While the natural structure of rainforest landscapes appears to support diversification and specialisation of inhabitants, these same characteristics may require large adaptive turnover and promote spatially disparate responses under rapid environmental change. Meanwhile, savannah fish appear to face homogenisation of genomic adaptation in a highly connected landscape, but display remarkable flexibility in their physiological responses to environment. These differences genomic and phenotypic relationships with environmental and neutral patterns highlight the benefits of integrating multiple biological datasets in studies of selection. Such findings are not only important from a theoretical perspective, but may become critical for appropriate management in the context of anthropogenic habitat alteration.

Chapter 4: Comparative transcriptomics and resilience to future climates of rainforest and savannah rainbowfish

Abstract

Thermal response capacity will be a key factor determining persistence under global warming, and may be affected not only by static traits, but by the plasticity of regulatory mechanisms. Transcriptional plasticity may be an important mechanism for survival under warming stress, however little is so far known about local adaptation of plastic resilience. Here, we investigate bioregional intraspecies variation in the tropical rainbowfish *Melanotaenia splendida splendida*, hypothesising a positive relationship between upper thermal tolerance and gene expression plasticity in different climatic ecotypes. We used common-garden experiments to compare short-term responses to climate warming among rainforest and savannah ecotypes, as well as in relation to previously studied temperate, desert, and subtropical rainbowfish ecotypes. We assessed rapid acclimation capacity within and between ecotypes via tests of critical thermal maxima. We then compared plastic transcriptional responses to projected 2070 summer temperatures using differential gene expression analysis. We identified 189 differentially expressed (DE) genes as candidates for response to future thermal conditions, including eight hub genes related to heat shock and lipid metabolism central to induced expression networks. We found both the greatest thermal tolerance and transcriptional flexibility (139 DE genes) in the savannah ecotype, which may assist in plastic responses to the hot and variable conditions of its native environment. However, despite high thermal tolerance, plasticity of the rainforest ecotype was limited to 88 DE genes, which may be reflective of greater specialisation of thermal responses. When compared with the three higher latitude rainbowfishes, we found a strong positive relationship between induced transcriptional responses and upper thermal tolerance, both of which were greater in warm-adapted species. These findings support our hypothesis that transcriptional plasticity to future climates varies biogeographically and might facilitate thermal resilience in Australian rainbowfishes, with implications for patterns of population persistence under climate change.

Introduction

As climate change exposes organisms to thermal conditions outside their expected ranges, impacts will depend not only on the magnitudes of warming, but on populations' existing physiological traits, the plasticity of those traits, and the capacity for evolutionary adaptation to new norms (Stillman 2003, Hoffmann and Sgro 2011, Catullo et al. 2015). These factors are likely to be influenced by the environment in which an organism evolved, leading to the hypothesis that resilience will vary among geographic bioregions (Thomas et al. 2004, Tewksbury et al. 2008, Sunday et al. 2012). In this context, an obvious research priority is characterising spatial patterns in thermal limits, as well as the evolutionary mechanisms governing divergent responses (Pörtner et al. 2006, Bennett et al. 2021a). Organisms that evolved in stable climates may develop specialised thermal physiologies, yet their breadth and flexibility of tolerance are more often limited than those which adapted under variable conditions (Janzen 1967, Payne and Smith 2017, Bennett et al. 2021a). This raises concern for tropical species, which are not only reported as living closer to their critical thermal maxima (CT_{MAX}), but may have less acclimation capacity, and opportunity for behavioural avoidance, than those of higher latitudes (Ghalambor et al. 2006, Deutsch et al. 2008, Tewksbury et al. 2008, Huey et al. 2009). There is likely to be additional variation in climatic adaptation among regional tropical bioclimates, for example between rainforest and savanna; however, we have not yet developed a strong understanding of mechanisms for thermal resilience at this scale (Moritz et al. 2012, Polato et al. 2018).

Thermal adaptation is challenging to study because of the pervasiveness of temperature in biological functioning (Angilletta Jr 2009). In ectotherms, body temperature affects almost all major components of physiology and behaviour (Angilletta et al. 2002, Hochachka and Somero 2002, Huey et al. 2009). Moreover, thermal tolerance itself may be influenced by a range of extraneous environmental factors (Beitinger 1990, Pörtner et al. 2017). Climate change is also expected to increase both the averages and the variability of environmental temperatures (IPCC 2014), each of which may select for slightly different thermal response traits (Gilchrist 1995, Angilletta Jr 2009). A potentially important mechanism for warming responses is phenotypic plasticity, that is, the ability of a single genotype to

produce multiple phenotypes as a function of environmental exposure (Scheiner 1993, Pigliucci 2001, Kelly et al. 2011, Sultan 2021). Plasticity may broaden individuals' thermal performance capacities, not only buffering against short term stress response, but potentially facilitating long-term adaptation to novel conditions (Pfennig et al. 2010, Wund 2012, Logan and Cox 2020, Bailey et al. 2021, Levis and Pfennig 2021). Plasticity may effectively 'buy time' until genomic adaptation can take place (Diamond and Martin 2021), or contribute to evolutionary feedback loops which accelerate adaptive evolution (Fusco and Minelli 2010, Bailey et al. 2021). Plastic traits might be particularly important for climate adaptation in dispersal-restricted taxa (e.g., freshwater obligates), which have limited ability to translocate, and receive little inflow of novel genetic variation (Muñoz et al. 2016, Brauer et al. 2017).

Plasticity itself is a trait which may evolve in response to selection, being in many cases heritable (McCairns and Bernatchez 2012, McCairns et al. 2016, Goldstein and Ehrenreich 2021), and varying among taxa and environmental conditions as to the extent of fitness costs or benefits (DeWitt et al. 1998, Snell-Rood and Ehlman 2021). Like patterns of genetic variation, these factors permit the possibility of geographic variation in adaptive plasticity (Richards et al. 2006, Crispo 2008). Selection for plasticity predicted in a range of scenarios, but especially where individuals are likely to be exposed to variable environmental extremes, whether across time or space (Van Kleunen and Fischer 2001, Baythavong 2011, Snell-Rood and Ehlman 2021). Although high plasticity can sometimes inhibit genetic adaptation (Oostra et al. 2018, Fox et al. 2019), plasticity has also frequently been reported as co-gradient to directional selection, potentially providing additive or facultative effects (Robinson and Wilson 1996, Gilchrist and Huey 2004, Gonzalo-Turpin and Hazard 2009, Jasienski 2009). Fitness costs of phenotypic plasticity have been reported relatively rarely, however formerly plastic traits may be lost via the process of genetic assimilation. This is hypothesised to be likely in stable environments where specialisation is favoured over generalist traits (Kelly et al. 2017, Kelly 2019, Scheiner and Levis 2021).

One of the most important mechanisms for plasticity is gene expression modification, which can facilitate acclimation to a range of ambient conditions (Schlichting and Smith 2002, López-Maury et al. 2008, Logan and Cox 2020, Rivera et al. 2021). Occurring primarily at the level of transcription, this may occur via quantitative changes in gene expression levels, or through processes such as alternative splicing (Marden 2008, De Wit et al. 2012, Nonaka et al. 2015). Studies of gene expression can inform about the precise biochemical pathways being regulated during responses to environmental stimulus, as well as identifying possible targets of selection under long-term change (Alvarez et al. 2015, Gerken et al. 2015, Logan and Cox 2020). This is important for traits like thermal response, where regulatory processes may be obscure, and adaptive phenotypes unapparent in advance of an environmental transition (Schlichting 2008). Comparisons of gene expression patterns among populations or across environmental gradients can also provide insight about local reaction norms, which alongside physiological indicators such as tolerance, may help to elucidate patterns of adaptive plasticity (McCairns and Bernatchez 2010, Whitehead 2012, Rivera et al. 2021).

High-throughput transcriptome profiling using RNA sequencing (RNA-seq) allows both discovery and quantification of mRNA transcripts within a cell at the time of sampling, allowing comparison among individuals and environmental treatments (Wang et al. 2009, Alvarez et al. 2015, Conesa et al. 2016). Expression plasticity can therefore be assessed by comparing the magnitudes of expression differences, as well as the numbers and identities of responsive genes (McCairns and Bernatchez 2010, Alvarez et al. 2015). Transcriptional flexibility may be an important determinant of physiological stress resilience (Ghalambor et al. 2015, Bay et al. 2017, Kelly 2019), and positive correlations between thermal tolerance and expression plasticity have been described for teleost fishes (Garvin et al. 2015, Narum and Campbell 2015, Wellband and Heath 2017, Sandoval-Castillo et al. 2020, Komoroske et al. 2021). In Australian rainbowfishes (*Melanotaenia* spp.; Sandoval-Castillo et al. (2020)), these responses also diverged across climatic bioregions, with a greater number of thermally responsive genes and higher thermal tolerances demonstrated in warmer, lower-latitude ecotypes. Despite these strong trends, it may be context-dependent as to whether a superior regulatory response will be characterised by plasticity of

a larger number of specialised genes, or by a streamlined response requiring fewer regulatory changes (Logan and Cox 2020). Moreover, geographic studies of gene expression plasticity are so far uncommon (Logan and Buckley 2015, King et al. 2018), making it difficult to extrapolate inferences to other species and bioregions. This makes predictions even more difficult for tropical organisms, where warmer temperatures may demand greater thermal response capacities, but stable conditions may promote greater specialisation or assimilation of those responses (Gilchrist 1995, Tewksbury et al. 2008, Kelly 2019).

In this chapter, we return to a comparative approach between rainforest and savannah populations of the tropical-endemic eastern rainbowfish (*Melanotaenia splendida splendida*), investigating physiological resilience and molecular responses to climate warming. Chapter 3 provided genetic and morphological evidence for distinct hydroclimatic adaptation among individuals from neighbouring rainforest and savannah biomes, which we therefore suggest may be referred to as climatic 'ecotypes', *sensu* Engelhard et al. (2010). Among their native bioregions, the savannah ecotype experiences both greater average temperatures and greater temporal variation in thermal extremes, in contrast to milder and more stable rainforest conditions (Supplemental Figure 1). Given the apparent importance of climatic adaptation on other aspects of rainbowfish biology, we expect that ecotype-specific patterns may also exist for thermal plasticity and upper thermal tolerance.

We use an integrated experimental approach, specifically comparing CT_{MAX} and global gene expression profiles in response to temperatures projected for summer 2070 in a high emissions scenario. For simplicity, and for consistency with previous rainbowfish work, this addresses only what may be referred to as 'activational plasticity': expression changes which may be induced, and often reversed, in response to environmental fluctuations within an individual's lifetime (Novoplansky 2002, Snell-Rood and Ehlman 2021). We ask whether thermal tolerance differs among climatic regions, and if so, whether it covaries with plasticity of transcriptional responses. Based on previous rainbowfish findings,

we expect to find greater thermal resilience, and a greater number of thermally responsive genes, in the warmer-adapted savannah ecotype. Meanwhile, due to milder temperatures and lower variability of rainforest conditions, we expect a less flexible response consistent with genetic assimilation in the rainforest ecotype. Further to these objectives, we build upon previous work in Australian rainbowfishes by contrasting thermal tolerance and plastic capacity with that of subtropical, desert, and temperate congeners, interrogating broader biogeographic patterns of response to future climates. We hypothesise that transcriptional plasticity may be facilitating thermal resilience and will therefore be reflected by a positive relationship between upper thermal limits and the number of genes differentially expressed under warming.

Methods

Sample collection

During March 2017, wild eastern rainbowfish (*M. s. splendida*) individuals were sampled from a rainforest site, Cassowary Creek; and a savannah site, Laura River; located respectively in the Normanby and Mossman River catchments in Cape York Peninsula in north-eastern Australia (Figure 4.1; Supplementary Table A1). Fish from these localities are considered as separate populations based on SNP-based population genomic evidence in Chapter 3. Live fish were captured by seine netting and transported by road in closed containers fitted with battery-running air pumps, before transferral to the Flinders University Animal House Facility in Adelaide by air freight. There, they were acclimatised at 21°C for at least 60 days prior to warming experiments. This was done in aquaria (~20 fish/ 100L) while exposed to 12 h light/12 h dark. They were fed once per day with a combination of blood worms and fish pellets.
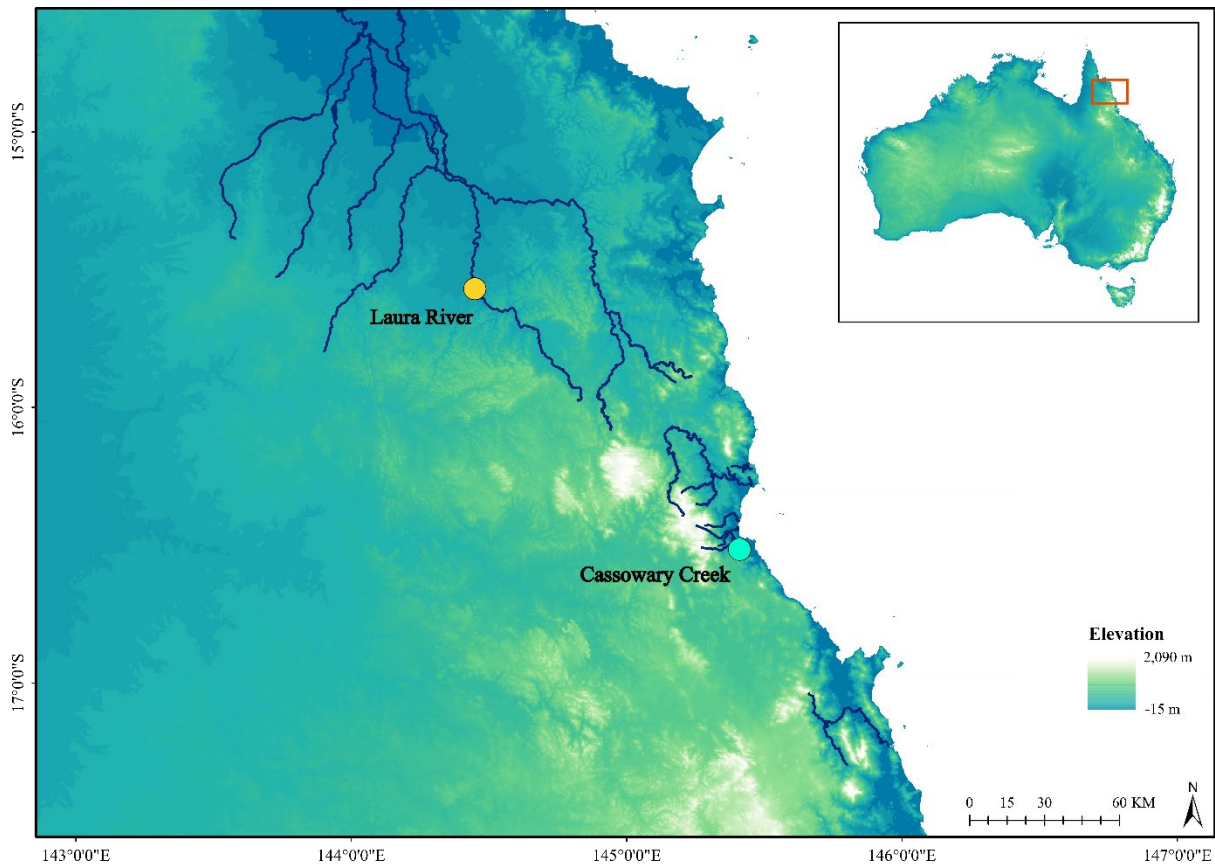
Figure 4.1. Sampling locations of rainforest (Cassowary Creek, Mossman drainage; green icon) and savannah (Laura River, Normanby drainage; yellow icon) *Melanotaenia splendida splendida* collected in March 2017 in north-eastern Australia. Navy lines highlight the creeks and major river channels sampled in throughout this thesis. Inset: extent indicator of main map relative to the Australian continent.

Characterising critical thermal maxima

We determined the upper thermal limits for organised locomotory activity (CT_{MAX}) for each ecotype, based on methods described by Becker and Genoway (1979) that were used in previous rainbowfish studies (McCairns et al. 2016, Sandoval-Castillo et al. 2020). We used ten similarly sized adult females from each of the 21°C acclimated rainforest and savannah populations. Fish were placed individually in a 5 L glass beaker containing 3.5 L of aquarium water, which was partially submerged in a digital water bath SWBD (Stuart®). The water bath was used to increase the temperature in the beaker by approximately 1°C every three minutes (0.33°C/min) until CT_{MAX} was reached (Becker and Genoway 1979). CT_{MAX} was determined by a 'loss of righting response', in which fish were unable to maintain

normal dorsal-ventral orientation for at least one minute, as described by Monirian et al. (2010). This endpoint was chosen because it represents a scenario in which the animal is no longer able to maintain essential functions nor a means of escape (Becker and Genoway 1979, Monirian et al. 2010). Once a loss of righting response was reached, the time and temperature were recorded, and fish were placed in a recovery tank of aerated, acclimation-temperature water. Fish were monitored in the 24 hours following the experiment for behavioural abnormalities or death. The CT_{MAX} for a given ecotype was obtained by taking an average of the 10 independent replicates. We tested significance of differences between ecotypes using two-sample *t*-Tests assuming equal variances.

Temperature trial for projected future climates

To assess short-term responses to contemporary (21°C) and 2070-projected (33°C) average summer temperatures, individuals of each ecotype (similarly sized adult males) were randomly assigned to a treatment or a control group (n = 6 per group, per ecotype). The treatment temperature (33°C) reflects a projected average summer temperature for eastern Australia in 2070 in a high emission scenario (RCP8.5) estimated by the International Panel on Climate Change, to be directly comparable with that used in previous warming experiments using Australian rainbowfishes (Smith et al. 2013, Sandoval-Castillo et al. 2020). Temperatures in climate change treatment tanks were increased by 2°C per day over a six-day period, towards the 33°C target, and were subsequently maintained for 14 days. Control groups were maintained at 21°C throughout the experiment. Then, between 9:00 am and 11:00 am, fish from both treatment and control groups were euthanised using an overdose of anaesthetic sedative (AQUI-S®: 175mg/L, 20 minutes) following the Australian Code of Practice for the Care and Use of Animals for Scientific Purpose 2013. Upon death, individuals were immediately dissected to extract the liver. We focused on liver due to its established relevance in metabolic conditioning during heat stress responses and because it contains a relatively homogeneous distribution of cell types (Rabergh et al. 2000, Smith et al. 2013). Liver tissue was placed in RNAlater (Ambion), and incubated at 4°C for 12 hours before transferral to -80°C.

RNA extraction, library preparation and sequencing

Total RNA was extracted from preserved liver samples of the 24 *M. s. splendida* individuals using MagMAX™-96 Total RNA Isolation Kit (Ambion) following the manufacturer's protocol. This involved homogenisation of liver tissues with a lysis/binding solution to solubilise cellular membranes and inactivate nucleases. Nucleic acids were then purified through the magnetic capture of RNA using nucleic acid binding beads and washed to remove proteins and cell debris. Finally, the RNA was treated with DNase to cleave DNA contaminants and purified from the reaction mixture for resuspension in a low salt buffer. Extractions were assessed for quantity and quality using a Bioanalyzer 2100 (Agilent Technologies) according to protocol from the Agilent RNA 6000 Nano Kit Quick Start guide.

Total RNA was converted into complementary DNA (cDNA) libraries for sequencing, following TruSeq RNA™ Sample Preparation Low Throughput (LT) Protocol (Illumina, 2010). In the first step of library preparation, poly-A containing messenger RNA (mRNA) molecules were purified using magnetic beads. Two rounds of purification were performed, in which RNA was also fragmented and primed for cDNA synthesis with random hexamers. First-strand cDNA were then synthesised using reverse transcriptase and random primers, while second-strand synthesis involved the removal of RNA templates and the generation of double stranded cDNA using Second Strand Master Mix. End-repair was performed by removing 3'overhangs and filling in 5'overhangs resulting from fragmentation. Adenlyation of 3' ends was performed to prevent chimera forming during ligation. Unique indexing adaptors (Illumina MID tags 2, 4–7, 12–16, 18, 19) were ligated to each sample to allow identification of individual samples despite pooled sequencing. The only modification of protocols was during the PCR clean-up of the enrichment step, in which the ratio of beads was reduced from 1: to 4:5 to minimise concentration of short fragments (>200 bp). Concentrations of RNA in individual samples was normalised by dilution, and pooled in groups of 12 individuals per lane following successful work by Smith et al. (2013). Sequencing was performed on a HiSeq2500 (Illumina) genomic platform located at the Novogene, Hong Kong, to produce paired-end, 100 base reads.

Bioinformatics: quality trimming, genome-guided assembly, and quality assessment

We used TRIMMOMATIC V0.36 to trim sequences with low-quality (Q<20) bases, as well as adapter sequences, and reads shorter than 45 bp. Reads were then mapped to the *Melanotaenia* transcriptome assembled by Sandoval-Castillo et al. (2020), and based on this alignment, a transcriptome was assembled for *M. s. splendida* using TRINITY V2.5.1. The assembly was evaluated using read content statistics (% raw reads present), contig length distribution (N50), annotation-based metrics (% full length transcripts). Candidate protein coding regions were obtained using TRANSDECODER V3.0, which identified and extracted all open reading frames (ORFs) of length ≥ 100 peptides. Where two or more transcripts showed 80% or higher similarity, only the longest transcripts were retained to produce a non-redundant set of transcripts, referred to as 'unigenes'. These were queried against the UniprotKB database using BLASTX against *Danio rerio*, with a 1 x 10-2 e-value cut-off (UniProt-Consortium). Transcripts with 50% or higher similarity to bacterial, fungal, or viral genes were removed from the dataset.

Differential expression and network analyses

To test differential expression between experimental groups and among ecotypes, reads for each sampled individual were mapped back to the *M. s. splendida* predicted protein coding regions using BOWTIE2 V2.2.7, before estimating gene-level abundance using RSEM V1.2.19. We then normalised read counts by cross-sample normalisation using trimmed mean of M values, which were then used as input for the DE analysis, performed using DESeq2 V1.10.1 (89). We used a conventional threshold to define DE genes following Sandoval-Castillo et al. (2020), whereby transcript expression showed ≥ $\log_2$ fold-change (5% FDR) between any two groups (i.e., experimental vs. control, rainforest vs. savannah). To test for relationships between expression plasticity and upper thermal tolerance, we used a linear regression to compare the number of DE genes identified between experiment and control for each ecotype. This analysis incorporated the results of DE genes and thermal tolerance previously characterised for subtropical *M. duboulayi*, desert *M. s. tatei*, and temperate *M. fluviatilis* rainbowfishes (Sandoval-Castillo et al. 2020) with values of CT_{MAX}..

To explore system-level functionality among thermally induced genes, and to identify those central to expression responses, we conducted a network analysis used CYTOSCAPE V3.7 (Rakshit et al. 2014). We first constructed protein interaction networks using thermally DE genes specific to rainforest, savannah, and combined datasets, respectively. This involved creating 'edges' between genes listed in the STRING database (Szklarczyk et al. 2016) reported to have physical or functional interactions in zebrafish (*Danio rerio*). We evaluated relative importance of proteins by their connectivity in the network which was calculated by node degrees. Following Rakshit et al. (2014) and Sandoval-Castillo et al. (2020), we identified highly connected genes with node degrees ≥ the mean plus 2SD of the node degree distribution, considering these as 'hubs' for interactivity within the thermal response networks.

Results

Gene expression differences among temperature treatments and ecotypes

All but one individual survived until the culmination of the projected future climate experiment, allowing us to obtain high quality transcriptomic datasets from 12 rainforest and 11 savannah individuals. The non-surviving savannah individual was part of the 33°C treatment group but was removed from the experiment after acclimation to only 26°C, close to the annual mean temperature in its natural habitat (Supplemental Figure 4.1). Therefore, we suggest that an underlying condition, and not the temperature increase, was likely responsible.

Illumina HiSeq sequencing produced ~1.4 billion paired end reads (2 x 100 bp), of which ~912 million (~65%) were retained after quality trimming (Supplemental Table 1). The *M. s. splendida* transcriptome assembly comprised 320,364 contigs and 284,807 'Trinity genes', of which 51,091 were identified as ORFs. A final subset of 30,874 'unigenes' were found to be non-redundant and used for subsequent DE

analyses. We found that of these unigenes, 26,705 (91.5%) were present in both tropical *M. s. splendida* ecotypes, and 23,604 (86.5%) were shared with the previously studied subtropical *M. duboulayi*, desert *M. s. tatei*, and temperate *M. fluviatilis* (Sandoval-Castillo et al. 2020) (Figure 4.2a).

Pairwise comparisons of gene expression profiles among *M. s. splendida* individuals revealed the strongest clustering among experimental and control groups for future climate warming. On the other hand, the expression profiles among individuals in the same thermal treatment group clustered by lineage (Figures 4.3, 4.4). In other words, while thermal response was the most important factor driving pairwise gene expression differences among individuals, lineage-specific responses drove expression differences within treatments.
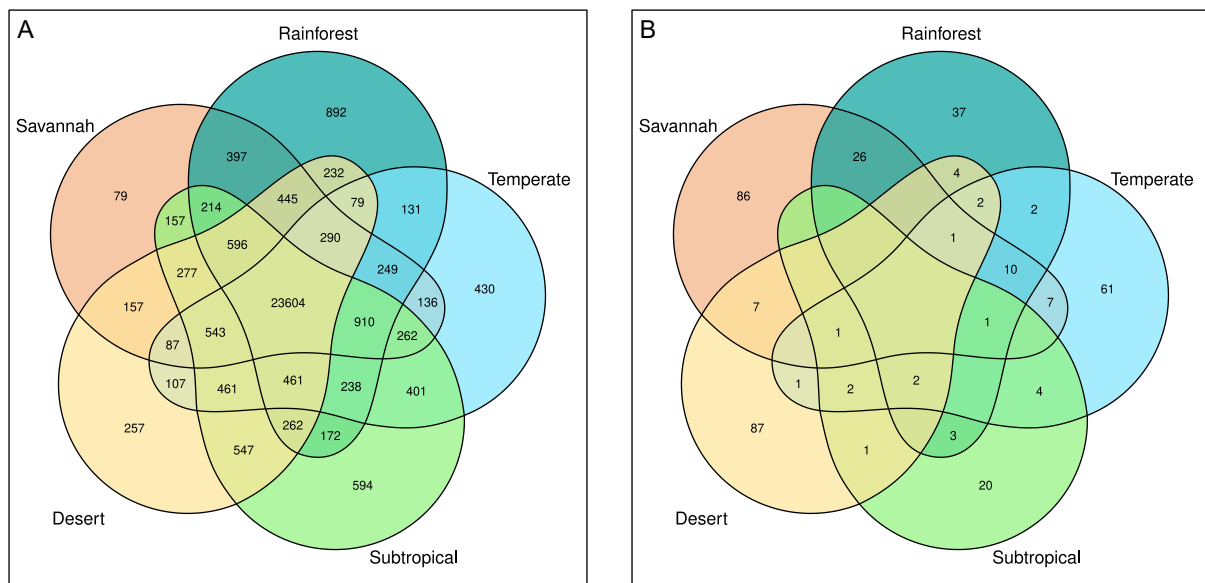
Figure 4.2: Venn diagram of unigenes shared among the five *Melanotaenia* ecotypes, based on A) all 34,815 identified *Melanotaenia* unigenes, and B) unigenes differentially expressed between control (21°C) and projected 2070 summer treatment (33°C) groups (blank segments indicate no shared responses).

Comparisons among thermal treatment groups for all *M. s. splendida* revealed 189 significantly DE unigenes as candidates for warming response, displaying plasticity of expression induced by projected

future thermal conditions. Warming treatments invoked shared DE responses between rainforest and savannah ecotypes in 38 unigenes. However, the savannah ecotype regulated a greater total number of genes in response to temperature, with 139 thermal candidates identified in comparison to only 88 identified for rainforest (Figure 4.2b, Figure 4.5). In the context of previous experimental results from temperate, desert and subtropical ecotypes, savannah individuals exhibited the most flexible transcriptional response to warming. The rainforest ecotype's plasticity, on the other hand, was limited to fewer genes than either subtropical or desert ecotypes. The rainforest ecotype only exceeded the plastic response of the temperate ecotype, which showed 39 DE genes (Figure 4.5).
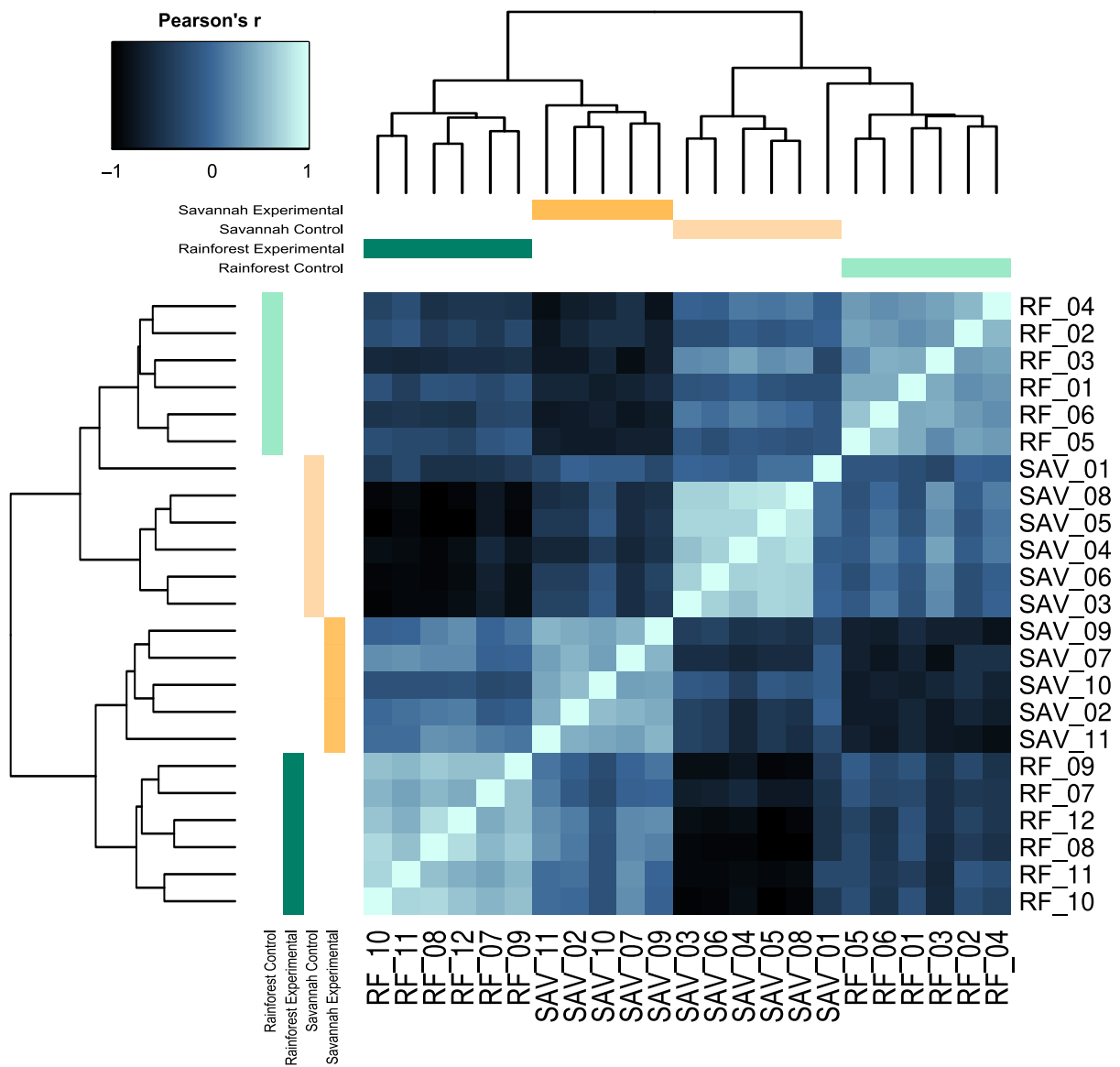
Figure 4.3. Correlation matrix for pairwise log$_2$ gene expression profiles among rainforest and savannah *Melanotaenia splendida splendida*. Coloured bars under sample dendrograms represent ecotypes and experimental treatments: dark green = rainforest experimental group, light green = rainforest control group, dark gold = savannah experimental group, light gold = savannah control group.
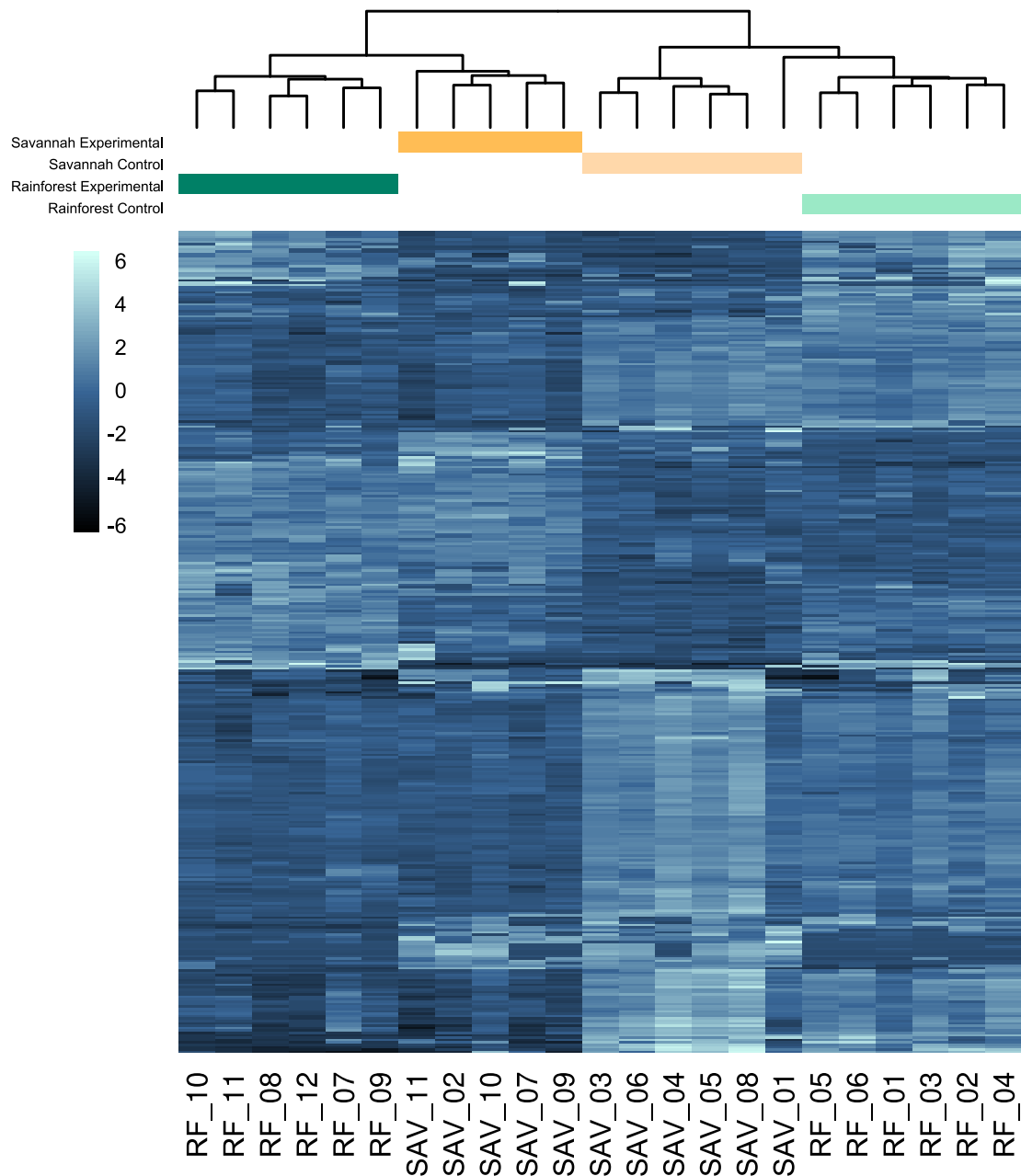
Figure 4.4. Hierarchical clusters of all DE transcripts according to similarity of expression, with columns representing sampled *Melanotaenia splendida splendida* individuals and rows representing transcripts. The coloured bars represent ecotypes and experimental groups: dark green = rainforest experimental group, light green = rainforest control group, dark gold = savannah experimental group, light gold = savannah control group.

Upper thermal tolerance

Critical thermal maximums among individuals ranged from 37.5°C to 39.0°C and were on average higher in the savannah (38.4°C, SD = 0.3°C) than in the rainforest (38.2°C, SD = 0.5°C) (Supplemental

Table 2). Although this difference was not significant (two-sample t-test $p = 0.209$), the mean upper thermal tolerance of tropical *M. s. splendida* overall (38.3°C, SD = 0.4°C) was significantly higher ($p < 0.05$), than that of subtropical (38.0°C, SD = 0.4°C), desert (37.2°C, SD = 0.5°C), or temperate (34.9°C, SD = 1.2°C) rainbowfishes (Supplemental Tables 5, 6). Among the five ecotypes, a significant linear relationship was detected between CT_{MAX} and the number of genes DE between contemporary and future climate treatments (r = 0.909, Figure 4.5, Supplemental Table 3).
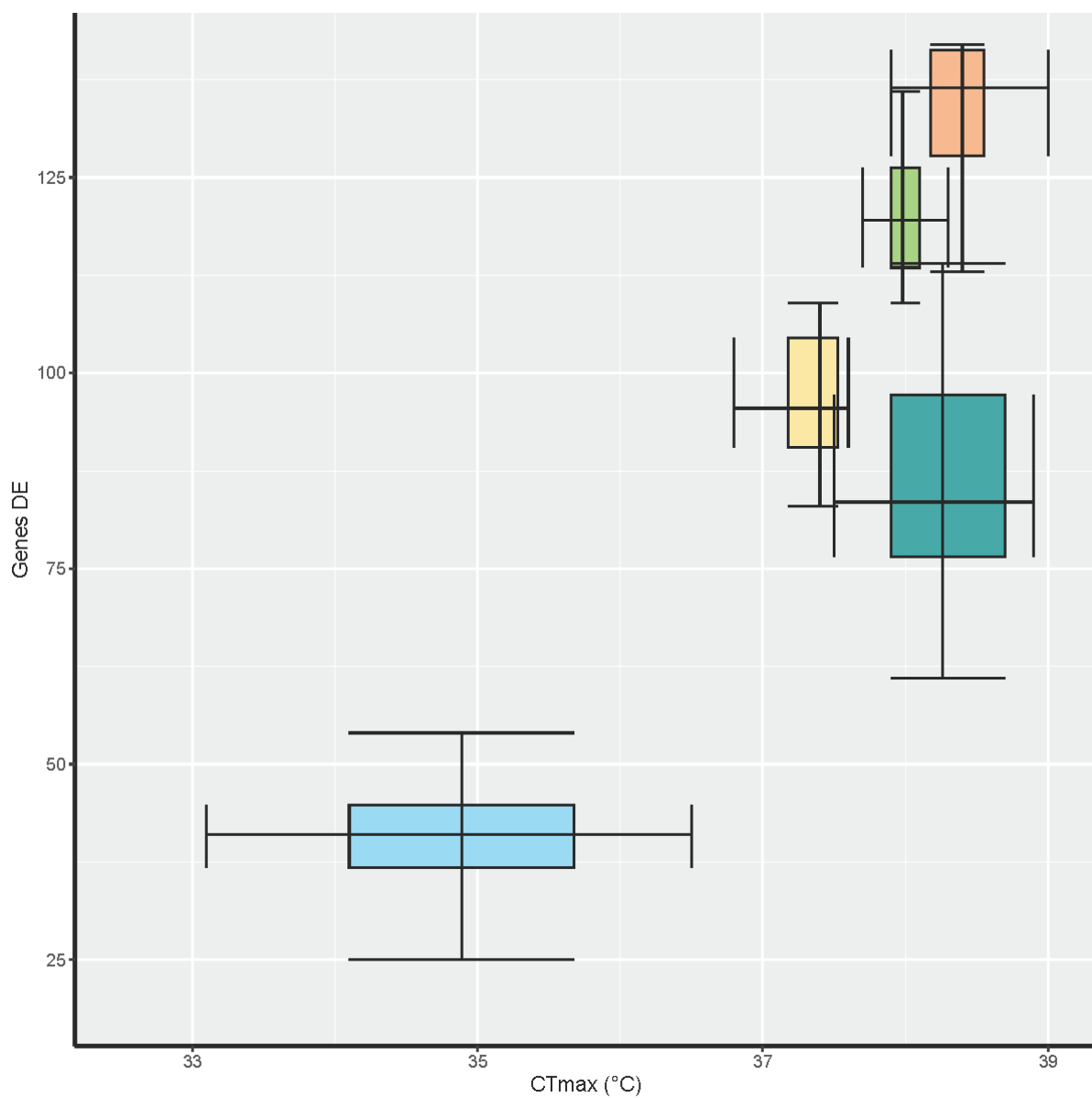
Figure 4.5. Associations between CT_{MAX} and the number of unigenes differentially expressed between control (21°C) and projected 2070 summer treatment (33°C) groups among five Australian *Melanotaenia* ecotypes (r = 0.909). The box plots display the upper and lower quartiles, whiskers represent 95th and 5th percentiles, and their intersections represent the median. Orange = savannah *Melanotaenia splendida splendida*, and dark green = rainforest *M. s. splendida*, light green = subtropical *M. duboulayi*, yellow = desert *M. s. tatei*, and light blue = temperate *M. fluviatilis*.

Functional annotation and network analysis

Transcript annotation produced 24,276 protein hits, 23,596 (97.2%) of which were assigned to 293,876 gene ontology (GO) terms (Supplemental Table 4). For the subset of unigenes DE under warming treatments, we received 77 protein hits corresponding to 1,226 GO terms for the rainforest, and 131 protein hits corresponding to 1,633 GO terms for the savannah. Protein networks for annotated DE genes were able to be constructed without requiring additional interactions, including for both rainforest- and savannah-specific subsets. From the network analyses, we identified eight hub genes for warming responses across the two ecotypes, defined by high degrees of interaction within protein networks. Of these, four were thermally induced in both ecotypes (FASN, ACLY, SCD, and FADS2; see Supplemental Figure 2), while three genes were DE only in savannah individuals (HAPA5, HMGCS1, and HYOU1; Figure 4.7), and one was DE only in rainforest individuals (ELOVL6; Figure 4.6).
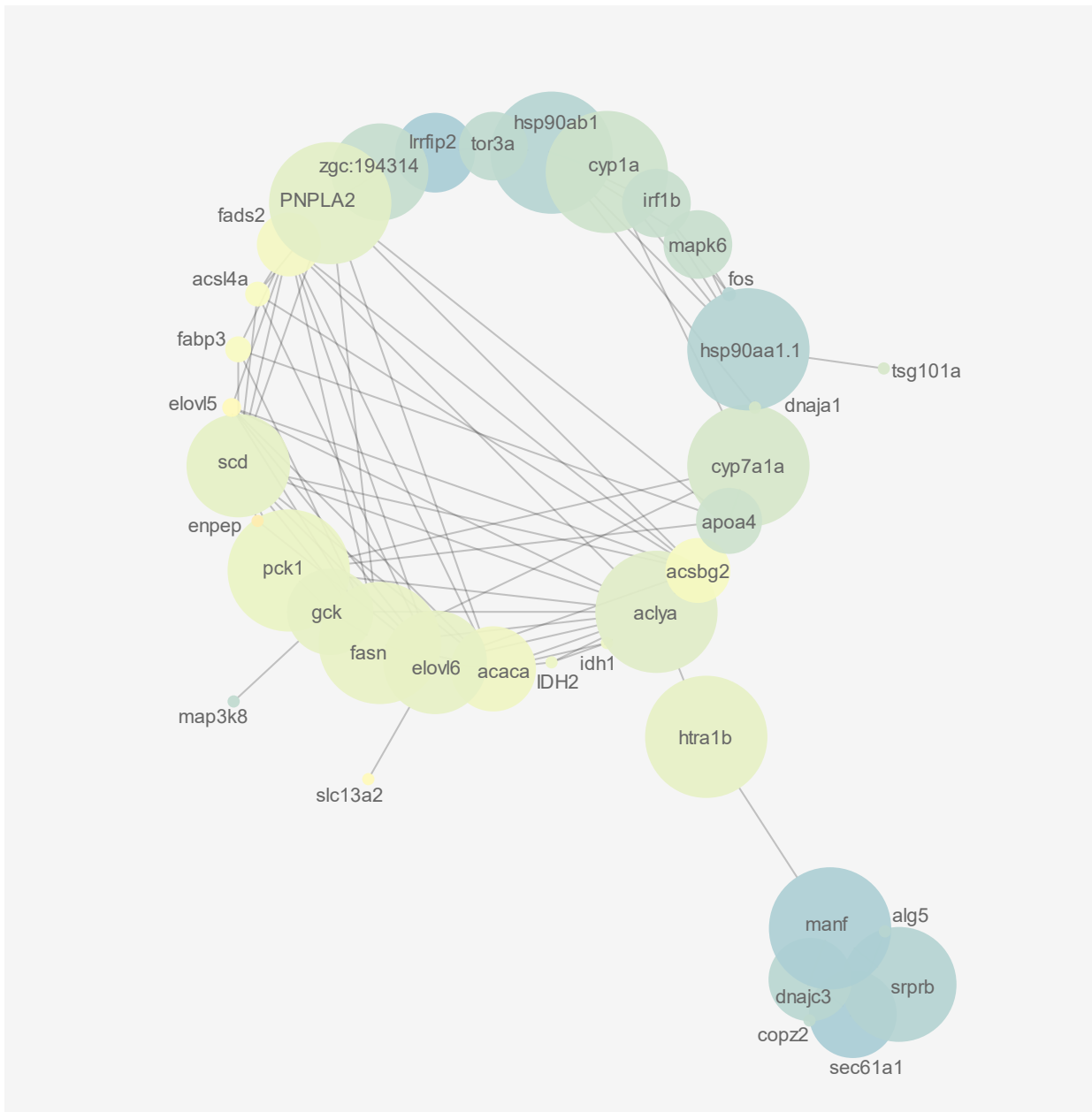
Figure 4.6. Protein interaction network for climate warming responses in tropical rainforest *Melanotaenia splendida splendida*, based on 88 unigenes differentially expressed between control (21°C) and projected 2070 summer treatment (33°C) groups. Node sizes are proportional to centrality in the network (betweenness centrality), while shading indicates the relative number of direct interaction (neighbourhood connectivity; blue = fewer interactions, orange = more interactions).
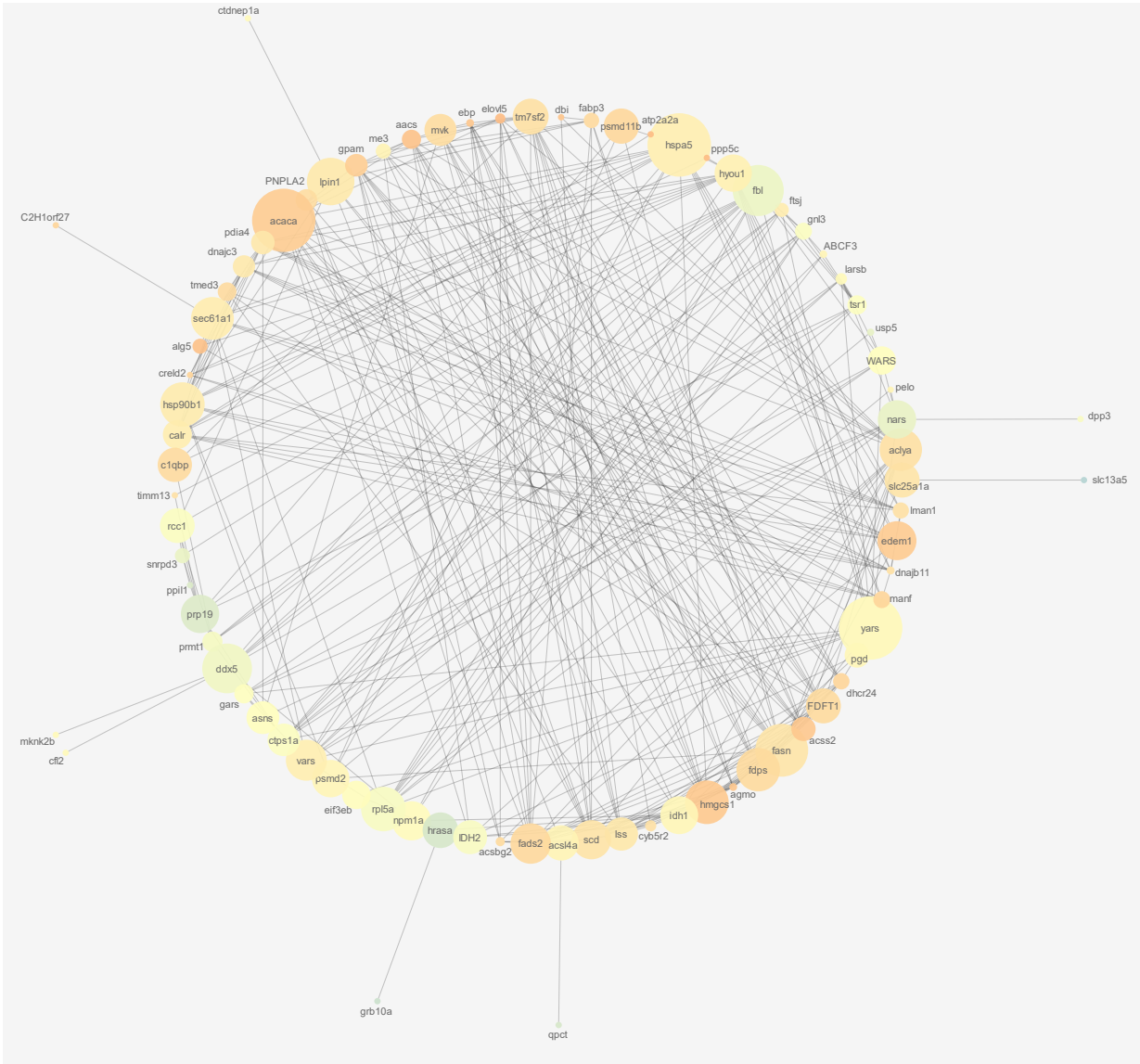
Figure 4.7. Protein interaction network for climate warming responses in tropical savannah *Melanotaenia splendida splendida*, based on 139 unigenes differentially expressed between control (21°C) and projected 2070 summer treatment (33°C) groups. Node sizes are proportional to centrality in the network (betweenness centrality), while shading indicates the relative number of direct interaction (neighbourhood connectivity; green = fewer interactions, orange = more interactions).

Discussion

Regional bioclimatic differences can produce substantial evolutionary variation in organismal physiology, including that of thermal tolerance (Cohet et al. 1980, Compton et al. 2007, Sunday et al. 2019). As such, adaptive resilience to climate change is expected to vary geographically (Thomas et al. 2004, Román-Palacios and Wiens 2020, Trisos et al. 2020). While phenotypic plasticity is likely to be important in facilitating thermal performance, the involved molecular mechanisms and their covariance with environment are not well understood (Oomen and Hutchings 2017, Logan and Cox 2020, Rivera et al. 2021). Here, we found gene expression plasticity in response to projected summer temperatures in rainbowfish *M. s. splendida* from both tropical rainforest and savannah biomes. However, we found much greater capacity for transcriptional response in the savannah ecotype, in addition to slightly superior thermal performance, both of which may provide advantage under warm and variable conditions. Meanwhile, we propose that the more limited plasticity in the rainforest ecotype could reflect greater specialisation of thermal responses due to milder and more temporally stable conditions. When comparing with previous results for three higher latitude rainbowfish ecotypes, we found broad support for our hypothesis that transcriptional plasticity is facilitating thermal resilience in Australian rainbowfishes. In fact, there was a strong positive relationship between thermally induced transcriptional responses and thermal tolerance among the five ecotypes. These results have implications for understanding how adaptation of plastic responses may differ among climatic bioregions and informing about mechanisms shaping resilience under warming climates.

Plastic capacity and thermal resilience

High survivorship during acclimation and the two-week exposure period to projected 2070 summer temperatures suggest that both ecotypes are preadapted to withstand short-term exposure to these magnitudes of warming, if other ecological factors are amenable. This could even be described as a hidden reaction norm (*sensu* Schlichting and Smith (2002)) in the rainforest ecotype, which is unlikely to encounter such high thermal extremes in its contemporary habitat (Supplemental Figure 1). Despite this, the greatest differences in individual gene expression occurred between thermal treatment and

control groups, consistent with large transcriptional responses common during thermal warming stress in ectotherms (López-Maury et al. 2008, Smith et al. 2013, Porcelli et al. 2015, Oomen and Hutchings 2017, Logan and Cox 2020). Moreover, all hub genes identified for shared (across-ecotype) responses to warming were related to lipid biosynthesis and metabolism, a long recognised component of heat shock response in eukaryotes, and necessary for maintaining cellular membrane integrity and function during thermal stress (Vigh et al. 1998, Mejía et al. 1999, Balogh et al. 2013). Being central in both rainforest and savannah thermal expression networks, these hub genes were closely connected to heat shock proteins, which are highly conserved mitigators of cellular damage during environmental stress (Chen et al. 2018a). Together, these results suggest that in both rainforest and savannah wild populations, a substantial divergence of physiological baselines will be necessary for maintaining normal cellular functions in future climates, either via evolutionary adaptation (e.g. Kelly et al. (2017)) or by continued use of flexible mechanisms for thermal response (e.g. Kingsolver and Buckley (2017)).

Despite these common heat stress indicators, thermal expression responses were shared among rainforest and savannah ecotypes in only 38 (~20%) of the 189 identified thermally DE unigenes (DE $\geq \log_2$ fold-change). Almost half of the 88 unigenes DE in rainforest thermal responses were also DE in the savannah fish; however, a much greater 139 unigenes were DE in savannah, making 66% of these uniquely responsive. This contrasts with the fact that the majority of sequenced unigenes (91.5%) were detected in both ecotypes. This suggests that constitutive expression may have been more highly conserved between rainforest and savannah, while either selective or demographic influences could have contributed to thermally induced expression profiles specific to each ecotype (Whitehead and Crawford 2006a, b). Selection may theoretically influence plasticity via changes to the number and identity of expressed genes, in addition to the magnitude of gene expression differences (Schlichting and Smith 2002, Komoroske et al. 2021). However, our previous work in Australian rainbowfishes found that the higher thermal maxima of warmer-climate ecotypes was particularly associated with greater numbers of thermally responsive unigenes (Sandoval-Castillo et al. 2020). This led to our expectation that the savannah ecotype, from a warmer contemporary habitat, would show plastic

responses to warming in a greater number of genes than the milder-climate rainforest ecotype. This was supported by the 157% more DE unigenes in the savannah compared to the rainforest, alongside a slightly higher average CT_{MAX}.

Ecotype-specific responses were also reflected by protein network differences. With fewer induced genes in the rainforest, the constructed network was smaller and therefore received lower connectivity values. Only one of its central hub genes (ELOVL6, another membrane protein responsible for lipid biosynthesis (Chen et al. 2018b, Xie et al. 2021)) was uniquely induced in this ecotype. Meanwhile, three uniquely induced genes were identified as hubs within the savannah network, including the heat shock protein HSPA5, the lipid synthesising HMGCS1, and the hypoxia up-regulated protein HYOU1. From this, we infer that different thermal response pathways have been induced by rainforest and savannah, with the greater diversity of molecular functions observable in the savannah ecotype's responses. Given that genetic diversity was found to be similar in rainforest and savannah in Chapter 3, rainforest responses seem unlikely to have been constrained by an unavailability of standing genetic variation. Overall, these results suggest that both the number and identity of expressed unigenes are contributing to physiological phenotypic differences in thermal responses between ecotypes. To further explore possible relationships between plasticity and thermal response capacity, we compared these results with experimental data from the congeneric subtropical, desert, and temperate rainbowfishes (Sandoval-Castillo et al. 2020). In the context of all five ecotypes (including the two tropical representatives), we found a strong positive relationship between the number of DE genes and an ecotype's average CT_{MAX}, with the savannah ecotype emerging as both the most thermally tolerant, and as having the most flexible transcriptional response to projected future climates. Although we cannot infer direct causation, this is consistent with our hypothesis that transcriptional plasticity could facilitate greater thermal performance in warmer-climate rainbowfishes.

It is becoming well-established that trait plasticity may evolve via ecological selection, as a phenotypic trait in its own right (Scheiner 1993, Pigliucci 2001, Chevin and Lande 2015, Bailey et al. 2021, Bond et al. 2021). Because it can facilitate acclimation to a greater range of conditions, plasticity is expected to be particularly advantageous under variable or novel environments (Scheiner 1993, Fusco and Minelli 2010, Snell-Rood and Ehlman 2021). However, plasticity can also evolve as a by-product of directional selection regardless of levels of environmental variation (Harshman et al. 1991, Garland Jr and Kelly 2006, Snell-Rood and Ehlman 2021), and may provide additive or even facultative roles to concurrent genomic adaptation (Chevin and Lande 2011, Bailey et al. 2021). Similar to the trend in this study, positive associations between gene expression plasticity and ecologically adaptive thermal tolerance have been reported in teleosts (*Oncorhynchus mykiss gairdneri* ecotypes, Narum and Campbell (2015); *Neogobius melanostomus* versus *Proterorhinus semilunaris*, Wellband and Heath (2017), *Menidia beryllina* versus *Hypomesus transpacificus*, Komoroske et al. (2021)), and oysters (*Crassostrea angulate* versus *Crassostrea gigas*, Li et al. (2021)).

To complicate matters however, there may sometimes be fitness costs to maintaining plasticity (Callahan et al. 2008, Scheiner et al. 2020). Even where plastic traits may have facilitated environmental adaptation, they can eventually be lost through processes of genetic assimilation or canalisation (Kelly 2019, Scheiner and Levis 2021). For instance, Kelly et al. (2017) experimentally selected for heat tolerance in the copepod *Tigriopus californicus*, finding that transcriptional plasticity decreased as generations became better adapted to the consistently high thermal stimulus. This phenomenon is thought to be especially likely where environmental fluctuations are minimal, emphasising the idea that environmental variability, and not just the magnitude of environmental challenges, may contribute to adaptation of plastic responses (Scheiner 1993, Scheiner and Levis 2021, Snell-Rood and Ehlman 2021). This may help to explain the fact that the tropical rainforest ecotype in this study exhibited relatively low expression plasticity despite its high thermal tolerance. While its average CT_{MAX} was second only to the savannah ecotype, the number of thermally DE genes were lower than that of both the subtropical and desert ecotypes. It is therefore possible that thermal responses are more genetically

assimilated in the rainforest, which experiences the most climatically stable conditions and may therefore benefit from the efficiency of a more standardised, or specialised, genetic response. It is also important to consider that different genes can have different effect sizes on resultant physiology and fitness, or may even be expressed maladaptively (Ghalambor et al. 2007, Logan and Cox 2020). For these reasons, we should still consider it possible that even linear relationships between expression plasticity and thermal resilience may mask multifaceted evolutionary mechanisms.

Biogeographic implications for future climates

Given the assumption that populations are adapted to the environments they experience, Janzen (1967) predicted that the low variability of tropical climates would produce thermal specialisation of endemic organisms, while thermal generalists would be more likely to proliferate in temperate climates. This framework has since been extensively tested in latitudinal studies, supporting the generalisation that low latitude (tropical) organisms tend to exhibit higher thermal maxima but tolerate smaller ranges of temperature fluctuation than high latitude (temperate) organisms (Addo-Bediako et al. 2000, Ghalambor et al. 2006, Deutsch et al. 2008, Sunday et al. 2011, Sunday et al. 2019). Meanwhile, within tropical latitudes, several regionally focussed studies have found higher thermal maxima in ectotherms from ecotone or savannah habitats compared to rainforest centres, despite the greater variability of conditions (Moritz et al. 2012, Frishkoff et al. 2015, Nowakowski et al. 2017, Dongmo et al. 2021). The latter trend was supported here among our tropical ecotypes by a 0.2°C higher average CT_{MAX} in the savannah compared to the rainforest. The difference was not statistically significant; however, we suggest this may be a product of sample size. Following CT_{MAX} experiments in previous rainbowfish work (Sandoval-Castillo et al. 2020), we included only ten individuals per treatment, which potentially limited power for detecting differences at this narrower geographic scale.

Further, and more analogous to the abovementioned latitudinal studies, we found that the average CT_{MAX} of the tropical ecotypes was significantly higher than those of other rainbowfishes, whose

thermal tolerance decreased with distance from the equator. These differences in thermal adaptation are probably not attributed to phylogenetic constraints; while the tropical (*M. s. splendida*) and desert (*M. s. tatei*) ecotypes are both *splendida* subspecies, the desert has a surprisingly low CT_{MAX}. Moreover, the relatively warm-tolerant subtropical ecotype (*M. duboulayi*) is closely related to the temperate congener (*M. fluviatilis*) (Unmack et al. 2013, Sandoval-Castillo et al. 2020)), which was the least tolerant of all ecotypes. This again lends favourability to the hypothesis of climatic adaptation; yet, as with gene expression plasticity, interpretation appears to require consideration of both the average conditions and the variability of local climates.

It has been theorised that adaptation to highly variable climates may produce trade-offs limiting upper thermal performance (Pörtner et al. 2006, Payne and Smith 2017). This could have contributed to the observed latitudinal patterns in rainbowfishes' CT_{MAX}, as discussed by Sandoval-Castillo et al. (2020) in relation to the desert ecotype's low thermal resilience. By the same rationale, the savannah's variable habitat conditions could pose a trade-off for maximum tolerance relative to conditions in the rainforest. However, although savannah's warm thermal extremes are substantially higher (~2.2°C), cold extremes are only slightly lower (~0.4°C; Supplemental Figure 1), minimising potential selective pressures for accommodation of cold extremes. Savannah organisms would therefore be likely to benefit more generally from warm adaptation than the rainforest ecotype, as is likely reflected by their greater thermal tolerance and associated expression plasticity. Flexibility of thermal responses may be a key factor for persistence under warmer and more variable future climates (Logan and Buckley 2015, Diamond and Martin 2021), suggesting that the savannah ecotype may have the greatest preadapted resilience of ecotypes so far studied. The rainforest ecotype also has relatively high thermal tolerance; yet given evidence for climatic specialisation here and in previous chapters, it may be more restricted in its versatility of responses to conditions outside the expected range.

Realised patterns of vulnerability will depend not only on existing adaptations, but also on the extent of local environmental change (Huntley et al. 1995, Sykes et al. 1996), so future studies should benefit from distribution modelling under projected future climates. Our results highlight stark differences in plastic capacity and thermal tolerance among closely related rainbowfish lineages, warning against the common practice in distribution forecasts of treating species as single homogeneous units (Pearman et al. 2010, Reed et al. 2011, King et al. 2019). Notably, even with the finer scale mechanistic data presented here, there remain many challenges to inferring future adaptive potential from contemporary patterns. For instance, different responses may be advantageous under acute thermal stress conditions compared to warmer long-term averages (Gerken et al. 2015), both of which are anticipated under climate change modelling (IPCC 2014, O'Neill et al. 2017). Despite this, acute periods of warming such as heat waves may produce the strongest selective effects, relying on accuracy of heat stress responses. Both heat shock and lipid metabolic processes have therefore been suggested as determinants of resilience, as well as targets of selection, under rapid climatic change (Logan and Cox 2020, Zhang and Dong 2021). We therefore consider the DE genes identified here as candidates for rainbowfishes' future climate adaptation, particularly those central to expression networks. In that regard, a promising framework to test if divergent selection has influenced the evolution of expression variation in these candidate genes is the comparative phylogenetic Expression Variance and Evolution (EVE) model (Rohlfs and Nielsen 2015). The EVE framework uses a phylogenetic tree to model gene expression as a quantitative trait across a phylogeny. It estimates the ratio of among-lineage expression divergence to within-lineage expression diversity, and in this way detects gene responses subjected to ecotype-specific directional selection (Rohlfs and Nielsen 2015). This framework has been applied for Australian freshwater fishes in transcriptomic studies of wild populations found across hydroclimatic gradients (Brauer et al. 2017) and in our comparative experimental study of rainbowfish ecotypes (Sandoval-Castillo et al. 2020). It is anticipated that the EVE framework will be incorporated into the work reported in this chapter prior to its journal submission, enabling us to asses the contribution of divergent selection on gene expression to the adaptive evolution of climatically defined ecotypes.

Linking molecular mechanisms and physiological responses to warming is a key step for predicting and mitigating biodiversity loss in future climates. A comprehensive understanding of the role of plasticity in climate change responses should include a broader range of co-distributed taxa, as well as experiments using a greater range of sublethal temperatures under both laboratory and wild conditions. Nonetheless, the strong biogeographic pattern in both warming tolerance and expression plasticity in Australian rainbowfishes provides support for ecological adaptation of thermal plasticity in this group. These results may signify greater flexibility in the savannah ecotype compared to the rainforest ecotype in response to future climates, in line with established concerns for the future of tropical rainforest organisms under warmer and more unpredictable conditions. Overall, our study suggests an important role for plasticity in rapid climatic adaptation, which is expected to influence distributions and resilience in coming decades.

Chapter 5: Conclusions and perspectives

Climate is well established as a selective force in natural populations (Franks and Hoffmann 2012, Anderson and Song 2020), and regional bioclimatic variation is expected to influence contemporary adaptive diversity, as well as future climatic responses (Somero 2010, Chen et al. 2018c, Buckley and Kingsolver 2021). Tropical organisms are known for their narrow thermal niches, and as such have been hypothesised to be particularly vulnerable to changing climates (Tewksbury et al. 2008, Huey et al. 2009, Sunday et al. 2011). However, not enough is currently known about how climatic variation in tropical ecosystems is likely to affect patterns of adaptation, plasticity, and persistence of local populations.

The objectives of this thesis were to evaluate how hydroclimatic selection and landscape structure influence adaptation and evolution in the tropical-endemic rainbowfish, *Melanotaenia splendida splendida*. We also aimed to inform about factors influencing resilience of freshwater organisms in rainforest and savannah in a rapidly changing climate. Across the north-eastern Australian study region, we found significant intraspecies divergence among 17 sampled localities, but particularly between rainforest and savannah regions, where genetic, morphological, and gene expression variation were sufficient to distinguish local ecotypes. Some of this was attributable to neutral processes, particularly among drainage divides. However, integrative approaches based on landscape genomics and morphometrics identified strong signals of thermal and hydrological adaptation, with local variation better explained by environment than by estimations of neutral genetic structure. Further mechanistic experiments found greater gene expression plasticity, and slightly greater thermal tolerance, in the savannah compared to the rainforest ecotype, echoing positive associations previously suggested to facilitate thermal responses in warm-adapted rainbowfish ecotypes (Sandoval-Castillo et al. 2020). Our results support the influence of both contemporary climates and population connectivity on environmentally relevant traits, suggesting several implications for resilience to climate change among regional tropical ecotypes. In this final chapter, we provide a broad overview of the findings in relation

to our aims, as well as in relation to their broader contribution to conservation and evolutionary research. We also review the limitations of our work, and outline opportunities to expand upon this research.

Hydroclimatic adaptation and response capacity

The role of ecological adaptation in local divergence has implications for understanding the processes generating and sustaining tropical biodiversity, as well for identifying areas of vulnerability and resilience under rapid change. In the rainforest-focused Chapter 2, we found that despite being able to link strong hierarchical demographic structure to the five sampled drainage divisions, RDA modelling of both genotype-environment associations (GEAs) and phenotype-environment associations (PEAs) revealed a greater proportion of overall genomic and morphological divergence associated with the included ecological variables. This pattern was reiterated in Chapter 3, where ecological variables again had a high power to explain intraspecies variation, despite there being less overall divergence within the well-connected system. Between systems, the overall greatest genetic and morphological divergences occurred across the rainforest-savannah boundary, and were similarly associated more closely to environment than to measures of neutral genetic structure. In both Chapters 2 and 3, we found surprising differences in the extent to which genetic and morphological variation could be explained by environment relative to neutral explanatory variables. Across all sampling localities, environment best explained approximately ten times more body shape variation than did neutral structure, versus only three times more genetic variation. This relative resistance of phenotypes to neutral influences, especially relative to genomic patterns, suggests there may be functional constraints on body shape variation (e.g., McKay et al. (2001), Clegg et al. (2002)).

Supporting the hypothesised role of hydroclimate in local adaptation, we found that in all GEAs and PEAs, the top environmental explanatory variables related to hydrological or thermal variables, and were most often identical among RDA and BAYPASS approaches. Between rainforest and savannah ecotypes, we found both genomic and morphological selective signals most strongly associated with

average annual rainfall and summer mean runoff. This differed slightly at a regional level, with annual means (rainfall and temperature) most associated within the rainforest, and seasonal means (runoff) more prominent in savannah analyses. The GEAs provided a suite of loci as candidates for local adaptation, including 1,004 within rainforest, 987 within savannah and 1,284 across systems. Further, using genotype x phenotype x environment (GxPxE) associations, we identified a small yet significant subset of loci which were closely associated with morphological variation, to be considered as candidates for heritable phenotypic adaptation. PEAs revealed that the main climate-associated morphological differences between rainforest and savannah individuals were relative body and caudal peduncle depths, which have established relevance to swimming biomechanics in teleosts (Gatz 1979, Leavy and Bonner 2009, Langerhans and Reznick 2010).We investigated morphology at a finer scale within the rainforest in Chapter 2, finding hydrology-associated variation in fin position similar to that attributed to streamflow adaptations in congeneric *M. duboulayi* and *M. eachamensis* (McGuigan et al. 2003, McGuigan et al. 2005), which further supported inferences of hydrological relevance.

While Chapters 2 and 3 explored biological variation along climatic gradients, Chapter 4 allowed us to test differences in physiological mechanisms for climatic response across ecotypes. In response to exposure to projected summer temperatures for eastern Australia in 2070, we found greater plasticity of gene expression in the savannah compared to the rainbowfish ecotype, with 139 and 88 warming-induced genes, respectively. As we found in previous transcriptomic work with rainbowfishes from higher latitudes (Sandoval-Castillo et al. 2020), the more plastic ecotype had slightly higher thermal tolerance, which may be advantageous in warmer savannah conditions. Meanwhile, stable conditions have long been suggested to favour thermal specialisation (Devictor et al. 2008, Afonso Silva et al. 2017), which may help to explain the rainforest ecotype's less flexible transcriptional response. When patterns were assessed alongside earlier datasets from subtropical, desert, and temperate ecotypes (from Sandoval-Castillo et al. (2020)), we found a strong positive relationship between expression plasticity and thermal tolerance, supporting our hypothesis that transcriptional plasticity is facilitating thermal responses among Australian rainbowfish ecotypes.

Influences of terrain structure on neutral and adaptive diversity

In addition to assessing climatic influences on divergence across rainforest and savannah ecotypes, we also investigated the role of river system connectivity, which has previously been established as an influence on wide-ranging aspects of freshwater biology (Pusey and Kennard 1996, Unmack 2001, Wong et al. 2004, Carvajal-Quintero et al. 2019). Here, our results suggested an important influence of contemporary drainage networks on patterns of intraspecies divergence. In Chapter 2, both neutral genetic clustering and environmental associations found divergences among drainages, providing evidence that gene flow barriers have helped to define broader patterns of diversity. Clustering methods typically grouped individuals by their drainage system of origin, suggesting hierarchical patterns of population structure common in lotic environments (Brauer et al. 2018, Grummer et al. 2019, Smith et al. 2020). In Chapter 3, we subsequently found that differences in drainage structure produced distinct patterns of population connectivity among ecotypes; while individuals from the hydrologically connected savannah system comprised a single population, five populations were ascribed among sampled drainages in the mountainous rainforest environment.

Considering that connectivity can affect not only neutral genetic structuring, but the flow of adaptive traits and alleles across heterogeneous landscapes (Garant et al. 2007, Yeaman and Otto 2011, Nosil 2012, Tigano and Friesen 2016), we further considered that drainage structure may have divergent effects on adaptive evolution within each bioregion. Supporting this hypothesis, we found that signals of locally adaptive genetic divergence were weaker in the more connected savannah region in both ecoregion-specific and combined-systems GEAs, despite similar magnitudes of environmental variation among sampling localities in each region. This was indicated by the savannah-specific pRDA models' lower overall variance, weaker local clustering of individual adaptive variation, and weaker locus-specific environmental associations than in rainforest-specific analyses. Furthermore, we found a relative decoupling of genomic and morphological associations, with GxPxEs explaining less variance and displaying weaker local clustering in the savannah compared to the rainforest ecotype. Together,

these results suggested that greater drainage connectivity in the savannah may have a homogenising influence on adaptive variation, in contrast to relatively independent adaptative responses to local selection in the naturally fragmented rainforest system.

Interestingly, despite this evidence for genetic homogenisation, we found that morphological associations with environment were just as strong, or even stronger, in the higher gene flow system. This highlighted a tentative role for plasticity in local body shape adaptation in the savannah ecotype, which has been suggested for systems with both high gene flow and environmental heterogeneity (Sultan and Spencer 2002, Crispo 2008). Although it was outside the scope of this project to further test the proposition, it is worth reiterating the result from Chapter 4 that thermally responsive expression plasticity was greater in the savannah ecotype than in the rainforest. In the context of broader biogeographic patterns in rainbowfishes, we considered this most likely to result from warm adaptation and a more temporally variable climate; however, within our current dataset we cannot extricate the possibility that gene flow differences among systems may also contribute to this plastic divergence and associated differences in thermal tolerance.

Resilience in future climates

As discussed above, environmental heterogeneity has the power to affect both neutral and adaptive evolutionary process across landscapes. This is expected to shape not only organisms' capacity to respond to existing environmental pressures, but their adaptive potential under novel challenges (Somero 2010, Chen et al. 2018c, Buckley and Kingsolver 2021). In general, where a large proportion of biological variation has evolved in response to local selection, a similarly large evolutionary turnover could be necessary to prevent fitness loss in changing conditions (Fitzpatrick and Keller 2015, Bay et al. 2017). Given the large proportion of adaptation associated with local hydroclimates in both rainforest and savannah rainbowfishes, and similarly identified in an increasing number of tropical taxa (Ntie et al. 2017, Termignoni-García et al. 2017, Zhen et al. 2017, Lam et al. 2018, Jaffé et al. 2019, Miller et al. 2020, Morgan et al. 2020), we expect that climate change may have substantial detrimental effects

across both of these tropical bioregions. Furthermore, although the extent of local impacts will depend on the magnitudes and rates of change, the rainforest ecotype in particular displays stronger local evolutionary divergence apparent in GEAs. This may highlight the potential for greater vulnerability, especially in the context of their more limited opportunity to translocate to favourable conditions (Atkins and Travis 2010, Thomas et al. 2017, Aguirre-Liguori et al. 2021).

More broadly, the connectivity differences among rainforest and savannah may pose trade-offs between local specialisation and system-wide resilience. From a genomic perspective, fragmented systems such as the rainforest may produce steadier evolutionary responses to local selective pressures, but will be constrained by the requirement for novel adaptive variation to arise independently within each deme (Tigano and Friesen 2016, Nosil et al. 2019). Meanwhile, well-connected systems such as the savannah may not experience locally adaptive shifts unless the wider system is driven to a selective 'tipping point', but in this event, gene flow is likely to benefit fitness by facilitating rapid and widespread adaptation (Nosil et al. 2019). From the perspective of phenotypic plasticity, similar trade-offs may exist between generalist and specialist tendencies (Pörtner et al. 2006, Olazcuaga et al. 2019, Snell-Rood and Ehlman 2021). For instance, if lower thermal expression plasticity in the rainforest ecotype has resulted from adaptation to a narrow range of conditions, it may enable more precise and efficient responses within the current range. On the other hand, the savannah's plasticity of thermal responses may be less specialised, yet the more flexible response capacity may be valuable in increasingly unpredictable climates.

Limitations, future directions, and concluding remarks

Some of the main limitations of this work are the same as those inherent in the study of natural populations more generally (useful reviews include Joost et al. (2013), Rellstab et al. (2015), Luikart et al. (2018) regarding landscape genomics; De Wit et al. (2012), Conesa et al. (2016) regarding gene expression analyses). Centrally, we seek to address patterns and processes occurring in complex and

uncontrollable ecological systems. Experimental frameworks therefore contain an exploratory element, and are unable to account for all possible confounding variables. In environmental association studies, some false positive signals of selections are generally expected to be found among genuine signals due to stochastic influences, genomic regions with low recombination rates, or untested environmental influences (Rellstab et al. 2015, Luikart et al. 2018). Moreover, the power for detecting genomic selection, as well as genotype-phenotype interactions, is limited to the subset of the genome sampled by the reduced representation sequencing (ddRADseq) strategy. Whole genome population resequencing data would have provided a high-resolution record of variants across the genome and information about causative genes, rather than information about markers as provided by ddRADseq and related methods. Despite these factors, the analytical methods used for environmental associations (RDA, BAYPASS) were chosen to suit the hierarchical population structure present in the study system, and due to the relative abundance and genetic diversity of wild *M. s. splendia*, we expect most false positives to add noise rather than large biases to reported patterns. Moreover, reduced representation sequencing is considered to provided sufficient marker density to study selection in many natural populations, and remains a powerful approach when linkage disequilibrium and other demographic influences are appropriately addressed (Catchen et al. 2017)

Uncontrollable aspects are potentially even greater for transcriptomics, entering the project not only at a population level, but during the lifespan of the individuals sampled (De Wit et al. 2012, Conesa et al. 2016). Given that rainforest and savannah populations were sampled within the same week, handled consistently, and were sequenced in the same Illumina lanes, these biases have been reduced as much as possible for comparisons among rainforest and savannah ecotypes. Early developmental influences resulting from the season and year of sampling could be further minimised by comparisons of lab raised F1s, however, this may ultimately reduce applicability of inferences to natural populations, given the introduction of new and different biases resulting from captive breeding and adaptation to captivity. The nature of all these approaches mean that inferences must be made with caution, which we have attempted to do in all three chapters. However, this should not discount their ability to uncover real

biological patterns in otherwise intractable systems (Catchen et al. 2017, Luikart et al. 2018). Given the urgency presented by rapid climate change, such approaches are not only valuable but are likely necessary for effective conservation management, and are already being implemented successfully in informing conservation decisions (Garner et al. 2016, Grummer et al. 2019)

A further limitation is the duration of a PhD project, and even with the confines of the existing datasets as there is much left to explore. At the time of writing, the manuscript from Chapter 2 is under consideration in *Heredity*. However, there are areas that we expect to address and improve in Chapters 3 and 4 prior to their submission for journal publication. Already mentioned was the intention to annotate candidate genes identified in landscape genomics approaches. There is also additional opportunity to compare those identified as candidates for adaptation with those identified in transcriptomics work in response to thermal stress. Further to identifying overlaps between thermal responses and adaptive signals, we intend to extend upon Chapter 4 results using the comparative phylogenetic Expression Variance and Evolution model (Rohlfs and Nielsen 2015). This will enable us to test whether divergent selection has influenced the evolution of expression variation in thermally induced genes. Additionally, both Chapters 3 and 4 can benefit from distribution modelling under future climates, as previously achieved in our study of higher latitudes rainbowfishes (Sandoval-Castillo et al. (2020). The existing resolution of the landscape genomic datasets will enable us to model projected turnover of loci and genomic vulnerability across landscapes (*sensu* Fitzpatrick and Keller (2015), rather than focusing on species-level modelling as has so far been more common. This is particularly important given the extent of intraspecific climate associated differences, even within connected populations of *M. s. splendida*, characterised throughout this thesis.

The combined results of these data chapters contribute towards broader understanding of contemporary environmental influences shaping tropical intraspecies variation at local and bioregional scales. Chapters 2 and 3 found genetic and morphological associations with hydroclimate across the rainforest

and savannah ranges of *M. s. splendida*, establishing the contained populations as distinct climatic ecotypes. Chapter 4 enabled us to characterise differences in physiological tolerance and plasticity among ecotypes, providing greater understanding of existing potential for responses to future climate change. We highlighted trade-offs between generalist and specialist adaptations among these regions, and the potential for greater risks within the rainforest compared to savannah ecotype. Future studies of genomic vulnerability and plastic adaptation in these, as well as co-distributed species, will increase the breadth of inferences for tropical resilience in future climates.

Appendices

1. Supplemental materials for Chapter 2

Part A: Supplemental Methods; Part B: Supplemental Results

A. Supplemental Methods

A1. Sample collection

Melanotaenia splendida splendida (eastern rainbowfish) were sampled from nine rainforest creek sites across five drainages in the Wet Tropics of Queensland, north-eastern Australia. To photograph individuals for morphometric data collection, each was positioned on a polystyrene tray immediately after death, submerged in a shallow layer of water to prevent distortion of shape by bending. Dissection pins were used to display the fish in a standard orientation (right-side-down) and to fix fins into their expanded state. Specimens were photographed using a Canon EOS 6D DSLR (EF-S 35mm f2/2.8 macro lens) attached to a horizontal mount positioned 45 cm directly above the specimens, and a ruler was included in each photograph for scaling.

Table A1. Localities and sample sizes (n) of *Melanotaenia splendida splendida* collected from the Wet Tropics of Queensland for genomic DNA and morphometric data.

Location	Catchment	Latitude	Longitude	Collected n	Final n (DNA)	Final n (Morpho)	Final n (GxPxE)
Little Mulgrave Creek	Mulgrave	-17.13	145.7	30	23	20	17
Cassowary Creek	Mossman	-16.51	145.41	30	23	30	23
Marrs Creek	Mossman	-16.47	145.36	24	20	19	15
Saltwater Creek	Saltwater Creek	-16.42	145.36	30	24	21	19
Stewart Creek	Daintree	-16.32	145.32	30	25	22	20
Douglas Creek	Daintree	-16.28	145.3	30	24	29	21
Doyle Creek	Daintree	-16.26	145.45	30	24	23	22

| Forest Creek | Daintree | -16.25 | 145.39 | 31 | 22 | 21 | 18 |
| McClean Creek | Hutchinson | -16.23 | 145.42 | 32 | 25 | 22 | 22 |

A2. DNA extraction

For DNA extractions by salting-out (modified from Sunnucks and Hales (1996), we placed approximately 5 mm^2 of each fin sample (crushed) in individual 1.5 mL microfuge tubes with 600 µL extraction buffer TNES, 20 µL proteinase K (10 µg/µL) and 10 µL RNase (10 µg/µL). Tubes were incubated at 37°C for three hours before adding 70 µL ammonium acetate, shaking for 15 seconds, chilling at -80°C for 5 minutes and centrifuging at 14,000 rpm for 5 minutes to precipitate proteins. Supernatant was decanted into a new 1.5 mL tube with 1 mL 99% ethanol, chilled at -80°C for 5 minutes, and centrifuged at 14,000 rpm for 5 minutes to precipitate DNA. Ethanol was removed and the DNA pellet was washed twice with 70% ethanol solution. The pellet was air-dried and resuspended in 17 µL of TE buffer. High-quality samples were diluted to 20 ng/µL and stored at -20°C.

A3. Library preparation

For each sample, 300 ng of genomic DNA was digested with SbfI-HF and MseI restriction enzymes (New England Biolabs). The cleaved fragments were ligated to adapter sequences and one of 96 unique 6-bp barcodes designed in-house. Groups of 12 individual samples were then pooled to create 8 libraries per lane and purified using AMPure XP beads (Agencourt) to remove small DNA fragments and other contaminants. Then, DNA size-selection was performed using automated gel electrophoresis (agarose, 1.5%) via Pippin Prep (Sage Science) to select fragments within a 250 – 800 bp range. A Qubit fluorometer (Life Technologies) was used to quantify library concentrations. Finally, libraries were amplified by polymerase chain reaction (PCR), using two 25 µL reactions per pool to minimise PCR clonal artefacts associated with larger volumes. Reactions were recombined, and a 2100 Bioanalyzer (Agilent Technologies) was used to verify that fragment size distribution was within the target range. Both the Qubit fluorometer (Life Technologies) and Real Time PCR were used to reconfirm quantity

of DNA, and each of the 8 libraries were pooled in equimolar concentrations to form five lanes of 96 uniquely barcoded samples.

A4. Bioinformatics: read trimming, alignment to genome, variant calling and filtering

Using VCFTOOLS 0.1.15 (Danecek et al. 2011), we removed loci with >20% missing data and minor allele frequency <3%, with the latter being biologically feasible but commonly related to calling errors. We also removed loci within indels, which can arise by different mechanisms and produce different functional effects than SNPs. We checked frequency of missing data per individual, and from the original unfiltered dataset, removed individuals with >30% missing data. The above filtering steps were then repeated for the unfiltered dataset with low coverage individuals removed to produce a filtration unbiased by low quality samples.

Also using VCFTOOLS, complex genotypes (e.g., multi-nucleotide polymorphisms) were decomposed and removed. We filtered by quality, compensating by coverage (QUAL / DP > 0.20) to prevent unrealistic inflation of locus quality scores (Li 2014). We removed loci with mapping quality >30, then calculated the mean depth of coverage and filtered by the mean +2SD to remove potentially merged paralogous sites. We also filtered for Hardy Weinberg Equilibrium (HWE) by sampling location, removing SNPs $< p = 0.05$ in 25% or more populations. Although large deviations from HWE are expected among populations due to non-random mating, these deviations can indicate erroneous variant calls when occurring within sampling sites.

Finally, we implemented a filter for linkage disequilibrium (LD) to reduce the likelihood of non-random associations among loci due to proximity in the genome. We first used VCFTOOLS to calculate the correlation coefficient between each pair of loci. In R (RC Team 2019), we fitted a spline to calculate the exponential decay of LD by physical distance (bp) and used a Tukey anomaly criteria (95%

probability distribution;) to select a cut-off (189 bp) where the rate of linkage decay was no longer significant. Given that R^2 values (and therefore LD) do not statistically decrease beyond this distance, most SNPs are expected to be unlinked. Where more than one of the identified SNPs occurred within the cut-off distance, all but one were excluded from the dataset. This left a total of 14,540 high quality SNPs for further analysis.

Table A4: Genome assembly summaries of the draft genome of the subtropical rainbowfish *Melanotaenia duboulayi* (Beheregaray et al. unpublished)

	Scaffold Size (bp)	Number	Contig Size (bp)	Number
N90	17,141	4,479	2,997	45,284
N80	65,581	2,168	7,159	29,442
N70	139,303	1,358	11,062	20,864
N60	222,945	915	15,334	14,998
N50	321,989	620	19,980	10,617
Longest	3,014,379	--	226,189	--
Total Size	785,682,952	--	766,736,644	--
Total number (>=100bp)	785,682,952	187,802	766,736,644	258,080
Total number (>=2kb)	743,062,104	9,685	705,878,805	51,681

A5. Differentiating putatively neutral versus outlier loci

Prior to assessing conformity of loci to neutral expectations we ran a preliminary structure analysis using FASTSTRUCTURE 1.0 (Raj et al. 2014) for the full filtered dataset of 14,540 SNPs. We first converted the VCF file to FASTSTRUCTURE format using PGDSPIDER 2.0 (Lischer and Excoffier 2012), then ran the model with the default convergence criterion of 10^{-6}, a simple prior, and ten replicate runs per a maximum of 10 K. The number of model components best able to explain structure in the data was determined using the function "chooseK.py".

A6. Genetic diversity and inference of population structure

To prepare input files for population genetic analyses, we converted the full SNP dataset and putatively neutral dataset from VCF to STRUCTURE (.str) format using PGDSPIDER . The same program was used to subsequently convert STRUCTURE files to FASTSTRUCTURE (.str), ARLEQUIN (.arl) and PAUP* (concatenated SNPs; phylip format) formats. For BAYPASS 2.2 (Gautier 2015), PGDSPIDER was first used to convert .str files to GESTE format, before using the script *geste2baypass* (Pina-Martins 2016) to create a BAYPASS (.txt) file with allele counts based on sampling locality. For packages implemented in R (e.g. ADEGENET, HIERFSTAT, VEGAN, and others), .str files were imported as GENIND objects using ADEGENET 2.0.0 (Jombart 2008).

To produce an unrooted Neighbour Joining Tree, we imported the neutral SNP dataset in concatenated (phylip) format to PAUP* 4.0 (Swofford and Sullivan 2003a). We ran the Neighbour Joining Tree analysis using pairwise TN93 distances (Tamura and Nei 1993), with other settings as default. *N.B.* where one individual was identified as an extreme outlier, photographic documentation was re-examined to confirm species identification error. The misidentified individual, confirmed as a co-distributed but non-hybridising *Melanotaenia maccullochi*, was removed from subsequent analyses, and prior population genetic analyses were repeated.

To produce a scaled covariance matrix of population allele frequencies (Ω), we used <small>BAYPASS</small> 2.2 (Gautier 2015) core model, based on the full SNP dataset. This hierarchical Bayesian model explicitly incorporates neutral correlation structure, providing an informative basis for demographic inference by accounting for structure resulting from shared history. The method follows from the BayEnv model proposed by (Coop et al. 2010, Günther and Coop 2013), but with several extensions to improve accuracy by estimation of prior distributions. The core model was executed using the command line, with default settings. From here, the resulting scaled covariance matrix (Ω) was visualised in R, using the *cov2cor* R function to produce a correlation matrix $\sum$, which was plotted as a correlation heatmap.

Using the neutral dataset, we re-examined population structure using <small>FASTSTRUCTURE</small> 1.0 (Raj et al. 2014), an algorithm for variational Bayesian inference of global ancestry. This method assesses allele frequency variations to find the number of clusters best approximating the log-marginal likelihood of parametric posterior distributions over hidden variables. We ran the model with the default convergence criterion of 10^{-6}, a simple prior, and ten replicate runs per a maximum of 10 K. The most likely number of clusters was selected using the function *chooseK*, and visualised using <small>DISTRUCT</small> 1.1 (Rosenberg 2004). We then used a Discriminant Analysis of Principal Components (DAPC) in <small>R</small> package <small>ADEGENET</small> to independently identify and describe the optimal number of genetic clusters present. DAPC considers both between- and within-group variance to best describe differences between groups, while minimising variation within. The function *find.clusters* was first used to transform the data using PCA, and then to run a k-means algorithm with increasing values of k (up to a possible 9 k, the number of rainforest sampling sites) using all PCs.

A7. Characterising environmental variation

National Environmental Stream Attributes v1.1.3 were obtained Geoscience Australia (Stein 2011), a custodian for national surface hydrology data. The National Environmental Stream Attributes describe both natural and anthropogenic characteristics of the stream and catchment environment supplied by

state and national jurisdictions to form a comprehensive national dataset. We initially downloaded lookup tables for all available attributes (>400) and, using $_{ARCMAP}$ 10.3 (ESRI 2011), connected the relevant attributes for each sampling site using raster files from the associated 9 Second DEM Derived Stream Network. Of the available variables, we pruned those for which there was no variation between sampling sites, were provided at a scale larger than the distance between most sampling sites (i.e. catchment level as opposed to stream level), or had missing data for any of the sampling sites. After this, ~83 variables remained. A Pearson correlation was performed in $_R$, and if two attributes were highly correlated ($|r| \geq 0.7$), one was removed from the dataset. While we recognise that there is not a perfect way of selecting which variables to keep, particularly where variables interact with each other, we prioritised retention of variables considered less likely to be derived in the system, and most likely to be important for the biology of the species, as indicated in previous studies of Australian freshwater fishes (e.g. Attard et al. (2018), Brauer et al. (2018)).

	STR ANN TEMP (°C)	STR ANN RAIN (mm)	RUN SUMMER MEAN (ML)	RDI (index: 0-1)	ASPECT (°)	STR DENSITY (km/km²)	
							HIGH
MSLM	23.95	2025.63	32734.99	0.010	127.01	1.01	
MSCA	24.47	2030.50	8630.67	0.070	338.10	0.97	
MSMA	24.46	2210.71	5887.23	0.124	25.33	0.93	
MSSA	24.33	2350.00	11915.01	0.024	51.19	1.14	
MSST	24.40	2742.62	51975.84	0.010	340.19	1.03	
MSDO	24.33	2764.57	31506.39	0.020	60.76	1.08	
MSDY	24.33	3173.78	4013.73	0.054	142.07	0.57	
MSAN	24.13	3153.86	2036.09	0.151	212.48	0.79	
MSMC	23.73	3181.89	1766.47	0.050	15.07	1.22	LOW

Figure A7. Raw climate data for each sampling locality of *Melanotaenia splendida splendida*. Shading represents relative variation among sites specific to each variable.

A8. Genotype-environment associations

The standard covariate model of BAYPASS 2.2 (Gautier 2015) tests linear associations between each SNP and each of a set of given environmental variables. The auxiliary model, used here, extends upon this method by introducing a Bayesian auxiliary variable for each regression coefficient to indicate whether a SNP is associated with a given climatic variable. Posterior distributions are then evaluated to produce a Bayes Factor (BFmc) indicating strength of evidence for each association. The method implicitly corrects for multiple-testing effects, whereby an increase in the number of explanatory variables can increase the likelihood of false positives. First, we centred and scaled environmental variables in R (*scale* function) to standardise comparisons relative to the total variation of each factor. We then ran the auxiliary model with default parameters to test associations between population-specific allele count data (14,540 SNPs) and the scaled environmental variables, while accounting for assumed population demographic structure (the scaled covariance matrix of population allele frequencies (Ω) resulting from the core model). Finally, the Bayes Factor estimates, and the underlying regression coefficients, were plotted in R using the *plot* function.

For the RDAs, we began with the same 14,540 quality-filtered and unlinked SNPs previously converted to a GENIND object using the R package ADEGENET. Genotypes were obtained from reference allele counts, then, missing data were replaced with the most common genotype for that locus. This is a conservative approach, in that it's more likely to minimise than exaggerate differences between sampled populations. We also used the same set of centred and scaled environmental variables as for the BAYPASS GEA analysis. To assess potential associations between genotype and environmental variables, we used the R package VEGAN 2.5-6 (Oksanen et al. 2019) to perform the following functions. First, an initial global RDA was run using the six environmental variables as explanatory factors, and the 14,540 SNPs used as the multivariate response (*rda* function). The variance inflation factor (VIF; *vif.cca*) for the model was calculated to ensure that no instances of multicollinearity remained between explanatory variables, with a VIF ≤ 5 considered acceptable. Analyses of variance (ANOVAs; *anova.cca*) were used with 999 permutations to test the significance of the global model, as well as each of the constrained axes. The *ordistep* function was then used with backwards-stepwise selection to determine the best

combination of explanatory variables and their relative contributions to the model. Only those found to have a significance of $p \leq 0.1$ were used in subsequent partial RDAs.

While some GEA algorithms (e.g., the BAYPASS auxiliary covariate model used above) implicitly account for the influence of neutral demographic variation, RDA methods require the partialing out of any potentially confounding explanatory factors by their inclusion in the model as conditional variables. Referred to as a partial RDA (pRDA), this method frequently incorporates a spatial conditional variable, either in the form of geographic coordinates or a measure of distance suited to the study system (e.g. river distances, as in Brauer et al. (2016)). However, neither of these measures could be said to be an accurate representation of the likelihood of gene flow in the tropical rainbowfish study system, in which some geographically distant sampling locations are connected by the same river system, while others in proximity are separated by catchment boundaries. Moreover, neither of these methods can account for effects to connectivity due to strength, direction and perenniality of river flow, or the presence of artificial barriers such as dams and weirs. We therefore chose to account for distance using genetic measures, including fixation index (F_{ST}; earlier obtained from analysis in ADEGENET) and covariance among population allele frequencies (Ω; earlier obtained from analysis in BAYPASS).

For each of these measures, population values were expanded to individual-level matrices. We then performed principal coordinate analyses (PCoA) on the respective distances (*pcoa* function implemented in R package APE 5.3 (Paradis and Schliep 2019)), retaining only the significant PCo axes. Partial RDAs were then performed controlling for each of the respective distance measures using explanatory variables identified as significant in the global model. As above, ANOVAs (999 permutations) were used to assess significance of the final RDA models, as well as the significance of the RDA axes within each model. Again, *ordistep* was used to assess the relative contribution of each of the explanatory variables. Finally, a list of candidate SNPs was established for each of the final RDAs (controlling for Fst, Ω and river distances respectively) by identifying outliers ± 3 standard deviations

(two-tailed *p*-value = 0.0027) from the mean loading (i.e. the correlation between the observed score and the latent score) of each significant RDA axis, following recommendations of Forester et al. (2018).

A9. Geometric morphometric analysis
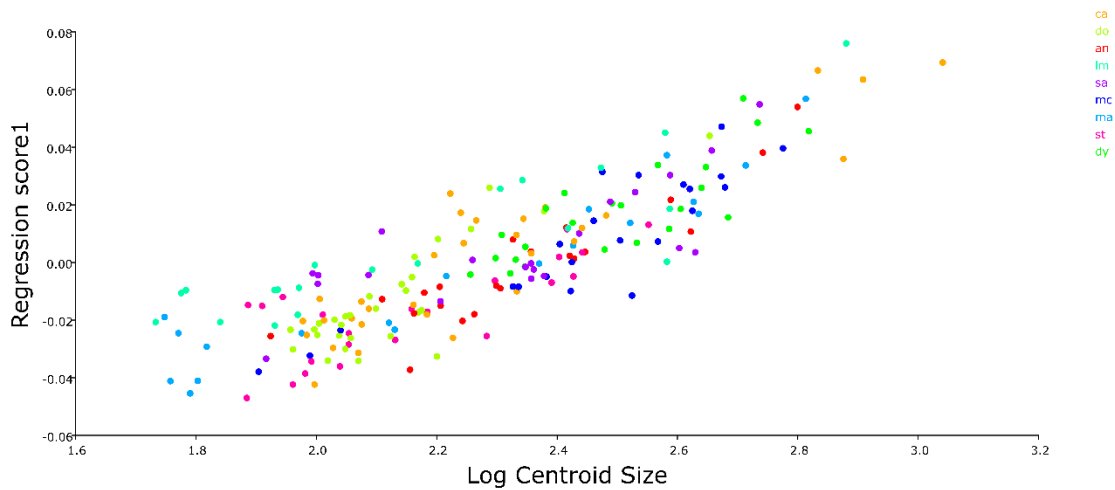
Figure A9. Regression of individual Procrustes coordinates against log centroid size pooled by sampling site, for *Melanotaenia splendida splendida* sampled from the Wet Tropics of Queensland, with predicted 30.8% of shape variation explained by size (p=<0.0001). Locality codes: LM = Little Mulgrave Creek, CA = Cassowary Creek, MA = Marrs Creek, SA = Saltwater Creek, ST = Stewart Creek, DO = Douglas Creek, DY = Doyle Creek, AN = Forest Creek, MC = McClean Creek.

A10. Phenotype-environment associations

To create the shape variable inputs, we processed the raw TPS files in $_R$ using functions developed by Claude (2008). We used individual landmark configurations to build an array (*array*), which was once again subjected to a Procrustes superimposition (*pgpa*). From the resulting configurations, shape data was extracted using orthogonal projection (*orp*) to create a response matrix of individual Procrustes values. We then ran a PCA on the Procrustes matrix (*prcomp*) and used a broken stick model (*screeplot*) to determine which components of shape variation exceeded random expectations, to be retained for the RDA. From the Procrustes matrix, we also extracted values of individual centroid size, which were

scaled (*scale*) and used to create a data frame for later inclusion as a covariable. Like genetic variation, body shape can also theoretically be influenced by adaptively neutral demographic structuring (Mitchell-Olds et al. 2007, Ho et al. 2017). As with the GEA analyses, we chose to account for neutral structure using fixation index (F_{ST}; earlier obtained from analysis in ADEGENET) and covariance among population allele frequencies (Ω; earlier obtained from analysis in BAYPASS). For each of these measures, we again expanded population values to individual-level matrices, before performing PCoAs (R package APE, retaining only significant PCo axes. *N.B.* It should be noted that although *M. s. splendida* is sexually dimorphic, we did not control for sex in final model. Sex of rainbowfishes is usually determined by fin length and colour, both of which were observed to occur on a spectrum. This meant that confident identification was not possible for all individuals, and exclusion of ambiguous individuals would have limited analytical power due to a reduced sample size. However, for the majority which were able to be identified, sex ratios did not vary significantly between sampling sites (11:14 m:f, Chi-Square *p* value = 0.987) and should therefore be unlikely to bias either morphometric or PEA results.

We then used the R package VEGAN to run an initial global RDA using the six environmental variables as explanatory factors, and the four significant PCs as the multivariate response (*rda*). ANOVAs (*anova.cca*) were run with 999 permutations to test the significance of the global model, as well as each of the constrained axes. Backwards-stepwise selection (*ordistep*) was used to determine the best combination of explanatory variables and their relative contribution. Only those with $p \leq 0.1$ were used in subsequent pRDAs. Two pRDAs were performed using explanatory environmental variables identified as significant in the global model, and the four significant PCs as the multivariate response (*rda*). They each controlled for the covariable of size, plus principal components of Ω or Fst respectively. We assessed significance of the final models, and the RDA axes contributing to each model, using ANOVA (*anova.cca*; 999 permutations). Finally, *ordistep* was used to assess the relative contribution of each of the explanatory variables.

A11. Genotype-phenotype-environment analysis

In R, we ran a global RDA using the four significant principal components of individual Procrustes distances as explanatory variables, and 864 putative adaptive alleles (identified in the genotype-environment pRDA controlling for Ω) as the multivariate response; *N.B.*, although we performed pRDAs controlling for both Ω and F_{ST} to confirm major patterns of environmental association, we chose, for simplicity, to use only adaptive candidates identified in the former analysis which has the advantage of model-based estimations of population covariance structure. The VIF (*vif.cca*) was calculated to ensure no multicollinearity between explanatory variables (VIF $\leq$ 5 considered acceptable). We used ANOVA (*anova.cca*, 999 permutations) to test significance of the global model, and the *ordistep* function to identify important explanatory variables. Those with significance of $p \leq$ 0.1 were used in the subsequent pRDA. This was performed in an identical manner, but with the introduction of size as a covariable. We again used ANOVA (*anova.cca*, 999 permutations) to test significance of the global model, as well as the significance of the RDA axes within each model. Backwards stepwise selection (*ordistep*) was used to assess the relative contribution of each explanatory shape PCo. A list of candidate SNPs was established for the partial RDA by identifying outliers ± 2 standard deviations (two-tailed *p*-value = 0.0455) from the mean loading each significant RDA axis. This cut-off is less stringent than for the original GEA analysis (± 3 std), allowing for the strong likelihood that body shape variation is polygenic in nature, and may be maintained by more subtle frequency shifts of individual alleles (Höllinger et al. 2019).

B. Supplemental Results

B1. Genome-wide SNP data

Table B1. Total number of variant sites retained after each filtering step for mapped ddRADseq reads for the eastern rainbowfish *Melanotaenia splendida splendida*.

Filtering Step	Number of SNPs
Raw catalogue	9,827,129
Genotyped in 80% of individuals, bi-allelic, minor allele frequency >0.03	62,277
Indels removed	56,745
Read quality (quality/coverage depth >0.2)	55,277
Mapping quality score > 30	41,177
Depth of coverage <mean+2SD	39,964
Missing data per locality <25%	39,157
Hardy–Weinberg equilibrium in >75% localities	37,344
Unlinked (>189 bp separation)	14,540
Putatively neutral (Bayescan)	14,478

B2. Pairwise F_{ST}

Table B2. Pairwise F_{ST} among *Melanotaenia splendida splendida* from nine rainforest sampling sites based on 14,478 putatively neutral SNPs. Locality abbreviations: LM = Little Mulgrave Creek, CA = Cassowary Creek, MA = Marrs Creek, SA = Saltwater Creek, ST = Stewart Creek, DO = Douglas Creek, DY = Doyle Creek, AN = Forest Creek, MC = McClean Creek.

	LM	CA	MA	SA	ST	DO	DY	AN
CA	0.127							
MA	0.126	0.026						
SA	0.158	0.075	0.071					

ST	0.105	0.087	0.084	0.111				
DO	0.108	0.088	0.086	0.113	0.017			
DY	0.119	0.099	0.097	0.124	0.029	0.028		
AN	0.109	0.090	0.089	0.115	0.021	0.019	0.028	
MC	0.208	0.174	0.174	0.202	0.127	0.130	0.141	0.132

B3. Discriminant Analysis of Principal Components
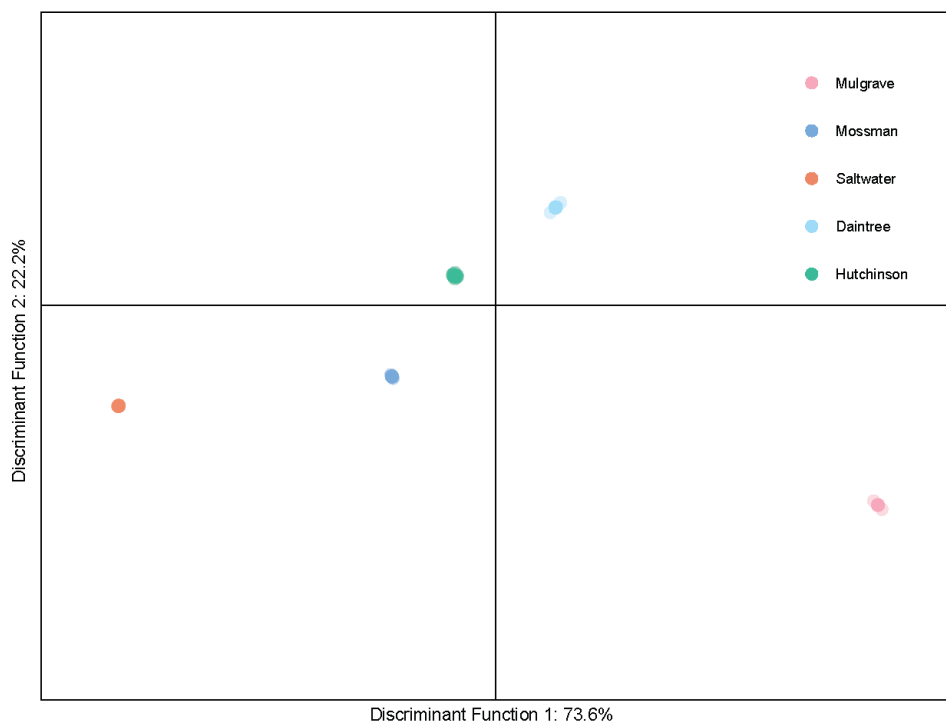
Figure B3. Discriminant analysis of principal components of putatively neutral genetic variation (14,478 SNPs) for the eastern rainbowfish (*Melanotaenia splendida splendida*) individuals sampled from nine localities among five drainage systems in the Wet Tropics of Queensland. Colours correspond simultaneously to drainage and the most likely group membership inferred by the model (K = 5).

B4. Neighbour-joining Tree
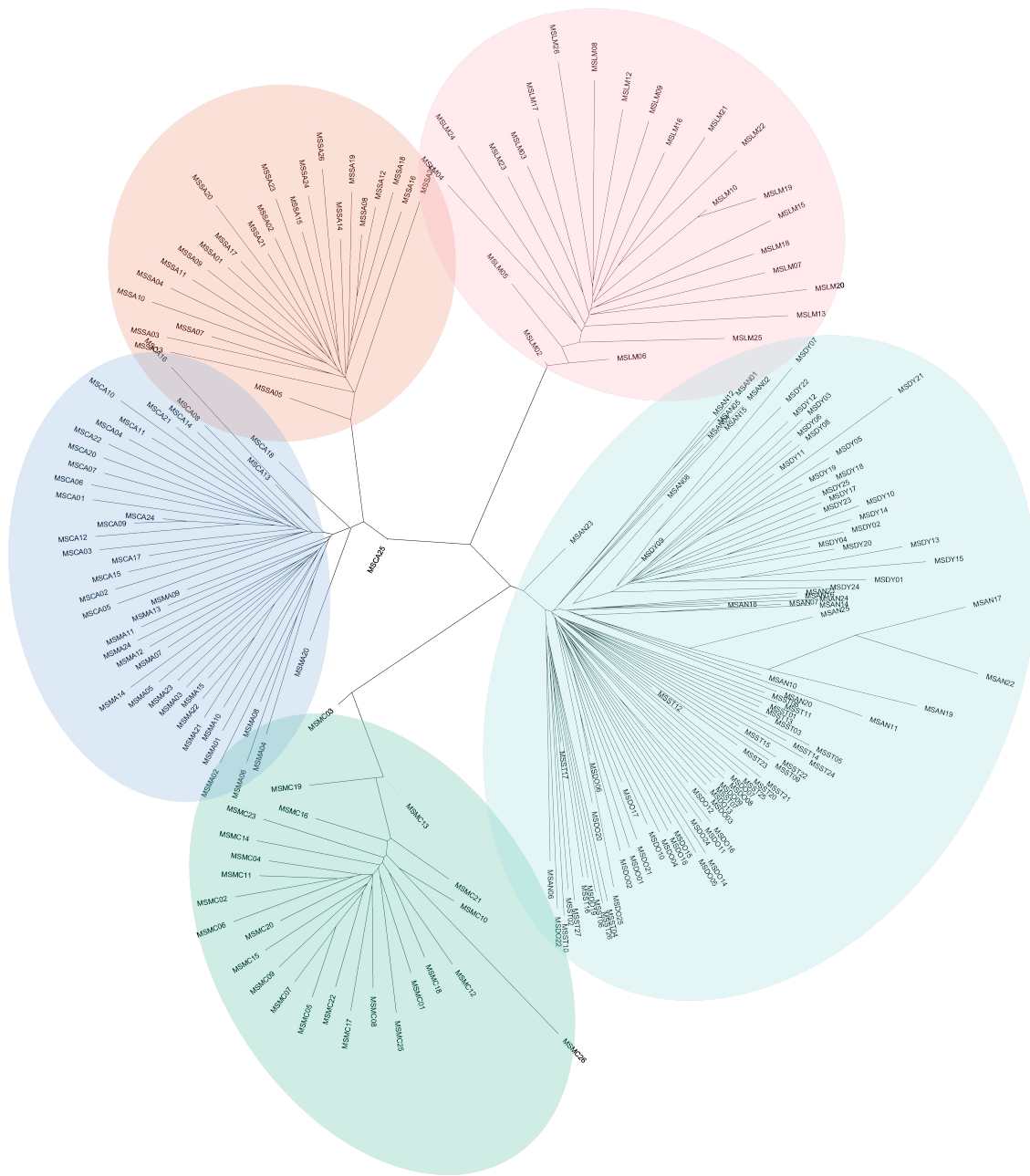
Figure B4. Unrooted neighbour-joining tree for individual genetic distances (TN93) based on 14,478 putatively neutral loci for the rainbowfish *Melanotaenia splendida splendida* in the Wet Tropics of Queensland. Colours loosely encircle individuals by drainage system of origin (Mulgrave, Mossman, Saltwater, Daintree, Hutchinson).

B5. Partial RDA model contributions
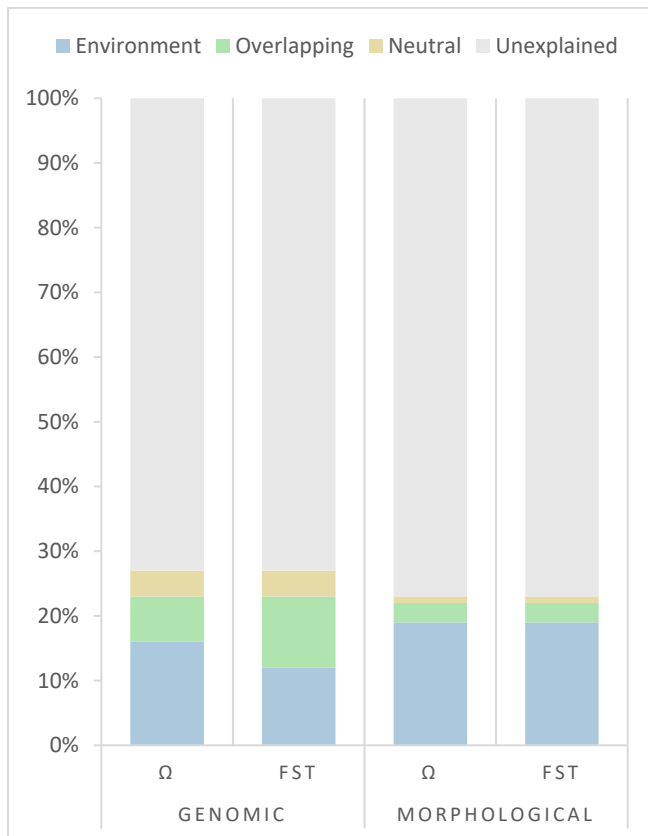
Figure B5. Percentage stacked column graph representing variance partitioning of pRDA response variables (genomic variation or morphological variation of *Melanotaenia splendida splendida*) among environmental explanatory variables (Table 2, main text) and neutral covariables (allelic covariance (Ω); F_{ST} distances (*F*ST)). Colours correspond to proportion of variation best explained by: environmental variables = "Environment"; by neutral variables = "Neutral"; by environmental or neutral variables equally = "Overlapping"; or by none of the variables included in the model = "unexplained".

B6. Global redundancy analysis of genotype-environment associations
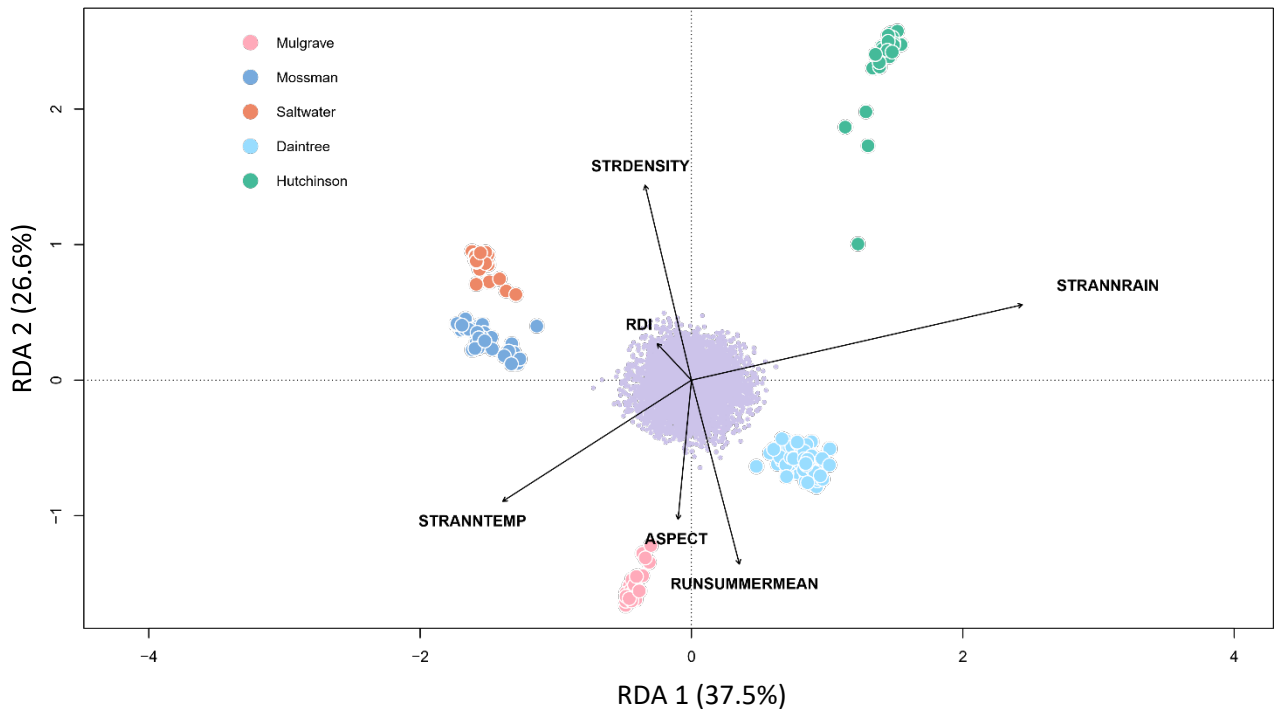
Figure B6. Ordination plot summarising the first two axes of a global redundancy analysis for genomic variation (14,540 SNPs) of *Melanotaenia splendida splendida* individuals as explained by six significantly associated environmental variables (p = <0.001). Large points represent individual-level responses, and are coloured by drainage system of origin. Small purple points represent SNP-level responses. Vectors represent the magnitude and direction of relationships with explanatory variables.

B7. GEA candidate loci identified by partial redundancy analysis, controlling for allelic covariance
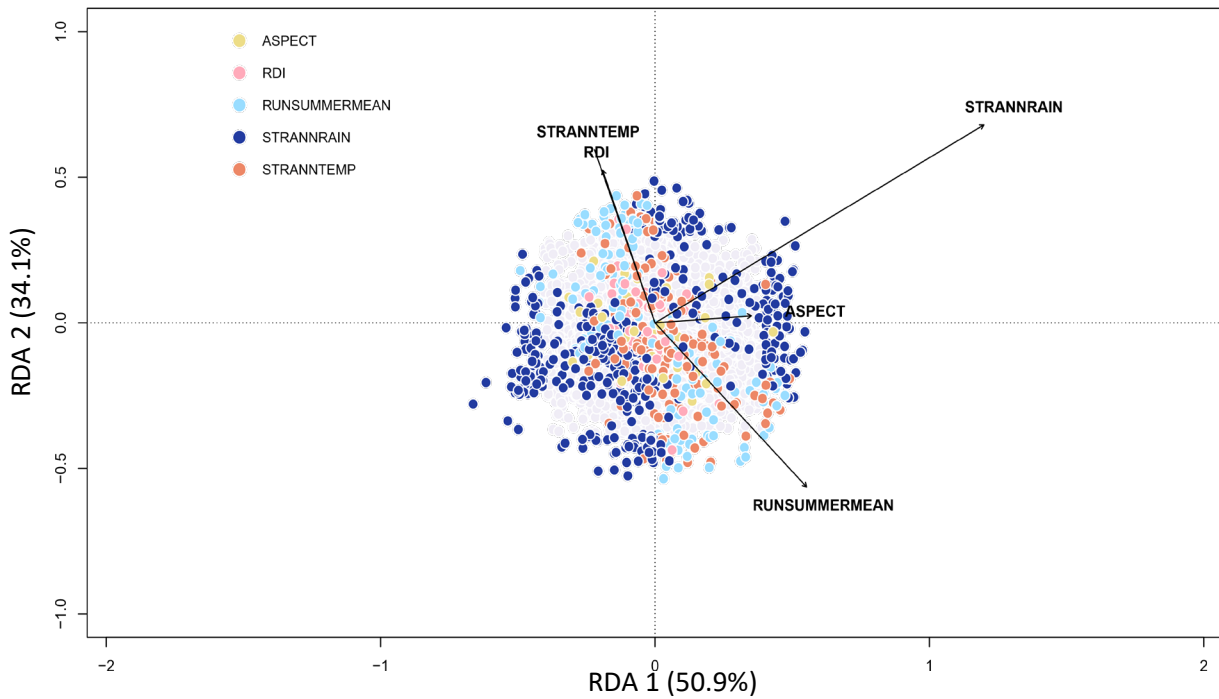
Figure B71. Partial redundancy analysis (pRDA) showing variation of 14540 SNPs from *Melanotaenia splendida splendida* rainforest individuals in relation to five environmental predictor variables, after controlling for Ω (allelic covariance) among sampling localities. The 864 SNPs represented by coloured points were strongly and significantly associated with at least one environmental predictor ($p \leq 0.0027$; colour key indicates best predictor variable), while SNPs represented by light grey points were unassociated. Vectors represent the magnitude and direction of relationships with explanatory variables.

Figure B8. Ordination plot summarising the first two axes of a partial redundancy analysis for genomic variation (14,540 SNPs) of *Melanotaenia splendida splendida* individuals as explained by six significantly associated environmental variables, (p = <0.001)after controlling for pairwise F_{ST} sampling localities. Large points represent individual-level responses, and are coloured by drainage system of origin. Small purple points represent SNP-level responses. Vectors represent the magnitude and direction of relationships with explanatory variables.

B9. Genotype environment associations using BAYPASS auxiliary covariate model
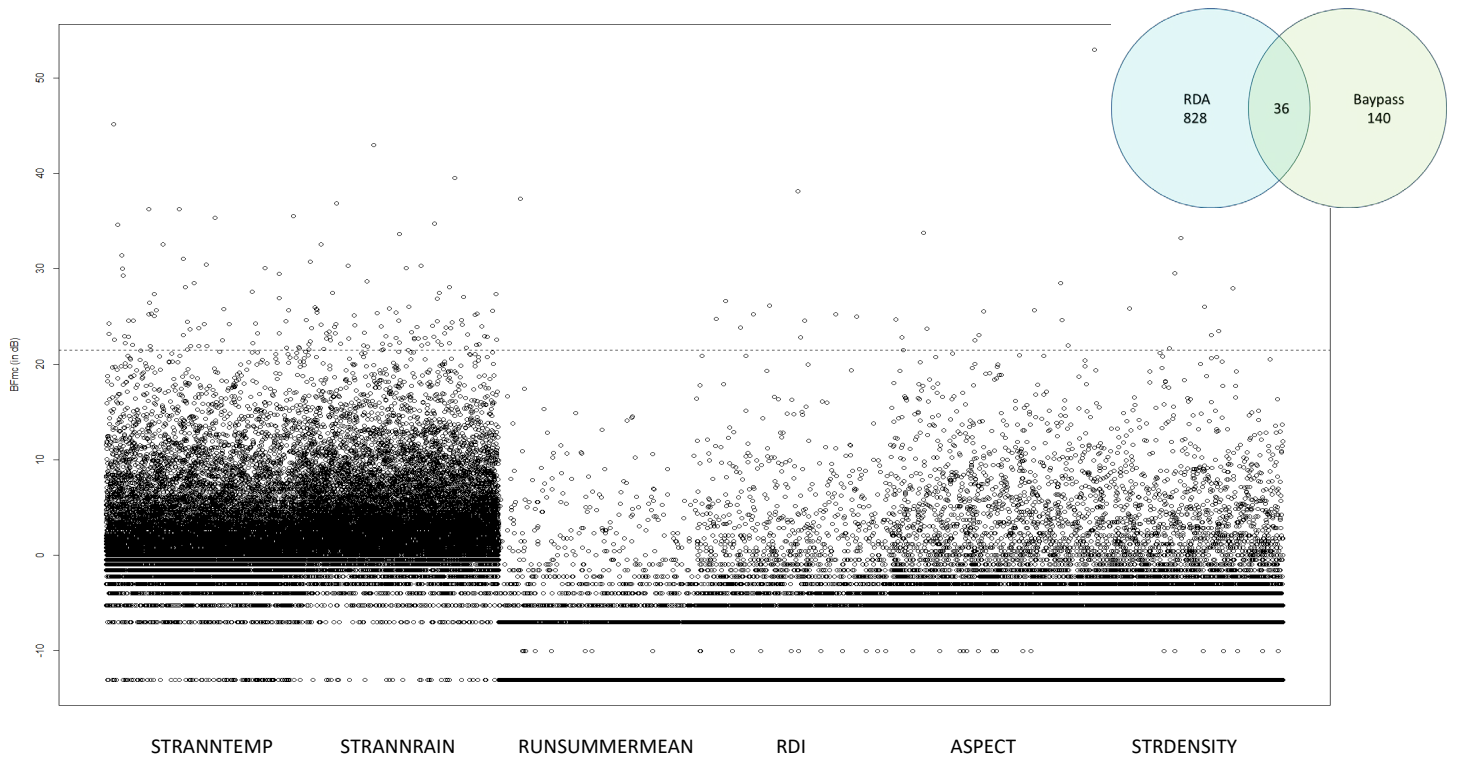
Figure B9. Climatic association of 14,540 SNPs from Melanotaenia splendida splendida across nine rainforest sampling sites against six independent environmental variables using BAYPASS auxiliary covariate model. Dashed line indicates Bayes Factor cutoff of 21.46 dB (99.8% probability), above which 176 loci were identified as candidates for climatic adaptation. Inset: 36 of these candidates (20%) were also identified using partial redundancy analysis (RDA).

B10. Morphometric variation among localities
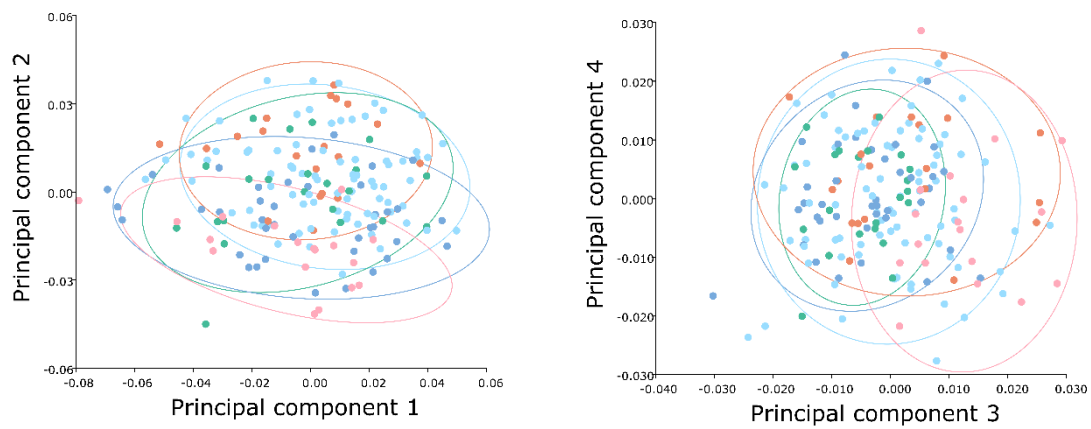
Figure B10. Significant principal components of body shape variation for *Melanotaenia splendida splendida* individuals sampled across the Wet Tropics of Queensland. PCA scatterplots show relative variation among individuals, with colours and equal frequency ellipses (90% probability) show for drainage system of origin (Mulgrave, Mossman, Saltwater, Daintree, Hutchinson).

B11. Canonical variate analysis of body shape variation
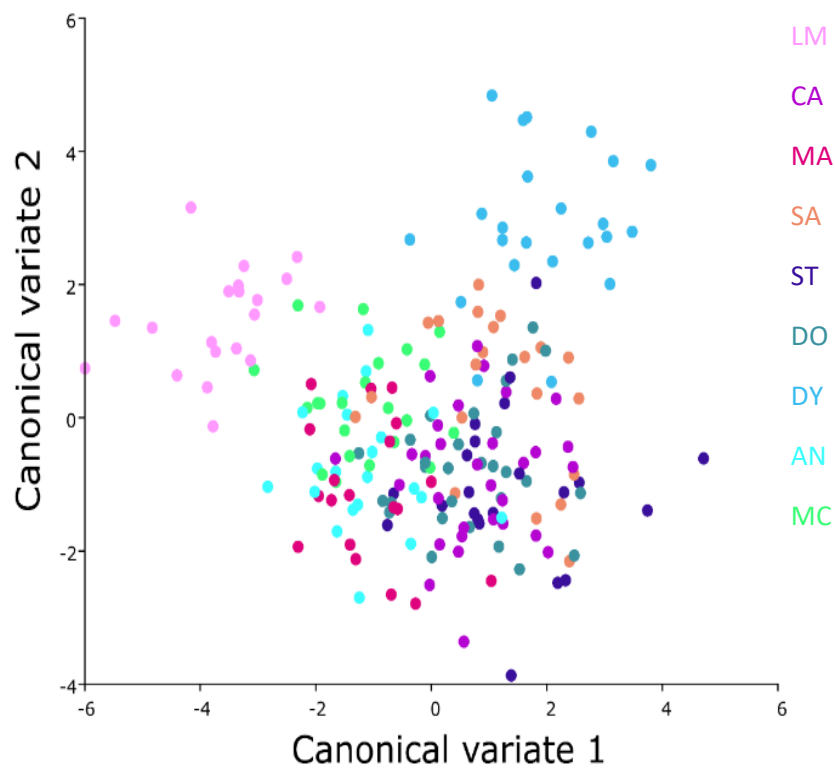
Figure B11. Canonical variate analysis of body shape variation of *Melanotaenia splendida splendida* among nine rainforest sampling sites. Locality codes: LM = Little Mulgrave Creek, CA = Cassowary Creek, MA = Marrs Creek, SA = Saltwater Creek, ST = Stewart Creek, DO = Douglas Creek, DY = Doyle Creek, AN = Forest Creek, MC = McClean Creek.

Table B11. Procrustes distances among sampling sites and among drainage systems, based on canonical variate analysis of body shape of *Melanotaenia splendida splendida*. Locality codes: LM = Little Mulgrave Creek, CA = Cassowary Creek, MA = Marrs Creek, SA = Saltwater Creek, ST = Stewart Creek, DO = Douglas Creek, DY = Doyle Creek, AN = Forest Creek, MC = McClean Creek. P-values from 10000 permutations: *** = $p<0.01$, ** = $p<0.05$, * = $p<0.10$.

	BY SAMPLING SITE							
	AN	CA	DO	DY	LM	MA	MC	SA
CA	0.014***							
DO	0.015***	0.016***						
DY	0.026***	0.029***	0.024***					
LM	0.033***	0.030***	0.035***	0.041***				
MA	0.015***	0.015***	0.015***	0.030***	0.025***			
MC	0.008	0.016***	0.014**	0.024***	0.034***	0.016***		
SA	0.024***	0.024***	0.016***	0.017***	0.040***	0.025***	0.021***	
ST	0.018***	0.023***	0.013**	0.023***	0.043***	0.024***	0.015**	0.015**

	BY DRAINAGE SYSTEM			
	Mulgrave	Mossman	Saltwater	Daintree
Mossman	0.027***			
Saltwater	0.040***	0.023***		
Daintree	0.036***	0.016***	0.013***	
Hutchinson	0.034***	0.014***	0.021***	0.012**

B12. GxPxE candidate loci identified by partial redundancy analysis
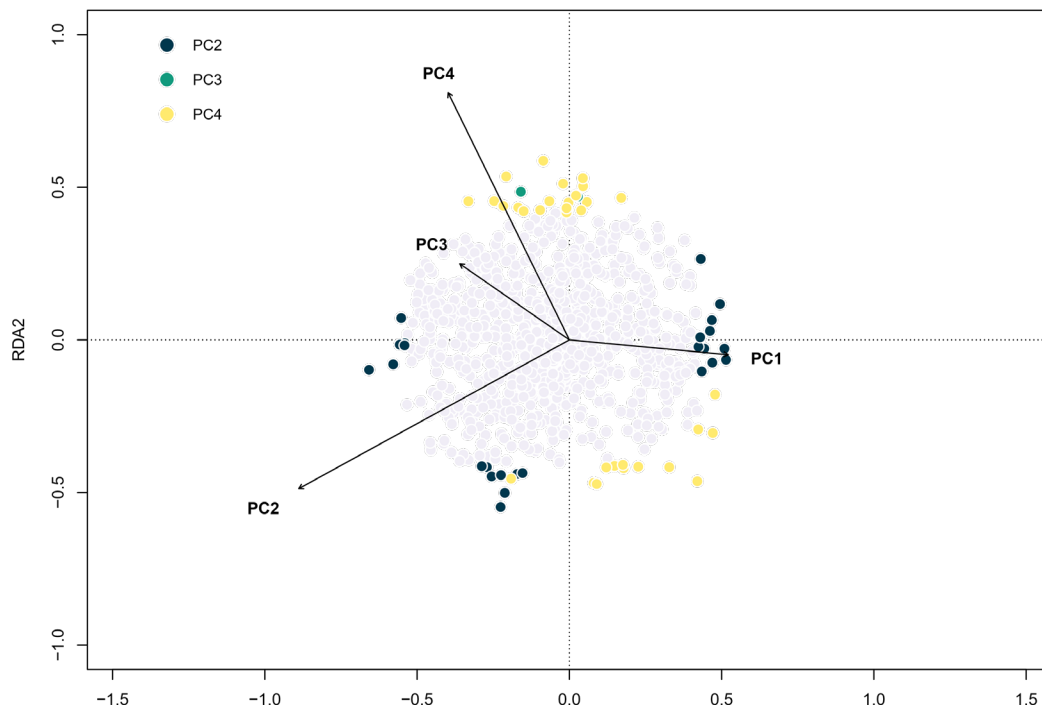
Figure B12. Partial redundancy analysis (RDA) showing variation of 864 SNPs from *Melanotaenia splendida splendida* rainforest individuals in relation to four principal components (PCs) of body shape, after cont. The 61 SNPs represented by coloured points were significantly associated with at least one body shape PC (p ≤ 0.0455; colour key indicates best predictor variable), while SNPs represented by light grey points were not. Vectors represent the magnitude and direction of relationships with explanatory variables.

2. Supplemental Material for Chapter 3

Part A: Supplemental Methods; Part B: Supplemental Results

A. Supplemental Methods

	STR ANN TEMP (°C)	STR ANN RAIN (mm)	RUN SUMMER MEAN (ML)	RUN WINTER MEAN (ML)	RDI (index: 0-1)	VALLEY SLOPE (%)	ASPECT (°)	STR DENSITY (km/km²)	
LM	23.95	2025.63	32734.99	841.00	0.01	0.85	127.01	1.01	HIGH
CA	24.47	2030.50	8630.67	14.67	0.07	0.32	338.10	0.97	
MA	24.46	2210.71	5887.23	10.44	0.12	0.62	25.33	0.93	
SA	24.33	2350.00	11915.01	153.05	0.02	0.22	51.19	1.14	
ST	24.40	2742.62	51975.84	601.22	0.01	0.12	340.19	1.03	
DO	24.33	2764.57	31506.39	205.31	0.02	0.43	60.76	1.08	
DY	24.33	3173.78	4013.73	44.02	0.05	5.51	142.07	0.57	
AN	24.13	3153.86	2036.09	21.18	0.15	9.24	212.48	0.79	
MC	23.73	3181.89	1766.47	21.67	0.05	9.41	15.07	1.22	
FA	21.77	1129.53	2166.42	0.33	0.06	4.04	18.59	0.81	
WN	23.10	1308.29	305467.60	345.83	0.05	0.20	354.11	1.01	
EN	23.08	1381.96	130284.80	241.02	0.09	0.13	337.75	0.94	
LA	24.70	976.38	453350.50	12.93	0.08	0.06	17.35	0.95	
KE	25.20	1017.09	259012.90	0.00	0.04	0.04	14.31	0.90	
NK	25.31	1044.46	64037.12	0.00	0.03	0.07	27.78	0.63	
HA	25.30	1070.00	173939.90	0.00	0.10	0.18	62.61	0.61	
MO	25.40	1073.47	341.29	0.00	0.05	0.37	109.16	1.38	LOW

Figure A1. Raw climate data for each sampling locality of *Melanotaenia splendida splendida*. Shading represents relative variation among sites specific to each variable. Locality abbreviations: refer to table A1. Compiled from Stein, J. L., Hutchison, M.F., Stein, J.A. . 2011. National Environmental Stream Attributes v1.1.3. Page http://pid.geoscience.gov.au/dataset/ga/73045   Geoscience Australia, Canberra. Accessed June 2017.
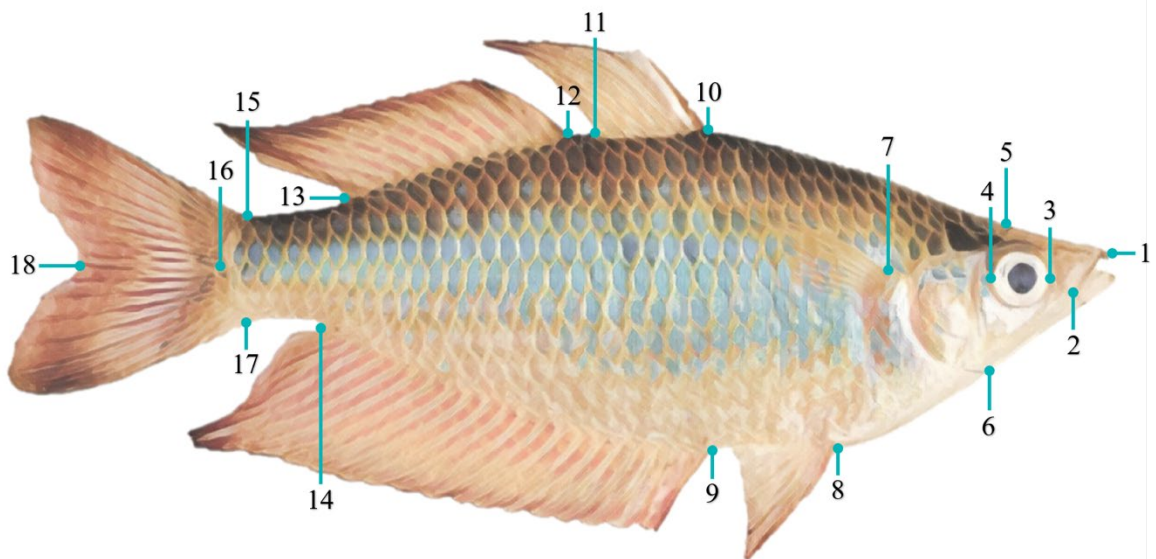
Figure A2. The 18 landmarks used for geometric morphometric analysis of the eastern rainbowfish *Melanotaenia splendida splendida*. 1: Anterior tip of head, where premaxillary bones articulate at midline; 2: Posterior tip of maxilla; 3: Anterior margin in maximum eye width; 4: Posterior margin in maximum eye width; 5: Dorsal margin of head at beginning of scales; 6: Ventral margin in the end of the head; 7: Dorsal insertion of pectoral fin; 8: Anterior insertion of the pelvic fin; 9: Anterior insertion of the anal fin; 10: Anterior insertion of the first dorsal fin; 11: Posterior insertion of the first dorsal fin; 12: Anterior insertion of the second dorsal fin; 13: Posterior insertion of the second dorsal fin; 14: Posterior insertion of the anal fin; 15: Dorsal insertion of the caudal fin; 16: Posterior margin of the caudal peduncle (at tip of lateral line); 17: Ventral insertion of the caudal fin; 18: Posterior margin of the caudal fin between dorsal and ventral lobes.

Table B1. Table B2. Pairwise F_{ST} among *Melanotaenia splendida splendida* from 17 sampling sites across in tropical north-eastern Australia, based on 14,478 putatively neutral SNPs. Locality abbreviations: refer to Table 1, main text.

	CA	MA	SA	ST	DO	DY	AN	MC	FA	WN	EN	LA	KE	NK	HA	MO
CA	0.128															
MA	0.126	0.026														
SA	0.158	0.075	0.071													
ST	0.105	0.087	0.084	0.111												
DO	0.108	0.088	0.086	0.113	0.017											
DY	0.119	0.099	0.097	0.125	0.029	0.027										
AN	0.109	0.090	0.089	0.115	0.021	0.019	0.027									
MC	0.208	0.174	0.174	0.202	0.127	0.130	0.141	0.132								
FA	0.134	0.155	0.153	0.184	0.127	0.131	0.141	0.131	0.227							
WN	0.138	0.159	0.159	0.188	0.129	0.134	0.144	0.135	0.232	0.030						
EN	0.144	0.165	0.166	0.194	0.134	0.138	0.148	0.139	0.237	0.040	0.019					
LA	0.124	0.146	0.145	0.174	0.118	0.123	0.132	0.123	0.215	0.017	0.024	0.032				
KE	0.124	0.147	0.146	0.175	0.118	0.123	0.133	0.124	0.218	0.027	0.029	0.037	0.019			
NK	0.121	0.142	0.145	0.172	0.113	0.117	0.127	0.119	0.214	0.029	0.033	0.041	0.025	0.024		
HA	0.116	0.139	0.138	0.168	0.113	0.117	0.127	0.117	0.210	0.029	0.033	0.041	0.023	0.021	0.020	
MO	0.115	0.138	0.136	0.166	0.111	0.114	0.124	0.115	0.209	0.029	0.033	0.041	0.024	0.023	0.020	0.014
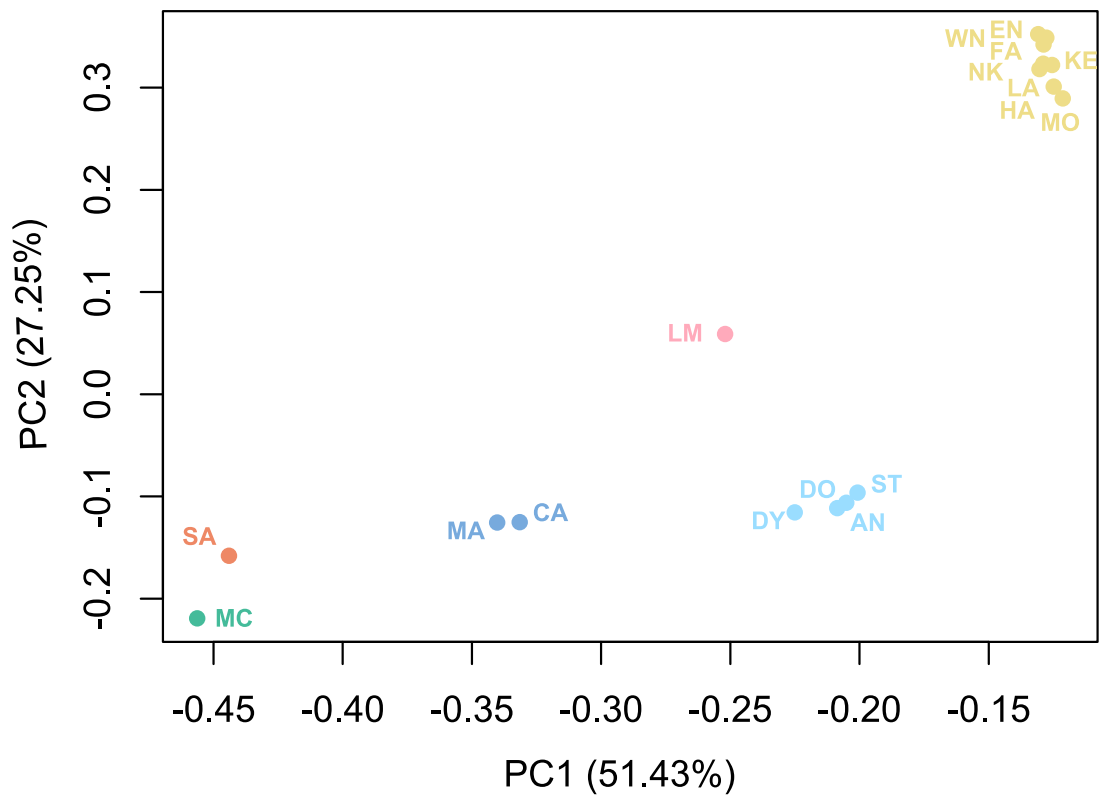
Figure B2. Eigen-decomposition of scaled covariance matrix of locality-specific allele frequencies for *Melanotaenia splendida splendida*, based on 14,540 SNPs. Points correspond to sampling sites, and are colour coded by drainage system of origin following Figure 1, main text.
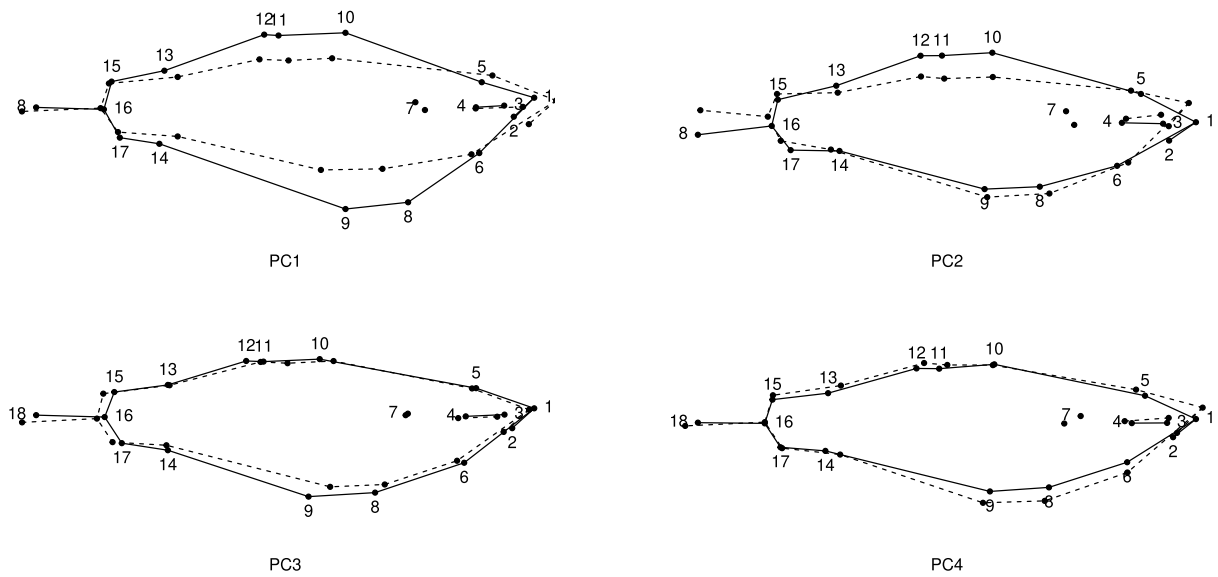
Figure B3. Principal component analysis of body shape of all M. s. splendida individuals produced four significant PCs under broken stick modelling Wireframe graphical representation of significant principal components of body shape variation based on 18 landmarks for 366 *Melanotaenia splendida splendida* individuals sampled across seventeen rainforest and savannah sampling localities in tropical north-eastern Australia. Solid and dashed frames respectively represent body shape at high and low extremes of each significant axis (scale factor = 1).
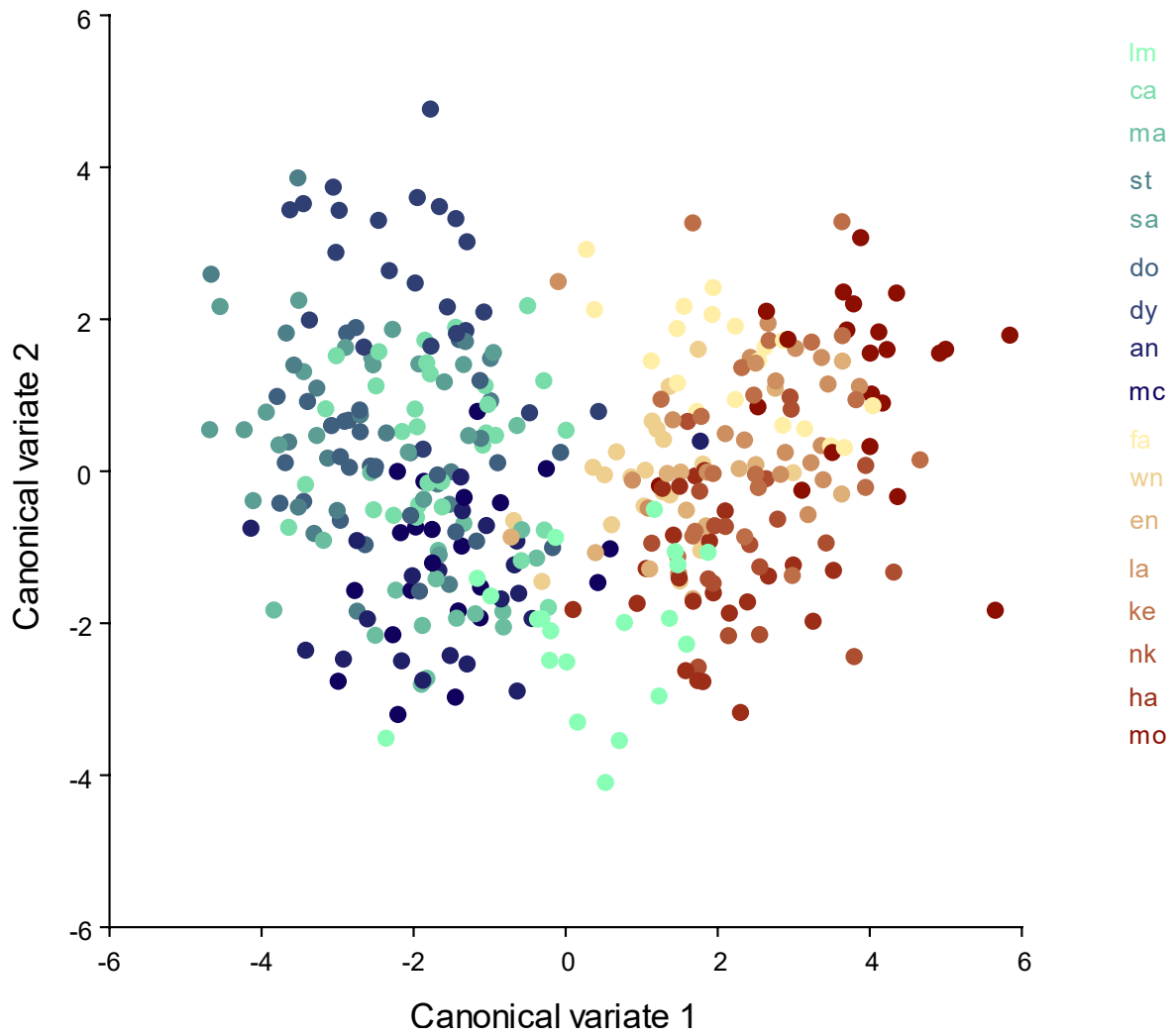
Figure B4. Individual canonical body shape variation of 366 *Melanotaenia splendida splendida* individuals sampled across seventeen rainforest and savannah sampling localities in tropical north-eastern Australia. Locality codes follow Figure A1.

Table B2. Procrustes distances among sampling sites, based on canonical variate analysis of body shape of *Melanotaenia splendida splendida* across rainforest and savannah localities (For codes refer to Figure A1). Significant differences ($p = <0.05$) are indicated by bold font.

	AN	CA	DO	DY	EN	FA	HA	KE	LA	LM	MA	MC	MO	NK	SA	ST
CA	**0.0138**															
DO	**0.0142**	**0.0165**														
DY	**0.0256**	**0.0266**	**0.0204**													
EN	**0.0282**	**0.0234**	**0.0339**	**0.0403**												
FA	**0.0338**	**0.0277**	**0.0391**	**0.0441**	0.0139											
HA	**0.0288**	**0.0243**	**0.0346**	**0.0412**	0.012	**0.0147**										
KE	**0.0321**	**0.0275**	**0.0355**	**0.0337**	**0.0186**	**0.0202**	**0.0193**									
LA	**0.0263**	**0.0214**	**0.0304**	**0.0322**	**0.0151**	**0.0197**	**0.0152**	0.0101								
LM	**0.0312**	**0.0289**	**0.0351**	**0.0368**	**0.0203**	**0.0267**	**0.0224**	**0.0186**	**0.0199**							
MA	**0.0138**	**0.0148**	**0.0156**	**0.0275**	**0.0247**	**0.0324**	**0.0254**	**0.0288**	**0.0234**	**0.0243**						
MC	0.008	**0.014**	0.012	**0.0241**	**0.0294**	**0.035**	**0.0297**	**0.032**	**0.026**	**0.0313**	0.0134					
MO	**0.0396**	**0.0354**	**0.0446**	**0.0412**	**0.0244**	**0.0229**	**0.0248**	**0.0121**	**0.0192**	**0.0263**	**0.0383**	**0.0403**				
NK	**0.0372**	**0.0324**	**0.0415**	**0.0442**	**0.0159**	**0.0163**	**0.0176**	**0.0152**	**0.0185**	**0.0197**	**0.032**	**0.0379**	**0.0183**			
SA	**0.0235**	**0.0237**	**0.0151**	**0.0153**	**0.0406**	**0.0445**	**0.0408**	**0.0362**	**0.0334**	**0.0384**	**0.0238**	**0.0209**	**0.0446**	**0.0451**		
ST	**0.0184**	**0.0244**	**0.0129**	**0.0222**	**0.0424**	**0.0476**	**0.0436**	**0.0428**	**0.0378**	**0.0434**	**0.0243**	**0.0163**	**0.0508**	**0.0501**	**0.0161**	
WN	**0.0176**	**0.0175**	**0.0224**	**0.0247**	**0.0194**	**0.0244**	**0.0217**	**0.0178**	**0.0152**	**0.0221**	**0.0187**	**0.0184**	**0.0249**	**0.0254**	0.026	**0.0285**
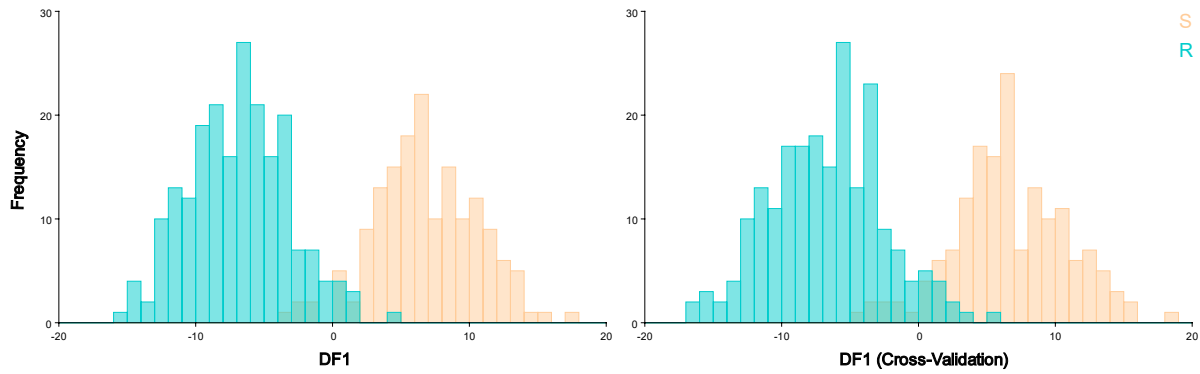
Figure B5. Frequencies of individual discriminant function (DF) scores among rainforest (n = 207) and savannah (n = 159) *Melanotaenia splendida splendida*, based on multivariate analysis of 18 morphometric landmarks, controlling for centroid size.

Table B3. Classification/misclassification tables for discriminant function analysis of 18 morphometric landmarks among rainforest (n = 207) and savannah (n = 159) *Melanotaenia splendida splendida*, controlling for centroid size. Differences between means = 0.0274 Procrustes distance, 3.705 Mahalanobis distance. *P*-value (parametric) = <.0001 for 1000 permutation runs.

Discriminant function	True origin	Allocated to		
		Rainforest	Savannah	Total
	Rainforest	200	8	208
	Savannah	5	154	159
Cross-validation	True origin	Allocated to		
		Rainforest	Savannah	Total
	Rainforest	195	13	208
	Savannah	8	151	159

Table B4. Model significance for pRDAs testing genotype-environment (GEA), phentoype-environment (PEA), and genotyoe-phenotype-environment (GxPxE) associations for *Melanotaenia spplendida splendida*, based on ANOVA-like permutation test for Constrained Correspondence Analysis (anova.cca) using 999 permutation rounds. For numbers of individuals in response datasets, refer to Table 1, main text.

Analysis	Response Dataset	Covariable	Df		Variance		F
			Model	Residual	Model	Residual	
GEA	Among-ecotypes	Allelic covariance	8	369	889.75	3076.13	13.341***
		F_{ST}	8	370	357.33	3042.78	5.431***
		river dist	8	370	376.59	3051.43	5.708***
	Rainforest-specific	Allelic covariance	5	201	625.55	2745.1	9.161***
		F_{ST}	6	201	456.47	2745.1	5.571***
	Savannah-specific	Allelic covariance	5	163	223.88	3041.22	2.3999***
		F_{ST}	5	163	126.18	3041.22	1.3525***
PEA	Among-ecotypes	Allelic covariance + size	6	294	0.000187	0.000397	23.03***
		F_{ST} + size	7	294	0.000086	0.000402	8.939***
		River distance + size	7	294	0.000086	0.000402	8.939***
	Rainforest-specific	Allelic covariance + size	4	171	0.000159	0.000486	13.969***
		F_{ST} + size	4	172	0.000137	0.000494	11.972***
	Savannah-specific	Allelic covariance + size	3	117	0.000062	0.000385	6.2968***
		F_{ST} + size	4	117	0.000077	0.000382	5.8896***
GxPxE	Among-ecotypes	Size	3	297	44.01	527.96	8.253***
	Rainforest-specific	Size	4	171	28.27	404.62	2.9866***
	Savannah-specific	Size	3	120	14.45	396.92	1.4563***

Table B5. Proportion of variation better explained by environment versus neutral factors in patrial RDAs

	Controlling for	Genomic	Morphological
Among-ecotypes	Allelic covariance	5	12
	F_{ST}	4	4
	River distance	2	9
Rainforest-specific	Allelic covariance	4	19
	F_{ST}	3	19
Savannah-specific	Allelic covariance	3	5
	F_{ST}	2	6
	Average	3.3	10.5
	Standard Deviation	1.0	5.9
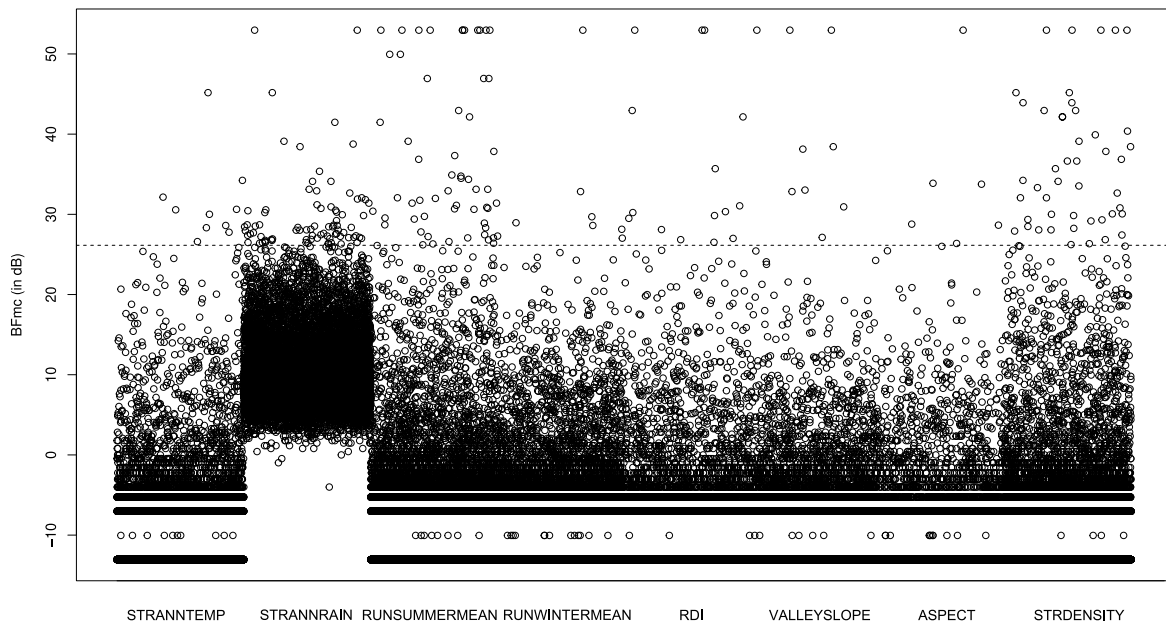
Figure B6. Environmental association of 14,540 SNPs for *Melanotaenia splendida splendida* across seventeen sampling sites, against eight independent environmental variables, using BAYPASS auxiliary covariate model. Dashed line indicates Bayes Factor cutoff of 26 dB (99.8% probability), above which 233 loci were identified as candidates for environmental adaptation.

3. Supplemental Material for Chapter 4

Supplemental Results

Table 1. Summary of assembly statistics for the transcriptome of *Melanotaenia splendida splendida*. ORF = open reading frame, bp = base pairs.

Raw read pairs	1,409,883,643
Retained filtered read pairs	911,546,879
Transcripts	320,364
Trinity "Genes"	284,807
Trinity "Genes" with ORFs	51,091
Uni-genes	30,874
N50	2053
Average contig length (bp)	1015
Assembled bases	565,956,118
ORF genes annotated	24,971

Table 2. Number of unigenes differentially expressed between control (21°C) and projected 2027 summer treatment (33°C) groups, and critical thermal maxima (CT$_{MAX}$) of five Australian *Melanotaenia* ecotypes versus. Savannah and Rainforest are *Melanotaenia splendida splendida*, Subtropical is *M. duboulayi*, Desert is *M. s. tatei*, Temperate is *M. fluviatilis*.

Ecotype	Genes DE	CT$_{MAX}$ (°C)
Temperate	39	34.8
Desert	98	37.2
Subtropical	120	37.9
Rainforest	88	38.2
Savannah	139	38.4

Table 3. Linear regression statistics for comparisons of CT$_{MAX}$ versus the number of unigenes differentially expressed between control (21°C) and projected 2027 summer treatment (33°C) groups among five Australian *Melanotaenia* ecotypes ($r = 0.909$; $R^2 = 0.827$). Savannah and Rainforest are *Melanotaenia splendida splendida*, Subtropical is *M. duboulayi*, Desert is *M. s. tatei*, Temperate is *M. fluviatilis*.

Regression Statistics					
Multiple R	0.909				
R Square	0.827				
Adjusted R Square	0.769				
Standard Error	0.706				
Observations	5				
ANOVA	df	SS	MS	F	Significance F
Regression	1	7.143	7.143	14.315	0.032
Residual	3	1.497	0.499		
Total	4	8.640			

Table 4. Gene annotations and ontology terms for unigenes differentially expressed by *Melanotaenia splendida splendida* between control (21°C) and projected 2027 summer treatments (33°C).

Gene ID	Gene Ontology Terms
BMAL2_CHICK	GO:0003700; GO:0005634; GO:0005667; GO:0005737; GO:0006351; GO:0042753; GO:0045893; GO:0046983; GO:0048511; GO:0070888
MANF_HUMAN	GO:0002576; GO:0003723; GO:0005576; GO:0005615; GO:0005634; GO:0005783; GO:0005788; GO:0005829; GO:0006986; GO:0008083; GO:0008289; GO:0031175; GO:0033018; GO:0071542; GO:1905897
SCD1_TACFU	GO:0004768; GO:0005789; GO:0006633; GO:0016021; GO:0046872
IDHC_BOVIN	GO:0000287; GO:0004450; GO:0005737; GO:0005829; GO:0006097; GO:0006099; GO:0006102; GO:0006103; GO:0006979; GO:0051287
FAS_CHICK	GO:0003697; GO:0004312; GO:0004313; GO:0004314; GO:0004315; GO:0004316; GO:0004320; GO:0005623; GO:0006089; GO:0006633; GO:0016295; GO:0016296; GO:0031177; GO:0032100; GO:0047117; GO:0047451; GO:0102131; GO:0102132
IDHP_BOVIN	GO:0000287; GO:0004450; GO:0005739; GO:0005743; GO:0005777; GO:0005829; GO:0006097; GO:0006099; GO:0006102; GO:0006103; GO:0051287
RDH11_MOUSE	GO:0001917; GO:0004745; GO:0005622; GO:0005789; GO:0016021; GO:0016062; GO:0016491; GO:0042572; GO:0042574; GO:0052650
CALR_RABIT	GO:0005509; GO:0006457; GO:0016529; GO:0030246; GO:0033018; GO:0050821; GO:0051082
HYOU1_DANRE	GO:0005524; GO:0005788
JARD2_DANRE	GO:0003677; GO:0003682; GO:0005634; GO:0006351; GO:0007275; GO:0016577; GO:0031061; GO:0035097; GO:0045892; GO:0048863; GO:0051574
ALG5_HUMAN	GO:0004576; GO:0004581; GO:0005789; GO:0006486; GO:0006487; GO:0007368; GO:0016020; GO:0016021; GO:0018279
ACLY_MOUSE	GO:0003878; GO:0005524; GO:0005654; GO:0005739; GO:0005829; GO:0005886; GO:0006084; GO:0006085; GO:0006101; GO:0006107; GO:0006633; GO:0008610; GO:0009346; GO:0046872; GO:0048037
LMAN1_MOUSE	GO:0000139; GO:0005537; GO:0005783; GO:0005789; GO:0005793; GO:0005794; GO:0006888; GO:0007029; GO:0007030; GO:0010638; GO:0015031; GO:0016021; GO:0030017; GO:0030134; GO:0033116; GO:0042802; GO:0043231; GO:0044220; GO:0046872
COF2_MOUSE	GO:0007015; GO:0007519; GO:0015629; GO:0016363; GO:0030018; GO:0030042; GO:0030043; GO:0030836; GO:0031674; GO:0045214; GO:0046716; GO:0051015
ELOV5_TACFU	GO:0005789; GO:0006636; GO:0009922; GO:0016021; GO:0019367; GO:0030425; GO:0034625; GO:0034626; GO:0035338; GO:0042761; GO:0102336; GO:0102337; GO:0102338; GO:0102756
S61A1_DANRE	GO:0005789; GO:0015031; GO:0016021; GO:0021986; GO:0039019
FAS_CHICK	GO:0003697; GO:0004312; GO:0004313; GO:0004314; GO:0004315; GO:0004316; GO:0004320; GO:0005623; GO:0006089; GO:0006633; GO:0016295; GO:0016296; GO:0031177; GO:0032100; GO:0047117; GO:0047451; GO:0102131; GO:0102132
DNJC3_HUMAN	GO:0004860; GO:0005576; GO:0005737; GO:0005783; GO:0005788; GO:0005790; GO:0005829; GO:0016020; GO:0019901; GO:0031205; GO:0035578; GO:0036494; GO:0036498; GO:0043066; GO:0043312; GO:0043687; GO:0044267; GO:0051087; GO:0051603; GO:0051607; GO:0051787; GO:0070062; GO:0070417; GO:1903561; GO:1903912
ERG7_RAT	GO:0000250; GO:0005789; GO:0006695; GO:0016125; GO:0043231
SYLC_HUMAN	GO:0002161; GO:0004819; GO:0004823; GO:0004832; GO:0005096; GO:0005524; GO:0005737; GO:0005764; GO:0005783; GO:0005829; GO:0006418; GO:0006425; GO:0006429; GO:0006438; GO:0006622; GO:0008361; GO:0010507; GO:0012505; GO:0016604; GO:0017101; GO:0034198; GO:0043547; GO:0071230; GO:0071233; GO:1904263; GO:1990253
ALKMO_DANRE	GO:0005506; GO:0005783; GO:0005789; GO:0006643; GO:0008610; GO:0016021; GO:0046485; GO:0050479
FPPS_CHICK	GO:0004161; GO:0004337; GO:0005737; GO:0006695; GO:0033384; GO:0045337; GO:0046872
PELO_DANRE	GO:0004519; GO:0005634; GO:0005737; GO:0006412; GO:0007049; GO:0032790; GO:0043022; GO:0046872; GO:0051301; GO:0070481; GO:0070651; GO:0070966; GO:0071025
DCAM_HUMAN	GO:0004014; GO:0005829; GO:0006557; GO:0006595; GO:0006597; GO:0008295; GO:0019810; GO:0046500
CASR_PIG	GO:0004930; GO:0005509; GO:0005513; GO:0005887; GO:0006874; GO:0007186; GO:0010628; GO:0016597; GO:0032781; GO:0042803; GO:0051924; GO:0070509
DDX5_HUMAN	GO:0000122; GO:0000380; GO:0000381; GO:0000398; GO:0000956; GO:0001837; GO:0003723; GO:0003724; GO:0003730; GO:0004004; GO:0005516; GO:0005524; GO:0005634; GO:0005654; GO:0005730; GO:0005737; GO:0006357; GO:0009299; GO:0010501; GO:0016020; GO:0019899; GO:0030509; GO:0030520; GO:0030521; GO:0035500; GO:0036002; GO:0043021; GO:0043517; GO:0045069; GO:0045445;

GO:0045667; GO:0046332; GO:0048306; GO:0048511; GO:0050681; GO:0060765; GO:0061614; GO:0070062; GO:0070412; GO:0070878; GO:0071013; GO:0072332; GO:1903800; GO:1990841; GO:1990904; GO:2001014

AACS_DANRE	GO:0005524; GO:0005829; GO:0006631; GO:0030729
ES8L2_MOUSE	GO:0001726; GO:0003779; GO:0005829; GO:0005886; GO:0007266; GO:0007605; GO:0016601; GO:0030676; GO:0032421; GO:0032426; GO:0032587; GO:0032991; GO:0035023; GO:0051015; GO:1900029
FLVC2_MOUSE	GO:0005886; GO:0015232; GO:0016021; GO:0020037
C1QBP_RAT	GO:0000122; GO:0001849; GO:0003714; GO:0003729; GO:0005080; GO:0005540; GO:0005615; GO:0005634; GO:0005730; GO:0005737; GO:0005759; GO:0005829; GO:0005886; GO:0006351; GO:0006397; GO:0006915; GO:0006955; GO:0006958; GO:0008134; GO:0008380; GO:0009986; GO:0014065; GO:0030449; GO:0030984; GO:0031690; GO:0032689; GO:0032695; GO:0039534; GO:0039536; GO:0042256; GO:0043065; GO:0045087; GO:0045785; GO:0048025; GO:0050687; GO:0051897; GO:0070131; GO:0090023; GO:0097177; GO:1900026; GO:1901165; GO:2000510
FDFT_HUMAN	GO:0004310; GO:0005783; GO:0005789; GO:0006694; GO:0006695; GO:0006696; GO:0008299; GO:0016021; GO:0019216; GO:0045338; GO:0045540; GO:0051996
FADS2_TACFU	GO:0005789; GO:0006636; GO:0016021; GO:0016213
ACLY_HUMAN	GO:0003878; GO:0005524; GO:0005576; GO:0005654; GO:0005829; GO:0005886; GO:0006085; GO:0006101; GO:0006107; GO:0006633; GO:0006695; GO:0008610; GO:0009346; GO:0015936; GO:0016020; GO:0031325; GO:0035578; GO:0043312; GO:0046872; GO:0046949; GO:0048037; GO:0070062; GO:1904813
CREL2_DANRE	GO:0005509; GO:0005576; GO:0005783
NB5R2_DANRE	GO:0001878; GO:0004128; GO:0016021; GO:0016126; GO:0016491
TIM13_DANRE	GO:0005743; GO:0008565; GO:0042719; GO:0045039; GO:0046872; GO:0072321
QPCT_BOIIR	GO:0005576; GO:0008270; GO:0016603; GO:0017186
TXTP_RAT	GO:0005743; GO:0006839; GO:0006843; GO:0015137; GO:0016021
MVD1_DANRE	GO:0004163; GO:0005524; GO:0005829; GO:0006695; GO:0019287
DYL1_DROME	GO:0000132; GO:0003774; GO:0005737; GO:0005814; GO:0005868; GO:0005874; GO:0006914; GO:0007018; GO:0007283; GO:0007290; GO:0007291; GO:0007476; GO:0008092; GO:0008407; GO:0010970; GO:0022416; GO:0030286; GO:0032991; GO:0034454; GO:0035071; GO:0035220; GO:0042623; GO:0042803; GO:0045505; GO:0048477; GO:0051017; GO:0051959; GO:0060271; GO:0097718; GO:1904801; GO:2000582
ACSL4_HUMAN	GO:0004467; GO:0005524; GO:0005737; GO:0005741; GO:0005778; GO:0005789; GO:0005811; GO:0006629; GO:0007584; GO:0008610; GO:0015908; GO:0016020; GO:0016021; GO:0019432; GO:0030307; GO:0031957; GO:0032307; GO:0035338; GO:0043025; GO:0044233; GO:0047676; GO:0060136; GO:0060996; GO:0070062; GO:0070672; GO:0102391
AT2A2_MOUSE	GO:0002026; GO:0005388; GO:0005509; GO:0005524; GO:0005654; GO:0005783; GO:0005789; GO:0006816; GO:0006874; GO:0006937; GO:0006984; GO:0006996; GO:0008022; GO:0010882; GO:0012506; GO:0014801; GO:0014883; GO:0014898; GO:0016020; GO:0016529; GO:0019899; GO:0031234; GO:0031775; GO:0032469; GO:0032470; GO:0032496; GO:0032991; GO:0033017; GO:0033292; GO:0034599; GO:0043434; GO:0044548; GO:0045822; GO:0048471; GO:0055119; GO:0070296; GO:0070588; GO:0086036; GO:0086039; GO:0090534; GO:0097470; GO:0098909; GO:1903233; GO:1903515; GO:1990036
ENPL_BOVIN	GO:0001666; GO:0003723; GO:0005524; GO:0005783; GO:0005788; GO:0005789; GO:0005829; GO:0005886; GO:0006457; GO:0019903; GO:0030433; GO:0030496; GO:0030970; GO:0031247; GO:0034663; GO:0042470; GO:0043066; GO:0043666; GO:0048471; GO:0050750; GO:0051082; GO:0071318
ERG1_MOUSE	GO:0004506; GO:0005783; GO:0005789; GO:0006725; GO:0008203; GO:0010033; GO:0016021; GO:0016126; GO:0031090; GO:0043231; GO:0050660
EBP_HUMAN	GO:0000247; GO:0001501; GO:0004769; GO:0004888; GO:0005635; GO:0005783; GO:0005789; GO:0005887; GO:0006695; GO:0008203; GO:0015238; GO:0030097; GO:0031410; GO:0033489; GO:0033490; GO:0047750
6PGD_HUMAN	GO:0004616; GO:0005634; GO:0005829; GO:0006098; GO:0009051; GO:0019322; GO:0019521; GO:0050661; GO:0055114; GO:0070062
DJB11_PONAB	GO:0005102; GO:0005615; GO:0005634; GO:0005788; GO:0006457; GO:0016556; GO:0050768; GO:0051082
ACACA_HUMAN	GO:0001650; GO:0001894; GO:0003989; GO:0004075; GO:0005524; GO:0005829; GO:0006084; GO:0006633; GO:0006853; GO:0015629; GO:0019538; GO:0031325; GO:0042802; GO:0045540; GO:0046872; GO:0046949; GO:0051289; GO:0055088; GO:0071380; GO:2001295
DPP3_RAT	GO:0005737; GO:0005829; GO:0005886; GO:0006508; GO:0008237; GO:0008239; GO:0008270; GO:0016607
ZP1_RABIT	GO:0005576; GO:0005886; GO:0007338; GO:0016021
ASNS_CHICK	GO:0004066; GO:0005524; GO:0006529; GO:0006541; GO:0042803; GO:0070981

GRB10_HUMAN	GO:0005070; GO:0005158; GO:0005737; GO:0005829; GO:0005886; GO:0007411; GO:0008286; GO:0030178; GO:0030949; GO:0032868; GO:0032991; GO:0042326; GO:0042327; GO:0042802; GO:0045719; GO:0046325; GO:0046627; GO:0048009; GO:0120162
PK1L1_ORYLA	GO:0003127; GO:0005262; GO:0005929; GO:0034704; GO:0050982; GO:0060170; GO:0070986; GO:0097730
BIP_CHICK	GO:0005524; GO:0005788; GO:0005793; GO:0005886; GO:0006983; GO:0008180; GO:0009986; GO:0016887; GO:0019904; GO:0021589; GO:0021680; GO:0030176; GO:0030335; GO:0030496; GO:0030512; GO:0030968; GO:0031398; GO:0031625; GO:0034663; GO:0035437; GO:0042149; GO:0043022; GO:0043066; GO:0043209; GO:0051603; GO:0051787; GO:0071353; GO:0090074; GO:1901998; GO:1903895
TOR3A_HUMAN	GO:0005524; GO:0005783; GO:0005788; GO:0016887; GO:0070062
EDEM1_HUMAN	GO:0000139; GO:0004571; GO:0005509; GO:0005783; GO:0006491; GO:0016235; GO:0030176; GO:0030433; GO:0036498; GO:0036510; GO:0044322; GO:0051787; GO:0097466; GO:1904154; GO:1904382
RL5_CHICK	GO:0000027; GO:0003735; GO:0005730; GO:0006412; GO:0008097; GO:0022625
STAR5_MOUSE	GO:0005739; GO:0015485; GO:0017127; GO:0032052; GO:0070508
SYNC_MOUSE	GO:0003676; GO:0004816; GO:0005524; GO:0005739; GO:0005829; GO:0006421
TMED3_RAT	GO:0005783; GO:0005789; GO:0005793; GO:0005794; GO:0015031; GO:0016021; GO:0030126; GO:0032580; GO:0033116
CP51A_PIG	GO:0005506; GO:0005783; GO:0005789; GO:0005886; GO:0008398; GO:0016021; GO:0020037; GO:0031090; GO:0033488
FBRL_XENLA	GO:0003723; GO:0005730; GO:0006364; GO:1990258; GO:1990259
ACBG2_XENLA	GO:0004467; GO:0005524; GO:0005737; GO:0102391
ODR4_MOUSE	GO:0016021
NPM_XENLA	GO:0003723; GO:0005654; GO:0005730; GO:0005737; GO:0006281; GO:0032071; GO:0042802; GO:0060699
NRDC_MOUSE	GO:0004222; GO:0005739; GO:0008233; GO:0046872; GO:0051044; GO:0052548; GO:0120163
ERG24_MOUSE	GO:0005783; GO:0006695; GO:0016126; GO:0016627; GO:0030176; GO:0031090; GO:0043231; GO:0043235; GO:0050613; GO:0050661
ANM1_RAT	GO:0005634; GO:0005654; GO:0005829; GO:0006355; GO:0006479; GO:0008276; GO:0008284; GO:0008327; GO:0008469; GO:0008757; GO:0016020; GO:0016274; GO:0016275; GO:0018216; GO:0019919; GO:0030519; GO:0032991; GO:0034709; GO:0035241; GO:0035242; GO:0035247; GO:0042802; GO:0043985; GO:0044020; GO:0045648; GO:0045652; GO:0045653; GO:0046985; GO:0051260; GO:0097421; GO:1900745; GO:1904047
PLPL2_HUMAN	GO:0004465; GO:0004806; GO:0005654; GO:0005737; GO:0005788; GO:0005789; GO:0005811; GO:0005829; GO:0005886; GO:0010891; GO:0010898; GO:0016020; GO:0016021; GO:0016411; GO:0019433; GO:0019915; GO:0034389; GO:0036155; GO:0043687; GO:0044267; GO:0055088
BIP_BOVIN	GO:0005524; GO:0005788; GO:0016887; GO:0030335; GO:0035437; GO:0090074; GO:1903895
KIME_BOVIN	GO:0000287; GO:0004496; GO:0005524; GO:0005777; GO:0005829; GO:0006695; GO:0019287; GO:0042802
SERPH_CHICK	GO:0003433; GO:0004867; GO:0005518; GO:0005783; GO:0005788; GO:0005793; GO:0030199; GO:0032964; GO:0045121; GO:0051082; GO:0051604
S35E3_DANRE	GO:0016021
CCD86_PONAB	GO:0005634
EI3EB_DANRE	GO:0001732; GO:0003743; GO:0005634; GO:0005852; GO:0006413; GO:0016282; GO:0033290; GO:0071540
FAS_CHICK	GO:0003697; GO:0004312; GO:0004313; GO:0004314; GO:0004315; GO:0004316; GO:0004320; GO:0005623; GO:0006089; GO:0006633; GO:0016295; GO:0016296; GO:0031177; GO:0032100; GO:0047117; GO:0047451; GO:0102131; GO:0102132
LPIN1_HUMAN	GO:0003713; GO:0005634; GO:0005635; GO:0005654; GO:0005737; GO:0005741; GO:0005789; GO:0005829; GO:0006351; GO:0006642; GO:0006646; GO:0006656; GO:0007077; GO:0008195; GO:0009062; GO:0019432; GO:0031100; GO:0031965; GO:0032869; GO:0045944; GO:0120162
NRDC_RAT	GO:0004222; GO:0008233; GO:0046872; GO:0120163
ACSA_HUMAN	GO:0003987; GO:0005524; GO:0005654; GO:0005737; GO:0005759; GO:0005829; GO:0006069; GO:0008610; GO:0016208; GO:0019413; GO:0019427; GO:0019542; GO:0043231
NCOA7_MOUSE	GO:0005622; GO:0005634; GO:0006351; GO:0030374; GO:0035257; GO:0045944; GO:1900408; GO:1902083; GO:1903204
SYWC_BOVIN	GO:0004830; GO:0005524; GO:0005634; GO:0005737; GO:0005829; GO:0006436; GO:0006469; GO:0010628; GO:0010835; GO:0019210; GO:0019901; GO:0019904; GO:0031334; GO:0032991; GO:0042803; GO:0045765
PRP19_BOVIN	GO:0000244; GO:0000245; GO:0000349; GO:0000398; GO:0000974; GO:0001833; GO:0004842; GO:0005634; GO:0005662; GO:0005737; GO:0005811; GO:0005819; GO:0006303; GO:0008610; GO:0010498; GO:0016607; GO:0034450; GO:0034613; GO:0035861; GO:0042802; GO:0045665; GO:0048026; GO:0048711; GO:0061630; GO:0070534; GO:0071006; GO:0071007; GO:0072422
HMCS1_CHICK	GO:0004421; GO:0005737; GO:0006695; GO:0008299

GARS_MOUSE	GO:0004081; GO:0004820; GO:0005524; GO:0005739; GO:0005829; GO:0006418; GO:0006426; GO:0015966; GO:0030141; GO:0030424; GO:0042802; GO:0046983; GO:0070062; GO:0070150
DHC24_HUMAN	GO:0000139; GO:0000246; GO:0005634; GO:0005783; GO:0005789; GO:0005829; GO:0005856; GO:0006695; GO:0006915; GO:0006979; GO:0007050; GO:0007265; GO:0008104; GO:0008285; GO:0009725; GO:0009888; GO:0016020; GO:0016021; GO:0016628; GO:0019899; GO:0030539; GO:0031639; GO:0033489; GO:0033490; GO:0042605; GO:0042987; GO:0043066; GO:0043154; GO:0043588; GO:0050614; GO:0055114; GO:0061024; GO:0071949; GO:1901214
SYVC_TAKRU	GO:0002161; GO:0004832; GO:0005524; GO:0005737; GO:0006438
ACBP_HUMAN	GO:0005788; GO:0005794; GO:0006637; GO:0008289; GO:0030156; GO:0036042; GO:0036151; GO:0046983; GO:0070062; GO:0097038
PDIA4_HUMAN	GO:0003723; GO:0003756; GO:0005615; GO:0005783; GO:0005788; GO:0006457; GO:0009306; GO:0009986; GO:0015037; GO:0034976; GO:0042470; GO:0045454; GO:0061077
ABCF3_MOUSE	GO:0005524; GO:0016887; GO:0051607
TXTP_BOVIN	GO:0005743; GO:0006839; GO:0006843; GO:0015137; GO:0016021
CP27B_HUMAN	GO:0004498; GO:0005506; GO:0005737; GO:0005739; GO:0005741; GO:0006766; GO:0006816; GO:0008285; GO:0010956; GO:0010980; GO:0020037; GO:0030282; GO:0030308; GO:0030500; GO:0032496; GO:0033280; GO:0034341; GO:0036378; GO:0042359; GO:0042369; GO:0043627; GO:0045618; GO:0046697; GO:0055074; GO:0070314; GO:0070564
RASH_HUMAN	GO:0000139; GO:0000165; GO:0001934; GO:0002223; GO:0003924; GO:0005525; GO:0005634; GO:0005737; GO:0005794; GO:0005829; GO:0005886; GO:0006897; GO:0006935; GO:0007050; GO:0007093; GO:0007165; GO:0007166; GO:0007265; GO:0008022; GO:0008283; GO:0008284; GO:0008285; GO:0009887; GO:0010629; GO:0010863; GO:0019003; GO:0030335; GO:0032729; GO:0034260; GO:0035900; GO:0042088; GO:0042832; GO:0043406; GO:0043410; GO:0043524; GO:0043547; GO:0045740; GO:0045944; GO:0046330; GO:0046579; GO:0048013; GO:0048169; GO:0048471; GO:0050679; GO:0050852; GO:0051291; GO:0070374; GO:0071480; GO:0090303; GO:0090314; GO:0090398; GO:0097193; GO:0098696; GO:0098978; GO:1900029; GO:2000251; GO:2000630
MKNK2_HUMAN	GO:0004674; GO:0004683; GO:0005516; GO:0005524; GO:0005634; GO:0005654; GO:0005737; GO:0006417; GO:0006468; GO:0007166; GO:0009931; GO:0016604; GO:0016605; GO:0018105; GO:0030097; GO:0035556; GO:0046777; GO:0046872; GO:0071243; GO:0097192
LRRF2_XENTR	GO:0006355; GO:0009950; GO:0016055; GO:0030275
TBB1_GADMO	GO:0003924; GO:0005200; GO:0005525; GO:0005737; GO:0005874; GO:0007017
SYYC_DANRE	GO:0000049; GO:0004831; GO:0005524; GO:0006418; GO:0006437; GO:0006974; GO:0017101; GO:0017102
CNEPA_DANRE	GO:0004721; GO:0004722; GO:0005635; GO:0005737; GO:0005789; GO:0006470; GO:0006998; GO:0010867; GO:0016021; GO:0031965; GO:0071595
TMED3_RAT	GO:0005783; GO:0005789; GO:0005793; GO:0005794; GO:0015031; GO:0016021; GO:0030126; GO:0032580; GO:0033116
PPA6_HUMAN	GO:0002244; GO:0003993; GO:0005737; GO:0005739; GO:0005759; GO:0006644; GO:0006654; GO:0052642; GO:2001311
CCD43_DANRE	
S13A5_HUMAN	GO:0005886; GO:0005887; GO:0015137; GO:0015141; GO:0015746; GO:0017153; GO:0035674
SPB1_CHICK	GO:0000453; GO:0000463; GO:0000466; GO:0005730; GO:0008650; GO:0016435; GO:0030687; GO:0030688; GO:0031167
BIP_CHICK	GO:0005524; GO:0005788; GO:0005793; GO:0005886; GO:0006983; GO:0008180; GO:0009986; GO:0016887; GO:0019904; GO:0021589; GO:0021680; GO:0030176; GO:0030335; GO:0030496; GO:0030512; GO:0030968; GO:0031398; GO:0031625; GO:0034663; GO:0035437; GO:0042149; GO:0043022; GO:0043066; GO:0043209; GO:0051603; GO:0051787; GO:0071353; GO:0090074; GO:1901998; GO:1903895
PYRG1_DANRE	GO:0003883; GO:0005524; GO:0006241; GO:0006541; GO:0044210
TNI3K_HUMAN	GO:0002027; GO:0004672; GO:0004674; GO:0005524; GO:0005634; GO:0005737; GO:0006468; GO:0008022; GO:0031013; GO:0035556; GO:0046872; GO:0055117; GO:0086069; GO:1903779
ACKR4_HUMAN	GO:0004950; GO:0005044; GO:0005769; GO:0005886; GO:0005887; GO:0006935; GO:0006955; GO:0007186; GO:0019956; GO:0055037
RCC1_XENLA	GO:0005085; GO:0005634; GO:0005694; GO:0005737; GO:0007049; GO:0051301
PESC_SALSA	GO:0000463; GO:0000466; GO:0005654; GO:0005730; GO:0008283; GO:0030687; GO:0043021; GO:0070545
PPIL1_BOVIN	GO:0000398; GO:0000413; GO:0003755; GO:0005634; GO:0006457; GO:0016018; GO:0071007; GO:0097718
FABPH_ONCMY	GO:0005737; GO:0008289
S13A2_HUMAN	GO:0005215; GO:0005886; GO:0005887; GO:0015361; GO:0016020; GO:0070062; GO:0098656
TBL2_MOUSE	GO:0005737; GO:0005783; GO:0019901; GO:0030968; GO:0031369; GO:0042149; GO:0051219; GO:0071456
GNL3_DANRE	GO:0000467; GO:0003407; GO:0003924; GO:0005525; GO:0005634; GO:0005730; GO:0007096; GO:0042127; GO:0045664
DEPD5_HUMAN	GO:0005096; GO:0005764; GO:0005765; GO:0005829; GO:0010506; GO:0032007; GO:0034198; GO:0035556; GO:0044877; GO:0048471; GO:1904262; GO:1990130

MKNK2_HUMAN	GO:0004674; GO:0004683; GO:0005516; GO:0005524; GO:0005634; GO:0005654; GO:0005737; GO:0006417; GO:0006468; GO:0007166; GO:0009931; GO:0016604; GO:0016605; GO:0018105; GO:0030097; GO:0035556; GO:0046777; GO:0046872; GO:0071243; GO:0097192
DCAM_XENLA	GO:0004014; GO:0006557; GO:0006597; GO:0008295
GPAT1_RAT	GO:0004366; GO:0005739; GO:0005741; GO:0005886; GO:0009750; GO:0010867; GO:0014823; GO:0016021; GO:0016024; GO:0031667; GO:0031966; GO:0032869; GO:0046686; GO:0102420
CN028_HUMAN	
DDX5_MOUSE	GO:0000122; GO:0000380; GO:0000381; GO:0000956; GO:0001837; GO:0003712; GO:0003723; GO:0003724; GO:0003730; GO:0004004; GO:0005516; GO:0005524; GO:0005634; GO:0005730; GO:0005737; GO:0006357; GO:0007623; GO:0009299; GO:0010501; GO:0019899; GO:0030509; GO:0030520; GO:0030521; GO:0033158; GO:0035500; GO:0036002; GO:0043021; GO:0043517; GO:0045069; GO:0045445; GO:0045667; GO:0045893; GO:0046332; GO:0048306; GO:0050681; GO:0060765; GO:0061614; GO:0070412; GO:0070878; GO:0071013; GO:0072332; GO:1903800; GO:1990841; GO:1990904; GO:2001014
PPP5_HUMAN	GO:0000165; GO:0000278; GO:0001933; GO:0001965; GO:0003723; GO:0004721; GO:0004722; GO:0005524; GO:0005634; GO:0005654; GO:0005829; GO:0005886; GO:0006281; GO:0006351; GO:0006470; GO:0008017; GO:0008289; GO:0010288; GO:0016576; GO:0016791; GO:0032991; GO:0035970; GO:0042802; GO:0043123; GO:0043204; GO:0043231; GO:0043278; GO:0043531; GO:0046872; GO:0051291; GO:0051879; GO:0070262; GO:0070301; GO:0071276; GO:0101031; GO:1901215; GO:1904550; GO:1990635; GO:2000324
NFM_HUMAN	GO:0005200; GO:0005883; GO:0008017; GO:0030424; GO:0033693; GO:0045111; GO:0061564; GO:0097418
MAON_HUMAN	GO:0004470; GO:0004471; GO:0004473; GO:0005739; GO:0005759; GO:0006090; GO:0006099; GO:0006108; GO:0008948; GO:0009060; GO:0046872; GO:0048037; GO:0051287; GO:0055114; GO:0072592
PDE8B_MOUSE	GO:0001662; GO:0004115; GO:0006198; GO:0007165; GO:0008542; GO:0035106; GO:0046676; GO:0046872; GO:0050885; GO:0061179; GO:0090032
ABCF3_PONAB	GO:0005524; GO:0016887; GO:0051607
PSMD2_BOVIN	GO:0005634; GO:0008540; GO:0022624; GO:0030234; GO:0034515; GO:0042176; GO:0043161
SMD3_HUMAN	GO:0000243; GO:0000245; GO:0000387; GO:0000398; GO:0003723; GO:0005654; GO:0005681; GO:0005682; GO:0005683; GO:0005685; GO:0005686; GO:0005687; GO:0005689; GO:0005697; GO:0005829; GO:0006369; GO:0006479; GO:0008334; GO:0008380; GO:0016604; GO:0019899; GO:0030532; GO:0030620; GO:0034709; GO:0034715; GO:0034719; GO:0051170; GO:0070034; GO:0071007; GO:0071010; GO:0071011; GO:0071013; GO:0071208; GO:0071209; GO:0097526; GO:1990446
PLPL2_RAT	GO:0004806; GO:0005737; GO:0005811; GO:0005886; GO:0010891; GO:0010898; GO:0016020; GO:0016021; GO:0019433; GO:0055088
PS11B_DANRE	GO:0005198; GO:0005634; GO:0005829; GO:0006511; GO:0008541; GO:0022624; GO:0043248; GO:0048863
TSR1_XENLA	GO:0005730; GO:0042254
PKHG7_HUMAN	GO:0005089; GO:0035023
UBP5_HUMAN	GO:0004197; GO:0004843; GO:0005764; GO:0005829; GO:0006511; GO:0008270; GO:0016579; GO:0032436; GO:0036459; GO:0043130; GO:0071108
FADS2_TACFU	GO:0005789; GO:0006636; GO:0016021; GO:0016213
HXK4_HUMAN	GO:0001678; GO:0004340; GO:0005524; GO:0005536; GO:0005654; GO:0005739; GO:0005829; GO:0006096; GO:0006110; GO:0006739; GO:0032024; GO:0032869; GO:0042593; GO:0043266; GO:0044320; GO:0045721; GO:0045725; GO:0050796; GO:0051156; GO:0051594; GO:0061621; GO:0070509
FAS_CHICK	GO:0003697; GO:0004312; GO:0004313; GO:0004314; GO:0004315; GO:0004316; GO:0004320; GO:0005623; GO:0006089; GO:0006633; GO:0016295; GO:0016296; GO:0031177; GO:0032100; GO:0047117; GO:0047451; GO:0102131; GO:0102132
SCD1_TACFU	GO:0004768; GO:0005789; GO:0006633; GO:0016021; GO:0046872
BMAL2_CHICK	GO:0003700; GO:0005634; GO:0005667; GO:0005737; GO:0006351; GO:0042753; GO:0045893; GO:0046983; GO:0048511; GO:0070888
ES8L2_MOUSE	GO:0001726; GO:0003779; GO:0005829; GO:0005886; GO:0007266; GO:0007605; GO:0016601; GO:0030676; GO:0032421; GO:0032426; GO:0032587; GO:0032991; GO:0035023; GO:0051015; GO:1900029
ELOV5_TACFU	GO:0005789; GO:0006636; GO:0009922; GO:0016021; GO:0019367; GO:0030425; GO:0034625; GO:0034626; GO:0035338; GO:0042761; GO:0102336; GO:0102337; GO:0102338; GO:0102756
FAS_CHICK	GO:0003697; GO:0004312; GO:0004313; GO:0004314; GO:0004315; GO:0004316; GO:0004320; GO:0005623; GO:0006089; GO:0006633; GO:0016295; GO:0016296; GO:0031177; GO:0032100; GO:0047117; GO:0047451; GO:0102131; GO:0102132
HOOK1_DANRE	GO:0005737; GO:0005813; GO:0005829; GO:0005874; GO:0007032; GO:0007040; GO:0008017; GO:0008333; GO:0015031; GO:0030705; GO:0031122; GO:0045022; GO:0051959; GO:0070695
CP1A1_LIZAU	GO:0005506; GO:0005789; GO:0020037; GO:0031090; GO:0070330

ACACA_HUMAN	GO:0001650; GO:0001894; GO:0003989; GO:0004075; GO:0005524; GO:0005829; GO:0006084; GO:0006633; GO:0006853; GO:0015629; GO:0019538; GO:0031325; GO:0042802; GO:0045540; GO:0046872; GO:0046949; GO:0051289; GO:0055088; GO:0071380; GO:2001295
DDX5_HUMAN	GO:0000122; GO:0000380; GO:0000381; GO:0000398; GO:0000956; GO:0001837; GO:0003723; GO:0003724; GO:0003730; GO:0004004; GO:0005516; GO:0005524; GO:0005634; GO:0005654; GO:0005730; GO:0005737; GO:0006357; GO:0009299; GO:0010501; GO:0016020; GO:0019899; GO:0030509; GO:0030520; GO:0030521; GO:0035500; GO:0036002; GO:0043021; GO:0043517; GO:0045069; GO:0045445; GO:0045667; GO:0046332; GO:0048306; GO:0048511; GO:0050681; GO:0060765; GO:0061614; GO:0070062; GO:0070412; GO:0070878; GO:0071013; GO:0072332; GO:1903800; GO:1990841; GO:1990904; GO:2001014
PELO_DANRE	GO:0004519; GO:0005634; GO:0005737; GO:0006412; GO:0007049; GO:0032790; GO:0043022; GO:0046872; GO:0051301; GO:0070481; GO:0070651; GO:0070966; GO:0071025
ACKR4_HUMAN	GO:0004950; GO:0005044; GO:0005769; GO:0005886; GO:0005887; GO:0006935; GO:0006955; GO:0007186; GO:0019956; GO:0055037
TOR3A_HUMAN	GO:0005524; GO:0005783; GO:0005788; GO:0016887; GO:0070062
ALG5_HUMAN	GO:0004576; GO:0004581; GO:0005789; GO:0006486; GO:0006487; GO:0007368; GO:0016020; GO:0016021; GO:0018279
CASR_PIG	GO:0004930; GO:0005509; GO:0005513; GO:0005887; GO:0006874; GO:0007186; GO:0010628; GO:0016597; GO:0032781; GO:0042803; GO:0051924; GO:0070509
PLPL2_HUMAN	GO:0004465; GO:0004806; GO:0005654; GO:0005737; GO:0005788; GO:0005789; GO:0005811; GO:0005829; GO:0005886; GO:0010891; GO:0010898; GO:0016020; GO:0016021; GO:0016411; GO:0019433; GO:0019915; GO:0034389; GO:0036155; GO:0043687; GO:0044267; GO:0055088
IDHP_BOVIN	GO:0000287; GO:0004450; GO:0005739; GO:0005743; GO:0005777; GO:0005829; GO:0006097; GO:0006099; GO:0006102; GO:0006103; GO:0051287
JARD2_DANRE	GO:0003677; GO:0003682; GO:0005634; GO:0006351; GO:0007275; GO:0016577; GO:0031061; GO:0035097; GO:0045892; GO:0048863; GO:0051574
ELOV6_DANRE	GO:0005783; GO:0006636; GO:0009922; GO:0019367; GO:0030148; GO:0030176; GO:0034625; GO:0034626; GO:0035338; GO:0042759; GO:0042761; GO:0102336; GO:0102337; GO:0102338; GO:0102756
ACLY_HUMAN	GO:0003878; GO:0005524; GO:0005576; GO:0005654; GO:0005829; GO:0005886; GO:0006085; GO:0006101; GO:0006107; GO:0006633; GO:0006695; GO:0008610; GO:0009346; GO:0015936; GO:0016020; GO:0031325; GO:0035578; GO:0043312; GO:0046872; GO:0046949; GO:0048037; GO:0070062; GO:1904813
HHIP_HUMAN	GO:0003824; GO:0005576; GO:0005634; GO:0005737; GO:0005887; GO:0007224; GO:0007405; GO:0008270; GO:0009953; GO:0009968; GO:0009986; GO:0040036; GO:0043066; GO:0045879; GO:0048705; GO:0060170; GO:0060441; GO:0097108
NFM_HUMAN	GO:0005200; GO:0005883; GO:0008017; GO:0030424; GO:0033693; GO:0045111; GO:0061564; GO:0097418
MANF_HUMAN	GO:0002576; GO:0003723; GO:0005576; GO:0005615; GO:0005634; GO:0005783; GO:0005788; GO:0005829; GO:0006986; GO:0008083; GO:0008289; GO:0031175; GO:0033018; GO:0071542; GO:1905897
LAYN_CRIGR	GO:0001726; GO:0009986; GO:0016021; GO:0030246
HS90A_PIG	GO:0005524; GO:0005634; GO:0005737; GO:0005886; GO:0006457; GO:0009408; GO:0009409; GO:0016887; GO:0030235; GO:0030911; GO:0042470; GO:0045429; GO:0046677; GO:0051082
NDUC2_MOUSE	GO:0005737; GO:0005739; GO:0005743; GO:0005747; GO:0006120; GO:0008137; GO:0010918; GO:0016021; GO:0032981; GO:0050727; GO:0060547; GO:1901223; GO:1903427; GO:2001171
FOS_TAKRU	GO:0003677; GO:0003700; GO:0005634; GO:0005667; GO:0006357
COPZ2_MOUSE	GO:0000139; GO:0005829; GO:0015031; GO:0016192; GO:0030126; GO:0030137; GO:0033116
CP2CE_RABIT	GO:0005506; GO:0005789; GO:0020037; GO:0031090; GO:0070330
GA45G_BOVIN	GO:0000185; GO:0005634; GO:0005737; GO:0006915; GO:0006950; GO:0007275; GO:0030154; GO:0043065; GO:0046330; GO:0051726; GO:1900745
IDHC_BOVIN	GO:0000287; GO:0004450; GO:0005737; GO:0005829; GO:0006097; GO:0006099; GO:0006102; GO:0006103; GO:0006979; GO:0051287
M3K8_MOUSE	GO:0000287; GO:0002376; GO:0004674; GO:0004709; GO:0005524; GO:0005737; GO:0005829; GO:0007049; GO:0007346; GO:0023014; GO:0031098; GO:0032147; GO:0042981
SYLC_HUMAN	GO:0002161; GO:0004819; GO:0004823; GO:0004832; GO:0005096; GO:0005524; GO:0005737; GO:0005764; GO:0005783; GO:0005829; GO:0006418; GO:0006425; GO:0006429; GO:0006438; GO:0006622; GO:0008361; GO:0010507; GO:0012505; GO:0016604; GO:0017101; GO:0034198; GO:0043547; GO:0071230; GO:0071233; GO:1904263; GO:1990253
ANM1_RAT	GO:0005634; GO:0005654; GO:0005829; GO:0006355; GO:0006479; GO:0008276; GO:0008284; GO:0008327; GO:0008469; GO:0008757; GO:0016020; GO:0016274; GO:0016275; GO:0018216; GO:0019919; GO:0030519; GO:0032991; GO:0034709; GO:0035241; GO:0035242;

GO:0035247; GO:0042802; GO:0043985; GO:0044020; GO:0045648; GO:0045652; GO:0045653; GO:0046985; GO:0051260; GO:0097421; GO:1900745; GO:1904047

TSN15_MOUSE   GO:0005886; GO:0005887; GO:0007166; GO:0009986; GO:0019899; GO:0031902; GO:0051604; GO:0072659; GO:0097197

SRPRB_MOUSE   GO:0005047; GO:0005525; GO:0005737; GO:0005785; GO:0005881; GO:0016020; GO:0016021; GO:0031625

S61A1_DANRE   GO:0005789; GO:0015031; GO:0016021; GO:0021986; GO:0039019

DNJA1_HUMAN   GO:0001664; GO:0001671; GO:0005524; GO:0005634; GO:0005739; GO:0005829; GO:0006457; GO:0006986; GO:0009408; GO:0015630; GO:0016020; GO:0030544; GO:0030957; GO:0031397; GO:0031625; GO:0043065; GO:0043066; GO:0043508; GO:0046872; GO:0048471; GO:0050750; GO:0051082; GO:0051087; GO:0051223; GO:0055131; GO:0070062; GO:0070585; GO:0098554; GO:1903748; GO:1905259

HS90B_HUMAN   GO:0001890; GO:0002134; GO:0002135; GO:0003723; GO:0003725; GO:0005524; GO:0005525; GO:0005576; GO:0005634; GO:0005654; GO:0005737; GO:0005739; GO:0005765; GO:0005829; GO:0006457; GO:0006805; GO:0006986; GO:0007004; GO:0009651; GO:0009986; GO:0016020; GO:0016234; GO:0016323; GO:0016324; GO:0017098; GO:0019062; GO:0019887; GO:0019900; GO:0019901; GO:0021955; GO:0023026; GO:0030010; GO:0030235; GO:0030511; GO:0030911; GO:0031072; GO:0031396; GO:0031526; GO:0031625; GO:0032092; GO:0032435; GO:0032516; GO:0032564; GO:0032991; GO:0033138; GO:0033160; GO:0034751; GO:0034774; GO:0035690; GO:0038096; GO:0042220; GO:0042277; GO:0042470; GO:0042623; GO:0042802; GO:0042803; GO:0042826; GO:0043008; GO:0043025; GO:0043312; GO:0043524; GO:0044294; GO:0044295; GO:0044325; GO:0045296; GO:0045429; GO:0045597; GO:0045793; GO:0046983; GO:0048156; GO:0048471; GO:0048675; GO:0050821; GO:0051082; GO:0051131; GO:0051248; GO:0051897; GO:0051973; GO:0060334; GO:0060338; GO:0070062; GO:0070182; GO:0071157; GO:0071353; GO:0071407; GO:0071902; GO:0097435; GO:0097718; GO:1900034; GO:1901389; GO:1901799; GO:1902949; GO:1903660; GO:1903827; GO:1904031; GO:1904813; GO:1905323; GO:1990226; GO:1990913; GO:1990917; GO:2000010

CP2F1_HUMAN   GO:0004497; GO:0005506; GO:0005789; GO:0006805; GO:0008392; GO:0008395; GO:0009636; GO:0016712; GO:0018931; GO:0018979; GO:0019373; GO:0019825; GO:0020037; GO:0031090; GO:0043231; GO:0070330

S13A2_HUMAN   GO:0005215; GO:0005886; GO:0005887; GO:0015361; GO:0016020; GO:0070062; GO:0098656

G0S2_MOUSE   GO:0005739; GO:0097191; GO:0120162; GO:2001238

GRB10_HUMAN   GO:0005070; GO:0005158; GO:0005737; GO:0005829; GO:0005886; GO:0007411; GO:0008286; GO:0030178; GO:0030949; GO:0032868; GO:0032991; GO:0042326; GO:0042327; GO:0042802; GO:0045719; GO:0046325; GO:0046627; GO:0048009; GO:0120162

AMPE_BOVIN   GO:0002003; GO:0003081; GO:0004177; GO:0005737; GO:0005886; GO:0006508; GO:0008217; GO:0008270; GO:0008283; GO:0016021; GO:0016477; GO:0042277; GO:0043171; GO:0070006

TT39A_DANRE

SERPH_CHICK   GO:0003433; GO:0004867; GO:0005518; GO:0005783; GO:0005788; GO:0005793; GO:0030199; GO:0032964; GO:0045121; GO:0051082; GO:0051604

SATL1_HUMAN   GO:0004145; GO:0005829; GO:0019809; GO:0032918; GO:0046208

CLAP1_XENTR   GO:0000777; GO:0005794; GO:0005815; GO:0005828; GO:0005881; GO:0007020; GO:0007049; GO:0031023; GO:0034453; GO:0043515; GO:0051010; GO:0051301

LRRF2_XENTR   GO:0006355; GO:0009950; GO:0016055; GO:0030275

FAS_CHICK   GO:0003697; GO:0004312; GO:0004313; GO:0004314; GO:0004315; GO:0004316; GO:0004320; GO:0005623; GO:0006089; GO:0006633; GO:0016295; GO:0016296; GO:0031177; GO:0032100; GO:0047117; GO:0047451; GO:0102131; GO:0102132

APOA4_HUMAN   GO:0001523; GO:0002227; GO:0005319; GO:0005507; GO:0005576; GO:0005615; GO:0005769; GO:0005788; GO:0005829; GO:0006695; GO:0006869; GO:0006982; GO:0007159; GO:0008203; GO:0008289; GO:0010873; GO:0010898; GO:0015485; GO:0016042; GO:0016209; GO:0017127; GO:0019430; GO:0030300; GO:0031102; GO:0031210; GO:0032374; GO:0033344; GO:0033700; GO:0034361; GO:0034364; GO:0034371; GO:0034372; GO:0034375; GO:0034378; GO:0034380; GO:0034445; GO:0035634; GO:0042157; GO:0042627; GO:0042632; GO:0042744; GO:0042802; GO:0042803; GO:0043691; GO:0044267; GO:0045723; GO:0046470; GO:0051006; GO:0055088; GO:0060228; GO:0062023; GO:0065005; GO:0070062; GO:0070328; GO:0072562

TS101_HUMAN   GO:0000813; GO:0001558; GO:0003677; GO:0003714; GO:0005730; GO:0005737; GO:0005768; GO:0005769; GO:0005770; GO:0005771; GO:0005815; GO:0005829; GO:0005886; GO:0006513; GO:0006858; GO:0007050; GO:0007175; GO:0008285; GO:0008333; GO:0010008; GO:0015031; GO:0016197; GO:0016236; GO:0019058; GO:0030216; GO:0030374; GO:0031625; GO:0031901; GO:0031902; GO:0036258; GO:0039702; GO:0042059; GO:0042803; GO:0043130; GO:0043162; GO:0043405; GO:0044877; GO:0045892; GO:0046755; GO:0046790; GO:0048306; GO:0048524; GO:0051301; GO:0070062; GO:0090543; GO:0097352; GO:1902188; GO:1903543; GO:1903551; GO:1903772; GO:1903774; GO:1990182; GO:2000397

TYSY_MOUSE   GO:0000166; GO:0000900; GO:0003729; GO:0004799; GO:0005542; GO:0005634; GO:0005730; GO:0005737; GO:0005739; GO:0005743; GO:0005759; GO:0006231; GO:0006235; GO:0006417; GO:0007568; GO:0007623; GO:0008144; GO:0017148; GO:0019088; GO:0019860;

GO:0032570; GO:0033189; GO:0034097; GO:0035999; GO:0042803; GO:0045471; GO:0046078; GO:0046683; GO:0048037; GO:0048589;

GO:0051216; GO:0051384; GO:0051593; GO:0060574; GO:0097421; GO:1990825

SEPT7_MOUSE GO:0000281; GO:0000777; GO:0001725; GO:0005525; GO:0005634; GO:0005819; GO:0005930; GO:0005938; GO:0005940; GO:0007283;

GO:0016020; GO:0016476; GO:0030496; GO:0030865; GO:0031105; GO:0031270; GO:0032154; GO:0032156; GO:0032160; GO:0032991;

GO:0042802; GO:0043005; GO:0043209; GO:0043679; GO:0044297; GO:0045202; GO:0046982; GO:0048668; GO:0051291; GO:0060271;

GO:0060997; GO:0097227; GO:0097730; GO:1902857

SVEP1_HUMAN GO:0003682; GO:0005509; GO:0005576; GO:0005737; GO:0007155; GO:0016020

S13A5_HUMAN GO:0005886; GO:0005887; GO:0015137; GO:0015141; GO:0015746; GO:0017153; GO:0035674

LORF2_HUMAN GO:0003964; GO:0006310; GO:0009036; GO:0032197; GO:0032199; GO:0046872; GO:0090305

PCKGC_CHICK GO:0003729; GO:0004550; GO:0004613; GO:0005525; GO:0005829; GO:0006089; GO:0006090; GO:0006094; GO:0006111; GO:0006522;

GO:0006531; GO:0006536; GO:0006541; GO:0006544; GO:0006560; GO:0006735; GO:0007296; GO:0007568; GO:0007586; GO:0008343;

GO:0008906; GO:0009069; GO:0009792; GO:0015743; GO:0016042; GO:0018991; GO:0019157; GO:0019543; GO:0019563; GO:0019953;

GO:0030145; GO:0030703; GO:0032496; GO:0032869; GO:0033993; GO:0042149; GO:0042594; GO:0043565; GO:0043950; GO:0045722;

GO:0045912; GO:0045913; GO:0046015; GO:0046898; GO:0047134; GO:0048562; GO:0048589; GO:0050692; GO:0050892; GO:0051379;

GO:0051384; GO:0051591; GO:0060259; GO:0070365; GO:0070741; GO:0071300; GO:0071320; GO:0071332; GO:0071333; GO:0071347;

GO:0071356; GO:0071361; GO:0071374; GO:0071377; GO:0071456; GO:0071549; GO:0072071; GO:1904640

FABPH_ONCMY GO:0005737; GO:0008289

IRF1_HUMAN GO:0000790; GO:0000978; GO:0000981; GO:0001077; GO:0002819; GO:0003677; GO:0005634; GO:0005654; GO:0005737; GO:0005829;

GO:0006366; GO:0006915; GO:0007050; GO:0007596; GO:0008285; GO:0032481; GO:0032728; GO:0034124; GO:0035458; GO:0043374;

GO:0045084; GO:0045088; GO:0045590; GO:0045892; GO:0045893; GO:0045944; GO:0051607; GO:0051726; GO:0060333; GO:0060337;

GO:0071260; GO:2000564

LIPO_RHIMB GO:0005576; GO:0036094

MK06_CHICK GO:0004707; GO:0005524; GO:0005634; GO:0005737; GO:0005829; GO:0007049; GO:0010468; GO:0019901; GO:0032156; GO:0032991;

GO:0046982; GO:0060999; GO:0071310

PRI1_HUMAN GO:0000082; GO:0003697; GO:0003896; GO:0005654; GO:0005658; GO:0006269; GO:0016020; GO:0032201; GO:0046872

ACBG2_XENLA GO:0004467; GO:0005524; GO:0005737; GO:0102391

CLC4M_NOMCO GO:0002250; GO:0005537; GO:0006897; GO:0016021; GO:0045087; GO:0046872

CP7A1_HUMAN GO:0005506; GO:0005789; GO:0006699; GO:0006707; GO:0008123; GO:0016125; GO:0019216; GO:0020037; GO:0031090; GO:0042632;

GO:0043231; GO:0070857; GO:0071333; GO:0071397

DNJC3_HUMAN GO:0004860; GO:0005576; GO:0005737; GO:0005783; GO:0005788; GO:0005790; GO:0005829; GO:0016020; GO:0019901; GO:0031205;

GO:0035578; GO:0036494; GO:0036498; GO:0043066; GO:0043312; GO:0043687; GO:0044267; GO:0051087; GO:0051603; GO:0051607;

GO:0051787; GO:0070062; GO:0070417; GO:1903561; GO:1903912

TREF1_MOUSE GO:0000118; GO:0003700; GO:0005634; GO:0005654; GO:0005667; GO:0005730; GO:0005829; GO:0006351; GO:0006357; GO:0008134;

GO:0044212; GO:0045893; GO:0046872

FAZ1_TRYB2 GO:0000281; GO:0005856; GO:0005929; GO:0020016; GO:0031514; GO:0060271

HS3SA_HUMAN GO:0000139; GO:0006024; GO:0008146; GO:0008467; GO:0016021; GO:0033872

CSRN1_HUMAN GO:0000981; GO:0001228; GO:0003700; GO:0005634; GO:0006915; GO:0009791; GO:0043565; GO:0045944; GO:0048008; GO:0048705;

GO:0060021; GO:0060325

ACSL4_HUMAN GO:0004467; GO:0005524; GO:0005737; GO:0005741; GO:0005778; GO:0005789; GO:0005811; GO:0006629; GO:0007584; GO:0008610;

GO:0015908; GO:0016020; GO:0016021; GO:0019432; GO:0030307; GO:0031957; GO:0032307; GO:0035338; GO:0043025; GO:0044233;

GO:0047676; GO:0060136; GO:0060996; GO:0070062; GO:0070672; GO:0102391

CAN5_HUMAN GO:0004198; GO:0005737; GO:0005925; GO:0006508; GO:0007165; GO:0009986; GO:0070062

DCAM_HUMAN GO:0004014; GO:0005829; GO:0006557; GO:0006595; GO:0006597; GO:0008295; GO:0019810; GO:0046500

SHH_XENLA GO:0005509; GO:0005615; GO:0005886; GO:0007267; GO:0007275; GO:0008233; GO:0008270; GO:0016539; GO:0045880

Table 5. Thermal tolerance comparisons based on critical thermal maximum (CT_{MAX}) of five rainbowfish ecotypes with a single factor ANOVA.

Species	Ecotype	n	Max CT_{MAX}	Min CT_{MAX}	Average	Variance
Melanotaenia splendida splendida	Tropical savannah	10	39.0	37.9	38.40	0.129
Melanotaenia splendida splendida	Tropical rainforest	10	38.9	37.5	38.23	0.293
Melanotaenia duboulayi	Subtropical	10	38.6	37.0	37.96	0.174
Melanotaenia splendida tatei	Desert	10	37.6	36.1	37.24	0.232
Melanotaenia fluviatilis	Temperate	10	36.5	33.1	34.88	1.633

Source of Variation	SS	df	MS	F	P-value	F crit
Between Groups	83.6168	4	20.9042	42.4786182	9.9E-15	2.578739184
Within Groups	22.145	45	0.49211111			
Total	105.7618	49				

Table 6. Thermal tolerance comparisons based on critical thermal maximum (CT_{MAX}) of five rainbowfish ecotypes using two-sample *t*-tests.

	Rainforest vs Savannah		Tropical vs Subtropical		Tropical vs Desert		Tropical vs Temperate	
	Variable 1	*Variable 2*	*Variable 1*	*Variable 2*	*Variable 1*	*Variable 2*	*Variable 1*	*Variable 2*
Mean	38.230	38.400	38.315	37.960	38.315	37.240	34.880	38.315
Variance	0.293	0.129	0.208	0.174	0.208	0.232	1.633	0.208
Observations	10.000	10.000	20.000	10.000	20.000	10.000	10.000	20.000
Pooled Variance	0.211		0.197		0.215			
Hypothesized Mean Difference	0.000		0.000		0.000		0.000	
df	18.000		28.000		28.000		10.000	
t Stat	-0.827		2.066		5.981		-8.243	
$P(T<=t)$ one-tail	0.209		0.024		0.000		0.000	
t Critical one-tail	1.734		1.701		1.701		1.812	
$P(T<=t)$ two-tail	0.419		0.048		0.000		0.000	
t Critical two-tail	2.101		2.048		2.048		2.228	
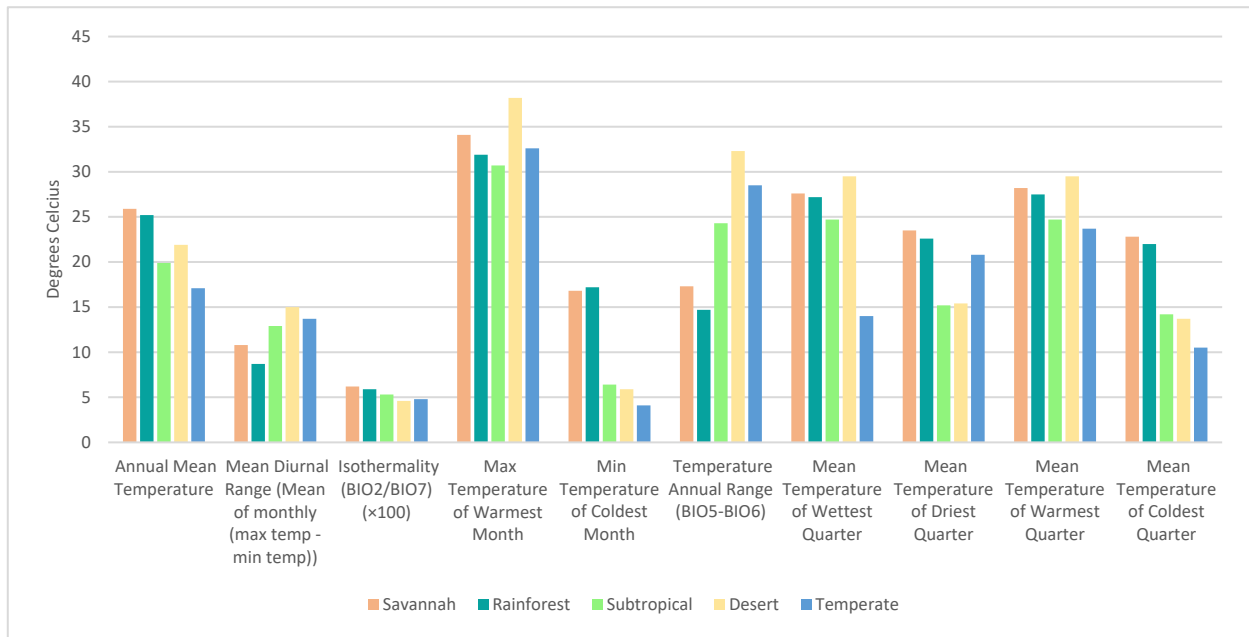
Figure 1. Overview of native thermal conditions at the sampling locality of five *Melanotaenia* rainbowfish ecotypes, based on ten contemporary BIOCLIM variables (Booth et al. 2014).
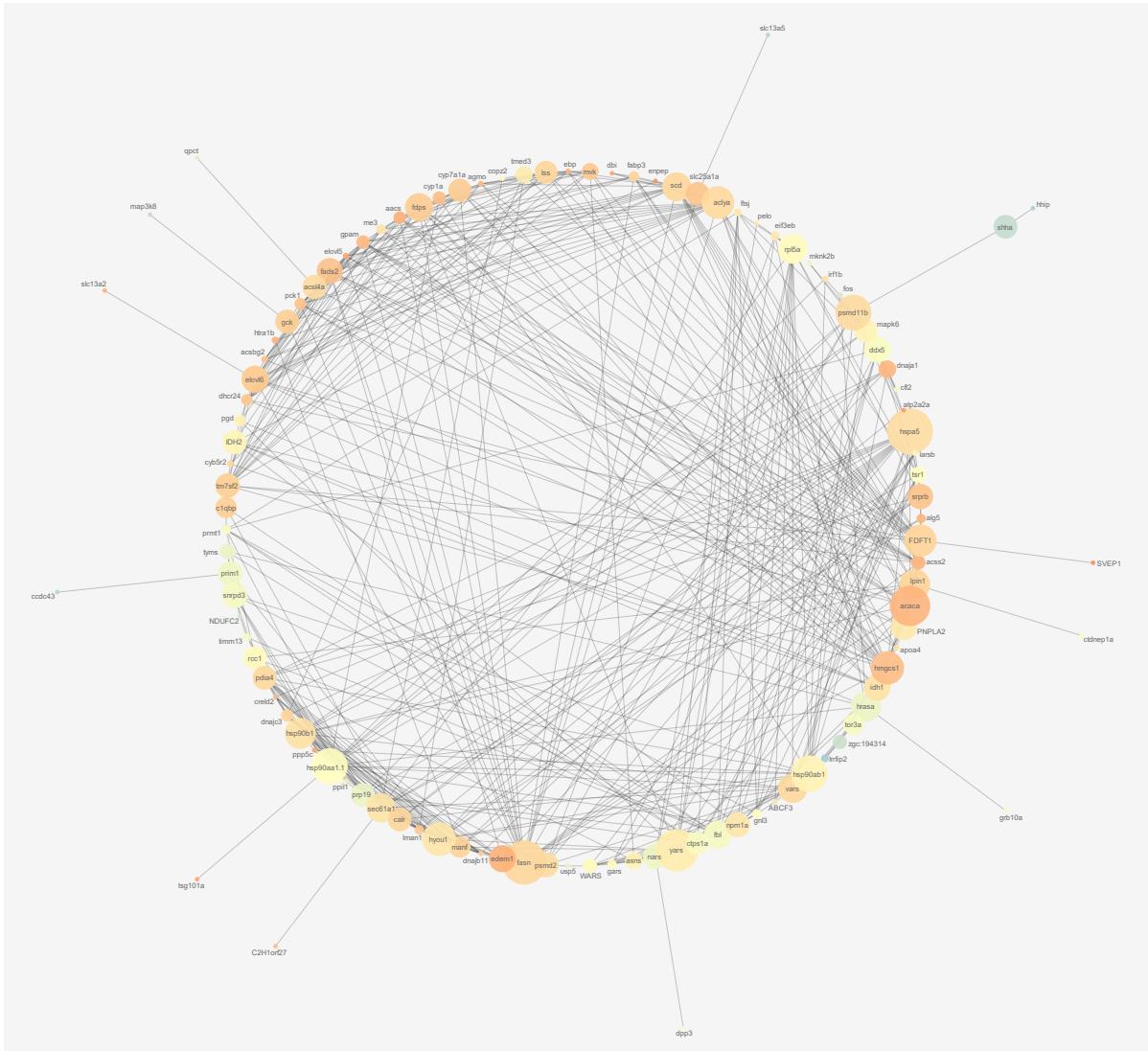
Figure 2. Protein interaction network for climate warming responses across rainforest and savannah *Melanotaenia splendida splendida*, based on 189 unigenes differentially expressed between control (21°C) and projected 2027 summer treatment (33°C) groups. Node sizes are proportional to centrality in the network (betweenness centrality), while shading indicates the relative number of direct interaction (neighbourhood connectivity; green = fewer interactions, orange = more interactions).

4. Companion publication

Full manuscript of Sandoval-Castillo et al. (2020), "Adaptation of plasticity to projected maximum temperatures and across climatically defined bioregions", Proceedings of the National Academy of Sciences, 117(29), 17112-17121.

Adaptation of plasticity to projected maximum temperatures and across climatically defined bioregions

Jonathan Sandoval-Castillo[a], Katie Gates[a], Chris J. Brauer[a], Steve Smith[a,b], Louis Bernatchez[c], and Luciano B. Beheregaray[a,1]

[a]Molecular Ecology Lab, Flinders University, Bedford Park, SA 5042, Australia; [b]Konrad Lorenz Institute of Ethology, University of Veterinary Medicine, 1160 Vienna, Austria; and [c]Institut de Biologie Intégrative et des Systèmes, Université Laval, Québec, QC G1V 0A6, Canada

Resilience to environmental stressors due to climate warming is influenced by local adaptations, including plastic responses. The recent literature has focused on genomic signatures of climatic adaptation, but little is known about how plastic capacity may be influenced by biogeographic and evolutionary processes. We investigate phenotypic plasticity as a target of climatic selection, hypothesizing that lineages that evolved in warmer climates will exhibit greater plastic adaptive resilience to upper thermal stress. This was experimentally tested by comparing transcriptomic responses within and among temperate, subtropical, and desert ecotypes of Australian rainbowfish subjected to contemporary and projected summer temperatures. Critical thermal maxima were estimated, and ecological niches delineated using bioclimatic modeling. A comparative phylogenetic expression variance and evolution model was used to assess plastic and evolved changes in gene expression. Although 82% of all expressed genes were found in the three ecotypes, they shared expression patterns in only 5 out of 236 genes that responded to the climate change experiment. A total of 532 genes showed signals of adaptive (i.e., genetic-based) plasticity due to ecotype-specific directional selection, and 23 of those responded to projected summer temperatures. Network analyses demonstrated centrality of these genes in thermal response pathways. The greatest adaptive resilience to upper thermal stress was shown by the subtropical ecotype, followed by the desert and temperate ecotypes. Our findings indicate that vulnerability to climate change will be highly influenced by biogeographic factors, emphasizing the value of integrative assessments of climatic adaptive traits for accurate estimation of population and ecosystem responses.

climate change | ecological genomics | teleosts | thermal biology | climatic variability hypothesis

Characterizing mechanisms underpinning variation in ecological adaptation can assist in identifying biogeographic patterns of vulnerability and resilience to environmental change. Climate change has promoted numerous range shifts and local extinctions due to exposure of populations to conditions outside their zones of tolerance (1–3). However, it is expected that some populations will be able to persist in situ if they are not already living at the edge of their tolerance limits or if they are able to acclimatize or adapt outside their current range of tolerance (4–7). Species' distributions are strongly influenced by thermal conditions in their native climates; it is expected that tolerance ranges and vulnerability to change will also be influenced by biogeographic factors (8–10). Exploring how molecular mechanisms influence upper thermal resilience is an important step for inferring responses to a warming environment (11). While plastic regulation of gene expression is expected to play an important role in adaptation, the effects of selection on plasticity are poorly understood and untangling them requires integrative approaches (12, 13).

Plasticity refers to a change in expressed phenotype as a function of the environment and occurs through direct effects of the environment on allelic expression, as well as changes in interactions among loci (14, 15). Here, we focus on plasticity as the ability or tendency of an individual to up- or down-regulate genes in response to the environment and, particularly, on how plasticity might provide adaptive resilience to climate change. For many genes, this occurs primarily at the level of transcription, and a complexity of responses (i.e., adaptive, maladaptive, or neutral) has been documented (16, 17). For instance, plasticity can act as a buffer against environmental pressures (16, 18) and can be a target of selection if genotypes differ in environmental sensitivity (19). Alternatively, initial plastic responses could be nonadaptive under novel environmental conditions (20). In the context of climate, gene expression can inform about the functional pathways relevant for persistence under given conditions, as well as the likely targets of selection (11, 21). This is especially important where phenotypes of ecological relevance are not obvious and may be difficult to distinguish using traditional approaches (22, 23). Relatively few studies have attempted to find signals of selection acting on gene expression. Challenges include controlling for internal and external environmental variables

Significance

Adaptation to climate change is expected to be influenced by thermal conditions experienced by species during their evolutionary history. We studied plastic capacity as a target of climatic selection, hypothesizing that populations that evolved under warmer climates have greater plastic adaptive resilience to climate change. This was tested experimentally by comparing upper thermal tolerance and gene expression in fish populations from desert, temperate, and subtropical regions of Australia. Divergent adaptive plastic responses to future climates were found across different bioregions, including in key heat stress genes. The greatest adaptive resilience was shown by the subtropical ecotype, followed by the desert and temperate ecotypes. These results have implications for large-scale assessments of climate impacts and for predictions of species distribution changes.

influencing expression (24), as well as for the effect of genetic distance on the variation in transcription between lineages (25).

Climatically defined bioregions provide a scale at which environmental variation drives meaningful differences in evolutionary and ecological processes (26, 27). The ability of populations to persist in a warmer climate is predicted to vary geographically (6, 28–31), making climatic bioregions valuable systems for comparative studies of adaptation. For instance, the climatic variability hypothesis (CVH) predicts a positive relationship between breadth of thermal tolerance and the level of climatic variability experienced by organisms as latitude increases (32). Studies of climate change impacts are increasingly seeking to integrate spatial modeling (e.g., climatic envelopes) to uncover associations between landscape features and evolutionary processes such as temperature adaptation (33–35). While a majority of species distribution models are primarily correlative, there has been an urgent call for an increase in mechanistic approaches for predicting species' responses to climate change (36–39). Mechanistic approaches have the advantage of explaining the underlying processes associated with observed trends, allowing for findings to be interpreted more generally (40).

Freshwater fishes represent an important component of vertebrate diversity. They are arguably the most threatened group of vertebrates and, as ectotherms, are especially vulnerable to thermal changes (41). The subjects of this study are Australian rainbowfishes of *Melanotaenia* (family Melanotaeniidae), a freshwater genus with evolutionary origins in tropical southern New Guinea (42). *Melanotaenia* spp. of the "australis" clade (43) provide an ideal model system to study climatic-driven adaptive evolution and to address predictions from the CVH. The clade contains a minimum of eight largely allopatric species that recently radiated into tropical, subtropical, desert, and temperate regions of mainland Australia (43). They show adaptive phenotypic divergence due to selection linked to the hydrological environment (44, 45), as well as adaptive genomic divergence associated with hydroclimatic variation (46). In terms of gene expression, common garden experiments in a subtropical australis species (*Melanotaenia duboulayi*) have tested the effect of 2070-projected summer temperatures on short-term (47) and long-term (48) transcriptional responses. Both studies indicated capacity for plastic responses to future climates and identified candidate genes for thermal adaptation (47, 48). In addition, a transgenerational experiment revealed pedigree-based evidence for heritability of observed plastic responses (48).

This work focuses on three closely related australis species, *Melanotaenia splendida tatei*, *M. fluviatilis*, and *M. duboulayi*. Their ranges show a striking concordance with three major contemporary climatic bioregions of the Australian continent (Fig. 1A), suggesting that their evolution has been influenced by selective pressures associated with climatic regimes. For this reason, we refer to them herein as climatic "ecotypes," *sensu* Engelhard, Ellis, Payne, ter Hofstede, and Pinnegar (49). We used an experimental approach (Fig. 2) to compare short-term transcriptional responses to a projected future temperature in subtropical, temperate, and desert rainbowfish ecotypes. In addition, we delineated ecological niches and assessed physiological tolerance to thermal stress and warming for each ecotype. We hypothesize that ecotype resilience in future climates will be dependent on the biogeographic region in which a given ecotype has evolved. As such, we predict to find evidence for adaptation of plastic responses to temperature among ecotypes. To test this, we applied a comparative phylogenetic expression variance and evolution (EVE) model framework (Fig. 2) to detect transcriptional responses subject to ecotype-specific directional selection. This enabled us to explore how divergent selection on gene expression may have contributed to differences in thermal tolerance and to adaptive evolution in climatically defined ecotypes.

Results

Differential Gene Expression.
Sequencing and de novo assemblies produced transcriptomes with high percentages of gene completeness for the three rainbowfish ecotypes (*SI Appendix,* Fig. S1 and Table S1). Of the 34,815 identified unigenes, 82% (28,483) were present in all ecotypes (Fig. 3A). Comparison of gene expression profiles among ecotypes and between climate change treatments identified 2,409 differentially expressed (DE) unigenes. Expression profiles showed a strong phylogenetic pattern (i.e., transcription responses are most highly correlated among individuals within ecotypes), followed by high correlation between experimental and control groups within each ecotype (Fig. 3B; see also below). On the other hand, when gene expression was compared exclusively between climate change treatments, 236 unigenes were identified (Fig. 3 C and D). Of these 236 unigenes responding plastically to climate change, 10 were shared by at least two ecotypes, with only five shared responses among all three ecotypes (Fig. 3D). In contrast, unique plastic responses to the projected summer temperature were observed for the temperate ecotype in 27 unigenes, the desert ecotype in 84 unigenes, and the subtropical ecotype in a much higher 109 unigenes. This indicates a strong phylogenetic effect on plastic gene expression but may also represent the effects of divergent selection and adaptation to different climatic ecoregions.

Divergent Selection on Gene Expression.
The phylogenetic tree provided strong support for reciprocal monophyly of each ecotype (Fig. 1B). This tree, which is consistent with previous studies (42) that indicated a sister relationship between the temperate (*M. fluviatilis*) and the subtropical (*M. duboulayi*) ecotypes, was used as the input phylogeny for the EVE analysis. Of the 34,815 unigenes assessed with EVE, 532 showed plasticity due to ecotype-specific directional selection (false discovery rate [FDR], 10%). These were genes that showed greater expression variance among rather than within ecotypes after controlling for phylogenetic effects. The dendrogram of expression level of these 532 genes was consistent with phylogenetic patterns (*SI Appendix,* Fig. S2). Twenty-three of these genes were also identified as responding to the climate change experiment (Fig. 4A). Only 1 of these 23 EVE candidate genes was DE between treatments in all ecotypes. This suggests that the plastic responses for these 23 genes are under divergent selection for resilience to thermal stress among ecotypes, with the greatest differences between desert and the other two ecotypes.

Functional Annotation, Enrichment Analysis, and Network Analyses.
From a total of 25,315 protein hits, 24,276 (96%) were assigned to 293,781 gene ontology (GO) terms (*SI Appendix,* Table S1). Enrichment analysis of GO terms assigned to the 236 DE unigenes between treatments (Fig. 3C) found terms for five molecular functions (MFs), 13 biological processes (BPs), and five cellular components (CCs) ($P < 0.01$; *SI Appendix,* Table S2). The same enrichment analysis using the 23 EVE candidates identified between treatments (Fig. 4A) found three MF, four BP, and two CC terms ($P < 0.01$; *SI Appendix,* Table S3). The protein network analysis identified six genes with very high degree of interaction, all of which were heat shock proteins (Fig. 4B and *SI Appendix,* Table S4). These hub genes included the only EVE candidate that is DE between treatments in all ecotypes. In addition, 16 candidates for shared plasticity found to be DE between treatments in two or more ecotypes, as well as all 23 EVE candidates identified between treatments, showed higher average node degrees compared with other DE genes (*SI Appendix,* Table S5). This suggests an important role of these genes in plastic and adaptive thermal stress responses of rainbowfish, respectively.

EVOLUTION

176
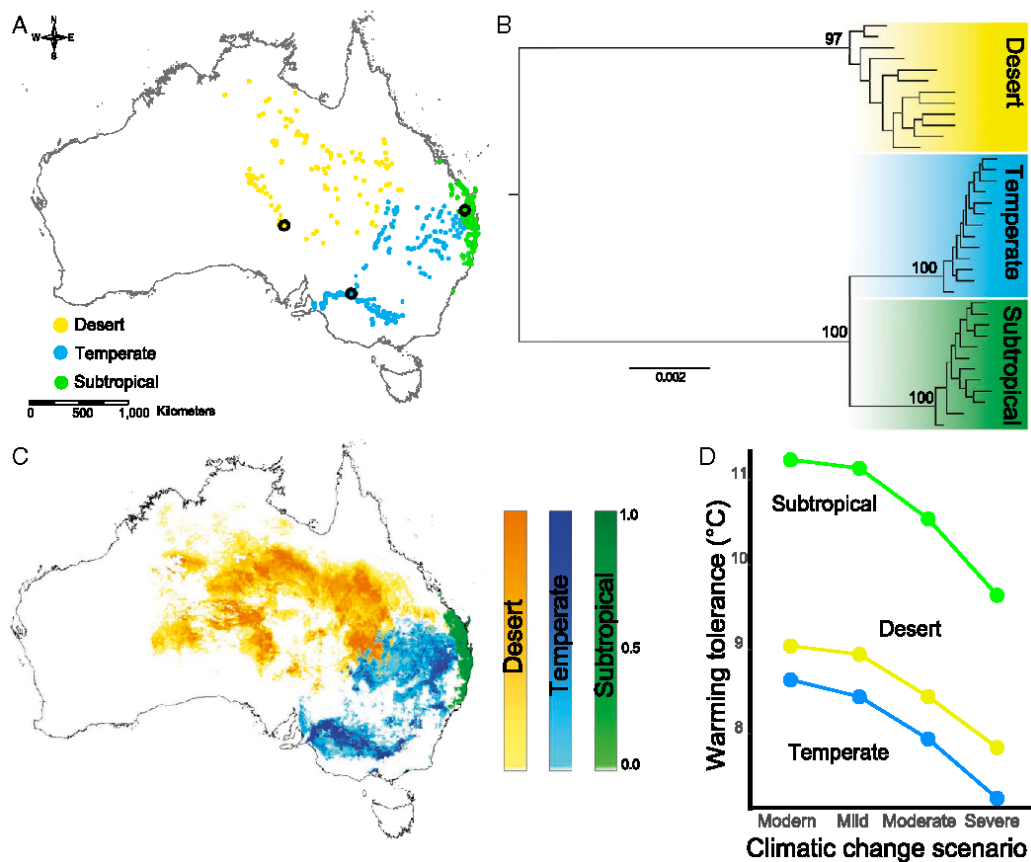
Fig. 1. (*A*) Map of Australia showing spatially and taxonomically validated records that depict the range of the three *Melanotaenia* ecotypes. The black circles show sampling localities for the transcriptomic and physiological experiments. (*B*) Maximum-likelihood tree depicting evolutionary relationships among 36 individuals of the three ecotypes based on ddRAD sequences of 1,799 loci and 156,581 bp. Numbers above nodes denote bootstrap support values. (*C*) Ecotype niche model based on 1,279 unique distribution records and nine bioclimatic variables generated in MaxEnt 3.4.1. Color tone indicates habitat suitability of each ecotype. (*D*) Physiological sensitivity of ecotypes across their ranges estimated by the warming tolerance quantity (41). Modern days are based on monthly average maximum temperature (BIOCLIM 2010 to 2018 data) and climatic projections are based on a global climate model (BCC-CSM2-MR) and on three shared socioeconomic pathways (SSPs) (mild, SSP126; moderate, SSP245; severe, SSP585).

Empirical Thermal Tolerance (CT$_{MAX}$). Upper thermal tolerance was significantly different among ecotypes (*P* = <0.001; *SI Appendix,* Table S5 and Fig. 5) with the highest CT$_{MAX}$ shown by the subtropical ecotype (38.0 °C; CI = 37 to 38.6 °C), followed by the desert (37.2 °C; CI = 36.1 to 37.6 °C) and finally the temperate ecotype (34.9 °C; CI = 33.1 to 36.5 °C). Interestingly, these estimates of CT$_{MAX}$ across ecotypes were correlated with the number of DE genes between climate change treatments displayed by each ecotype (*r* = 0.998; Fig. 5).

Ecological Niche Modeling and Warming Tolerance. Nine BIOCLIM variables were retained for analysis after correcting for data dimensionality and redundancy ($|r| > 0.8$) (*SI Appendix,* Fig. S3 and Table S6). The species distribution modeling (SDM) analyses revealed that the three ecotypes have markedly divergent bioclimatic niches (Fig. 1*C*), with near zero or zero niche overlap (*P* = <0.001; *SI Appendix,* Table S7). The ecotypes also showed

different physiological sensitivities based on the warming tolerance quantity, with the subtropical ecotype being the more tolerant, the desert being intermediate, and the temperate the less tolerant (Fig. 1*D*). This pattern was observed for modern as well as for the three projected climates (Fig. 1*D*) and remained unaffected if warming tolerance is estimated using the maximum temperature of the warmest month (*SI Appendix,* Fig. S4).

Discussion

We compared transcriptional plasticity to projected summer temperatures and physiological tolerance in three climatic ecotypes of Australian rainbowfish: temperate, desert, and subtropical. These ecotypes showed divergent bioclimatic niches and different physiological sensitivities to upper thermal stress and to environmental warming. Within ecotypes, individuals exhibited very similar changes in both the direction and the magnitude of expressed genes. However, gene response mechanisms to projected

Sandoval-Castillo et al.

177
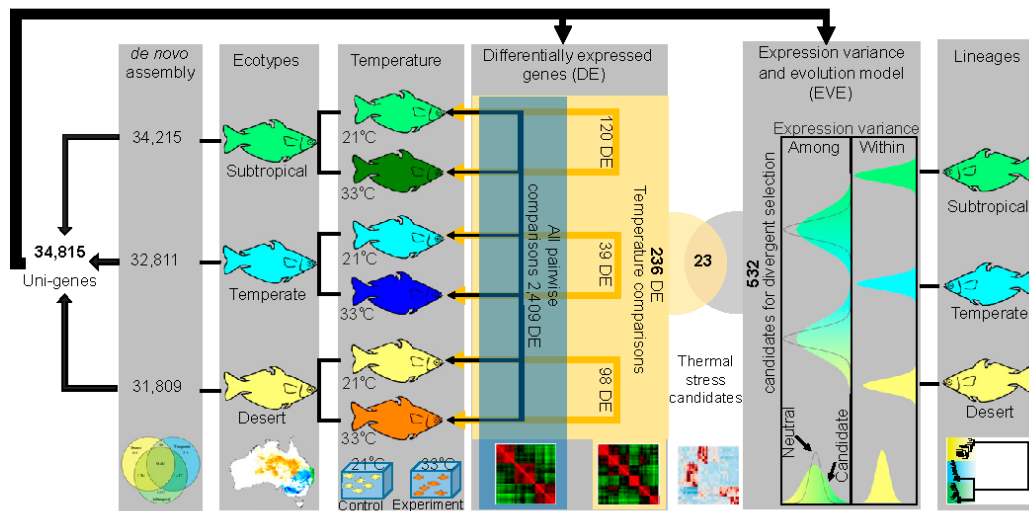
Fig. 2. Experimental design and pipeline of the comparative transcriptomic section. Wild-caught individuals from each *Melanotaenia* ecotype (subtropical, temperate, and desert) were subjected to control (21 °C) and experimental (33 °C) treatments. Their transcriptomes were assembled de novo. Expression profiles of 34,815 unigenes were used to identify 2,409 differentially expressed (DE) genes in all pairwise comparisons (blue shading, 15 comparisons), and 236 genes DE between temperature treatments for the same ecotype (orange shading, three comparisons). In parallel, an expression variance and evolution (EVE) model was used to identify genes for which expression plasticity is under divergent selection. Under a neutral model, the ratio of the expression variance between vs. within lineages (i.e., ecotypes) is the same for all genes, compared to a higher relative ratio for genes under divergent selection. This resulted in 532 EVE candidates for divergent selection on expression between ecotypes. Twenty-three genes (overlapping gray and orange area) that were DE between temperature treatments for the same ecotype and also identified by EVE were considered candidates for adaptation to projected upper thermal stress.

thermal stress differed remarkably among ecotypes. Interestingly, both plastic responses and estimates of physiological tolerance (i.e., CT_{MAX} results and environmental warming tolerance) varied in a biogeographically determined manner. Subtropical rainbowfish showed both the highest transcription response and tolerance among ecotypes, temperate rainbowfish showed the lowest responses and tolerance, and desert rainbowfish showed intermediate transcriptional responses and physiological tolerance.

Although all species mounted substantial plastic responses to 2070-projected summer temperatures, a striking result was that responses were ecotype-specific, with transcriptional changes for only five genes common to all three ecotypes. This is consistent with lineage-specific adaptation resulting from contrasting selective pressures across the climatically defined bioregions, but can also be associated with neutral mechanisms of evolution (25, 50, 51). For this reason, we incorporated a comparative phylogenetic model to control for the effects of neutral drift on gene expression (52). This approach identified a large suite of 532 candidates for divergent selection on gene expression between ecotypes, of which a subset of 23 genes also showed significant ecotype-specific response to thermal manipulation (Fig. 4). We consider these 23 genes as strong candidates for adaptive (i.e., genetic-based) plastic response to future increases in temperature. Network analyses demonstrated centrality of these genes in thermal response pathways, while also identifying several highly conserved hub genes. These genes appear to be of fundamental importance for modulating thermal response pathways and adaptive potential in the three ecotypes. Together, these results show that while integral expression responses can be conserved among ecotypes, the tendency for divergence in response to upper thermal stress is high. This divergence not only exceeds neutral expectations but corresponds to inferred ecotype differences in niche suitability and tolerance to environmental

warming across climatically defined bioregions, speaking to the importance of biogeographic history in considerations of climate-adaptive potential.

Adaptive Mechanisms Contribute to Gene Expression Plasticity among Ecotypes. Shifts in gene expression regulation have for a long time been hypothesized to contribute to adaptive diversity (53). However, the evolution of plastic responses by natural selection has been infrequently documented in empirical studies, particularly in natural populations (but see refs. 51 and 54–57). Although a diversity of mechanisms regulate gene expression (58), substantial empirical evidence supports heritability of expression responses (51, 59, 60), including for the subtropical Australian rainbowfish (*M. duboulayi*) (48). As such, plasticity is likely to be subject to the same broad evolutionary processes as other heritable traits. For instance, under directional selection, limited expression polymorphism is expected within ecotypes, while extensive divergence is expected between ecotypes (61). Under stabilizing selection, expression regulation is predicted to be highly consistent within and across ecotypes (16, 61). Meanwhile, under neutral evolution, patterns of gene expression are expected to correlate with evolutionary divergence (51), which we assessed using a phylogenetic-based approach. Our comparative analyses suggested that all of the above mechanisms have influenced gene expression responses to projected thermal limits in rainbowfishes. This fits with our understanding of thermal tolerance adaptation in ectotherms as highly complex, and involving multiple levels of biological organization (62, 63).

The majority of DE genes under 2070-projected temperature manipulation exhibited patterns of variation that could be associated with phylogenetic distance (Figs. 1*B* and 3*B*). This demonstrates that plastic responses to future climates can be

178
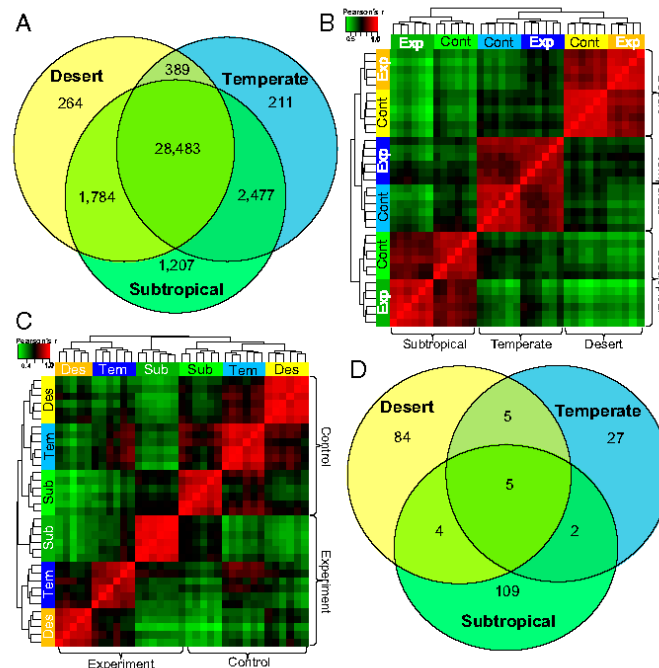
Fig. 3. (A) Venn diagram of unigenes identified in each ecotype of *Melanotaenia* as well as shared among ecotypes (based on a total of 34,815 unigenes). (B) Heatmap summarizing correlation among ecotypes in log₂ gene expression profiles. This analysis was based on 2,409 DE transcripts. The colored bars under the sample dendrograms represent the climate change experimental (Exp) and control (Cont) groups. (C) Heatmap summarizing correlation between treatments (control vs. experiment) in log₂ gene expression profiles. This analysis was based on 236 DE unigenes identified between control and experiment samples. Colored bars under the sample dendrograms represent the ecotypes, with climate change experimental groups represented by dark color variation and control groups represented by light color variation. (D) Venn diagram of DE unigenes shared between ecotypes.

highly constrained by demographic history. Nonetheless, we were able to reject neutral scenarios as the most parsimonious explanation for the variation in a large subset of DE genes. In the case of the EVE candidates for directional selection to thermal stress, there was very little expression variance within ecotypes, but high levels of divergence between ecotypes. We suggest that regulatory differences in these genes have helped to facilitate persistence of rainbowfish ecotypes within their respective thermal environments (Fig. 1C), bringing each closer to a local phenotypic optimum. While evidence of ecological selection on plasticity is rare, an example includes the gene expression divergence of a soil-dwelling hexapod (*Orchesella cincta*) in populations subsisting in contaminated mine sites (56). This was correlated with heavy metal tolerance, which resulted in a heritable increase in metal excretion efficiency. In fish, Brennan et al. (64) demonstrated a shift in salinity-specific expression responses in populations of killifish (*Fundulus heteroclitus*) adapted to habitats of contrasting salinity.

The center of the gene interaction network for the three rainbowfish ecotypes consisted largely of heat shock proteins that play an important role in thermal responses in a wide variety of taxa (65, 66). Patterns of plastic responses to temperature were most likely to be shared among ecotypes in these central "hub" genes (*SI Appendix*, Table S4). This indicates a conserved functional role, which may have been retained through purifying and possibly stabilizing selection. Hub genes influence the expression and activity of genes downstream in an expression

network and tend to be highly conserved in their expression between lineages (67). In genome-wide studies of model organisms, the deletion of hub genes is more likely to be deleterious than for nonhub genes. This can be due to either compromised network structure, or simply because they are more likely to be involved in essential interactions (68). However, the fact that the EVE candidates for divergent expression among ecotypes also exhibited greater average connectedness than other DE genes suggests the importance of these genes in the respective ecological adaptations they have likely facilitated. In fact, three EVE candidates were also identified as hub genes, and one of these shows plasticity in all ecotypes (HSP90AA1). A change in expression in one or a few hub genes could therefore translate to a completely different stress response pathway. Indeed, enrichment analyses indicate that functions as diverse as metabolism, immune response, oxidative stress response, DNA damage response, signal transduction, and other stress responses are contributing to local adaptation among ecotypes.

While the transcriptomic approaches used here directly address functional mechanisms for thermal response, we are not yet able to infer specific fitness effects of divergent expression patterns in warming climates. Despite this, the number of genes regulated in response to warming differed markedly between ecotypes, with the greatest number in the most heat-resilient subtropical ecotype (CT_{MAX}, 38.0°), and the smallest number responding in the least heat-resilient temperate ecotype (CT_{MAX}, 34.9°) (Fig. 5). This was consistent with range-wide

Sandoval-Castillo et al.

179
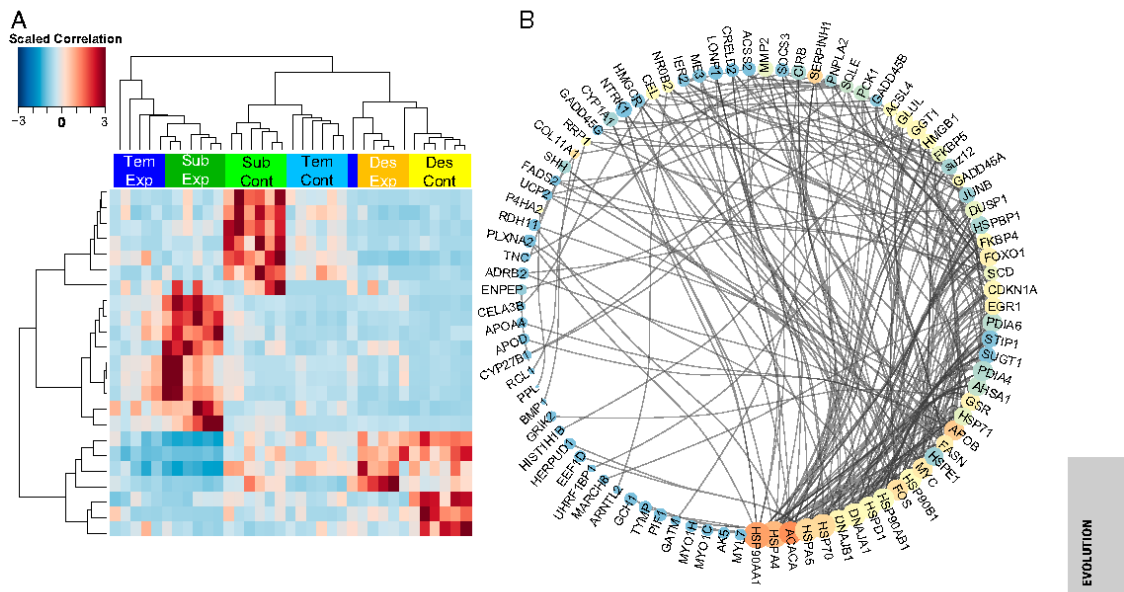
Fig. 4. (*A*) Hierarchical clusters of 23 transcripts identified as candidates for divergent selection on expression level and also showing significant differential expression between control and experiment. Color bars indicate the ecotype of the samples. DesCont, desert control (20 °C); DesExp, desert experimental (33 °C); SubCont, subtropical control (20 °C); SubExp, subtropical experimental (33 °C); TemCont, temperate control (20 °C); TemExp, temperate experimental (33 °C). (*B*) Protein interaction network containing 137 heat stress-associated proteins linked via 1,114 interactions. Size of node is proportional to its centrality in the network, color of node indicates the relative number of interactions it is directly involved in (blue, lower, to red, higher number of interactions), and both color and size of the node indicate relative importance of the protein in *Melanotaenia* heat stress response.

patterns of warming tolerance estimated for the ecotypes for both modern and projected climates (Fig. 1*D*). Similarly, previous work comparing montane and desert redband trout (*Oncorhynchus mykiss gairdneri*) found that the more resilient desert trout regulated a larger number of genes than the less resilient montane trout in response to acute warming conditions (69, 70). While the absolute number of transcripts regulated in a given condition can depend on many factors, including differences in constitutive expression or qualitative differences such as amino acid or regulatory changes (71), it is possible that a larger number of regulated genes may reflect a multifaceted [e.g., Chadwick et al. (72)] plastic response to environmental stressors. In rainbowfish, it is too early to say whether the observed increase in number of DE genes represents a more specialized adaptation to heat by the subtropical rainbowfish compared to desert and temperate ecotypes. However, the association between thermal tolerance and number of regulated transcripts does provide further evidence to support adaptive differences in the potential for expression-mediated phenotypic plasticity.

Physiological Thermal Tolerance Is Specific to Ecotype. It is generally assumed that organisms are adapted to or have the ability to acclimate to the temperatures normally encountered in their habitat range (29). It has been proposed that organisms that evolved in warmer climates will have higher thermal tolerances than those in cool climates (73), and that those that evolved in variable climates will have greater acclimation capacities and tolerance ranges than those in more stable climates (32). We found that ecotypes show different climatic envelopes and environmental warming tolerance and differed significantly in

CT_{MAX}. Although it is unclear how well CT_{MAX} predicts thermal tolerance in wild populations, a recent zebrafish study showed that tolerance to rapid warming correlates with tolerance to slow warming, indicating that CT_{MAX} is likely to be representative of resilience to longer episodes of warming, such as heat waves (74). Consistent with several studies assessing relationships between thermal tolerance and latitude (5, 10, 29, 41, 75, 76), and with Janzen's (32) CVH assumption that organisms adapt to the temperatures they normally encounter (29, 32), rainbowfish thermal tolerance increases with proximity to the equator. However, CT_{MAX} does not coincide entirely with average maximum summer temperatures (or average annual temperatures) in the climate of origin, with the hottest Australian temperatures found in the central deserts as opposed to the north-eastern subtropical region (*SI Appendix*, Table S5; ref. 77). Perhaps counterintuitively, this finding supports studies that emphasize the importance of temperature variability in relation to an organism's upper limits of thermal tolerance (5, 29, 76).

Although wider ranges of tolerance have been found at higher latitudes, these have been largely attributed to lower critical thermal minimums of temperate organisms (10, 29). Meanwhile, higher thermal tolerances have been observed in tropical regions, but with an inverse relationship to tolerance breadth (36). This has led to the use of the term "climate specialists" to describe tropical species, with an evolutionary trade-off suggested between upper thermal tolerance and the capacity to acclimate to a wide range of temperatures (36, 41, 78, 79). Due to this apparent trade-off, our findings may highlight an unforeseen risk for desert taxa, which are theoretically expected to show the greatest thermal plasticity. While the temperate ecotype showed

Sandoval-Castillo et al.

EVOLUTION

180
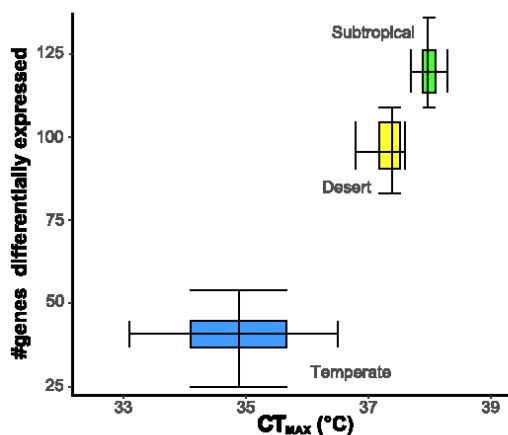
Fig. 5. Association between CT$_{MAX}$ and number of genes differentially expressed in response to projected climate in three ecotypes of *Melanotaenia* ($r = 0.998$). The box plots display the upper and lower quartiles, whiskers represent 95th and 5th percentiles, and their intersections represent the median.

the lowest transcription response and tolerance, the ability of the desert rainbowfish to adapt to extremely high temperatures may be compromised by the need to maintain a large window of tolerance. It is already common for ambient temperatures at the desert rainbowfish's sampling locations (77) to exceed its CT$_{MAX}$, although larger water bodies are unlikely to reach such extremes due to the fluctuation in diurnal temperatures (~15 °C/d) and slow rates of heat exchange between air and water (80). However, desert environments are predicted to experience more extreme heat waves and longer droughts under climate change scenarios (81). This is likely to not only increase the length of time in which organisms are exposed to thermal stress conditions, but decrease the overall volume of aquatic refugia, making them more susceptible to extreme ambient temperatures (82). In such circumstances, typical behavioral responses such as seeking shade or cool-water sites created by deeper water or inflowing tributaries may be unable to compensate for these effects (82, 83). The current poor understanding of desert ecosystems and the disparate approaches used to study climate change impacts in these regions (84) highlight the need for an integrated reassessment of dryland vulnerability to climate change.

Conclusions and Perspectives. Climate change is creating a discord between some organisms' physiologies and their environments. To predict the likelihood of range shifts, population declines, or local extinctions, it is useful to understand the distribution of adaptive diversity, including that of adaptive plasticity. However, despite extensive empirical studies about standing genetic variation and its effects on climate-related traits, the concept of adaptive plasticity remains relatively unaddressed. Our results supported the hypothesis that the capacity for plastic response to climate varies biogeographically, even within a closely related group. Moreover, by controlling for the effects of phylogeny, we showed that divergent selection on gene expression has contributed to observed differences in plastic capacity among ecotypes. By demonstrating immediate response mechanisms to upper thermal stress, as well as evidence for ecological selection on these mechanisms, our study emphasizes the key role of plasticity in both short- and long-term climatic adaptation. This has implications for broad biogeographic assessments of climate

impacts, as well as for more focused predictions of species distribution changes, which are only now beginning to account for intrataxonomic adaptive variation. This study represents a stride toward a more holistic understanding of climatic adaptive potential in natural populations.

Materials and Methods

Ecotype Range, Sampling, and Temperature Experiments. Our study system includes the crimson spotted rainbowfish (*Melanotaenia duboulayi*)—a species with a subtropical distribution along coastal catchments of eastern Australia; the Murray River rainbowfish (*M. fluviatilis*)—a temperate species found in the inland Murray-Darling Basin; and the desert rainbowfish (*M. splendida tatei*)—a species found in arid and semiarid catchments of central Australia (Fig. 1 *A* and *C*). *Melanotaenia duboulayi* individuals were collected using bait traps and hand nets from the upper section of the Brisbane River, near Fernvale in Queensland (subtropical; 27°26'37.39"S, 152°40'12.76"E). *Melanotaenia fluviatilis* were collected from the midsection of the Murray River, close to Gol Gol in New South Wales (temperate; 34°10'50.3"S 142°13' 16.8"E) using a seine net. *Melanotaenia splendida tatei* were collected from Algebuckina Waterhole in South Australia (desert; 27°51'53.9"S 135°53'57.1" E) using fyke nets. Between 42 and 60 individuals were collected at each locality, transported live to the Flinders University Animal House Facility and acclimatized at 21 °C for at least 60 d prior to temperature experiments. Individuals from each species were maintained in single-sex aquaria (~20 fish/100 L) at 21 °C under 12-h light/12-h dark and fed once daily with blood worms and fish pellets. To assess short-term responses to contemporary (21 °C) and 2070-projected (33 °C) average summer temperatures, individuals of each species were randomly assigned to an experimental or a control group ($n = 6$ per group, per species). Temperature in these "climate change treatments" was increased by 2 °C per d over 6 d toward the target of 33 °C, and then maintained for 14 d. The 33 °C is the projected average summer temperature for Australia's east coast in 2070 based on a high emission scenario (RCP8.5) of the International Panel on Climate Change (47, 85). Control groups were kept at 21 °C for the duration of the experiment. Fish were euthanized following the Australian Code of Practice for the Care and Use of Animals for Scientific Purposes 2013 and immediately dissected to extract the liver. Sampling procedures took place between 9:00 AM and 11:00 AM. Only adult males of similar length were used to control for sex- and age-related effects on transcription responses. Liver tissue was incubated at 4 °C for 12 h in RNAlater (Ambion) before storage at −80 °C. In addition to being a relatively homogenous tissue, liver was selected because metabolic conditioning and gene expression are known to respond to heat stress (47, 48).

Transcript Quantification and Differential Expression Analysis. Methodological details about RNA extraction, transcriptome sequencing, and assembly are provided in *SI Appendix*. For the differential expression tests between experimental groups and among ecotypes, reads for each sample were mapped back to the predicted protein coding regions using BOWTIE2 V2.2.7 (86), and then gene-level abundance was estimated with RSEM V1.2.19 (87). Read count estimations were cross-sample normalized using trimmed mean of M values (88). Normalized count data were then used as input in DESeq2 V1.10.1 (89). We used a conventional threshold (e.g., refs. 90 and 91) where transcripts with a minimum log$_2$ fold change of 2 between any two groups (i.e., experimental vs. control, ecotype vs. ecotype) were considered DE (FDR of 5%).

Gene Expression Plasticity and Divergent Selection. We implemented the EVE Model (52) to identify transcripts potentially under divergent selection for expression levels. Briefly, the model uses a phylogenetic tree and expression data to estimate a parameter β that represents the ratio of among-lineage expression divergence to within-lineage expression diversity. This ratio should be approximately constant over most genes if no divergent selection is acting between lineages. For each transcript (i), the EVE model assesses the null hypothesis that independent transcript β_i is not significantly different to a shared β_s for all transcripts; if β_i is higher than β_s, the model assumes that transcript i is subject to lineage-specific directional selection on expression level. We considered transcripts to be under divergent selection when β_i was significantly higher than β_s (FDR of 10%).

To calculate the expected expression covariance between lineages under shared and independent evolutionary scenarios, we constructed a phylogenetic tree using genome-wide SNP (single-nucleotide polymorphism) data from 12 samples of each ecotype. These data were obtained using reduced-

Sandoval-Castillo et al.

181

representation sequencing (ddRAD) for studies of population genomics of the three ecotypes (46) (*SI Appendix*, Table S8). The software PyRAD V3.0.6 (92) was used to align the ddRAD sequences and RAXML V8.2.1 (93) used to perform a maximum-likelihood phylogenetic analysis, with the GTRGAMMA model and 1,000 bootstrap replicates. The final concatenated dataset for the 36 rainbowfishes was based on 1799 ddRAD loci and 156,581 bp. The consensus phylogenetic tree was used as the input phylogeny for the EVE analysis.

GO Enrichment Analysis and Pathway Network Analysis. Enrichment analysis on the DE genes and on the EVE candidate genes relative to all genes were performed using TOPGO v2.34 (94) based on both Fisher's classic and weight tests ($P < 0.01$). To further understand the relative importance of candidate and shared plastic genes, a network analysis was conducted using CYTO-SCAPE V3.7 (95). First, a protein interaction network was created from the entire DE gene set by drawing edges between genes with physical and functional interactions reported for humans and with orthologous functions in zebrafish in the STRING database (96). The relative importance of a protein is correlated with its connectivity in an interactive network. We calculated the node degrees as an estimator of protein connectivity. We then identified highly connected genes (hubs) following ref. 97, as those with a node degree greater than or equal to the sum of the mean, plus twice the SD of the node degree distribution.

Thermal Tolerance (CT_{MAX}). We determined the thermal tolerance of each ecotype via short-term CT_{MAX} experiments following Becker and Genoway (98). To control for sex- and age-related effects, we sampled 10 adult females of similar length from each ecotype from the same populations used for the transcriptomic experiments. Each fish was placed individually in a 5-L glass beaker containing 3 L of water at 21 °C. Temperature was increased at a rate of 0.33 °C/min using a digital water bath until the fish showed both motor disorganization and loss of equilibrium for a period of 1 min (98). CT_{MAX} for a given ecotype was obtained by averaging over 10 independent replicates. An ANOVA test was used to assess statistical differences in CT_{MAX} among ecotypes.

Ecological Niche Modeling and Warming Tolerance. The ecological niche for each ecotype was obtained via SDM using MaxEnt 3.4 (99). This capitalized on extensive spatial records for the three ecotypes (Atlas of Living Australia; https://www.ala.org.au/) and on 19 BIOCLIM datasets (https://www.worldclim.org/) (35) that include variables known to influence hydroclimatic adaptation in Australian rainbowfish (46). Because BIOCLIM data are based on air temperature, we used a global standard regression model to calculate stream water temperature (100). Niche identity and overlap between ecotypes were assessed by calculating Schoener's D and Hellinger distance in ENMTools (101). Ecologically meaningful climatic envelopes were obtained with the Bayesian-based *Plateau* climate envelope function (102).

We estimated warming tolerance [*sensu* Deutsch et al. (41)] to assess physiological sensitivity of each ecotype across their ranges. This quantity approximates the average amount of environmental warming an ectotherm can tolerate before performance drops to fatal levels, and is defined as the difference between CT_{MAX} and the mean monthly maximum temperature experienced by an ecotype across its range (41). This was estimated for modern days based on monthly average maximum temperature (BIOCLIM 2010 to 2018 data) and for three projected warming scenarios based on the Beijing Climate Center Climate System Model (BCC-CSM2-MR) and three Shared Socioeconomic Pathways (SSPs) (mild, SSP126; moderate, SSP245; severe, SSP585). For comparison, we also estimated warming tolerance using the maximum temperature of the warmest month (*SI Appendix*, Fig. S4). Additional details for this section are in *SI Appendix*.

1. G. Grabherr, M. Gottfried, H. Pauli, Climate effects on mountain plants. *Nature* **369**, 448 (1994).
2. C. Parmesan *et al.*, Poleward shifts in geographical ranges of butterfly species associated with regional warming. *Nature* **399**, 579–583 (1999).
3. J. J. Wiens, Climate-related local extinctions are already widespread among plant and animal species. *PLoS Biol.* **14**, e2001104 (2016).
4. J. H. Stillman, Acclimation capacity underlies susceptibility to climate change. *Science* **301**, 65 (2003).
5. J. M. Sunday, A. E. Bates, N. K. Dulvy, Global analysis of thermal tolerance and latitude in ectotherms. *Proc. Biol. Sci.* **278**, 1823–1830 (2011).
6. R. A. Catullo, S. Ferrier, A. A. Hoffmann, Extending spatial modelling of climate change responses beyond the realized niche: Estimating, and accommodating, physiological limits and adaptive evolution. *Glob. Ecol. Biogeogr.* **24**, 1192–1202 (2015).
7. A. A. Hoffmann, C. M. Sgrò, Climate change and evolutionary adaptation. *Nature* **470**, 479–485 (2011).
8. Y. Cohet, J. Vouidibio, J. David, Thermal tolerance and geographic distribution: A comparison of cosmopolitan and tropical endemic *Drosophila* species. *J. Therm. Biol.* **5**, 69–74 (1980).
9. T. J. Compton, M. J. Rijkenberg, J. Drent, T. Piersma, Thermal tolerance ranges and climate variability: A comparison between bivalves from differing climates. *J. Exp. Mar. Biol. Ecol.* **352**, 200–211 (2007).
10. A. Addo-Bediako, S. L. Chown, K. J. Gaston, Thermal tolerance, climatic variability and latitude. *Proc. Biol. Sci.* **267**, 739–745 (2000).
11. L. M. Komoroske, R. E. Connon, K. M. Jeffries, N. A. Fangue, Linking transcriptional responses to organismal tolerance reveals mechanisms of thermal sensitivity in a mesothermal endangered fish. *Mol. Ecol.* **24**, 4960–4981 (2015).
12. Y. Gilad, A. Oshlack, S. A. Rifkin, Natural selection on gene expression. *Trends Genet.* **22**, 456–461 (2006).
13. R. J. McCairns, L. Bernatchez, Plasticity and heritability of morphological variation within and between parapatric stickleback demes. *J. Evol. Biol.* **25**, 1097–1112 (2012).
14. S. M. Scheiner, Genetics and evolution of phenotypic plasticity. *Annu. Rev. Ecol. Syst.* **24**, 35–68 (1993).
15. E. Nonaka, R. Svanbäck, X. Thibert-Plante, G. Englund, Å. Brännström, Mechanisms by which phenotypic plasticity affects adaptive divergence and ecological speciation. *Am. Nat.* **186**, E126–E143 (2015).
16. C. K. Ghalambor, J. K. McKay, S. P. Carroll, D. N. Reznick, Adaptive versus non-adaptive phenotypic plasticity and the potential for contemporary adaptation in new environments. *Funct. Ecol.* **21**, 394–407 (2007).
17. P. Gibert, V. Debat, C. K. Ghalambor, Phenotypic plasticity, global change, and the speed of adaptive evolution. *Curr. Opin. Insect Sci.* **35**, 34–40 (2019).
18. S. Grenier, P. Barre, I. Litrico, Phenotypic plasticity and selection: Nonexclusive mechanisms of adaptation. *Scientifica (Cairo)* **2016**, 7021701 (2016).
19. G. Fusco, A. Minelli, Phenotypic plasticity in development and evolution: Facts and concepts. Introduction. *Philos. Trans. R. Soc. Lond. B Biol. Sci.* **365**, 547–556 (2010).
20. C. K. Ghalambor *et al.*, Non-adaptive plasticity potentiates rapid adaptive evolution of gene expression in nature. *Nature* **525**, 372–375 (2015).
21. T. E. Reed, D. E. Schindler, R. S. Waples, Interacting effects of phenotypic plasticity and evolution on population persistence in a changing climate. *Conserv. Biol.* **25**, 56–63 (2011).
22. P. Nosil, *Ecological Speciation*, (Oxford University Press, 2012).
23. J. R. Nevins, A. Potti, Mining gene expression profiles: Expression signatures as cancer phenotypes. *Nat. Rev. Genet.* **8**, 601–609 (2007).
24. A. Conesa *et al.*, A survey of best practices for RNA-seq data analysis. *Genome Biol.* **17**, 13 (2016).
25. C. W. Dunn, X. Luo, Z. Wu, Phylogenetic analysis of gene expression. *Integr. Comp. Biol.* **53**, 847–856 (2013).
26. W. Jetz, P. V. Fine, Global gradients in vertebrate diversity predicted by historical area-productivity dynamics and contemporary environment. *PLoS Biol.* **10**, e1001292 (2012).
27. P. V. Fine, Ecological and evolutionary drivers of geographic variation in species diversity. *Annu. Rev. Ecol. Evol. Syst.* **46**, 369–392 (2015).
28. C. D. Thomas *et al.*, Extinction risk from climate change. *Nature* **427**, 145–148 (2004).
29. C. K. Ghalambor, R. B. Huey, P. R. Martin, J. J. Tewksbury, G. Wang, Are mountain passes higher in the tropics? Janzen's hypothesis revisited. *Integr. Comp. Biol.* **46**, 5–17 (2006).

EVOLUTION

182

30. S. N. Aitken, M. C. Whitlock, Assisted gene flow to facilitate local adaptation to climate change. *Annu. Rev. Ecol. Evol. Syst.* **44**, 367–388 (2013).

31. N. R. Polato et al., Narrow thermal tolerance and low dispersal drive higher speciation in tropical mountains. *Proc. Natl. Acad. Sci. U.S.A.* **115**, 12471–12476 (2018).

32. D. H. Janzen, Why mountain passes are higher in the tropics. *Am. Nat.* **101**, 233–249 (1967).

33. D. M. Summers, B. A. Bryan, N. D. Crossman, W. S. Meyer, Species vulnerability to climate change: Impacts on spatial conservation priorities and species representation. *Glob. Change Biol.* **18**, 2335–2348 (2012).

34. M. B. Araújo, R. J. Whittaker, R. J. Ladle, M. Erhard, Reducing uncertainty in projections of extinction risk from climate change. *Glob. Ecol. Biogeogr.* **14**, 529–538 (2005).

35. T. H. Booth, H. A. Nix, J. R. Busby, M. F. Hutchinson, BIOCLIM: The first species distribution modelling package, its early applications and relevance to most current MAXENT studies. *Divers. Distrib.* **20**, 1–9 (2014).

36. L. Comte, J. D. Olden, Evolutionary and environmental determinants of freshwater fish thermal tolerance and plasticity. *Glob. Change Biol.* **23**, 728–736 (2017).

37. M. A. Cavaleri, S. C. Reed, W. K. Smith, T. E. Wood, Urgent need for warming experiments in tropical forests. *Glob. Change Biol.* **21**, 2111–2121 (2015).

38. M. E. K. Evans, C. Merow, S. Record, S. M. McMahon, B. J. Enquist, Towards process-based range modeling of many species. *Trends Ecol. Evol. (Amst.)* **31**, 860–871 (2016).

39. R. A. Bay et al., Predicting responses to contemporary environmental change using evolutionary response architectures. *Am. Nat.* **189**, 463–473 (2017).

40. M. Kearney, W. Porter, Mechanistic niche modelling: Combining physiological and spatial data to predict species' ranges. *Ecol. Lett.* **12**, 334–350 (2009).

41. C. A. Deutsch et al., Impacts of climate warming on terrestrial ectotherms across latitude. *Proc. Natl. Acad. Sci. U.S.A.* **105**, 6668–6672 (2008).

42. K. McGuigan, D. Zhu, G. R. Allen, C. Moritz, Phylogenetic relationships and historical biogeography of melanotaeniid fishes in Australia and New Guinea. *Mar. Freshw. Res.* **51**, 713–723 (2000).

43. P. Unmack, G. Allen, J. Johnson, Phylogeny and biogeogeography of rainbowfishes (Teleostei: Melanotaeniidae). *Mol. Phylogenet. Evol.* **67**, 15–27 (2013).

44. K. McGuigan, S. F. Chenoweth, M. W. Blows, Phenotypic divergence along lines of genetic variance. *Am. Nat.* **165**, 32–43 (2005).

45. K. McGuigan, C. E. Franklin, C. Moritz, M. W. Blows, Adaptation of rainbow fish to lake and stream habitats. *Evolution* **57**, 104–118 (2003).

46. C. J. Brauer, P. J. Unmack, S. Smith, L. Bernatchez, L. B. Beheregaray, On the roles of landscape heterogeneity and environmental variation in determining population genomic structure in a dendritic system. *Mol. Ecol.* **27**, 3484–3497 (2018).

47. S. Smith, L. Bernatchez, L. B. Beheregaray, RNA-seq analysis reveals extensive transcriptional plasticity to temperature stress in a freshwater fish species. *BMC Genomics* **14**, 375 (2013).

48. R. J. S. McCairns, S. Smith, M. Sasaki, L. Bernatchez, L. B. Beheregaray, The adaptive potential of subtropical rainbowfish in the face of climate change: Heritability and heritable plasticity for the expression of candidate genes. *Evol. Appl.* **9**, 531–545 (2016).

49. G. H. Engelhard, J. R. Ellis, M. R. Payne, R. ter Hofstede, J. K. Pinnegar, Ecotypes as a concept for exploring responses to climate change in fish assemblages. *ICES J. Mar. Sci.* **68**, 580–591 (2010).

50. A. Whitehead, Comparative genomics in ecological physiology: Toward a more nuanced understanding of acclimation and adaptation. *J. Exp. Biol.* **215**, 884–891 (2012).

51. A. Whitehead, D. L. Crawford, Neutral and adaptive variation in gene expression. *Proc. Natl. Acad. Sci. U.S.A.* **103**, 5425–5430 (2006).

52. R. V. Rohlfs, R. Nielsen, Phylogenetic ANOVA: The expression variance and evolution model for quantitative trait evolution. *Syst. Biol.* **64**, 695–708 (2015).

53. M.-C. King, A. C. Wilson, Evolution at two levels in humans and chimpanzees. *Science* **188**, 107–116 (1975).

54. R. J. McCairns, L. Bernatchez, Adaptive divergence between freshwater and marine sticklebacks: Insights into the role of phenotypic plasticity from an integrated analysis of candidate gene expression. *Evolution* **64**, 1029–1047 (2010).

55. C. D. Kenkel, M. V. Matz, Gene expression plasticity as a mechanism of coral adaptation to a variable environment. *Nat. Ecol. Evol.* **1**, 14 (2016).

56. D. Roelofs et al., Adaptive differences in gene expression associated with heavy metal tolerance in the soil arthropod *Orchesella cincta*. *Mol. Ecol.* **18**, 3227–3239 (2009).

57. J. G. Kingsolver, L. B. Buckley, Evolution of plasticity and adaptive responses to climate change along climate gradients. *Proc. Biol. Sci.* **284**, 20170386 (2017).

58. G. Orphanides, D. Reinberg, A unified theory of gene expression. *Cell* **108**, 439–451 (2002).

59. C. Roberge, H. Guderley, L. Bernatchez, Genomewide identification of genes under directional selection: Gene transcription Q(ST) scan in diverging Atlantic salmon subpopulations. *Genetics* **177**, 1011–1022 (2007).

60. E. E. Schadt et al., Genetics of gene expression surveyed in maize, mouse and man. *Nature* **422**, 297–302 (2003).

61. A. Hodgins-Davis, J. P. Townsend, Evolving gene expression: From G to E to GxE. *Trends Ecol. Evol. (Amst.)* **24**, 649–658 (2009).

62. J. K. Pritchard, A. Di Rienzo, Adaptation—not by sweeps alone. *Nat. Rev. Genet.* **11**, 665–667 (2010).

63. A. Cossins, *Temperature Biology of Animals*, (Springer Science and Business Media, 2012).

64. R. S. Brennan, F. Galvez, A. Whitehead, Reciprocal osmotic challenges reveal mechanisms of divergence in phenotypic plasticity in the killifish *Fundulus heteroclitus*. *J. Exp. Biol.* **218**, 1212–1222 (2015).

65. M. E. Feder, G. E. Hofmann, Heat-shock proteins, molecular chaperones, and the stress response: Evolutionary and ecological physiology. *Annu. Rev. Physiol.* **61**, 243–282 (1999).

66. Z. Chen, A. P. Farrell, A. Matala, S. R. Narum, Mechanisms of thermal adaptation and evolutionary potential of conspecific populations to changing environments. *Mol. Ecol.* **27**, 659–674 (2018).

67. T. G. Evans, Considerations for the use of transcriptomics in identifying the "genes that matter" for environmental adaptation. *J. Exp. Biol.* **218**, 1925–1935 (2015).

68. X. He, J. Zhang, Why do hubs tend to be essential in protein networks? *PLoS Genet.* **2**, e88 (2006).

69. M. R. Garvin, G. H. Thorgaard, S. R. Narum, Differential expression of genes that control respiration contribute to thermal adaptation in redband trout (*Oncorhynchus mykiss gairdneri*). *Genome Biol. Evol.* **7**, 1404–1414 (2015).

70. S. R. Narum, N. R. Campbell, Transcriptomic response to heat stress among ecologically divergent populations of redband trout. *BMC Genomics* **16**, 103 (2015).

71. G. N. Somero, The physiology of climate change: How potentials for acclimatization and genetic adaptation will determine "winners" and "losers". *J. Exp. Biol.* **213**, 912–920 (2010).

72. W. Chadwick et al., Minimal peroxide exposure of neuronal cells induces multifaceted adaptive responses. *PLoS One* **5**, e14352 (2010).

73. F. J. Vernberg, Studies on the physiological variation between tropical and temperate zone fiddler crabs of the genus Uca. II. Oxygen consumption of whole organisms. *Biol. Bull.* **117**, 163–184 (1959).

74. E. R. Åsheim, A. H. Andreassen, R. Morgan, F. Jutfelt, Rapid-warming tolerance correlates with tolerance to slow warming but not growth at non-optimal temperatures in zebrafish. https://doi.org/10.32942/osf.io/u6dpj (8 May 2020).

75. Á. J. Aguilar-Kirigin, D. E. Naya, Latitudinal patterns in phenotypic plasticity: The case of seasonal flexibility in lizards' fat body size. *Oecologia* **173**, 745–752 (2013).

76. S. Magozzi, P. Calosi, Integrating metabolic performance, thermal tolerance, and plasticity enables for more accurate predictions on species vulnerability to acute and chronic effects of global warming. *Glob. Change Biol.* **21**, 181–194 (2015).

77. Bureau of Meteorology, Bureau of Meteorology Climate Data Online (2014). http://www.bom.gov.au/. Accessed 2 March 2016.

78. J. J. Tewksbury, R. B. Huey, C. A. Deutsch, Ecology. Putting the heat on tropical animals. *Science* **320**, 1296–1297 (2008).

79. N. L. Payne, J. A. Smith, An alternative explanation for global trends in thermal tolerance. *Ecol. Lett.* **20**, 70–77 (2017).

80. D. M. Livingstone, A. F. Lotter, The relationship between air and water temperatures in lakes of the Swiss plateau: A case study with palæolimnological implications. *J. Paleolimnol.* **19**, 181–198 (1998).

81. IPCC, *Climate Change 2014—Impacts, Adaptation and Vulnerability: Regional Aspects*, (Cambridge University Press, 2014).

82. D. D. Magoulick, R. M. Kobza, The role of refugia for fishes during drought: A review and synthesis. *Freshw. Biol.* **48**, 1186–1198 (2003).

83. C. Breau, R. A. Cunjak, S. J. Peake, Behaviour during elevated water temperatures: Can physiology explain movement of juvenile Atlantic salmon to cool water? *J. Anim. Ecol.* **80**, 844–853 (2011).

84. F. T. Maestre, R. Salguero-Gómez, J. L. Quero, It is getting hotter in here: Determining and projecting the impacts of global environmental change on drylands. *Philos. Trans. R. Soc. Lond. B Biol. Sci.* **367**, 3062–3075 (2012).

85. CSIRO, Climate Change in Australia: Australian Climate Futures Tool (2016). https://www.climatechangeinaustralia.gov.au/. Accessed 2 March 2016.

86. B. Langmead, S. L. Salzberg, Fast gapped-read alignment with Bowtie 2. *Nat. Methods* **9**, 357–359 (2012).

87. B. Li, C. N. Dewey, RSEM: Accurate transcript quantification from RNA-seq data with or without a reference genome. *BMC Bioinformatics* **12**, 323 (2011).

88. M. D. Robinson, A. Oshlack, A scaling normalization method for differential expression analysis of RNA-seq data. *Genome Biol.* **11**, R25 (2010).

89. M. I. Love, W. Huber, S. Anders, Moderated estimation of fold change and dispersion for RNA-seq data with DESeq2. *Genome Biol.* **15**, 550 (2014).

90. G. A. McCulloch et al., Comparative transcriptomic analysis of a wing-dimorphic stonefly reveals candidate wing loss genes. *Evodevo* **10**, 21 (2019).

91. C. J. Brauer, P. J. Unmack, L. B. Beheregaray, Comparative ecological transcriptomics and the contribution of gene expression to the evolutionary potential of a threatened fish. *Mol. Ecol.* **26**, 6841–6856 (2017).

92. D. A. Eaton, PyRAD: Assembly of de novo RADseq loci for phylogenetic analyses. *Bioinformatics* **30**, 1844–1849 (2014).

183

93. A. Stamatakis, RAxML version 8: A tool for phylogenetic analysis and post-analysis of large phylogenies. *Bioinformatics* **30**, 1312–1313 (2014).

94. A. Alexa, J. Rahnenfuhrer, topGO: Enrichment Analysis for Gene Ontology (R package, Version 2, 2010). https://bioconductor.org/packages/release/bioc/html/topGO.html. Accessed 4 July 2016.

95. P. Shannon *et al.*, Cytoscape: A software environment for integrated models of biomolecular interaction networks. *Genome Res.* **13**, 2498–2504 (2003).

96. D. Szklarczyk *et al.*, The STRING database in 2017: Quality-controlled protein-protein association networks, made broadly accessible. *Nucleic Acids Res.* **45**, D362–D368 (2017).

97. H. Rakshit, N. Rathi, D. Roy, Construction and analysis of the protein-protein interaction networks based on gene expression profiles of Parkinson's disease. *PLoS One* **9**, e103047 (2014).

98. C. D. Becker, R. G. Genoway, Evaluation of the critical thermal maximum for determining thermal tolerance of freshwater fish. *Environ. Biol. Fishes* **4**, 245–256 (1979).

99. S. J. Phillips, R. P. Anderson, M. Dudík, R. E. Schapire, M. E. Blair, Opening the black box: An open-source release of Maxent. *Ecography* **40**, 887–893 (2017).

100. M. Punzet, F. Voß, A. Voß, E. Kynast, I. Bärlund, A global approach to assess the potential impact of climate change on stream water temperatures and related instream first-order decay rates. *J. Hydrometeorol.* **13**, 1052–1065 (2012).

101. D. L. Warren, R. E. Glor, M. Turelli, ENMTools: A toolbox for comparative studies of environmental niche models. *Ecography* **33**, 607–611 (2010).

102. M. J. Brewer, R. B. O'Hara, B. J. Anderson, R. Ohlemüller, Plateau: A new method for ecologically plausible climate envelopes for species distribution modelling. *Methods Ecol. Evol.* **7**, 1489–1502 (2016).

EVOLUTION

Sandoval-Castillo et al.

5. Code used in R for environmental association analyses

RDA: GEA

```
###########################################################
###RDA: Detecting genomic adaptation within tropical rainforest ###
###########################################################
```

```
setwd("C:/Users/kgate/Desktop/Dryad/RDA_GEA")
```

```
# load required packages
library(vegan)      #ordination (RDA)
library(adegenet)   #to import snp dataset
```

```
#import predictor dataset
rfenvunsc = read.table("env_rf_unscaled.txt", row.names = 1, header = TRUE)
```

```
#Scale and check inputs
rfenviro <- scale(rfenvunsc)
rfenviro = as.data.frame(rfenviro)
```

```
# import genotypes (counts of reference allele) which was taken from full snp dataset of all indivs RDA
rfsnps = read.table("rfsnps.txt", row.names = 1, header = TRUE)
rfsnps[1:10,1:10]
```

```
# check total % missing data
(sum(is.na(rfsnps)))/(dim(rfsnps)[1]*dim(rfsnps)[2])*100
#2.549876
```

```
# impute missing data with most common genotype
rfsnps <- apply(rfsnps, 2, function(x) replace(x, is.na(x), as.numeric(names(which.max(table(x))))))
```

```
# check % missing data again
(sum(is.na(rfsnps)))/(dim(rfsnps)[1]*dim(rfsnps)[2])*100
#[1] 0
rfsnps[1:10,1:10]


#check rownames against other inputs
stopifnot(all(row.names(rfsnps) == row.names(rfenviro)))


###########################
#Run initial global RDA
#RDA
globalrda_rf=rda(rfsnps ~ RUNSUMMERMEAN
        +STRANNTEMP
        +STRANNRAIN
        +RDI
        +ASPECT
        +STRDENSITY,
        data=rfenviro)



#double check variables are uncorrelated (vif < 5)
vif.cca(globalrda_rf)
#RUNSUMMERMEAN   STRANNTEMP   STRANNRAIN      RDI     ASPECT   STRDENSITY
#2.659303      1.653336     1.402749    2.259543   1.613286   1.739524



#Check the plots
plot(globalrda_rf, scaling=3)
screeplot(globalrda_rf)



#test significanc of the model
model.sig_rf = anova.cca(globalrda_rf, nperm=999)
#Df            Variance    F       Pr(>F)
#Model     6      876.88     10.222  0.001 ***
```

#Residual 203   2902.49

#backwards-stepwise selection to determine the best combination

#of explanatory variables and their relative contributions to the model

ordistep(globalrda_rf)

#Df   AIC   F Pr(>F)

#- ASPECT   1 1688.0 2.5093 0.005 **

- RDI   1 1688.6 3.1267 0.005 **

- RUNSUMMERMEAN 1 1694.6 9.1333 0.005 **

- STRDENSITY   1 1696.5 10.9838 0.005 **

- STRANNTEMP   1 1698.4 13.0030 0.005 **

- STRANNRAIN   1 1703.6 18.3791 0.005 **

Signif. codes: 0 '***' 0.001 '**' 0.01 '*' 0.05 '.' 0.1 ' ' 1

#Call: rda(formula = rfsnps ~ RUNSUMMERMEAN + STRANNTEMP + STRANNRAIN + RDI +

ASPECT + STRDENSITY, data = rfenviro)

#Inertia Proportion Rank

#Total   3779.370   1.000

#Constrained   876.878   0.232   6

#Unconstrained 2902.492   0.768 203

#Inertia is variance

#Eigenvalues for constrained axes:

RDA1 RDA2 RDA3 RDA4 RDA5 RDA6

#328.7 233.6 200.1 47.2 40.9 26.4

#Eigenvalues for unconstrained axes:

PC1   PC2   PC3   PC4   PC5   PC6   PC7   PC8

#108.50 55.77 38.96 33.68 24.21 23.00 21.74 21.47

#(Showing 8 of 203 unconstrained eigenvalues)

#test significance of explanatory variables

187

```
margin.sig_rf = anova.cca(globalrda_rf, by="margin", nperm=999)
#   Df Variance       F Pr(>F)
#   RUNSUMMERMEAN  1   130.59  9.1333  0.001 ***
#   STRANNTEMP      1   185.92 13.0030  0.001 ***
#   STRANNRAIN      1   262.78 18.3791  0.001 ***
#   RDI             1    44.71  3.1267  0.001 ***
#   ASPECT          1    35.88  2.5093  0.001 ***
#   STRDENSITY      1   157.05 10.9838  0.001 ***
#   Residual      203  2902.49
#---
#  Signif. codes:  0 '***' 0.001 '**' 0.01 '*' 0.05 '.' 0.1 ' ' 1


#Test significance of each constrained axis
axis.sig = anova.cca(globalrda_rf, by="axis", nperm=999)




#### Plot global RDA ####
#by catchment


#get location names
rfloc = read.table("rfloc.txt", row.names = 1, header = TRUE)
rfloc = as.data.frame(rfloc[1:210,])
stopifnot(all(row.names(rfloc) == row.names(rfenviro)))
rfenvloc = cbind(rfenviro, rfloc)


#Set catchment as factor
factor(rfenvloc$Catchment, as.character(unique(rfenvloc$Catchment)))
rfcat <- rfenvloc$Catchment


#Set colours and legend labels
rfleglab = c("Mulgrave", "Mossman", "Saltwater", "Daintree", "Hutchinson")
rflegcol <- c("#FFAABB","#77AADD","#EE8866","#99DDFF","#44BB99")
rfcatcol <- c("#99DDFF","#44BB99","#77AADD","#FFAABB", "#EE8866")


#Make the plot
plot(globalrda_rf, type="n", scaling=3)
```

```
points(globalrda_rf, display="sites", pch=21, cex=2, col="white", scaling=3, bg=rfcatcol[rfcat])

points(globalrda_rf, display="species", pch=20, cex=0.7, col="#ccc3ea", scaling=3)

text(globalrda_rf, scaling=3, display="bp", col="black", font=2, cex=1)

legend("topleft", legend = rfleglab, col=rflegcol, pch=21, pt.cex=2, cex=0.9, xpd=1, box.lty = 0, pt.bg=rflegcol,
bg= "transparent")




###############################################


# partial RDA (pRDA) controlling for neutral structure (allelic covariance; omega)


#import omega values (first 3 PCs)

rfom = read.table("rfomeg.txt", row.names = 1, header = TRUE)

stopifnot(all(row.names(rfom) == row.names(rfenviro)))

stopifnot(all(row.names(rfom) == row.names(rfsnps)))




#Partial RDA

rfpartialrdaOM=rda(rfsnps ~ RUNSUMMERMEAN

            +STRANNTEMP

            +STRANNRAIN

            +RDI

            +ASPECT

            +STRDENSITY

            + Condition(rfom$Axis.1 + rfom$Axis.2 + rfom$Axis.3),

            data=rfenviro)


plot(rfpartialrdaOM, scaling=3)

screeplot(rfpartialrdaOM)


ordistep(rfpartialrdaOM)

#Df    AIC      F Pr(>F)

#- ASPECT                  1 1680.0  2.2519  0.005 **

# - RDI                    1 1681.3  3.5229  0.005 **

# - RUNSUMMERMEAN          1 1681.5  3.7060  0.005 **

# - STRANNTEMP             1 1690.7 12.8449  0.005 **
```

- STRANNRAIN   1 1697.6 19.9651 0.005 **

- Condition(rfom$Axis.1 + rfom$Axis.2 + rfom$Axis.3) 3 1696.5

#---

Signif. codes: 0 '***' 0.001 '**' 0.01 '*' 0.05 '.' 0.1 ' ' 1

#Call: rda(formula = rfsnps ~ RUNSUMMERMEAN + STRANNTEMP + STRANNRAIN + RDI +

ASPECT + Condition(rfom$Axis.1 + rfom$Axis.2 + rfom$Axis.3), data = rfenviro)

Inertia   Proportion Rank

#Total   3779.3703   1.0000

#Conditional   408.7206   0.1081   3

#Constrained   625.5521   0.1655   5

#Unconstrained 2745.0976   0.7263 201

#Inertia is variance

#Eigenvalues for constrained axes:

RDA1 RDA2 RDA3 RDA4 RDA5

#318.6 213.4 43.4 27.0 23.1

#Eigenvalues for unconstrained axes:

PC1 PC2 PC3 PC4 PC5 PC6 PC7 PC8

#40.48 33.86 24.21 23.02 21.83 21.48 21.27 20.95

#(Showing 8 of 201 unconstrained eigenvalues)

model.sigOMrf = anova.cca(rfpartialrdaOM, nperm=999)

#Df Variance   F Pr(>F)

#Model   5   625.55 9.1608 0.001 ***

Residual 201 2745.10

axis.sigOMRF = anova.cca(rfpartialrdaOM, by="axis", nperm=999)

#Model: rda(formula = rfsnps ~ RUNSUMMERMEAN + STRANNTEMP + STRANNRAIN + RDI + ASPECT
+ STRDENSITY + Condition(rfom$Axis.1 + rfom$Axis.2 + rfom$Axis.3), data = rfenviro)

#Df Variance   F   Pr(>F)

RDA1   1   318.58 23.3266 0.001 ***

RDA2   1   213.43 15.6279 0.001 ***

RDA3   1   43.42 3.1789 0.001 ***

```
# RDA4      1   27.03  1.9794  0.001 ***

# RDA5      1   23.09  1.6910  0.001 ***

# Residual 201 2745.10


margin.sigOMrf = anova.cca(rfpartialrdaOM, by="margin", nperm=999)




#### Plots ###########################

#by catchment


plot(rfpartialrdaOM, type="n", scaling=3)

points(rfpartialrdaOM, display="species", pch=20, cex=0.7, col="#ccc3ea", scaling=3)

points(rfpartialrdaOM, display="sites", pch=21, cex=2, col="white", scaling=3, bg=rfcatcol[rfcat])

text(rfpartialrdaOM, scaling=3, display="bp", col="black", font=2, cex=1)

legend("bottomright", legend = rfleglab, col=rflegcol, pch=21, pt.cex=2, cex=0.9, xpd=1, box.lty = 0,
pt.bg=rflegcol, bg= "transparent")




################################################################

#####Identify candidate SNPs involved in local adaptation#####

################################################################


rfload.rda <- scores(rfpartialrdaOM, choices=c(1:5), display="species")  # Scores for the first three constrained
axes


hist(rfload.rda[,1], main="Loadings on RDA1")

hist(rfload.rda[,2], main="Loadings on RDA2")

hist(rfload.rda[,3], main="Loadings on RDA3")

hist(rfload.rda[,4], main="Loadings on RDA4")

hist(rfload.rda[,5], main="Loadings on RDA5")


rfoutliers <- function(x,z){

  lims <- mean(x) + c(-1, 1) * z * sd(x)     # find loadings +/-z sd from mean loading

  x[x < lims[1] | x > lims[2]]            # locus names in these tails

}
```

```
rfcand1 <- rfoutliers(rfload.rda[,1],3)

length(rfcand1) #181

rfcand2 <- rfoutliers(rfload.rda[,2],3)

length(rfcand2) #187

rfcand3 <- rfoutliers(rfload.rda[,3],3)

length(rfcand3) #172

rfcand4 <- rfoutliers(rfload.rda[,4],3)

length(rfcand4) #169

rfcand5 <- rfoutliers(rfload.rda[,5],3)

length(rfcand5) #199


rfncand <- length(rfcand1) + length(rfcand2) + length(rfcand3) + length(rfcand4) + length(rfcand5)

rfncand #908 with first 5 axes



#Organize results by making one data frame with the axis, SNP name, loading, & correlation with each predictor:


rfcand1 <- cbind.data.frame(rep(1,times=length(rfcand1)), names(rfcand1), unname(rfcand1))

rfcand2 <- cbind.data.frame(rep(2,times=length(rfcand2)), names(rfcand2), unname(rfcand2))

rfcand3 <- cbind.data.frame(rep(3,times=length(rfcand3)), names(rfcand3), unname(rfcand3))

rfcand4 <- cbind.data.frame(rep(4,times=length(rfcand4)), names(rfcand4), unname(rfcand4))

rfcand5 <- cbind.data.frame(rep(5,times=length(rfcand5)), names(rfcand5), unname(rfcand5))


colnames(rfcand1) <- colnames(rfcand2) <- colnames(rfcand3) <- colnames(rfcand4) <- colnames(rfcand5) <-
c("axis","snp","loading")


rfcand <- rbind(rfcand1, rfcand2, rfcand3, rfcand4, rfcand5)

rfcand$snp <- as.character(rfcand$snp)



#Add in correlations of each candidate SNP with the environmental predictors:

#Remove uncorrelated explanatory variable and put in desired order

write.csv(rfenviro, "rfen.csv")

rfen = read.table("rfen5vars.txt", row.names = 1, header = TRUE)


#Add in correlations of each candidate SNP with the environmental predictors:
```

```r
rffoo <- matrix(nrow=(rfncand), ncol=5)  # 8 columns for 8 predictors
colnames(rffoo) <- c("ASPECT", "RDI", "RUNSUMMERMEAN", "STRANNTEMP", "STRANNRAIN")


for (i in 1:length(rfcand$snp)) {
  nam <- rfcand[i,2]
  rfsnp.gen <- rfsnps[,nam]
  rffoo[i,] <- apply(rfen,2,function(x) cor(x,rfsnp.gen))
}


rfcand <- cbind.data.frame(rfcand,rffoo)
head(rfcand)


#look for duplicates
length(rfcand$snp[duplicated(rfcand$snp)])  # 44 on more than one axis
# remove duplicate detections
rfcand <- rfcand[!duplicated(rfcand$snp),] #[1] 0
#How many unique SNPs then?
length(rfcand$snp)
# 864


#Which predictor is each candidate SNP most strongly correlated with?
for (i in 1:length(rfcand$snp)) {
  bar <- rfcand[i,]
  rfcand[i,9] <- names(which.max(abs(bar[4:8]))) # gives the variable
  rfcand[i,10] <- max(abs(bar[4:8]))             # gives the correlation
}


colnames(rfcand)[9] <- "predictor"
colnames(rfcand)[10] <- "correlation"


table(rfcand$predictor)
#ASPECT   RDI   RUNSUMMERMEAN   STRANNRAIN   STRANNTEMP
#34      52    155             455          168



##########################################################################
```

###PLOT THE SNPS###

rfsel <- rfcand$snp

rfen <- rfcand$predictor

rfen[rfen=="ASPECT"] <- "#EEDD88"

rfen[rfen=="RDI"] <- "#FFAABB"

rfen[rfen=="RUNSUMMERMEAN"] <- "#99DDFF"

rfen[rfen=="STRANNRAIN"] <- "#223ba1"

rfen[rfen=="STRANNTEMP"] <- "#EE8866"

color by predictor:

rfcol.pred <- rownames(rfpartialrdaOMCCAv) # pull the SNP names

for (i in 1:length(rfsel)) {   # color code rfcandidate SNPs

  rffoo <- match(rfsel[i],rfcol.pred)

  rfcol.pred[rffoo] <- rfen[i]

}

rfcol.pred[grep("SNP",rfcol.pred)] <- '#f1eef6' # non-candidate SNPs

rfempty <- rfcol.pred

rfempty[grep("#f1eef6",rfempty)] <- rgb(0,1,0, alpha=0) # transparent

rfempty.outline <- ifelse(rfempty=="#00FF0000","#00FF0000","white")

rfbg <- c("#EEDD88","#FFAABB","#99DDFF","#223ba1","#EE8866")

#Plot it

axes 1 & 2

plot(rfpartialrdaOM, type="n", scaling=3, xlim=c(-1,1), ylim=c(-1,1))

points(rfpartialrdaOM, display="species", pch=21, cex=1.5, col="white", bg=rfcol.pred, scaling=3)

points(rfpartialrdaOM, display="species", pch=21, cex=1.5, col=rfempty.outline, bg=rfempty, scaling=3)

text(rfpartialrdaOM, scaling=3, display="bp", col="black", font=2, cex=1)

legend("topleft", legend=c("ASPECT","RDI","RUNSUMMERMEAN","STRANNRAIN","STRANNTEMP"),

    bty="n", col="white", pch=21, cex=0.9, pt.cex=2, pt.bg=rfbg)

axes 3 & 4

plot(rfpartialrdaOM, type="n", scaling=3, xlim=c(-1,1), ylim=c(-1,1), choices=c(3,4))

points(rfpartialrdaOM, display="species", pch=21, cex=1.5, col="white", bg=rfcol.pred, scaling=3, choices=c(3,4))

points(rfpartialrdaOM, display="species", pch=21, cex=1.5, col=rfempty.outline, bg=rfempty, scaling=3, choices=c(3,4))

text(rfpartialrdaOM, scaling=3, display="bp", col="black", font=2, cex=1, choices=c(3,4))

legend("topleft", legend=c("ASPECT","RDI","RUNSUMMERMEAN","STRANNRAIN","STRANNTEMP"),

   bty="n", col="white", pch=21, cex=0.9, pt.cex=2, pt.bg=rfbg)

##

##########Partial RDA (controlling for Fst)#######################

##

#PARTIAL RDA USING FST

#import fst matrix

rf_fstmatrix <-data.matrix(read.table("rf_fstmatrix.csv", sep = ",", header = TRUE, row.names = 1))

#convert to euclidian distances

library(ade4)

rf_FstLTM2<-quasieuclid(as.dist(rf_fstmatrix))

rf_FstLTM2

#principal coordinate analysis

library(ape)

#pcoa_fst$values

rf_pcoa_fst <- pcoa(rf_FstLTM2)

rf_pcoa_fst

#determine how many pcos are relevant by plotting broken stick externally

#(here we choose two)

```
rf_Fst_PcoaAxes <- data.frame(rf_pcoa_fst$vectors)

rf_FST_PCOA <- rf_Fst_PcoaAxes[,c(1,2)]

rf_FST_PCOA


write.csv(rf_FST_PCOA, "rf_Fst_PCoA.csv")
#Take these, which are pop level, and align them against individuals


rffst = read.table("rf_FstDistInput.txt", row.names = 1, header = TRUE)

stopifnot(all(row.names(rffst) == row.names(rfenviro)))

stopifnot(all(row.names(rffst) == row.names(rfsnps)))




#######################################


#Partial RDA controlling for neutral dist (Fst)


rfpartialrda_fst=rda(rfsnps ~ ASPECT

            +RDI

            +RUNSUMMERMEAN

            +STRANNRAIN

            +STRANNTEMP

            +STRDENSITY

          + Condition(rffst$Axis.1 + rffst$Axis.2),

          data=rfenviro)


#Inertia Proportion Rank

#Total        3779.3703    1.0000

#Conditional   577.8066    0.1529    2

#Constrained   456.4661    0.1208    6

#Unconstrained 2745.0976   0.7263  201

#Inertia is variance


#Eigenvalues for constrained axes:

# RDA1  RDA2  RDA3  RDA4  RDA5  RDA6

#233.09 101.99  43.26  28.64  26.42  23.07
```

#Eigenvalues for unconstrained axes:

PC1 PC2 PC3 PC4 PC5 PC6 PC7 PC8

#40.48 33.86 24.21 23.02 21.83 21.48 21.27 20.95

#(Showing 8 of 201 unconstrained eigenvalues)


```
plot(rfpartialrda_fst, scaling=3)
screeplot(rfpartialrda_fst)
```


```
modsig_rfpartialrda_fst = anova.cca(rfpartialrda_fst, nperm=999)
```

#Df Variance   F Pr(>F)

#Model   6   456.47 5.5705 0.001 ***

Residual 201 2745.10


```
ordistep(rfpartialrda_fst)
```

#Start: rfsnps ~ ASPECT + RDI + RUNSUMMERMEAN + STRANNRAIN + STRANNTEMP + STRDENSITY + Condition(rffst$Axis.1 + rffst$Axis.2)

#Df   AIC   F Pr(>F)

- RUNSUMMERMEAN   1 1679.9 2.1458 0.005 **

- ASPECT   1 1680.0 2.2515 0.005 **

- STRDENSITY   1 1680.3 2.5684 0.005 **

- RDI   1 1680.4 2.6300 0.005 **

- STRANNTEMP   1 1681.8 3.9772 0.005 **

- STRANNRAIN   1 1685.2 7.3229 0.005 **

- Condition(rffst$Axis.1 + rffst$Axis.2) 2 1687.4

#---

Signif. codes: 0 '***' 0.001 '**' 0.01 '*' 0.05 '.' 0.1 ' ' 1

#Call: rda(formula = rfsnps ~ ASPECT + RDI + RUNSUMMERMEAN + STRANNRAIN +

STRANNTEMP + STRDENSITY + Condition(rffst$Axis.1 + rffst$Axis.2), data = rfenviro)

#Inertia Proportion Rank

#Total   3779.3703   1.0000

#Conditional   577.8066   0.1529   2

#Constrained   456.4661   0.1208   6

#Unconstrained 2745.0976   0.7263   201

```
#Inertia is variance


#Eigenvalues for constrained axes:

# RDA1  RDA2  RDA3  RDA4  RDA5  RDA6

#233.09 101.99  43.26  28.64  26.42  23.07


#Eigenvalues for unconstrained axes:

# PC1  PC2  PC3  PC4  PC5  PC6  PC7  PC8

#40.48 33.86 24.21 23.02 21.83 21.48 21.27 20.95

#(Showing 8 of 201 unconstrained eigenvalues)



#axis sig

axissigrf_fst = anova.cca(rfpartialrda_fst, by="axis", nperm=999)

##Df Variance      F Pr(>F)

# RDA1      1  233.09 17.0672  0.001 ***

# RDA2      1  101.99  7.4677  0.001 ***

# RDA3      1   43.26  3.1675  0.001 ***

# RDA4      1   28.64  2.0972  0.001 ***

# RDA5      1   26.42  1.9345  0.001 ***

# RDA6      1   23.07  1.6890  0.001 ***

# Residual 201  2745.10

#---

# Signif. codes:  0 '***' 0.001 '**' 0.01 '*' 0.05 '.' 0.1 ' ' 1



#### Plots ###########################

#by catchment


plot(rfpartialrda_fst, type="n", scaling=3)

#with(rfenviro, text(rfpartialrda_fst, display = "sites", col = rfcatcol[rfenvloc$Catchment], scaling=3, cex=0.4,
bg= "transparent"))

points(rfpartialrda_fst, display="species", pch=20, cex=0.7, col="#ccc3ea", scaling=3)

points(rfpartialrda_fst, display="sites", pch=21, cex=2, col="white", scaling=3, bg=rfcatcol[rfcat])

text(rfpartialrda_fst, scaling=3, display="bp", col="black", font=2, cex=1)

legend("topleft", legend = rfleglab, col=rflegcol, pch=21, pt.cex=2, cex=0.9, xpd=1, box.lty = 0, pt.bg=rflegcol,
bg= "transparent")
```

```
################################################################
#####Identify candidate SNPs involved in local adaptation#####
################################################################


rffst_load.rda <- scores(rfpartialrda_fst, choices=c(1:6), display="species")  # Species scores for the first three
constrained axes


hist(rffst_load.rda[,1], main="Loadings on RDA1")

hist(rffst_load.rda[,2], main="Loadings on RDA2")

hist(rffst_load.rda[,3], main="Loadings on RDA3")

hist(rffst_load.rda[,4], main="Loadings on RDA4")

hist(rffst_load.rda[,5], main="Loadings on RDA5")

hist(rffst_load.rda[,6], main="Loadings on RDA6")


rffst_outliers <- function(x,z){

  lims <- mean(x) + c(-1, 1) * z * sd(x)     # find loadings +/-z sd from mean loading

  x[x < lims[1] | x > lims[2]]           # locus names in these tails

}


rffst_cand1 <- rffst_outliers(rffst_load.rda[,1],3)

length(rffst_cand1) #166

rffst_cand2 <- rffst_outliers(rffst_load.rda[,2],3)

length(rffst_cand2) #213

rffst_cand3 <- rffst_outliers(rffst_load.rda[,3],3)

length(rffst_cand3) #161

rffst_cand4 <- rffst_outliers(rffst_load.rda[,4],3)

length(rffst_cand4) #198

rffst_cand5 <- rffst_outliers(rffst_load.rda[,5],3)

length(rffst_cand5) #155

rffst_cand6 <- rffst_outliers(rffst_load.rda[,6],3)

length(rffst_cand6) #200


rffst_ncand <- length(rffst_cand1) + length(rffst_cand2) + length(rffst_cand3) + length(rffst_cand4) +
length(rffst_cand5)+ length(rffst_cand6)
```

rffst_ncand #1093 with 6 axes

#Next, we'll organize our results by making one data frame with the axis, SNP name, loading, & correlation with each predictor:


```
rffst_cand1 <- cbind.data.frame(rep(1,times=length(rffst_cand1)), names(rffst_cand1), unname(rffst_cand1))

rffst_cand2 <- cbind.data.frame(rep(2,times=length(rffst_cand2)), names(rffst_cand2), unname(rffst_cand2))

rffst_cand3 <- cbind.data.frame(rep(3,times=length(rffst_cand3)), names(rffst_cand3), unname(rffst_cand3))

rffst_cand4 <- cbind.data.frame(rep(4,times=length(rffst_cand4)), names(rffst_cand4), unname(rffst_cand4))

rffst_cand5 <- cbind.data.frame(rep(5,times=length(rffst_cand5)), names(rffst_cand5), unname(rffst_cand5))

rffst_cand6 <- cbind.data.frame(rep(6,times=length(rffst_cand6)), names(rffst_cand6), unname(rffst_cand6))


colnames(rffst_cand1) <- colnames(rffst_cand2) <- colnames(rffst_cand3) <- colnames(rffst_cand4) <- colnames(rffst_cand5)<- colnames(rffst_cand6) <- c("axis","snp","loading")


rffst_cand <- rbind(rffst_cand1, rffst_cand2, rffst_cand3, rffst_cand4, rffst_cand5, rffst_cand6)

rffst_cand$snp <- as.character(rffst_cand$snp)
```


#Add in correlations of each candidate SNP with the six environmental predictors:

```
write.csv(rfenviro, "rfen.csv")

rffst_en = read.table("rfenfst.txt", row.names = 1, header = TRUE)


rffst_foo <- matrix(nrow=(rffst_ncand), ncol=6)

colnames(rffst_foo) <- c("ASPECT", "RDI", "RUNSUMMERMEAN", "STRANNTEMP", "STRANNRAIN", "STRDENSITY")


for (i in 1:length(rffst_cand$snp)) {
  nam <- rffst_cand[i,2]
  rffst_snp.gen <- rfsnps[,nam]
  rffst_foo[i,] <- apply(rffst_en,2,function(x) cor(x,rffst_snp.gen))
}


rffst_cand <- cbind.data.frame(rffst_cand,rffst_foo)

head(rffst_cand)
```

```
#look for duplicates
length(rffst_cand$snp[duplicated(rffst_cand$snp)])  # 64 on more than one axis
# remove duplicate detections
rffst_cand <- rffst_cand[!duplicated(rffst_cand$snp),] #[1] 0
#How many unique SNPs then?
length(rffst_cand$snp)
# 1029


#Which predictor is each candidate SNP most strongly correlated with?
for (i in 1:length(rffst_cand$snp)) {
  rffstbar <- rffst_cand[i,]
  rffst_cand[i,10] <- names(which.max(abs(rffstbar[4:9]))) # gives the variable
  rffst_cand[i,11] <- max(abs(rffstbar[4:9]))           # gives the correlation
}


colnames(rffst_cand)[10] <- "predictor"
colnames(rffst_cand)[11] <- "correlation"


table(rffst_cand$predictor)
#ASPECT   RDI RUNSUMMERMEAN   STRANNRAIN   STRANNTEMP   STRDENSITY
#54      68     122        335       277        173




##############################################################################


###PLOT THE SNPS###


rffst_sel <- rffst_cand$snp
rffst_en <- rffst_cand$predictor
rffst_en[rffst_en=="ASPECT"] <- "#EEDD88"
rffst_en[rffst_en=="RDI"] <- "#FFAABB"
rffst_en[rffst_en=="RUNSUMMERMEAN"] <- "#99DDFF"
rffst_en[rffst_en=="STRANNRAIN"] <- "#223ba1"
rffst_en[rffst_en=="STRANNTEMP"] <- "#EE8866"
rffst_en[rffst_en=="STRDENSITY"] <- "#5d2e6e"
```

```
# color by predictor:

rffst_col.pred <- rownames(rfpartialrda_fst$CCA$v) # pull the SNP names


for (i in 1:length(rffst_sel)) {          # color code SNPs
  rffst_foo <- match(rffst_sel[i],rffst_col.pred)
  rffst_col.pred[rffst_foo] <- rffst_en[i]
}


rffst_col.pred[grep("SNP",rffst_col.pred)] <- '#f1eef6' # non-candidate SNPs
rffst_empty <- rffst_col.pred
rffst_empty[grep("#f1eef6",rffst_empty)] <- rgb(0,1,0, alpha=0) # transparent
rffst_empty.outline <- ifelse(rffst_empty=="#00FF0000","#00FF0000","white")
rffst_bg <- c("#EEDD88","#FFAABB","#99DDFF","#223ba1","#EE8866","#5d2e6e")
#theirs
#bg <- c('#1f78b44b4b4','#a6cee3','#6a3d9a','#e31a1c','#33a02c','#ffff33','#fb9a99','#b2df8a')


#Plot it
# axes 1 & 2
plot(rfpartialrda_fst, type="n", scaling=3, xlim=c(-1,1), ylim=c(-1,1))
points(rfpartialrda_fst, display="species", pch=21, cex=1.5, col="white", bg=rffst_col.pred, scaling=3)
points(rfpartialrda_fst, display="species", pch=21, cex=1.5, col=rffst_empty.outline, bg=rffst_empty, scaling=3)
text(rfpartialrda_fst, scaling=3, display="bp", col="black", font=2, cex=1)
legend("topleft",   legend=c("ASPECT","RDI","RUNSUMMERMEAN","STRANNRAIN","STRANNTEMP",
"STRDENSITY"),
     bty="n", col="white", pch=21, cex=0.9, pt.cex=2, pt.bg=rffst_bg)



# axes 3 & 4
plot(rfpartialrda_fst, type="n", scaling=3, xlim=c(-1,1), ylim=c(-1,1), choices=c(3,4))
points(rfpartialrda_fst, display="species", pch=21, cex=1.5, col="white", bg=rffst_col.pred, scaling=3,
choices=c(3,4))
points(rfpartialrda_fst, display="species", pch=21, cex=1.5, col=rffst_empty.outline, bg=rffst_empty, scaling=3,
choices=c(3,4))
text(rfpartialrda_fst, scaling=3, display="bp", col="black", font=2, cex=1, choices=c(3,4))
legend("topright", legend=c("ASPECT","RDI","RUNSUMMERMEAN","STRANNRAIN","STRANNTEMP"),
     bty="n", col="white", pch=21, cex=0.9, pt.cex=2, pt.bg=rffst_bg)
```

RDA: PEA

#RAINFOREST ONLY

```
setwd("C:/Users/kgate/Desktop/Dryad/RDA_PEA")
library(vegan)

##import variables
#body shape (response variables)
FORMRF = read.table("formrf.txt")
#Environmental variables (explanatory variables)
unsc_predictors_RF_ind = read.table("PredictorsInputUnscaledforomeg.txt", row.names=1, header=TRUE)
#Body size and neutral genetic varation (covariables)
unsc_cov_RF = read.table("OmegaSizeCovar_unsc.txt")


#Scale inputs
covariables_RF <- scale(unsc_cov_RF)
rainenv = scale(unsc_predictors_RF_ind)
rfenv = as.data.frame(rainenv)
covariables_RF = as.data.frame(covariables_RF)


# check if all data frames have identical row names
stopifnot(all(row.names(FORMRF) == row.names(rfenv)))
stopifnot(all(row.names(FORMRF) == row.names(unsc_cov_RF)))
stopifnot(all(row.names(rfenv) == row.names(unsc_cov_RF)))


###########GLOBAL RDA ################
#RDA
rda.indiv.RF1=rda(FORMRF ~ RUNSUMMERMEAN
        +STRANNTEMP
```

```
          +STRANNRAIN

          +RDI

          +ASPECT

          +STRDENSITY, data=rfenv)


rda.indiv.RF1
#Inertia Proportion Rank
#Total        0.0011518  1.0000000
#Constrained   0.0002538  0.2203206    4
##Unconstrained 0.0008980  0.7796794    4
#Inertia is variance


#Eigenvalues for constrained axes:
#  RDA1    RDA2    RDA3    RDA4
#1.228e-04 9.637e-05 2.715e-05 7.440e-06


#Eigenvalues for unconstrained axes:
#  PC1    PC2    PC3    PC4
#0.0005328 0.0001837 0.0001034 0.0000781


RsquareAdj(rda.indiv.RF1)
#$r.squared
#[1] 0.2203206


#$adj.r.squared
#[1] 0.1932797


plot(rda.indiv.RF1)
screeplot(rda.indiv.RF1)


#test significanc of the model
model_sig_ind_RF1 = anova.cca(rda.indiv.RF1, nperm=999)
#Df   Variance      F Pr(>F)
#Model     6 0.00025376 8.1477  0.001 ***
#Residual 173 0.00089803
```

#How much variance explained by each variable

margin_sig_ind_RF1 = anova.cca(rda.indiv.RF1, by="margin", nperm=999)

#Df   Variance   F Pr(>F)

#RUNSUMMERMEAN   1 0.00005215 10.0467 0.001 ***

#STRANNTEMP   1 0.00006196 11.9354 0.001 ***

#STRANNRAIN   1 0.00009480 18.2629 0.001 ***

#RDI   1 0.00004625 8.9089 0.001 ***

#ASPECT   1 0.00001002 1.9303 0.108

#STRDENSITY   1 0.00005559 10.7093 0.001 ***

#Residual   173 0.00089803

#How much variance explained by each constrained axis

axis_sig_ind_RF1 = anova.cca(rda.indiv.RF1, by="axis", nperm=999)

#Df   Variance   F Pr(>F)

#RDA1   1 0.00012280 23.9309 0.001 ***

#RDA2   1 0.00009637 18.7801 0.001 ***

#RDA3   1 0.00002715 5.2910 0.085 .

#RDA4   1 0.00000744 1.4493 0.887

#Residual 175 0.00089803

#variance inflation factor

vif.cca(rda.indiv.RF1)

#RUNSUMMERMEAN   STRANNTEMP   STRANNRAIN   RDI

#2.531422   1.694709   1.435550   2.227260

#ASPECT   STRDENSITY

#1.597518   1.732636

#backwards-stepwise selection to determine the best combination

#of explanatory variables and their relative contributions to the model

ordistep(rda.indiv.RF1)

#Remove any predictor variables with P value >0.1 (Aspect)

#Remove any predictor variables contributing to collinearity (VIF > 5) (N/A)

##

##

```
#PARTIAL RDA

#controlling for neutral gen distance and size

rda.indiv.RF=rda(FORMRF ~ RUNSUMMERMEAN

        +STRANNTEMP

        +STRANNRAIN

        +RDI

        +STRDENSITY

        + Condition(covariables_RF$Axis.1

                +covariables_RF$Axis.2

                +covariables_RF$Axis.3

                +covariables_RF$Size), data=rfenv)


rda.indiv.RF

#Inertia Proportion Rank

#Total        0.0011518  1.0000000

#Conditional   0.0005071  0.4402596   4

#Constrained   0.0001630  0.1414907   4

#Unconstrained 0.0004817  0.4182497   4

#Inertia is variance


#Eigenvalues for constrained axes:

## RDA1     RDA2     RDA3     RDA4

#1.149e-04 3.760e-05 9.760e-06 7.000e-07


#Eigenvalues for unconstrained axes:

# PC1      PC2      PC3      PC4

#0.00020814 0.00011271 0.00010297 0.00005793


RsquareAdj(rda.indiv.RF)

#$r.squared

#[1] 0.1414907


#$adj.r.squared

#[1] 0.1321421
```

```
plot(rda.indiv.RF)
screeplot(rda.indiv.RF)


#test significanc of the model
model_sig_ind_RF = anova.cca(rda.indiv.RF, nperm=999)
#Df   Variance     F Pr(>F)
#Model    5 0.00016297 11.502  0.001 ***
#Residual 170 0.00048174


#How much variance explained by each variable
margin_sig_ind_RF = anova.cca(rda.indiv.RF, by="margin", nperm=999)
#Df   Variance     F Pr(>F)
# RUNSUMMERMEAN   1 0.00000834  2.9427  0.036 *
# STRANNTEMP     1 0.00004915 17.3461  0.001 ***
# STRANNRAIN     1 0.00000419  1.4776  0.206
# RDI         1 0.00001621  5.7202  0.001 ***
# STRDENSITY     1 0.00000981  3.4615  0.021 *
# Residual     170 0.00048174


#How much variance explained by each constrained axis
axis_sig_ind_RF = anova.cca(rda.indiv.RF, by="axis", nperm=999)
#Df   Variance     F Pr(>F)
#RDA1     1 0.00011490 40.7873  0.001 ***
# RDA2     1 0.00003760 13.3471  0.001 ***
# RDA3     1 0.00000976  3.4650  0.112
#RDA4     1 0.00000070  0.2486  0.996
#Residual 171 0.00048174


ordistep(rda.indiv.RF)
#F
#- RUNSUMMERMEAN     9.5034
#- RDI           11.6685
#- STRDENSITY     19.9812
#- STRANNTEMP      34.8260
```

###

#FINAL MODEL

rda_RF=rda(FORMRF ~ RUNSUMMERMEAN

    +STRANNTEMP

    +RDI

    +STRDENSITY

    + Condition(covariables_RF$Axis.1

        +covariables_RF$Axis.2

        +covariables_RF$Axis.3

        +covariables_RF$Size), data=rfenv)

rda_RF

#Inertia Proportion Rank

#Total   0.0011518 1.0000000

#Conditional   0.0005071 0.4402596   4

#Constrained   0.0001588 0.1378553   4

#Unconstrained 0.0004859 0.4218851   4

#Inertia is variance

#Eigenvalues for constrained axes:

RDA1   RDA2   RDA3   RDA4

#0.00011164 0.00003758 0.00000901 0.00000055

#Eigenvalues for unconstrained axes:

PC1   PC2   PC3   PC4

#0.00021057 0.00011272 0.00010330 0.00005933

RsquareAdj(rda_RF)

#$r.squared

#[1] 0.1378553

#$adj.r.squared

#[1] 0.1309121

```
plot(rda_RF)

screeplot(rda_RF)


#test significanc of the model

model_RF = anova.cca(rda_RF, nperm=999)

#Df    Variance      F Pr(>F)

#Model     4 0.00015878 13.969  0.001 ***

# Residual 171 0.00048592


#How much variance explained by each variable

margin_RF = anova.cca(rda_RF, by="margin", nperm=999)

#Df    Variance       F Pr(>F)

# RUNSUMMERMEAN   1 0.00002701  9.5034  0.001 ***

# STRANNTEMP      1 0.00009896 34.8260  0.001 ***

# RDI             1 0.00003316 11.6685  0.001 ***

# STRDENSITY      1 0.00005678 19.9812  0.001 ***

# Residual      171 0.00048592


#How much variance explained by each constrained axis

axis_RF = anova.cca(rda_RF, by="axis", nperm=999)

#Df    Variance       F Pr(>F)

#RDA1      1 0.00011164 39.2872  0.001 ***

# RDA2     1 0.00003758 13.2232  0.001 ***

# RDA3     1 0.00000901  3.1706  0.075 .

#RDA4      1 0.00000055  0.1951  0.936

#Residual 171 0.00048592




################################################################################

#plots


locationinfo <- read.table("LocationData.txt", row.names = 1, header = TRUE)

rfloc = as.data.frame(locationinfo[1:180,])

stopifnot(all(row.names(rfenv) == row.names(rfloc)))

rfsite <- factor(as.character(rfloc$Site))
```

```
rfcatch <- factor(as.character(rfloc$Catchment))

rfenv <- cbind(rfenv, rfsite, rfcatch)



rflegendlab = c("Mulgrave", "Mossman", "Saltwater", "Daintree", "Hutchinson")

rflegendcol <- c("#FFAABB","#77AADD","#EE8866","#99DDFF","#44BB99")

rfcatchcol <- c("#99DDFF","#44BB99","#77AADD","#FFAABB","#EE8866")



plot(rda_RF, type="n", scaling=3)

points(rda_RF, display="sites", pch=21, cex=1.5, col="white", scaling=3, bg=rfcatchcol[rfcatch])

points(rda_RF, display="species", pch=17, cex=2, col="gray32", scaling=3)

text(rda_RF, scaling=3, display="bp", col="black", font=2, cex=1)

legend("bottomleft", legend = rflegendlab, col=rflegendcol, pch=21, pt.cex=1, cex=0.9, xpd=1, box.lty = 0,
        pt.bg=rflegendcol, bg= "transparent")




################################################################

#Control for fst

FstSizeUnscaled = read.table("FstSizeUnscaled.txt", row.names=1, header=TRUE)

stopifnot(all(row.names(FORMRF) == row.names(FstSizeUnscaled)))

covar = scale(FstSizeUnscaled)

covar = as.data.frame(covar)


#controling for neutral gen distance and size

rda.fst=rda(FORMRF ~ RUNSUMMERMEAN

        +STRANNTEMP

        +STRANNRAIN

        +RDI

        +STRDENSITY

        + Condition(covar$Axis.1

                +covar$Axis.2
```

+covar$Size), data=rfenv)

rda.fst

#Inertia Proportion Rank

#Total   0.0011518 1.0000000

#Conditional   0.0005206 0.4519898   3

#Constrained   0.0001429 0.1241039   4

#Unconstrained 0.0004883 0.4239063   4

#Inertia is variance

#Eigenvalues for constrained axes:

RDA1   RDA2   RDA3   RDA4

#0.00010736 0.00002378 0.00001009 0.00000171

#Eigenvalues for unconstrained axes:

PC1   PC2   PC3   PC4

#0.00020816 0.00011486 0.00010486 0.00006036

RsquareAdj(rda.fst)

#$r.squared

#[1] 0.1241039

#$adj.r.squared

#[1] 0.1136131

plot(rda.fst)

screeplot(rda.fst)

#test significanc of the model

model_sig_ind_RF = anova.cca(rda.fst, nperm=999)

#Df   Variance   F Pr(>F)

#Model   5 0.00014294 10.012 0.001 ***

Residual 171 0.00048825

#How much variance explained by each variable

margin_sig_ind_RF = anova.cca(rda.fst, by="margin", nperm=999)

```
#Df  Variance      F Pr(>F)
# RUNSUMMERMEAN  1 0.00001145 4.0094 0.012 *
# STRANNTEMP     1 0.00000548 1.9186 0.136
# STRANNRAIN     1 0.00001897 6.6444 0.002 **
# RDI            1 0.00002909 10.1878 0.001 ***
# STRDENSITY     1 0.00000901 3.1544 0.031 *
# Residual      171 0.00048825
```

#How much variance explained by each constrained axis

axis_sig_ind_RF = anova.cca(rda.fst, by="axis", nperm=999)

```
#Df  Variance      F Pr(>F)
#RDA1    1 0.00010736 37.8212 0.001 ***
# RDA2    1 0.00002378 8.3776 0.001 ***
# RDA3    1 0.00001009 3.5549 0.114
#RDA4    1 0.00000171 0.6014 0.962
#Residual 172 0.00048825
```

ordistep(rda.fst)

```
#Inertia Proportion Rank
#Total        0.0011518 1.0000000
#Conditional  0.0005206 0.4519898  3
#Constrained  0.0001375 0.1193478  4
#Unconstrained 0.0004937 0.4286624  4
```

#Inertia is variance

```
#Df   AIC      F Pr(>F)
# - STRDENSITY                    1 -1355.2 2.1220 0.090 .
# - RUNSUMMERMEAN                 1 -1349.3 7.9636 0.005 **
# - STRANNRAIN                    1 -1347.3 9.9646 0.005 **
# - RDI                           1 -1345.3 11.9697 0.005 **
# - Condition(covar$Axis.1 + covar$Axis.2 + covar$Size) 3 -1238.8
```

#without STRANNTEMP

rfpartialrda_fst=rda(FORMRF ~ RUNSUMMERMEAN

    +STRANNRAIN

```
            +RDI

            +STRDENSITY

          + Condition(covar$Axis.1

                  +covar$Axis.2

                  +covar$Size), data=rfenv)
```

#Inertia Proportion Rank

#Total   0.0011518 1.0000000

#Conditional   0.0005206 0.4519898   3

#Constrained   0.0001375 0.1193478   4

#Unconstrained 0.0004937 0.4286624   4

#Inertia is variance

#Eigenvalues for constrained axes:

RDA1   RDA2   RDA3   RDA4

#0.00010491 0.00002378 0.00000820 0.00000057 #

#Eigenvalues for unconstrained axes:

PC1   PC2   PC3   PC4

#0.00021130 0.00011513 0.00010532 0.00006198

RsquareAdj(rfpartialrda_fst)

#[1] 0.1193478

#$adj.r.squared

#[1] 0.1112433

plot(rfpartialrda_fst)

screeplot(rfpartialrda_fst)

#test significanc of the model

model_sig_ind_RF = anova.cca(rfpartialrda_fst, nperm=999)

#Df   Variance   F Pr(>F)

#Model   4 0.00013746 11.972 0.001 ***

Residual 172 0.00049373

#How much variance explained by each variable

margin_sig_ind_RF = anova.cca(rfpartialrda_fst, by="margin", nperm=999)

#Df   Variance   F Pr(>F)

RUNSUMMERMEAN   1 0.00002286 7.9636 0.001 ***

STRANNRAIN   1 0.00002860 9.9646 0.001 ***

RDI   1 0.00003436 11.9697 0.001 ***

STRDENSITY   1 0.00000609 2.1220 0.101

#Residual   172 0.00049373

#How much variance explained by each constrained axis

axis_sig_ind_RF = anova.cca(rfpartialrda_fst, by="axis", nperm=999)

#Df   Variance   F Pr(>F)

RDA1   1 0.00010491 36.5471 0.001 ***

RDA2   1 0.00002378 8.2845 0.001 ***

RDA3   1 0.00000820 2.8568 0.106

RDA4   1 0.00000057 0.1996 0.931

#Residual 172 0.00049373

RDA: GxPxE

```
############################################################

###RDA: GEA candidates against morphology #########################

############################################################


#Set working directory
#setwd("C:/")


# load required packages
library(vegan)      #ordination (RDA)
library(adegenet)   #import snp dataset


#import predictor dataset
formraw = read.table("formrawrf.txt", row.names = 1, header = TRUE)
#PCA on procruste matrix
pca_form<-prcomp(formraw)
summary(pca_form)
#brokenstick (identify PC with more variation than randomly expected)
screeplot(pca_form, bstick = TRUE, type = "lines")
#here I kept the first four
formpcs=pca_form$x[,1:4]
#make it a data frame
form = as.data.frame(formpcs)



#import genetic data (from str file) to create genind object
gen    =    read.structure("CandidateSNPs.str",    row.marknames=1,    onerowperind=FALSE,    n.ind=177,
      n.loc=864,col.lab=1,col.pop=2)


# get allele counts
alleles <- gen@tab
alleles[1:10,1:10]
```

```
# get genotypes (counts of reference allele) and clean up locus names
snps <- alleles[,seq(1,ncol(alleles),2)]
colnames(snps) <- locNames(gen)
snps[1:10,1:10]


# check total % missing data
(sum(is.na(snps)))/(dim(snps)[1]*dim(snps)[2])*100
#2.549876


# impute missing data with most common genotype
snps <- apply(snps, 2, function(x) replace(x, is.na(x), as.numeric(names(which.max(table(x))))))


# check % missing data again
(sum(is.na(snps)))/(dim(snps)[1]*dim(snps)[2])*100
#[1] 0
snps[1:10,1:10]



#check rownames against other inputs
stopifnot(all(row.names(snps) == row.names(form)))



###########################
#Run initial (global) RDA
#RDA
rda_GxPxE=rda(snps ~ PC1
              +PC2
              +PC3
              +PC4,
              data=form)


#Check plots
plot(rda_GxPxE)
screeplot(rda_GxPxE)


#Permutation test - is the model significant?
```

model.sig = anova.cca(rda_GxPxE, nperm=999)

#Df Variance   F Pr(>F)

#Model   4   29.78 3.1355 0.001 ***

Residual 172   408.38

#backwards-stepwise selection to determine the best combination

#of explanatory variables and their relative contributions to the model

ordistep(rda_GxPxE)

#Start: snps ~ PC1 + PC2 + PC3 + PC4

#Df   AIC   F Pr(>F)

- PC1 1 1073.0 1.7774 0.040 *

- PC3 1 1073.1 1.9062 0.030 *

- PC4 1 1074.8 3.5613 0.005 **

- PC2 1 1076.5 5.2969 0.005 **

Signif. codes:

0 '***' 0.001 '**' 0.01 '*' 0.05 '.' 0.1 ' ' 1

#Call: rda(formula = snps ~ PC1 + PC2 + PC3 +

PC4, data = form)

#Inertia Proportion Rank

#Total   438.15466   1.00000

#Constrained   29.77788   0.06796   4

#Unconstrained 408.37678   0.93204 172

#Inertia is variance

#Eigenvalues for constrained axes:

RDA1 RDA2 RDA3 RDA4

#15.768 7.960 3.561 2.488

#Eigenvalues for unconstrained axes:

PC1 PC2 PC3 PC4 PC5 PC6 PC7 PC8

#65.09 32.40 23.52 8.69 7.26 6.78 5.77 4.13

#(Showing 8 of 172 unconstrained eigenvalues)

217

#How much variance explained by each constrained axis?

axis.sig = anova.cca(rda_GxPxE, by="axis", nperm=999)

#Df Variance   F Pr(>F)

#RDA1   1   15.77 6.6411 0.001 ***

#RDA2   1   7.96 3.3528 0.002 **

#RDA3   1   3.56 1.4999 0.172

#RDA4   1   2.49 1.0481 0.315

#Residual 172   408.38

Plot Global RDA

#by catchment

#Get location/catchment codes for each individual

loc = read.table("rfloc.txt", row.names = 1, header = TRUE)

stopifnot(all(row.names(loc) == row.names(form)))

formloc = cbind(form, loc)

factor(formloc$Catchment, as.character(unique(formloc$Catchment)))

cat <- formloc$Catchment

#Asign colours and labels for figure and legends

leglab = c("Mulgrave", "Mossman", "Saltwater", "Daintree", "Hutchinson")

legcol <- c("#FFAABB","#77AADD","#EE8866","#99DDFF","#44BB99")

catcol <- c("#99DDFF","#44BB99","#77AADD","#FFAABB","#EE8866")

#Plot it

plot(rda_GxPxE, type="n", scaling=3)

points(rda_GxPxE, display="species", pch=20, cex=0.7, col="#ccc3ea", scaling=3) #snps

points(rda_GxPxE, display="sites", pch=21, cex=2, col="white", scaling=3, bg=catcol[cat]) #individuals

text(rda_GxPxE, scaling=3, display="bp", col="black", font=2, cex=1)   #bodyshape

legend("topleft", legend = leglab, col=legcol, pch=21, pt.cex=2, cex=0.9, xpd=1, box.lty = 0, pt.bg=legcol, bg=
     "transparent")

```
################################################
#####CONTROL FOR SIZE USING PARTIAL RDA#####
################################################


#import size data to control for
sizeunsc = read.table("sizerf.txt", row.names = 1, header = TRUE)
size = scale(sizeunsc)
stopifnot(all(row.names(size) == row.names(form)))
stopifnot(all(row.names(snps) == row.names(size)))


#RDA
partrda_GxPxE=rda(snps ~ PC1
            +PC2
            +PC3
            +PC4
            + Condition(size),
            data=form)


plot(partrda_GxPxE)
screeplot(partrda_GxPxE)


partmodel.sig = anova.cca(partrda_GxPxE, nperm=999)
#Df Variance      F Pr(>F)
#  Model    4    28.27 2.9866  0.001 ***
#  Residual 171   404.62


ordistep(partrda_GxPxE)
#Start: snps ~ PC1 + PC2 + PC3 + PC4 + Condition(size)


#Df    AIC      F Pr(>F)
#  - PC3          1 1073.0 1.3994  0.060 .
#  - PC1          1 1073.2 1.6727  0.025 *
#  - PC4          1 1074.4 2.8242  0.005 **
#  - PC2          1 1074.9 3.3324  0.005 **
#  - Condition(size)  1 1073.2
#---
```

Signif. codes: 0 '***' 0.001 '**' 0.01 '*' 0.05 '.' 0.1 ' ' 1

#Call: rda(formula = snps ~ PC1 + PC2 + PC3 + PC4 + Condition(size), data = form)

#Inertia Proportion Rank

#Total   438.15466   1.00000

#Conditional   5.26680   0.01202   1

#Constrained   28.26778   0.06452   4

#Unconstrained 404.62008   0.92346 171

#Inertia is variance

#Eigenvalues for constrained axes:

RDA1 RDA2 RDA3 RDA4

#15.471 7.576 3.359 1.861

#Eigenvalues for unconstrained axes:

PC1 PC2 PC3 PC4 PC5 PC6 PC7 PC8

#64.90 30.91 23.40 8.62 7.26 6.62 5.70 4.10

#(Showing 8 of 171 unconstrained eigenvalues)

#How much variance explained by each constrained axis

partaxis.sig = anova.cca(partrda_GxPxE, by="axis", nperm=999)

#Df Variance   F Pr(>F)

#RDA1   1   15.47 6.5384 0.001 ***

#RDA2   1   7.58 3.2019 0.001 ***

#RDA3   1   3.36 1.4197 0.199

#RDA4   1   1.86 0.7865 0.863

#Residual 171   404.62

Plots

#by catchment

loc = read.table("rfloc.txt", row.names = 1, header = TRUE)

stopifnot(all(row.names(loc) == row.names(form)))

```
formloc = cbind(form, loc)


factor(formloc$Catchment, as.character(unique(formloc$Catchment)))
cat <- formloc$Catchment


leglab = c("Mulgrave", "Mossman", "Saltwater", "Daintree", "Hutchinson")
legcol <- c("#FFAABB","#77AADD","#EE8866","#99DDFF","#44BB99")
catcol <- c("#99DDFF","#44BB99","#77AADD","#FFAABB","#EE8866")


plot(partrda_GxPxE, type="n", scaling=3)
points(partrda_GxPxE, display="species", pch=20, cex=0.7, col="#ccc3ea", scaling=3)  #snps
points(partrda_GxPxE, display="sites", pch=21, cex=2, col="white", scaling=3, bg=catcol[cat])  #individuals
text(partrda_GxPxE, scaling=3, display="bp", col="black", font=2, cex=1)          #bodyshape
legend("bottomleft", legend = leglab, col=legcol, pch=21, pt.cex=2, cex=0.9, xpd=1, box.lty = 0, pt.bg=legcol,
      bg= "transparent")




#############################################################################################
#####Identify GxPxE candidates from full list of climate associated SNPs #########
#############################################################################################


load.rda <- scores(partrda_GxPxE, choices=c(1:2), display="species")  # Species scores for the first three
      constrained axes


hist(load.rda[,1], main="Loadings on RDA1")
hist(load.rda[,2], main="Loadings on RDA2")


#Using 2 standard deviations
outliers <- function(x,z){
  lims <- mean(x) + c(-1, 1) * 2 * sd(x)     # find loadings +/-z sd from mean loading
  x[x < lims[1] | x > lims[2]]             # locus names in these tails
}


cand1 <- outliers(load.rda[,1],3) # 20
cand2 <- outliers(load.rda[,2],3) # 41
length(cand1)
length(cand2)
```

```
formloc = cbind(form, loc)


factor(formloc$Catchment, as.character(unique(formloc$Catchment)))
cat <- formloc$Catchment


leglab = c("Mulgrave", "Mossman", "Saltwater", "Daintree", "Hutchinson")
legcol <- c("#FFAABB","#77AADD","#EE8866","#99DDFF","#44BB99")
catcol <- c("#99DDFF","#44BB99","#77AADD","#FFAABB","#EE8866")


plot(partrda_GxPxE, type="n", scaling=3)
points(partrda_GxPxE, display="species", pch=20, cex=0.7, col="#ccc3ea", scaling=3)  #snps
points(partrda_GxPxE, display="sites", pch=21, cex=2, col="white", scaling=3, bg=catcol[cat])  #individuals
text(partrda_GxPxE, scaling=3, display="bp", col="black", font=2, cex=1)          #bodyshape
legend("bottomleft", legend = leglab, col=legcol, pch=21, pt.cex=2, cex=0.9, xpd=1, box.lty = 0, pt.bg=legcol,
      bg= "transparent")




#############################################################################################
#####Identify GxPxE candidates from full list of climate associated SNPs #########
#############################################################################################


load.rda <- scores(partrda_GxPxE, choices=c(1:2), display="species")  # Species scores for the first three
      constrained axes


hist(load.rda[,1], main="Loadings on RDA1")
hist(load.rda[,2], main="Loadings on RDA2")


#Using 2 standard deviations
outliers <- function(x,z){
  lims <- mean(x) + c(-1, 1) * 2 * sd(x)     # find loadings +/-z sd from mean loading
  x[x < lims[1] | x > lims[2]]             # locus names in these tails
}


cand1 <- outliers(load.rda[,1],3) # 20
cand2 <- outliers(load.rda[,2],3) # 41
length(cand1)
length(cand2)
```

```r
ncand <- length(cand1) + length(cand2)
#[1] 61 with all 2 axes



#Organize results by making data frame with axis, SNP name, loading, & correlation with each predictor:
cand1 <- cbind.data.frame(rep(1,times=length(cand1)), names(cand1), unname(cand1))
cand2 <- cbind.data.frame(rep(2,times=length(cand2)), names(cand2), unname(cand2))

colnames(cand1) <- colnames(cand2) <- c("axis","snp","loading")

cand <- rbind(cand1, cand2)
cand$snp <- as.character(cand$snp)



formpc = as.data.frame(form)

#Let's add in the correlations of each candidate SNP with the eight environmental predictors:
foo <- matrix(nrow=(ncand), ncol=4)  # 8 columns for 8 predictors
colnames(foo) <- c("PC1","PC2","PC3","PC4")

for (i in 1:length(cand$snp)) {
  nam <- cand[i,2]
  snp.gen <- snps[,nam]
  foo[i,] <- apply(formpc,2,function(x) cor(x,snp.gen))
}

cand <- cbind.data.frame(cand,foo)
head(cand)

#look for duplicates
length(cand$snp[duplicated(cand$snp)])  # 0
# remove duplicate detections
cand <- cand[!duplicated(cand$snp),] #[1] 0
#How many unique SNPs then?
length(cand$snp)
```

#[1] 61

#Which predictor is each candidate SNP most strongly correlated with?

```
for (i in 1:length(cand$snp)) {
  bar <- cand[i,]
  cand[i,8] <- names(which.max(abs(bar[4:7]))) # gives the variable
  cand[i,9] <- max(abs(bar[4:7]))          # gives the correlation
}


colnames(cand)[8] <- "predictor"
colnames(cand)[9] <- "correlation"


write.csv(cand, "GxPxE_candidates.csv")
table(cand$predictor)
```
#PC2 PC3 PC4

#26   2 33

References

Addo-Bediako, A., S. L. Chown, and K. J. Gaston. 2000. Thermal tolerance, climatic variability and latitude. Proceedings of the Royal Society B: Biological Sciences **267**:739-745.

Afonso Silva, A. C., J. G. Bragg, S. Potter, C. Fernandes, M. M. Coelho, and C. Moritz. 2017. Tropical specialist vs. climate generalist: diversification and demographic history of sister species of Carlia skinks from northwestern Australia. Molecular Ecology **26**:4045-4058.

Aguirre-Liguori, J. A., S. Ramírez-Barahona, and B. S. Gaut. 2021. The evolutionary genomics of species' responses to climate change. Nature Ecology & Evolution **5**:1350-1360.

ALA. 2020. Atlas of Living Australia occurence records. https://bie.ala.org.au/species/ Accessed January 2020.

Alexandre, C. M., B. R. Quintella, A. F. Ferreira, F. A. Romão, and P. R. Almeida. 2014. Swimming performance and ecomorphology of the Iberian barbel Luciobarbus bocagei (Steindachner, 1864) on permanent and temporary rivers. Ecology of Freshwater Fish **23**:244-258.

Alvarez, M., A. W. Schrey, and C. L. Richards. 2015. Ten years of transcriptomics in wild populations: What have we learned about their ecology and evolution? Molecular Ecology **24**:710-725.

Andersen, A. N., L. T. van Ingen, and R. I. Campos. 2008. Contrasting rainforest and savanna ant faunas in monsoonal northern Australia: a rainforest patch in a tropical savanna landscape. Australian Journal of Zoology **55**:363-369.

Anderson, J. T., and B. H. Song. 2020. Plant adaptation to climate change—Where are we? Journal of Systematics and Evolution **58**:533-545.

Andrew, R. L., L. Bernatchez, A. Bonin, C. A. Buerkle, B. C. Carstens, B. C. Emerson, D. Garant, T. Giraud, N. C. Kane, and S. M. Rogers. 2013. A road map for molecular ecology. Molecular Ecology **22**:2605-2626.

Angilletta Jr, M. J. 2009. Thermal adaptation: a theoretical and empirical synthesis. Oxford University Press, New York, N.Y., USA.

Angilletta, M. J., P. H. Niewiarowski, and C. A. Navas. 2002. The evolution of thermal physiology in ectotherms. Journal of Thermal Biology **27**:249-268.

Ash, J. 1988. The location and stability of rainforest boundaries in north-eastern Queensland, Australia. Journal of Biogeography:619-630.

Atkins, K., and J. Travis. 2010. Local adaptation and the evolution of species' ranges under climate change. Journal of Theoretical Biology **266**:449-457.

Attard, C. R., C. J. Brauer, J. Sandoval-Castillo, L. K. Faulks, P. J. Unmack, D. M. Gilligan, and L. B. Beheregaray. 2018. Ecological disturbance influences adaptive divergence despite high gene flow in golden perch (Macquaria ambigua): implications for management and resilience to climate change. Molecular Ecology **27**:196-215.

Ayres, J. M., and T. Clutton-Brock. 1992. River boundaries and species range size in Amazonian primates. The American Naturalist **140**:531-537.

Azihou, A. F., R. G. Kakaï, R. Bellefontaine, and B. Sinsin. 2013. Distribution of tree species along a gallery forest–savanna gradient: patterns, overlaps and ecological thresholds. Journal of Tropical Ecology **29**:25-37.

Bailey, N. W., C. Desjonquères, A. Drago, J. G. Rayner, S. L. Sturiale, and X. Zhang. 2021. A neglected conceptual problem regarding phenotypic plasticity's role in adaptive evolution: The importance of genetic covariance and social drive. Evolution Letters **5**:444-457.

Balkenhol, N., R. Y. Dudaniec, K. V. Krutovsky, J. S. Johnson, D. M. Cairns, G. Segelbacher, K. A. Selkoe, S. von der Heyden, I. J. Wang, and O. Selmoni. 2017. Landscape genomics: understanding relationships between environmental heterogeneity and genomic characteristics of populations. Pages 261-322 Population Genomics. Springer.

Balogh, G., M. Péter, A. Glatz, I. Gombos, Z. Török, I. Horváth, J. L. Harwood, and L. Vígh. 2013. Key role of lipids in heat stress management. FEBS Letters **587**:1970-1980.

Barlow, J., F. França, T. A. Gardner, C. C. Hicks, G. D. Lennox, E. Berenguer, L. Castello, E. P. Economo, J. Ferreira, B. Guénard, C. Gontijo Leal, V. Isaac, A. C. Lees, C. L. Parr, S. K. Wilson, P. J. Young, and N. A. J. Graham. 2018. The future of hyperdiverse tropical ecosystems. Nature **559**:517-526.

Barreto, S. B., L. L. Knowles, P. R. A. d. M. Affonso, and H. Batalha-Filho. 2020. Riverscape properties contribute to the origin and structure of a hybrid zone in a Neotropical freshwater fish. Journal of evolutionary biology **33**:1530-1542.

Bay, R. A., N. Rose, R. Barrett, L. Bernatchez, C. K. Ghalambor, J. R. Lasky, R. B. Brem, S. R. Palumbi, and P. J. T. A. N. Ralph. 2017. Predicting responses to contemporary environmental change using evolutionary response architectures. **189**:463-473.

Baythavong, B. S. 2011. Linking the spatial scale of environmental variation and the evolution of phenotypic plasticity: selection favors adaptive plasticity in fine-grained environments. Am Nat **178**:75-87.

Becker, C. D., and R. G. Genoway. 1979. Evaluation of the critical thermal maximum for determining thermal tolerance of freshwater fish. Environmental Biology of Fishes **4**:245.

Beheregaray, L. B. 2008. Twenty years of phylogeography: the state of the field and the challenges for the Southern Hemisphere. Molecular Ecology **17**:3754-3774.

Beheregaray, L. B., G. M. Cooke, N. L. Chao, and E. L. Landguth. 2015. Ecological speciation in the tropics: insights from comparative genetic studies in Amazonia. Frontiers in genetics **5**:477.

Beitinger, T. L. 1990. Behavioral reactions for the assessment of stress in fishes. Journal of Great Lakes Research **16**:495-528.

Benham, P. M., and C. C. Witt. 2016. The dual role of Andean topography in primary divergence: functional and neutral variation among populations of the hummingbird, Metallura tyrianthina. BMC Evolutionary Biology **16**:22.

Bennett, J. M., J. Sunday, P. Calosi, F. Villalobos, B. Martínez, R. Molina-Venegas, M. B. Araújo, A. C. Algar, S. Clusella-Trullas, and B. A. Hawkins. 2021a. The evolution of critical thermal limits of life on Earth. Nature communications **12**:1-9.

Bennett, K. L., W. O. McMillan, and J. R. Loaiza. 2021b. The genomic signal of local environmental adaptation in Aedes aegypti mosquitoes. Evolutionary applications.

Bernatchez, L. 2016. On the maintenance of genetic variation and adaptation to environmental change: considerations from population genomics in fishes. Journal of Fish Biology **89**:2519-2556.

Bond, M. N., S. B. Piertney, T. G. Benton, and T. C. Cameron. 2021. Plasticity is a locally adapted trait with consequences for ecological dynamics in novel environments. Ecology and Evolution **11**:10868-10879.

Booth, T. H., H. A. Nix, J. R. Busby, and M. F. Hutchinson. 2014. BIOCLIM: the first species distribution modelling package, its early applications and relevance to most current MAXENT studies. Diversity and Distributions **20**:1-9.

Bourret, V., M. Dionne, and L. Bernatchez. 2014. Detecting genotypic changes associated with selective mortality at sea in Atlantic salmon: polygenic multilocus analysis surpasses genome scan. Molecular Ecology **23**:4444-4457.

Bowman, D. M. J. S., G. K. Brown, M. F. Braby, J. R. Brown, L. G. Cook, M. D. Crisp, F. Ford, S. Haberle, J. Hughes, Y. Isagi, L. Joseph, J. McBride, G. Nelson, and P. Y. Ladiges. 2010. Biogeography of the Australian monsoon tropics. Journal of Biogeography **37**:201-216.

Bragg, J. G., M. A. Supple, R. L. Andrew, and J. O. Borevitz. 2015. Genomic variation across landscapes: insights and applications. New Phytologist **207**:953-967.

Brandon, K. 2014. Ecosystem services from tropical forests: review of current science. Center for Global Development. Washington, DC, USA.

Brauer, C. J., and L. B. Beheregaray. 2020. Recent and rapid anthropogenic habitat fragmentation increases extinction risk for freshwater biodiversity. Evolutionary applications **13**:2857-2869.

Brauer, C. J., M. P. Hammer, and L. B. Beheregaray. 2016. Riverscape genomics of a threatened fish across a hydroclimatically heterogeneous river basin. Molecular Ecology **25**:5093-5113.

Brauer, C. J., P. J. Unmack, and L. B. Beheregaray. 2017. Comparative ecological transcriptomics and the contribution of gene expression to the evolutionary potential of a threatened fish. Molecular Ecology **26**:6841-6856.

Brauer, C. J., P. J. Unmack, S. Smith, L. Bernatchez, and L. B. Beheregaray. 2018. On the roles of landscape heterogeneity and environmental variation in determining population genomic structure in a dendritic system. Molecular Ecology **27**:3484-3497.

Brousseau, L., M. Foll, C. Scotti-Saintagne, and I. Scotti. 2015. Neutral and adaptive drivers of microgeographic genetic divergence within continuous populations: the case of the neotropical tree Eperua falcata (Aubl.). PloS one **10**:e0121394.

Brown, S. C., T. M. Wigley, B. L. Otto-Bliesner, C. Rahbek, and D. A. Fordham. 2020. Persistent Quaternary climate refugia are hospices for biodiversity in the Anthropocene. Nature Climate Change **10**:244-248.

Buckley, L. B., and J. G. Kingsolver. 2021. Evolution of Thermal Sensitivity in Changing and Variable Climates. Annual Review of Ecology, Evolution, and Systematics **52**.

Butlin, R. K., J. Galindo, and J. W. Grahame. 2008. Sympatric, parapatric or allopatric: the most important way to classify speciation? Philosophical Transactions of the Royal Society B: Biological Sciences **363**:2997-3007.

Cadena, C. D., K. H. Kozak, J. P. Gómez, J. L. Parra, C. M. McCain, R. C. Bowie, A. C. Carnaval, C. Moritz, C. Rahbek, and T. E. Roberts. 2012. Latitude, elevational climatic zonation and speciation in New World vertebrates. Proceedings of the Royal Society B: Biological Sciences **279**:194-201.

Callahan, H. S., H. Maughan, and U. K. Steiner. 2008. Phenotypic plasticity, costs of phenotypes, and costs of plasticity: toward an integrative view. Annals of the New York Academy of Sciences **1133**:44-66.

Carlston, C. W. 1963. Drainage density and streamflow. US Government Printing Office, Washington, DC, USA.

Carvajal-Quintero, J., F. Villalobos, T. Oberdorff, G. Grenouillet, S. Brosse, B. Hugueny, C. Jézéquel, and P. A. Tedesco. 2019. Drainage network position and historical connectivity explain global patterns in freshwater fishes' range size. Proceedings of the National Academy of Sciences **116**:13434-13439.

Carvalho, C. S., B. R. Forester, S. K. Mitre, R. Alves, V. L. Imperatriz-Fonseca, S. J. Ramos, L. C. Resende-Moreira, J. O. Siqueira, L. C. Trevelin, and C. F. Caldeira. 2021. Combining genotype, phenotype, and environmental data to delineate site-adjusted provenance strategies for ecological restoration. Molecular Ecology Resources **21**:44-58.

Catchen, J. M., P. A. Hohenlohe, L. Bernatchez, W. C. Funk, K. R. Andrews, and F. W. Allendorf. 2017. Unbroken: RADseq remains a powerful tool for understanding the genetics of adaptation in natural populations. Molecular Ecology Resources **17**:362-365.

Cattin, L., J. Schuerch, N. Salamin, and S. Dubey. 2016. Why are some species older than others? A large-scale study of vertebrates. BMC Evolutionary Biology **16**:90.

Catullo, R. A., S. Ferrier, and A. A. Hoffmann. 2015. Extending spatial modelling of climate change responses beyond the realized niche: estimating, and accommodating, physiological limits and adaptive evolution. Global ecology and Biogeography **24**:1192-1202.

Chen, B., M. E. Feder, and L. Kang. 2018a. Evolution of heat-shock protein expression underlying adaptive responses to environmental stress. Molecular Ecology **27**:3040-3054.

Chen, J., Y. Cui, J. Yan, J. Jiang, X. Cao, and J. Gao. 2018b. Molecular characterization of elongase of very long-chain fatty acids 6 (elovl6) genes in Misgurnus anguillicaudatus and their potential roles in adaptation to cold temperature. Gene **666**:134-144.

Chen, Z., A. P. Farrell, A. Matala, and S. R. Narum. 2018c. Mechanisms of thermal adaptation and evolutionary potential of conspecific populations to changing environments. Molecular Ecology **27**:659-674.

Chevin, L.-M., and R. Lande. 2015. Evolution of environmental cues for phenotypic plasticity. Evolution **69**:2767-2775.

Chevin, L. M., and R. Lande. 2011. Adaptation to marginal habitats by evolution of increased phenotypic plasticity. Journal of evolutionary biology **24**:1462-1476.

Ciemer, C., N. Boers, M. Hirota, J. Kurths, F. Müller-Hansen, R. S. Oliveira, and R. Winkelmann. 2019. Higher resilience to climatic disturbances in tropical vegetation exposed to more variable rainfall. Nature Geoscience **12**:174-179.

Clarke, B. C. 1979. The evolution of genetic diversity. Proceedings of the Royal Society of London. Series B. Biological Sciences **205**:453-474.

Clarke, D. A., P. H. York, M. A. Rasheed, and T. D. Northfield. 2017. Does Biodiversity–Ecosystem Function Literature Neglect Tropical Ecosystems? Trends in ecology & evolution **32**:320-323.

Claude, J. 2008. Morphometrics with R. Springer Science & Business Media, New York, NY, USA.

Clegg, S. M., S. M. Degnan, C. Moritz, A. Estoup, J. Kikkawa, and I. P. Owens. 2002. Microevolution in island forms: the roles of drift and directional selection in morphological divergence of a passerine bird. Evolution **56**:2090-2099.

Cohet, Y., J. Vouidibio, and J. David. 1980. Thermal tolerance and geographic distribution: a comparison of cosmopolitan and tropical endemic Drosophila species. Journal of Thermal Biology **5**:69-74.

Compton, T. J., M. J. Rijkenberg, J. Drent, and T. Piersma. 2007. Thermal tolerance ranges and climate variability: a comparison between bivalves from differing climates. Journal of Experimental Marine Biology and Ecology **352**:200-211.

Conesa, A., P. Madrigal, S. Tarazona, D. Gomez-Cabrero, A. Cervera, A. McPherson, M. W. Szcześniak, D. J. Gaffney, L. L. Elo, X. Zhang, and A. Mortazavi. 2016. A survey of best practices for RNA-seq data analysis. Genome Biology **17**:13.

Conover, D. O., and E. T. Schultz. 1995. Phenotypic similarity and the evolutionary significance of countergradient variation. Trends in ecology & evolution **10**:248-252.

Cook, B. D., and J. M. Hughes. 2010. Historical population connectivity and fragmentation in a tropical freshwater fish with a disjunct distribution (pennyfish, Denariusa bandata). Journal of the North American Benthological Society **29**:1119-1131.

Cooke, G., N. Chao, and L. Beheregaray. 2012a. Natural selection in the water: freshwater invasion and adaptation by water colour in the Amazonian pufferfish. Journal of evolutionary biology **25**:1305-1320.

Cooke, G. M., N. L. Chao, and L. B. Beheregaray. 2012b. Divergent natural selection with gene flow along major environmental gradients in Amazonia: insights from genome scans, population genetics and phylogeography of the characin fish Triportheus albus. Molecular Ecology **21**:2410-2427.

Cooke, G. M., E. L. Landguth, and L. B. Beheregaray. 2014. Riverscape genetics identifies replicated ecological divergence across an Amazonian ecotone. Evolution **68**:1947-1960.

Coop, G., D. Witonsky, A. Di Rienzo, and J. K. Pritchard. 2010. Using environmental correlations to identify loci underlying local adaptation. Genetics **185**:1411-1423.

Crispo, E. 2008. Modifying effects of phenotypic plasticity on interactions among natural selection, adaptation and gene flow. Journal of evolutionary biology **21**:1460-1469.

Dagallier, L. P. M., S. B. Janssens, G. Dauby, A. Blach-Overgaard, B. A. Mackinder, V. Droissart, J. C. Svenning, M. S. Sosef, T. Stévart, and D. J. Harris. 2020. Cradles and museums of generic plant diversity across tropical Africa. New Phytologist **225**:2196-2213.

Danecek, P., A. Auton, G. Abecasis, C. A. Albers, E. Banks, M. A. DePristo, R. E. Handsaker, G. Lunter, G. T. Marth, S. T. Sherry, G. McVean, R. Durbin, and G. Genomes Project Analysis. 2011. The variant call format and VCFtools. Bioinformatics (Oxford, England) **27**:2156-2158.

Davis, C. D., C. W. Epps, R. L. Flitcroft, and M. A. Banks. 2018. Refining and defining riverscape genetics: How rivers influence population genetic structure. Wiley Interdisciplinary Reviews: Water **5**:e1269.

De Wit, P., M. H. Pespeni, J. T. Ladner, D. J. Barshis, F. Seneca, H. Jaris, N. O. Therkildsen, M. Morikawa, and S. R. Palumbi. 2012. The simple fool's guide to population genomics via RNA-Seq: an introduction to high-throughput sequencing data analysis. Molecular Ecology Resources **12**:1058-1067.

Deutsch, C. A., J. J. Tewksbury, R. B. Huey, K. S. Sheldon, C. K. Ghalambor, D. C. Haak, and P. R. Martin. 2008. Impacts of climate warming on terrestrial ectotherms across latitude. Proceedings of the National Academy of Sciences **105**:6668-6672.

Devictor, V., R. Julliard, and F. Jiguet. 2008. Distribution of specialist and generalist species along spatial gradients of habitat disturbance and fragmentation. Oikos **117**:507-514.

DeWitt, T. J., A. Sih, and D. S. Wilson. 1998. Costs and limits of phenotypic plasticity. Trends in ecology & evolution **13**:77-81.

Diamond, S. E., and R. A. Martin. 2021. Buying Time: Plasticity and Population Persistence. Pages 185-209 *in* D. W. Pfennig, editor. Phenotypic Plasticity & Evolution: Causes, Consequences, Controversies. CRC Press, Boca Raton, FL, USA.

Dias, M. S., J.-F. Cornu, T. Oberdorff, C. A. Lasso, and P. A. Tedesco. 2013. Natural fragmentation in river networks as a driver of speciation for freshwater fishes. Ecography **36**:683-689.

Döll, P., and J. Zhang. 2010. Impact of climate change on freshwater ecosystems: a global-scale analysis of ecologically relevant river flow alterations. Hydrology and Earth System Sciences **14**:783-799.

Dongmo, M. A. K., R. Hanna, T. B. Smith, K. K. M. Fiaboe, A. Fomena, and T. C. Bonebrake. 2021. Local adaptation in thermal tolerance for a tropical butterfly across ecotone and rainforest habitats. Biology Open **10**.

Eguiguren-Velepucha, P. A., J. A. M. Chamba, N. A. Aguirre Mendoza, T. L. Ojeda-Luna, N. S. Samaniego-Rojas, M. J. Furniss, C. Howe, and Z. H. Aguirre Mendoza. 2016. Tropical ecosystems vulnerability to climate change in southern Ecuador. Tropical Conservation Science **9**:1940082916668007.

Eklöv, P., and R. Svanbäck. 2006. Predation risk influences adaptive morphological variation in fish populations. The American Naturalist **167**:440-452.

Endler, J. A. 1982. Problems in distinguishing historical from ecological factors in biogeography. American Zoologist **22**:441-452.

Engelhard, G. H., J. R. Ellis, M. R. Payne, R. ter Hofstede, and J. K. Pinnegar. 2010. Ecotypes as a concept for exploring responses to climate change in fish assemblages. ICES Journal of Marine Science: Journal du Conseil.

ESRI. 2011. ArcGIS Desktop: Release 10. Redlands, CA: Environmental Systems Research Institute.

Excoffier, L., and H. E. Lischer. 2010. Arlequin suite ver 3.5: a new series of programs to perform population genetics analyses under Linux and Windows. Molecular Ecology Resources **10**:564-567.

Faleiro, F. V., R. B. Machado, and R. D. Loyola. 2013. Defining spatial conservation priorities in the face of land-use and climate change. Biological Conservation **158**:248-257.

Farré, M., V. M. Tuset, F. Maynou, L. Recasens, and A. Lombarte. 2016. Selection of landmarks and semilandmarks in fishes for geometric morphometric analyses: a comparative study based on analytical methods. Scientia Marina **80**:175-186.

Fensham, R. 1995. Floristics and environmental relations of inland dry rainforest in north Queensland, Australia. Journal of Biogeography:1047-1063.

Fisher, R. 1950. Gene frequencies in a cline determined by selection and diffusion. Biometrics **6**:353-361.

Fitzpatrick, B. M. 2012. Underappreciated consequences of phenotypic plasticity for ecological speciation. International Journal of Ecology **2012**.

Fitzpatrick, M. C., and S. R. Keller. 2015. Ecological genomics meets community-level modelling of biodiversity: mapping the genomic landscape of current and future environmental adaptation. Ecology letters **18**:1-16.

Fjeldsaå, J., D. Ehrlich, E. Lambin, and E. Prins. 1997. Are biodiversity 'hotspots' correlated with current ecoclimatic stability? A pilot study using the NOAA-AVHRR remote sensing data. Biodiversity & Conservation **6**:401-422.

Foll, M., and O. Gaggiotti. 2008. A genome-scan method to identify selected loci appropriate for both dominant and codominant markers: a Bayesian perspective. Genetics **180**:977-993.

Forester, B. R., J. R. Lasky, H. H. Wagner, and D. L. Urban. 2018. Comparing methods for detecting multilocus adaptation with multivariate genotype–environment associations. Molecular Ecology **27**:2215-2233.

Fox, R. J., J. M. Donelson, C. Schunter, T. Ravasi, and J. D. Gaitán-Espitia. 2019. Beyond buying time: the role of plasticity in phenotypic adaptation to rapid environmental change. The Royal Society.

França, F. M., C. E. Benkwitt, G. Peralta, J. P. Robinson, N. A. Graham, J. M. Tylianakis, E. Berenguer, A. C. Lees, J. Ferreira, and J. Louzada. 2020. Climatic and local stressor interactions threaten tropical forests and coral reefs. Philosophical Transactions of the Royal Society B **375**:20190116.

Frankham, R. 2015. Genetic rescue of small inbred populations: Meta-analysis reveals large and consistent benefits of gene flow. Molecular Ecology **24**:2610-2618.

Franks, S. J., and A. A. Hoffmann. 2012. Genetics of climate change adaptation. Annual review of genetics **46**:185-208.

Freedman, A. H., H. A. Thomassen, W. Buermann, and T. B. Smith. 2010. Genomic signals of diversification along ecological gradients in a tropical lizard. Molecular Ecology **19**:3773-3788.

Frishkoff, L. O., E. A. Hadly, and G. C. Daily. 2015. Thermal niche predicts tolerance to habitat conversion in tropical amphibians and reptiles. Global Change Biology **21**:3901-3916.

Fuller, M. R., M. W. Doyle, and D. L. Strayer. 2015. Causes and consequences of habitat fragmentation in river networks. Annals of the New York Academy of Sciences **1355**:31-51.

Furness, E. N., R. J. Garwood, P. D. Mannion, and M. D. Sutton. 2021. Evolutionary simulations clarify and reconcile biodiversity-disturbance models. Proceedings of the Royal Society B **288**:20210240.

Fusco, G., and A. Minelli. 2010. Phenotypic Plasticity in Development and Evolution: Facts and Concepts. Philosophical transactions of the Royal Society of London Series B **365**:547-556.

Gallego-García, N., G. Forero-Medina, M. Vargas-Ramírez, S. Caballero, and H. B. Shaffer. 2019. Landscape genomic signatures indicate reduced gene flow and forest-associated adaptive divergence in an endangered neotropical turtle. Molecular Ecology **28**:2757-2771.

Garant, D., S. E. Forde, and A. P. Hendry. 2007. The multifarious effects of dispersal and gene flow on contemporary adaptation. Functional ecology **21**:434-443.

Garland Jr, T., and S. A. Kelly. 2006. Phenotypic plasticity and experimental evolution. Journal of Experimental Biology **209**:2344-2361.

Garner, B. A., B. K. Hand, S. J. Amish, L. Bernatchez, J. T. Foster, K. M. Miller, P. A. Morin, S. R. Narum, S. J. O'Brien, G. Roffler, W. D. Templin, P. Sunnucks, J. Strait, K. I. Warheit, T. R. Seamons, J. Wenburg, J. Olsen, and G. Luikart. 2016. Genomics in Conservation: Case Studies and Bridging the Gap between Data and Application. Trends Ecol Evol **31**:81-83.

Garvin, M. R., G. H. Thorgaard, and S. R. Narum. 2015. Differential expression of genes that control respiration contribute to thermal adaptation in redband trout (Oncorhynchus mykiss gairdneri). Genome biology and evolution **7**:1404-1414.

Gaston, K. J., and T. M. Blackburn. 1996. The tropics as a museum of biological diversity: an analysis of the New World avifauna. Proceedings of the Royal Society of London. Series B: Biological Sciences **263**:63-68.

Gates, K., J. Sandoval-Castillo, L. Bernatchez, and L. B. Beheregaray. 2017. De novo transcriptome assembly and annotation for the desert rainbowfish (Melanotaenia splendida tatei) with comparison with candidate genes for future climates. Marine Genomics **35**:63-68.

Gates, K., J. Sandoval-Castillo, C. J. Brauer, P. J. Unmack, M. Laporte, L. Bernatchez, and L. B. Beheregaray. 2021, under submission. Environmental selection, rather than neutral processes, best explain patterns of diversity in a tropical rainforest fish

Gatz, J. 1979. Ecological Morphology of Freshwater Streamfishes Tulane Studies in Zoology and Botany 21: 91-123.

Gatz Jr, A. J. 1979. Community organization in fishes as indicated by morphological features. Ecology **60**:711-718.

Gautier, M. 2015. Genome-wide scan for adaptive divergence and association with population-specific covariates. Genetics **201**:1555-1579.

Gerken, A. R., O. C. Eller, D. A. Hahn, and T. J. Morgan. 2015. Constraints, independence, and evolution of thermal plasticity: probing genetic architecture of long-and short-term thermal acclimation. Proceedings of the National Academy of Sciences **112**:4399-4404.

Ghalambor, C. K., K. L. Hoke, E. W. Ruell, E. K. Fischer, D. N. Reznick, and K. A. Hughes. 2015. Non-adaptive plasticity potentiates rapid adaptive evolution of gene expression in nature. Nature **525**:372.

Ghalambor, C. K., R. B. Huey, P. R. Martin, J. J. Tewksbury, and G. Wang. 2006. Are mountain passes higher in the tropics? Janzen's hypothesis revisited. Integrative and Comparative Biology **46**:5-17.

Ghalambor, C. K., J. K. McKay, S. P. Carroll, and D. N. Reznick. 2007. Adaptive versus non-adaptive phenotypic plasticity and the potential for contemporary adaptation in new environments. Functional ecology **21**:394-407.

Gibson, L., A. J. Lynam, C. J. A. Bradshaw, F. He, D. P. Bickford, D. S. Woodruff, S. Bumrungsri, and W. F. Laurance. 2013. Near-Complete Extinction of Native Small Mammal Fauna 25 Years After Forest Fragmentation. Science **341**:1508-1510.

Gilchrist, G. W. 1995. Specialists and Generalists in Changing Environments. I. Fitness Landscapes of Thermal Sensitivity. The American Naturalist **146**:252-270.

Gilchrist, G. W., and R. B. Huey. 2004. Plastic and genetic variation in wing loading as a function of temperature within and among parallel clines in Drosophila subobscura. Integrative and Comparative Biology **44**:461-470.

Goldstein, I., and I. M. Ehrenreich. 2021. Genetic Variation in Phenotypic Plasticity. Pages 91-111 *in* D. W. Pfennig, editor. Phenotypic Plasticity & Evolution: Causes, Consequences, Controversies. CRC Press, Boca Raton, FL, USA.

Gonzalo-Turpin, H., and L. Hazard. 2009. Local adaptation occurs along altitudinal gradient despite the existence of gene flow in the alpine plant species Festuca eskia. Journal of Ecology **97**:742-751.

Goudet, J. 2005. Hierfstat, a package for R to compute and test hierarchical F-statistics. Molecular Ecology Notes **5**:184-186.

Grace, J., J. S. José, P. Meir, H. S. Miranda, and R. A. Montes. 2006. Productivity and carbon fluxes of tropical savannas. Journal of Biogeography **33**:387-400.

Grummer, J. A., L. B. Beheregaray, L. Bernatchez, B. K. Hand, G. Luikart, S. R. Narum, and E. B. Taylor. 2019. Aquatic landscape genomics and environmental effects on genetic variation. Trends in ecology & evolution **34**:641-654.

Günther, T., and G. Coop. 2013. Robust identification of local adaptation from allele frequencies. Genetics **195**:205-220.

Haffer, J. 1969. Speciation in Amazonian forest birds. Science **165**:131-137.

Haffer, J. r. 1997. Alternative models of vertebrate speciation in Amazonia: an overview. Biodiversity & Conservation **6**:451-476.

Haldane, J. 1930. Theoretical genetics of autopolyploids. Journal of genetics **22**:359-372.

Haldane, J. 1948. The theory of a cline. Journal of genetics **48**:277-284.

Hansen, M. M., I. Olivieri, D. M. Waller, E. E. Nielsen, and G. W. Group. 2012. Monitoring adaptive genetic responses to environmental change. Molecular Ecology **21**:1311-1329.

Hanson, K. C., and S. J. Cooke. 2009. Why does size matter? A test of the benefits of female mate choice in a teleost fish based on morphological and physiological indicators of male quality. Physiological and Biochemical Zoology **82**:617-624.

Harshman, L., J. Ottea, and B. Hammock. 1991. Evolved environment-dependent expression of detoxication enzyme activity in Drosophila melanogaster. Evolution:791-795.

Hattori, A., and K. Warburton. 2003. Microhabitat use by the rainbowfish Melanotaenia duboulayi in a subtropical Australian stream. Journal of Ethology **21**:15-22.

Hau, M. 2001. Timing of breeding in variable environments: tropical birds as model systems. Hormones and behavior **40**:281-290.

Hawkins, B. A., R. Field, H. V. Cornell, D. J. Currie, J.-F. Guégan, D. M. Kaufman, J. T. Kerr, G. G. Mittelbach, T. Oberdorff, and E. M. O'Brien. 2003. Energy, water, and broad-scale geographic patterns of species richness. Ecology **84**:3105-3117.

Hendry, A. P. 2015. Key Questions on the Role of Phenotypic Plasticity in Eco-Evolutionary Dynamics. Journal of Heredity **107**:25-41.

Hendry, A. P., and E. B. Taylor. 2004. How much of the variation in adaptive divergence can be explained by gene flow? An evaluation using lake-stream stickleback pairs. Evolution **58**:2319-2331.

Hilbert, D. W. 2008. The Dynamic forest landscape of the Australian Wet Tropics: present, past and future. Pages 107-123 *in* N. Stork and S. Turton, editors. Living in a dynamic tropical forest landscape. Blackwell Publishing, Carlton, VIC, Australia.

Hirota, M., M. Holmgren, E. H. Van Nes, and M. Scheffer. 2011. Global resilience of tropical forest and savanna to critical transitions. Science **334**:232-235.

Ho, W.-C., Y. Ohya, and J. Zhang. 2017. Testing the neutral hypothesis of phenotypic evolution. Proceedings of the National Academy of Sciences **114**:12219-12224.

Hochachka, P. W., and G. N. Somero. 2002. Biochemical adaptation: mechanism and process in physiological evolution. Oxford university press.

Hoffmann, A., P. Griffin, S. Dillon, R. Catullo, R. Rane, M. Byrne, R. Jordan, J. Oakeshott, A. Weeks, and L. Joseph. 2015. A framework for incorporating evolutionary genomics into biodiversity conservation and management. Climate Change Responses **2**:1.

Hoffmann, A. A., P. D. Rymer, M. Byrne, K. X. Ruthrof, J. Whinam, M. McGeoch, D. M. Bergstrom, G. R. Guerin, B. Sparrow, and L. Joseph. 2019. Impacts of recent climate change on terrestrial flora and fauna: Some emerging Australian examples. Austral Ecology **44**:3-27.

Hoffmann, A. A., and C. M. Sgro. 2011. Climate change and evolutionary adaptation. Nature **470**:479-485.

Holderegger, R., U. Kamm, and F. Gugerli. 2006. Adaptive vs. neutral genetic diversity: implications for landscape genetics. Landscape Ecology **21**:797-807.

Holderegger, R., and H. H. Wagner. 2008. Landscape genetics. AIBS Bulletin **58**:199-207.

Höllinger, I., P. S. Pennings, and J. Hermisson. 2019. Polygenic adaptation: From sweeps to subtle frequency shifts. PLoS genetics **15**:e1008035.

Hooker, O., J. Barry, T. Van Leeuwen, A. Lyle, J. Newton, P. Cunningham, and C. Adams. 2016. Morphological, ecological and behavioural differentiation of sympatric profundal and pelagic Arctic charr (Salvelinus alpinus) in Loch Dughaill Scotland. Hydrobiologia **783**:209-221.

Howley, C., J. Shellberg, K. Stephan, and A. Brooks. 2013. Normanby Catchment Water Quality Management Plan. Australian Rivers Institute, Griffith University.

Hu, Z.-M., K.-L. Zhong, F. Weinberger, D.-L. Duan, S. G. A. Draisma, and E. A. Serrão. 2020. Linking Ecology to Genetics to Better Understand Adaptation and Evolution: A Review in Marine Macrophytes. Frontiers in Marine Science **7**:545102.

Huey, R. B., C. A. Deutsch, J. J. Tewksbury, L. J. Vitt, P. E. Hertz, H. J. Á. Pérez, and T. Garland. 2009. Why tropical forest lizards are vulnerable to climate warming. Proceedings of the Royal Society of London B: Biological Sciences **276**:1939-1948.

Huntley, B., P. M. Berry, W. Cramer, and A. P. McDonald. 1995. Special Paper: Modelling Present and Potential Future Ranges of Some European Higher Plants Using Climate Response Surfaces. Journal of Biogeography **22**:967-1001.

Hurwood, D., and J. Hughes. 2001. Historical interdrainage dispersal of eastern rainbowfish from the Atherton Tableland, north-eastern Australia. Journal of Fish Biology **58**:1125-1136.

Ibanez, T., J. Munzinger, C. Gaucherel, T. Curt, and C. Hély. 2013. Inferring savannah–rainforest boundary dynamics from vegetation structure and composition: a case study in New Caledonia. Australian Journal of Botany **61**:128-138.

IPCC. 2014. Climate Change 2014–Impacts, Adaptation and Vulnerability: Regional Aspects. Cambridge University Press.

Jaffé, R., J. C. Veiga, N. S. Pope, É. C. Lanes, C. S. Carvalho, R. Alves, S. C. Andrade, M. C. Arias, V. Bonatti, and A. T. Carvalho. 2019. Landscape genomics to the rescue of a tropical bee threatened by habitat loss and climate change. Evolutionary applications **12**:1164-1177.

Janzen, D. H. 1967. Why Mountain Passes are Higher in the Tropics. The American Naturalist **101**:233-249.

Jardim de Queiroz, L., G. Torrente-Vilara, C. Quilodran, C. Rodrigues da Costa Doria, and J. I. Montoya-Burgos. 2017. Multifactorial genetic divergence processes drive the onset of speciation in an Amazonian fish. PloS one **12**:e0189349.

Jasienski, M. 2009. Cogradient platicity of growth in montane and lowland larvae of Rana temporaria (L.) at two levels of temperature. Polish Journal of Ecology **57**:353-361.

Jensen, J. D., and D. Bachtrog. 2011. Characterizing the influence of effective population size on the rate of adaptation: Gillespie's Darwin domain. Genome biology and evolution **3**:687-701.

Jiménez-Cisneros, B., T. Oki, N. Arnell, G. Benito, J. Cogley, P. Döll, T. Jiang, and S. Mwakalila. 2014. Freshwater resources in climate change 2014: Impacts, adaptation, and vulnerability. Part a: global and sectoral aspects. . Pages 229-269 *in* C. Field, V. Barros, D. Dokken, K. Mach, M. Mastrandrea, T. Bilir, M. Chatterjee, K. Ebi, Y. Estrada, R. Genova, B. Girma, E. Kissel, A. Levy, S. MacCracken, P. Mastrandrea, and L. White, editors. Contribution of working group II to the fifth assessment report of the intergovernmental panel on climate change. Cambridge University Press, Cambridge, UK.

Jombart, T. 2008. adegenet: a R package for the multivariate analysis of genetic markers. Bioinformatics **24**:1403-1405.

Jombart, T., and I. Ahmed. 2011. adegenet 1.3-1: new tools for the analysis of genome-wide SNP data. Bioinformatics **27**:3070-3071.

Joost, S., A. Bonin, M. W. Bruford, L. Després, C. Conord, G. Erhardt, and P. Taberlet. 2007. A spatial analysis method (SAM) to detect candidate loci for selection: towards a landscape genomics approach to adaptation. Molecular Ecology **16**:3955-3969.

Joost, S., S. Vuilleumier, J. D. Jensen, S. Schoville, K. Leempoel, S. Stucki, I. Widmer, C. Melodelima, J. Rolland, and S. Manel. 2013. Uncovering the genetic basis of adaptive change: on the intersection of landscape genomics and theoretical population genetics. Molecular Ecology **22**:3659-3665.

Kellermann, V., B. Van Heerwaarden, C. M. Sgrò, and A. A. Hoffmann. 2009. Fundamental evolutionary limits in ecological traits drive Drosophila species distributions. Science **325**:1244-1246.

Kelley, J. L., P. M. Davies, S. P. Collin, and P. F. Grierson. 2017. Morphological plasticity in a native freshwater fish from semiarid Australia in response to variable water flows. Ecology and Evolution **7**:6595-6605.

Kelly, M. 2019. Adaptation to climate change through genetic accommodation and assimilation of plastic phenotypes. Philosophical Transactions of the Royal Society B **374**:20180176.

Kelly, M. W., M. S. Pankey, M. B. DeBiasse, and D. C. Plachetzki. 2017. Adaptation to heat stress reduces phenotypic and transcriptional plasticity in a marine copepod. Functional ecology **31**:398-406.

Kelly, S. A., T. M. Panhuis, and A. M. Stoehr. 2011. Phenotypic plasticity: molecular mechanisms and adaptive significance. Comprehensive Physiology **2**:1417-1439.

Kern, E. M., and R. B. Langerhans. 2018. Urbanization drives contemporary evolution in stream fish. Global Change Biology **24**:3791-3803.

Kier, G., J. Mutke, E. Dinerstein, T. H. Ricketts, W. Küper, H. Kreft, and W. Barthlott. 2005. Global patterns of plant diversity and floristic knowledge. Journal of Biogeography **32**:1107-1116.

Killen, S. S., D. S. Glazier, E. L. Rezende, T. D. Clark, D. Atkinson, A. S. Willener, and L. G. Halsey. 2016. Ecological influences and morphological correlates of resting and maximal metabolic rates across teleost fish species. The American Naturalist **187**:592-606.

King, N. G., N. J. McKeown, D. A. Smale, and P. J. Moore. 2018. The importance of phenotypic plasticity and local adaptation in driving intraspecific variability in thermal niches of marine macrophytes. Ecography **41**:1469-1484.

King, N. G., N. J. McKeown, D. A. Smale, D. C. Wilcockson, L. Hoelters, E. A. Groves, T. Stamp, and P. J. Moore. 2019. Evidence for different thermal ecotypes in range centre and trailing edge kelp populations. Journal of Experimental Marine Biology and Ecology **514-515**:10-17.

Kingsolver, J. G., and L. B. Buckley. 2017. Evolution of plasticity and adaptive responses to climate change along climate gradients. Proc. R. Soc. B **284**:20170386.

Kirschel, A. N., H. Slabbekoorn, D. T. Blumstein, R. E. Cohen, S. R. de Kort, W. Buermann, and T. B. Smith. 2011. Testing alternative hypotheses for evolutionary diversification in an African songbird: rainforest refugia versus ecological gradients. Evolution **65**:3162-3174.

Klingenberg, C. P. 2011. MorphoJ: an integrated software package for geometric morphometrics. Molecular Ecology Resources **11**:353-357.

Knutson, T. R., J. L. McBride, J. Chan, K. Emanuel, G. Holland, C. Landsea, I. Held, J. P. Kossin, A. Srivastava, and M. Sugi. 2010. Tropical cyclones and climate change. Nature Geoscience **3**:157.

Komoroske, L. M., K. M. Jeffries, A. Whitehead, J. L. Roach, M. Britton, R. E. Connon, C. Verhille, S. M. Brander, and N. A. Fangue. 2021. Transcriptional flexibility during thermal challenge corresponds with expanded thermal tolerance in an invasive compared to native fish. Evolutionary applications **14**:931-949.

Kooyman, R. M., M. Rossetto, H. Sauquet, and S. W. Laffan. 2013. Landscape patterns in rainforest phylogenetic signal: isolated islands of refugia or structured continental distributions? PloS one **8**:e80685.

Kramer, D. L., and M. McClure. 1982. Aquatic surface respiration, a widespread adaptation to hypoxia in tropical freshwater fishes. Environmental Biology of Fishes **7**:47-55.

Kutt, A. S., G. C. Perkins, N. Colman, E. P. Vanderduys, and J. J. Perry. 2012. Temporal variation in a savanna bird assemblage: what changes over 5 years? Emu-Austral Ornithology **112**:32-38.

Lam, A. W., M. Gueuning, C. Kindler, M. Van Dam, N. Alvarez, R. Panjaitan, H. Shaverdo, L. T. White, G. K. Roderick, and M. Balke. 2018. Phylogeography and population genomics of a lotic water beetle across a complex tropical landscape. Molecular Ecology **27**:3346-3356.

Langerhans, R. B. 2008. Predictability of phenotypic differentiation across flow regimes in fishes. Integrative and Comparative Biology **48**:750-768.

Langerhans, R. B., C. A. Layman, A. M. Shokrollahi, and T. J. DeWitt. 2004. Predator-driven phenotypic diversification in Gambusia affinis. Evolution **58**:2305-2318.

Langerhans, R. B., and D. N. Reznick. 2010. Ecology and evolution of swimming performance in fishes: predicting evolution with biomechanics. Pages 200-248 *in* P. Domenici and B. G. Kapoor, editors. Fish locomotion: an eco-ethological perspective. Science Publishers, Enfield, NH, USA.

Langmead, B., and S. L. Salzberg. 2012. Fast gapped-read alignment with Bowtie 2. Nature methods **9**:357.

Laporte, M., S. A. Pavey, C. Rougeux, F. Pierron, M. Lauzent, H. Budzinski, P. Labadie, E. Geneste, P. Couture, M. Baudrimont, and L. Bernatchez. 2016. RAD sequencing reveals within-generation polygenic selection in response to anthropogenic organic and metal contamination in North Atlantic Eels. Molecular Ecology **25**:219-237.

Leavy, T. R., and T. H. Bonner. 2009. Relationships among swimming ability, current velocity association, and morphology for freshwater lotic fishes. North American Journal of Fisheries Management **29**:72-83.

Lévêque, C. 1997. Biodiversity dynamics and conservation: the freshwater fish of tropical Africa. Cambridge University Press, Cambridge, UK.

Levis, N. A., and D. W. Pfennig. 2021. Innovation and Diversification Via Plasticity-Led Evolution. Pages 211-240 *in* D. W. Pfennig, editor. Phenotypic Plasticity & Evolution: Causes, Consequences, Controversies. CRC Press, Boca Raton, FL, USA.

Lewis Jr, W. M. 1970. Morphological adaptations of cyprinodontoids for inhabiting oxygen deficient waters. Copeia **2**:319-326.

Lewontin, R., and J. Krakauer. 1973. Distribution of gene frequency as a test of the theory of the selective neutrality of polymorphisms. Genetics **74**:175-195.

Li, A., L. Li, Z. Zhang, S. Li, W. Wang, X. Guo, and G. Zhang. 2021. Noncoding variation and transcriptional plasticity promote thermal adaptation in oysters by altering energy metabolism. Molecular biology and evolution **38**:5144-5155.

Li, H. 2011. A statistical framework for SNP calling, mutation discovery, association mapping and population genetical parameter estimation from sequencing data. Bioinformatics (Oxford, England) **27**:2987-2993.

Li, Y., X.-X. Zhang, R.-L. Mao, J. Yang, C.-Y. Miao, Z. Li, and Y.-X. Qiu. 2017. Ten years of landscape genomics: challenges and opportunities. Frontiers in Plant Science **8**:2136.

Lischer, H. E., and L. Excoffier. 2012. PGDSpider: an automated data conversion tool for connecting population genetics and genomics programs. Bioinformatics **28**:298-299.

Lisney, T. J., S. P. Collin, and J. L. Kelley. 2020. The effect of ecological factors on eye morphology in the western rainbowfish, Melanotaenia australis. Journal of Experimental Biology **223**.

Lo, M., J. Reed, L. Castello, E. A. Steel, E. A. Frimpong, and A. Ickowitz. 2020. The Influence of Forests on Freshwater Fish in the Tropics: A Systematic Review. BioScience **70**:404-414.

Logan, C. A., and B. A. Buckley. 2015. Transcriptomic responses to environmental temperature in eurythermal and stenothermal fishes. The Journal of Experimental Biology **218**:1915-1924.

Logan, M. L., and C. L. Cox. 2020. Genetic constraints, transcriptome plasticity, and the evolutionary response to climate change. Frontiers in genetics **11**:1088.

López-Maury, L., S. Marguerat, and J. Bähler. 2008. Tuning gene expression to changing environments: from rapid responses to evolutionary adaptation. Nature Reviews Genetics **9**:583.

Lostrom, S., J. P. Evans, P. F. Grierson, S. P. Collin, P. M. Davies, and J. L. Kelley. 2015. Linking stream ecology with morphological variability in a native freshwater fish from semi-arid Australia. Ecology and Evolution **5**:3272-3287.

Luikart, G., P. R. England, D. Tallmon, S. Jordan, and P. Taberlet. 2003. The power and promise of population genomics: from genotyping to genome typing. Nature Reviews Genetics **4**:981.

Luikart, G., M. Kardos, B. K. Hand, O. P. Rajora, S. N. Aitken, and P. A. Hohenlohe. 2018. Population genomics: advancing understanding of nature. Pages 3-79 *in* O. P. Rajora, editor. Population genomics. Springer Nature Switzerland, Cham, Switzerland.

Ma, X., A. Huete, Q. Yu, N. R. Coupe, K. Davies, M. Broich, P. Ratana, J. Beringer, L. B. Hutley, and J. Cleverly. 2013. Spatial patterns and temporal dynamics in savanna vegetation phenology across the North Australian Tropical Transect. Remote sensing of Environment **139**:97-115.

Maestri, R., R. Fornel, G. L. Gonçalves, L. Geise, T. R. O. de Freitas, and A. C. Carnaval. 2016. Predictors of intraspecific morphological variability in a tropical hotspot: comparing the influence of random and non-random factors. Journal of Biogeography **43**:2160-2172.

Manel, S., and R. Holderegger. 2013. Ten years of landscape genetics. Trends in ecology & evolution **28**:614-621.

Manel, S., S. Joost, B. K. Epperson, R. Holderegger, A. Storfer, M. S. Rosenberg, K. T. Scribner, A. Bonin, and M. J. FORTIN. 2010. Perspectives on the use of landscape genetics to detect genetic adaptive variation in the field. Molecular Ecology **19**:3760-3772.

Manel, S., M. K. Schwartz, G. Luikart, and P. Taberlet. 2003. Landscape genetics: combining landscape ecology and population genetics. Trends in ecology & evolution **18**:189-197.

Marden, J. 2008. Quantitative and evolutionary biology of alternative splicing: how changing the mix of alternative transcripts affects phenotypic plasticity and reaction norms. Heredity **100**:111-120.

Mayr, E., and R. J. O'Hara. 1986. The biogeographic evidence supporting the Pleistocene forest refuge hypothesis. Evolution **40**:55-67.

McCairns, R. J. S., S. Smith, M. Sasaki, L. Bernatchez, and L. B. Beheregaray. 2016. The adaptive potential of subtropical rainbowfish in the face of climate change: heritability and heritable plasticity for the expression of candidate genes. Evolutionary applications **9**:531-545.

McCairns, R. S., and L. J. E. I. J. o. O. E. Bernatchez. 2010. Adaptive divergence between freshwater and marine sticklebacks: insights into the role of phenotypic plasticity from an integrated analysis of candidate gene expression. **64**:1029-1047.

McCairns, R. S., and L. J. J. o. E. B. Bernatchez. 2012. Plasticity and heritability of morphological variation within and between parapatric stickleback demes. **25**:1097-1112.

McGuigan, K., S. F. Chenoweth, and M. W. Blows. 2005. Phenotypic divergence along lines of genetic variance. The American Naturalist **165**:32-43.

McGuigan, K., C. E. Franklin, C. Moritz, and M. W. Blows. 2003. Adaptation of rainbow fish to lake and stream habitats. Evolution **57**:104-118.

McGuigan, K., D. Zhu, G. R. Allen, and C. Moritz. 2000. Phylogenetic relationships and historical biogeography of melanotaeniid fishes in Australia and New Guinea. Marine and Freshwater Research **51**:713-723.

McKay, J. K., J. G. Bishop, J.-Z. Lin, J. H. Richards, A. Sala, and T. Mitchell-Olds. 2001. Local adaptation across a climatic gradient despite small effective population size in the rare sapphire rockcress. Proceedings of the Royal Society of London. Series B: Biological Sciences **268**:1715-1721.

Mejía, R., M. C. Gómez-Eichelmann, and M. S. Fernández. 1999. Fatty acid profile of Escherichia coli during the heat-shock response. IUBMB Life **47**:835-844.

Merilä, J. 2015. Perplexing effects of phenotypic plasticity. Nature **525**:326-327.

Merilä, J., and A. P. Hendry. 2014. Climate change, adaptation, and phenotypic plasticity: the problem and the evidence. Evolutionary applications **7**:1-14.

Metcalfe, D. J., and A. J. Ford. 2009. Floristics and plant biodiversity of the rainforests of the Wet Tropics. Pages 123-132 *in* N. Stork and S. Turton, editors. Living in a dynamic tropical forest landscape. Blackwell Publishing, Carlton, VIC, Australia.

Miller, C., G. T. Taboue, E. Fokam, K. Morgan, Y. Zhen, R. Harrigan, V. Le Underwood, K. Ruegg, P. S. Clee, and S. Ntie. 2020. Environmental variation predicts patterns of phenotypic and genomic variation in an African tropical forest frog. Authorea Preprints.

Mitchell-Olds, T., J. H. Willis, and D. B. Goldstein. 2007. Which evolutionary processes influence natural genetic variation for phenotypic traits? Nature Reviews Genetics **8**:845-856.

Monirian, J., Z. Sutphin, and C. Myrick. 2010. Effects of holding temperature and handling stress on the upper thermal tolerance of threadfin shad Dorosoma petenense. Journal of Fish Biology **76**:1329-1342.

Morgan, K., J.-F. Mboumba, S. Ntie, P. Mickala, C. A. Miller, Y. Zhen, R. J. Harrigan, V. Le Underwood, K. Ruegg, and E. B. Fokam. 2020. Precipitation and vegetation shape patterns of genomic and craniometric variation in the central African rodent Praomys misonnei. Proceedings of the Royal Society B **287**:20200449.

Moritz, C. 2002. Strategies to Protect Biological Diversity and the Evolutionary Processes That Sustain It. Systematic biology **51**:238-254.

Moritz, C., G. Langham, M. Kearney, A. Krockenberger, J. VanDerWal, and S. Williams. 2012. Integrating phylogeography and physiology reveals divergence of thermal traits between central and peripheral lineages of tropical rainforest lizards. Philosophical Transactions of the Royal Society B: Biological Sciences **367**:1680-1687.

Moritz, C., and K. McDonald. 2005. Evolutionary approaches to the conservation of tropical rainforest vertebrates. Pages 532-557 *in* E. Bermingham, C. W. Dick, and C. Moritz, editors. Tropical rainforests: past, present and future. University of Chicago Press, Chicago, IL, USA.

Moritz, C., J. Patton, C. Schneider, and T. Smith. 2000. Diversification of rainforest faunas: an integrated molecular approach. Annual review of ecology and systematics **31**:533-563.

Muñoz, D. J., K. Miller Hesed, E. H. Campbell Grant, and D. A. Miller. 2016. Evaluating within-population variability in behavior and demography for the adaptive potential of a dispersal-limited species to climate change. Ecology and Evolution **6**:8740-8755.

Murphy, B. P., and D. M. Bowman. 2012. What controls the distribution of tropical forest and savanna? Ecology letters **15**:748-758.

Muschick, M., M. Barluenga, W. Salzburger, and A. Meyer. 2011. Adaptive phenotypic plasticity in the Midas cichlid fish pharyngeal jaw and its relevance in adaptive radiation. BMC Evolutionary Biology **11**:116-116.

Myers, N., R. A. Mittermeier, C. G. Mittermeier, G. A. Da Fonseca, and J. Kent. 2000. Biodiversity hotspots for conservation priorities. Nature **403**:853.

Narum, S. R., and N. R. Campbell. 2015. Transcriptomic response to heat stress among ecologically divergent populations of redband trout. BMC Genomics **16**:103.

Nonaka, E., R. Svanbäck, X. Thibert-Plante, G. Englund, and Å. Brännström. 2015. Mechanisms by Which Phenotypic Plasticity Affects Adaptive Divergence and Ecological Speciation. The American Naturalist **186**:E126-E143.

Nosil, P. 2012. Ecological speciation. Oxford University Press, Oxford, UK.

Nosil, P., and D. J. Funk. 2008. 9. Comparative Analyses Of Ecological Speciation. Pages 117-135 Specialization, speciation, and radiation. University of California Press.

Nosil, P., V. Soria-Carrasco, J. L. Feder, S. M. Flaxman, and Z. Gompert. 2019. Local and system-wide adaptation is influenced by population connectivity. Conservation Genetics **20**:45-57.

Nott, J. 2005. The origin and evolution of Australia's eastern highlands. Pages 322-335 *in* E. Bermingham, C. W. Dick, and C. Moritz, editors. Tropical rainforests: past, present, and future. University of Chicago Press, Chicago, IL, USA.

Novoplansky, A. 2002. Developmental plasticity in plants: implications of non-cognitive behavior. Evolutionary Ecology **16**:177-188.

Nowakowski, A. J., J. I. Watling, S. M. Whitfield, B. D. Todd, D. J. Kurz, and M. A. Donnelly. 2017. Tropical amphibians in shifting thermal landscapes under land-use and climate change. Conservation Biology **31**:96-105.

Ntie, S., A. Davis, K. Hils, P. Mickala, H. Thomassen, K. Morgan, H. Vanthomme, M. Gonder, and N. Anthony. 2017. Evaluating the role of Pleistocene refugia, rivers and environmental variation in the diversification of central African duikers (genera Cephalophus and Philantomba). BMC Evolutionary Biology **17**:1-17.

O'Leary, S. J., J. B. Puritz, S. C. Willis, C. M. Hollenbeck, and D. S. Portnoy. 2018. These aren't the loci you'e looking for: Principles of effective SNP filtering for molecular ecologists. Wiley Online Library.

O'Neill, B. C., M. Oppenheimer, R. Warren, S. Hallegatte, R. E. Kopp, H. O. Pörtner, R. Scholes, J. Birkmann, W. Foden, and R. Licker. 2017. IPCC reasons for concern regarding climate change risks. Nature Climate Change **7**:28.

Ohta, T. 2002. Near-neutrality in evolution of genes and gene regulation. Proceedings of the National Academy of Sciences **99**:16134-16137.

Oksanen, J., F. G. Blanchet, M. Friendly, R. Kindt, P. Legendre, D. McGlinn, P. R. Minchin, R. O'Hara, G. L. Simpson, P. Solymos, M. H. H. Stevens, E. Szoecs, and H. Wagner. 2019. vegan: Community Ecology Package. R package version 2.5-6.

Olazcuaga, L., N. O. Rode, J. Foucaud, M. Gautier, C. Deschamps, A. Loiseau, N. Leménager, B. Facon, V. Ravigné, and R. A. Hufbauer. 2019. Evolution of trade-offs across environments following experimental evolution of the generalist Drosophila suzukii to different fruit media. bioRxiv:749945.

Oliveras, I., and Y. Malhi. 2016. Many shades of green: the dynamic tropical forest - savannah transition zones. Philosophical Transactions of the Royal Society B: Biological Sciences **371**:20150308.

Ondei, S., L. D. Prior, G. J. Williamson, T. Vigilante, and D. M. Bowman. 2017. Water, land, fire, and forest: Multi-scale determinants of rainforests in the Australian monsoon tropics. Ecology and Evolution **7**:1592-1604.

Oomen, R. A., and J. A. Hutchings. 2017. Transcriptomic responses to environmental change in fishes: Insights from RNA sequencing. Facets **2**:610-641.

Oostra, V., M. Saastamoinen, B. J. Zwaan, and C. W. Wheat. 2018. Strong phenotypic plasticity limits potential for evolutionary responses to climate change. Nature communications **9**:1-11.

Orr, H. A. 2005. The genetic theory of adaptation: a brief history. Nature Reviews Genetics **6**:119.

Paradis, E., and K. Schliep. 2019. ape 5.0: an environment for modern phylogenetics and evolutionary analyses in R. Bioinformatics **35**:526-528.

Parmesan, C. 2006. Ecological and evolutionary responses to recent climate change. Annu. Rev. Ecol. Evol. Syst. **37**:637-669.

Payne, N. L., and J. A. Smith. 2017. An alternative explanation for global trends in thermal tolerance. Ecology letters **20**:70-77.

Pearman, P. B., M. D'Amen, C. H. Graham, W. Thuiller, and N. E. Zimmermann. 2010. Within-taxon niche structure: niche conservatism, divergence and predicted effects of climate change. Ecography **33**:990-1003.

Pearson, R. G. 2005. Biodiversity of the freshwater invertebrates of the Wet Tropics region of Northeastern Australia: patterns and possible determinants. Pages 470-485 *in* E. Bermingham, C. W. Dick, and C. Moritz, editors. Tropical rainforests: past, present and future. University of Chicago Press, Chicago, IL, USA.

Pearson, R. G., N. M. Connolly, and L. Boyero. 2015. Ecology of streams in a biogeographic isolate—the Queensland Wet Tropics, Australia. Freshwater Science **34**:797-819.

Pease, J. E., T. B. Grabowski, A. A. Pease, and P. T. Bean. 2018. Changing environmental gradients over forty years alter ecomorphological variation in Guadalupe Bass Micropterus treculii throughout a river basin. Ecology and Evolution **8**:8508-8522.

Perrier, C., A. L. Ferchaud, P. Sirois, I. Thibault, and L. Bernatchez. 2017. Do genetic drift and accumulation of deleterious mutations preclude adaptation? Empirical investigation using RAD seq in a northern lacustrine fish. Molecular Ecology **26**:6317-6335.

Pert, P., J. Butler, J. Brodie, C. Bruce, M. Honzak, F. Kroon, D. Metcalfe, D. Mitchell, and G. Wong. 2010. A catchment-based approach to mapping hydrological ecosystem services using riparian habitat: a case study from the Wet Tropics, Australia. Ecological Complexity **7**:378-388.

Peterson, B. K., J. N. Weber, E. H. Kay, H. S. Fisher, and H. E. Hoekstra. 2012. Double digest RADseq: an inexpensive method for de novo SNP discovery and genotyping in model and non-model species. PloS one **7**:e37135.

Pfennig, D. W., M. A. Wund, E. C. Snell-Rood, T. Cruickshank, C. D. Schlichting, and A. P. Moczek. 2010. Phenotypic plasticity's impacts on diversification and speciation. Trends in ecology & evolution **25**:459-467.

Pigliucci, M. 2001. Phenotypic plasticity: beyond nature and nurture. Johns Hopkins University Press, Baltimore, Md. USA.

Pigliucci, M., C. J. Murren, and C. D. Schlichting. 2006. Phenotypic plasticity and evolution by genetic assimilation. Journal of Experimental Biology **209**:2362-2367.

Pina-Martins, F. 2016. geste2baypass. https://github.com/CoBiG2/RAD_Tools/blob/master/geste2baypass.py

Polato, N. R., B. A. Gill, A. A. Shah, M. M. Gray, K. L. Casner, A. Barthelet, P. W. Messer, M. P. Simmons, J. M. Guayasamin, and A. C. Encalada. 2018. Narrow thermal tolerance and low dispersal drive higher speciation in tropical mountains. Proceedings of the National Academy of Sciences **115**:12471-12476.

Pontes-da-Silva, E., W. E. Magnusson, B. Sinervo, G. H. Caetano, D. B. Miles, G. R. Colli, L. M. Diele-Viegas, J. Fenker, J. C. Santos, and F. P. Werneck. 2018. Extinction risks forced by climatic change and intraspecific variation in the thermal physiology of a tropical lizard. Journal of Thermal Biology **73**:50-60.

Porcelli, D., R. Butlin, K. Gaston, D. Joly, and R. Snook. 2015. The environmental genomics of metazoan thermal adaptation. Heredity **114**:502-514.

Pörtner, H.-O., C. Bock, and F. C. Mark. 2017. Oxygen-and capacity-limited thermal tolerance: bridging ecology and physiology. Journal of Experimental Biology **220**:2685-2696.

Pörtner, H. O., A. F. Bennett, F. Bozinovic, A. Clarke, M. A. Lardies, M. Lucassen, B. Pelster, F. Schiemer, and J. H. Stillman. 2006. Trade-offs in thermal adaptation: the need for a molecular to ecological integration. Physiol Biochem Zool **79**:295-313.

Primack, R. B., and R. Corlett. 2005. Tropical rain forests: an ecological and biogeographical comparison. Blackwell Publishing, Oxford, UK.

Pritchard, J. K., and A. Di Rienzo. 2010. Adaptation–not by sweeps alone. Nature Reviews Genetics **11**:665.

Puritz, J. B., C. M. Hollenbeck, and J. R. Gold. 2014. dDocent: a RADseq, variant-calling pipeline designed for population genomics of non-model organisms. PeerJ **2**:e431.

Pusey, B., M. J. Kennard, and A. H. Arthington. 2004. Freshwater fishes of north-eastern Australia. CSIRO Publishing, Melbourne, VIC, Australia.

Pusey, B. J., A. H. Arthington, and M. G. Read. 1995. Species richness and spatial variation in fish assemblage structure in two rivers of the Wet Tropics of northern Queensland, Australia. Environmental Biology of Fishes **42**:181-199.

Pusey, B. J., and M. J. Kennard. 1996. Species richness and geographical variation in assemblage structure of the freshwater fish fauna of the wet tropics region of northern Queensland. Marine and Freshwater Research **47**:563-573.

Rabergh, C., S. Airaksinen, A. Soitamo, H. Bjorklund, T. Johansson, M. Nikinmaa, and L. Sistonen. 2000. Tissue-specific expression of zebrafish (Danio rerio) heat shock factor 1 mRNAs in response to heat stress. Journal of Experimental Biology **203**:1817-1824.

Raj, A., M. Stephens, and J. K. Pritchard. 2014. fastSTRUCTURE: variational inference of population structure in large SNP data sets. Genetics **197**:573-589.

Rakshit, H., N. Rathi, and D. Roy. 2014. Construction and analysis of the protein-protein interaction networks based on gene expression profiles of Parkinson's disease. PloS one **9**:e103047.

Ralls, K., J. D. Ballou, M. R. Dudash, M. D. Eldridge, C. B. Fenster, R. C. Lacy, P. Sunnucks, and R. Frankham. 2018. Call for a paradigm shift in the genetic management of fragmented populations. Conservation Letters **11**:e12412.

RC Team. 2019. R: A language and environment for statistical computing. Pages https://www.R-project.org/. R Foundation for Statistical Computing, Vienna, Austria.

Reed, J. M. 1992. A system for ranking conservation priorities for Neotropical migrant birds based on relative susceptibility to extinction. Ecology and Conservation of Neotropical Migrant Landbirds. Smithsonian Institution Press, Washington, DC, USA.

Reed, T. E., D. E. Schindler, and R. S. Waples. 2011. Interacting effects of phenotypic plasticity and evolution on population persistence in a changing climate. Conservation Biology **25**:56-63.

Rellstab, C., F. Gugerli, A. J. Eckert, A. M. Hancock, and R. Holderegger. 2015. A practical guide to environmental association analysis in landscape genomics. Molecular Ecology **24**:4348-4370.

Richards, C. L., O. Bossdorf, N. Z. Muth, J. Gurevitch, and M. Pigliucci. 2006. Jack of all trades, master of some? On the role of phenotypic plasticity in plant invasions. Ecology letters **9**:981-993.

Ricklefs, R. E. 2005. Phylogenetic perspectives on patterns of regional and local species richness. Pages 16-40 *in* E. Bermingham, C. W. Dick, and C. Moritz, editors. Tropical rainforests: past, present and future. University of Chicago Press, Chicago, IL, USA.

Rivera, H. E., H. E. Aichelman, J. E. Fifer, N. G. Kriefall, D. M. Wuitchik, S. J. Wuitchik, and S. W. Davies. 2021. A framework for understanding gene expression plasticity and its influence on stress tolerance. Molecular Ecology **30**:1381-1397.

Robinson, B. W., and D. S. Wilson. 1996. Genetic variation and phenotypic plasticity in a trophically polymorphic population of pumpkinseed sunfish (Lepomis gibbosus). Evolutionary Ecology **10**:631-652.

Rohlf, F. 2017. Program TpsDig, version 2.31. Department of Ecology and Evolution, State University of New York at Stony Brook, Stony Brook, NY.

Rohlfs, R. V., and R. Nielsen. 2015. Phylogenetic ANOVA: the expression variance and evolution model for quantitative trait evolution. Systematic biology **64**:695-708.

Rohr, J. R., and B. D. Palmer. 2013. Climate change, multiple stressors, and the decline of ectotherms. Conservation Biology **27**:741-751.

Román-Palacios, C., and J. J. Wiens. 2020. Recent responses to climate change reveal the drivers of species extinction and survival. Proceedings of the National Academy of Sciences **117**:4211-4217.

Rosenberg, N. A. 2004. DISTRUCT: a program for the graphical display of population structure. Molecular Ecology Notes **4**:137-138.

Russell, D., T. Ryan, A. McDougall, S. Kistle, and G. Aland. 2003. Species diversity and spatial variation in fish assemblage structure of streams in connected tropical catchments in northern Australia with reference to the occurrence of translocated and exotic species. Marine and Freshwater Research **54**:813-824.

Salisbury, C. L., N. Seddon, C. R. Cooney, and J. A. Tobias. 2012. The latitudinal gradient in dispersal constraints: ecological specialisation drives diversification in tropical birds. Ecology letters **15**:847-855.

Salojärvi, J. 2018. Computational tools for population genomics. Pages 127-160 Population Genomics. Springer.

Sandoval-Castillo, J., K. Gates, C. J. Brauer, S. Smith, L. Bernatchez, and L. B. Beheregaray. 2020. Adaptation of plasticity to projected maximum temperatures and across climatically defined bioregions. Proceedings of the National Academy of Sciences **117**:17112-17121.

Sandoval-Castillo, J., N. A. Robinson, A. M. Hart, L. W. Strain, and L. B. Beheregaray. 2018. Seascape genomics reveals adaptive divergence in a connected and commercially important mollusc, the greenlip abalone (Haliotis laevigata), along a longitudinal environmental gradient. Molecular Ecology **27**:1603-1620.

Santure, A. W., and D. Garant. 2018. Wild GWAS—association mapping in natural populations. Molecular Ecology Resources **18**:729-738.

Scarnecchia, D. L. 1988. The importance of streamlining in influencing fish community structure in channelized and unchannelized reaches of a prairie stream. Regulated Rivers: Research & Management **2**:155-166.

Scheiner, S. M. 1993. Genetics and evolution of phenotypic plasticity. Annual review of ecology and systematics **24**:35-68.

Scheiner, S. M., M. Barfield, and R. D. Holt. 2020. The genetics of phenotypic plasticity. XVII. Response to climate change. Evolutionary applications **13**:388-399.

Scheiner, S. M., and N. A. Levis. 2021. The Loss of Phenotypic Plasticity Via Natural Selection: Genetic Assimilation. Pages 161-181 *in* D. W. Pfennig, editor. Phenotypic Plasticity & Evolution: Causes, Consequences, Controversies. CRC Press, Boca Raton, FL, USA.

Schlichting, C. D. 2008. Hidden reaction norms, cryptic genetic variation, and evolvability. Annals of the New York Academy of Sciences **1133**:187-203.

Schlichting, C. D., and H. Smith. 2002. Phenotypic plasticity: linking molecular mechanisms with evolutionary outcomes. Evolutionary Ecology **16**:189-211.

Schluter, D. 2001. Ecology and the origin of species. Trends in ecology & evolution **16**:372-380.

Schmid, M., and F. Guillaume. 2017. The role of phenotypic plasticity on population differentiation. Heredity **119**:214-225.

Schwartz, M. K., K. S. McKelvey, S. A. Cushman, and G. Luikart. 2010. Landscape genomics: a brief perspective. Pages 165-174 Spatial complexity, informatics, and wildlife conservation. Springer.

Seddon, N., G. M. Mace, S. Naeem, J. A. Tobias, A. L. Pigot, R. Cavanagh, D. Mouillot, J. Vause, and M. Walpole. 2016. Biodiversity in the Anthropocene: prospects and policy. Proceedings of the Royal Society B: Biological Sciences **283**:20162094.

Sgrò, C. M., A. J. Lowe, and A. A. Hoffmann. 2011. Building evolutionary resilience for conserving biodiversity under climate change. Evolutionary applications **4**:326-337.

Shuai, F., S. Yu, S. Lek, and X. Li. 2018. Habitat effects on intra-species variation in functional morphology: Evidence from freshwater fish. Ecology and Evolution **8**:10902-10913.

Siepielski, A. M., M. B. Morrissey, M. Buoro, S. M. Carlson, C. M. Caruso, S. M. Clegg, T. Coulson, J. DiBattista, K. M. Gotanda, and C. D. Francis. 2017. Precipitation drives global variation in natural selection. Science **355**:959-962.

Slatkin, M. 1987. Gene flow and the geographic structure of natural populations. Science **236**:787-792.

Smith, S., L. Bernatchez, and L. B. Beheregaray. 2013. RNA-seq analysis reveals extensive transcriptional plasticity to temperature stress in a freshwater fish species. BMC Genomics **14**:1-12.

Smith, S., C. J. Brauer, M. Sasaki, P. J. Unmack, G. Guillot, M. Laporte, L. Bernatchez, and L. B. Beheregaray. 2020. Latitudinal variation in climate-associated genes imperils range edge populations. Molecular Ecology **29**:4337–4349.

Smith, T. B., R. Calsbeek, R. K. Wayne, K. H. Holder, D. Pires, and C. Bardeleben. 2005. Testing alternative mechanisms of evolutionary divergence in an African rain forest passerine bird. Journal of evolutionary biology **18**:257-268.

Smith, T. B., H. A. Thomassen, A. H. Freedman, R. N. Sehgal, W. Buermann, S. Saatchi, J. Pollinger, B. Milá, D. Pires, and G. Valkiūnas. 2011. Patterns of divergence in the olive sunbird Cyanomitra olivacea (Aves: Nectariniidae) across the African rainforest–savanna ecotone. Biological Journal of the Linnean Society **103**:821-835.

Smith, T. B., R. K. Wayne, D. J. Girman, and M. W. Bruford. 1997. A role for ecotones in generating rainforest biodiversity. Science **276**:1855-1857.

Snell-Rood, E., and S. Ehlman. 2021. Ecology and Evolution of Plasticity. Pages 139-160 *in* D. W. Pfennig, editor. Phenotypic Plasticity & Evolution: Causes, Consequences, Controversies. CRC Press, Boca Raton, FL, USA.

Solomon, S. 2007. Climate change 2007-the physical science basis: Working group I contribution to the fourth assessment report of the IPCC. Cambridge university press.

Somero, G. 2010. The physiology of climate change: how potentials for acclimatization and genetic adaptation will determine 'winners' and 'losers'. Journal of Experimental Biology **213**:912-920.

Stapley, J., J. Reger, P. G. Feulner, C. Smadja, J. Galindo, R. Ekblom, C. Bennison, A. D. Ball, A. P. Beckerman, and J. Slate. 2010. Adaptation genomics: the next generation. Trends in ecology & evolution **25**:705-712.

Staver, A. C., S. Archibald, and S. A. Levin. 2011a. The global extent and determinants of savanna and forest as alternative biome states. Science **334**:230-232.

Staver, A. C., W. J. Bond, and E. C. February. 2011b. History matters: tree establishment variability and species turnover in an African savanna. Ecosphere **2**:1-12.

Stein, J. L., Hutchison, M.F., Stein, J.A. . 2011. National Environmental Stream Attributes v1.1.3. Page http://pid.geoscience.gov.au/dataset/ga/73045 Geoscience Australia, Canberra. Accessed June, 2017.

Stein, L. R., and A. M. Bell. 2019. The role of variation and plasticity in parental care during the adaptive radiation of three-spine sticklebacks. Evolution **73**:1037-1044.

Stillman, J. H. 2003. Acclimation capacity underlies susceptibility to climate change. Science **301**:65-65.

Storfer, A., M. Murphy, J. Evans, C. Goldberg, S. Robinson, S. Spear, R. Dezzani, E. Delmelle, L. Vierling, and L. Waits. 2007. Putting the 'landscape'in landscape genetics. Heredity **98**:128.

Storfer, A., and A. Sih. 1998. Gene flow and ineffective antipredator behavior in a stream-breeding salamander. Evolution **52**:558-565.

Sultan, S. E. 2021. Phenotypic Plasticity as an Intrinsic Property of Organisms. Pages 3-24 *in* D. W. Pfennig, editor. Phenotypic Plasticity & Evolution: Causes, Consequences, Controversies. CRC Press, Boca Raton, FL, USA.

Sultan, S. E., and H. G. Spencer. 2002. Metapopulation structure favors plasticity over local adaptation. The American Naturalist **160**:271-283.

Summers, D. M., B. A. Bryan, N. D. Crossman, and W. S. Meyer. 2012. Species vulnerability to climate change: impacts on spatial conservation priorities and species representation. Global Change Biology **18**:2335-2348.

Sunday, J., J. M. Bennett, P. Calosi, S. Clusella-Trullas, S. Gravel, A. L. Hargreaves, F. P. Leiva, W. C. Verberk, M. Á. Olalla-Tárraga, and I. Morales-Castilla. 2019. Thermal tolerance patterns across latitude and elevation. Philosophical Transactions of the Royal Society B **374**:20190036.

Sunday, J. M., A. E. Bates, and N. K. Dulvy. 2011. Global analysis of thermal tolerance and latitude in ectotherms. Proceedings of the Royal Society of London B: Biological Sciences **278**:1823-1830.

Sunday, J. M., A. E. Bates, and N. K. Dulvy. 2012. Thermal tolerance and the global redistribution of animals. Nature Climate Change **2**:686-690.

Sunnucks, P., and D. F. Hales. 1996. Numerous transposed sequences of mitochondrial cytochrome oxidase I-II in aphids of the genus Sitobion (Hemiptera: Aphididae). Molecular biology and evolution **13**:510-524.

Svenning, J. C. 1999. Microhabitat specialization in a species-rich palm community in Amazonian Ecuador. Journal of Ecology **87**:55-65.

Swofford, D. L., and J. Sullivan. 2003a. Phylogeny inference based on parsimony and other methods using PAUP*. The Phylogenetic Handbook: A Practical Approach to DNA and Protein Phylogeny, cáp **7**:160-206.

Swofford, D. L., and J. Sullivan. 2003b. Phylogeny inference based on parsimony and other methods using PAUP*. The phylogenetic handbook: a practical approach to DNA and protein phylogeny **160**.

Sykes, M. T., I. C. Prentice, and W. Cramer. 1996. A Bioclimatic Model for the Potential Distributions of North European Tree Species Under Present and Future Climates. Journal of Biogeography **23**:203-233.

Szklarczyk, D., J. H. Morris, H. Cook, M. Kuhn, S. Wyder, M. Simonovic, A. Santos, N. T. Doncheva, A. Roth, and P. Bork. 2016. The STRING database in 2017: quality-controlled protein–protein association networks, made broadly accessible. Nucleic acids research:gkw937.

Talbot, B., T.-W. Chen, S. Zimmerman, S. Joost, A. J. Eckert, T. M. Crow, D. Semizer-Cuming, C. Seshadri, and S. Manel. 2017. Combining genotype, phenotype, and environment to infer potential candidate genes. Journal of Heredity **108**:207-216.

Tamura, K., and M. Nei. 1993. Estimation of the number of nucleotide substitutions in the control region of mitochondrial DNA in humans and chimpanzees. Molecular biology and evolution **10**:512-526.

Ter Steege, H., D. SABATIER, H. CASTELLANOS, T. VAN ANDEL, J. DUIVENVOORDEN, A. A. DE OLIVEIRA, R. EK, R. LILWAH, P. MAAS, and S. MORI. 2000. An analysis of the floristic composition and diversity of Amazonian forests including those of the Guiana Shield. Journal of Tropical Ecology **16**:801-828.

Termignoni-García, F., J. P. Jaramillo-Correa, J. Chablé-Santos, M. Liu, A. J. Shultz, S. V. Edwards, and P. Escalante-Pliego. 2017. Genomic footprints of adaptation in a cooperatively breeding tropical bird across a vegetation gradient. Molecular Ecology **26**:4483-4496.

Terrain NRM. 2016. Catchment Profiles, Wet Tropics Plan for People and Country. Pages https://www.wettropicsplan.org.au/regional-themes/water/catchment-profiles/ accessed July 2020.

Tewksbury, J. J., R. B. Huey, and C. A. Deutsch. 2008. Putting the heat on tropical animals. SCIENCE-NEW YORK THEN WASHINGTON- **320**:1296.

Thomas, C. D., A. Cameron, R. E. Green, M. Bakkenes, L. J. Beaumont, Y. C. Collingham, B. F. Erasmus, M. F. De Siqueira, A. Grainger, and L. Hannah. 2004. Extinction risk from climate change. Nature **427**:145-148.

Thomas, L., W. J. Kennington, R. D. Evans, G. A. Kendrick, and M. Stat. 2017. Restricted gene flow and local adaptation highlight the vulnerability of high-latitude reefs to rapid environmental change. Global Change Biology **23**:2197-2205.

Thomaz, A. T., M. R. Christie, and L. L. Knowles. 2016. The architecture of river networks can drive the evolutionary dynamics of aquatic populations. Evolution **70**:731-739.

Tigano, A., and V. L. Friesen. 2016. Genomics of local adaptation with gene flow. Molecular Ecology **25**:2144-2164.

Trisos, C. H., C. Merow, and A. L. Pigot. 2020. The projected timing of abrupt ecological disruption from climate change. Nature **580**:496-501.

Turner, I. M. 2001. The ecology of trees in the tropical rain forest. Cambridge University Press, Cambridge, UK.

Unmack, P. J. 2001. Biogeography of Australian freshwater fishes. Journal of Biogeography **28**:1053-1089.

Unmack, P. J., G. R. Allen, and J. B. Johnson. 2013. Phylogeny and biogeography of rainbowfishes (Melanotaeniidae) from Australia and New Guinea. Mol Phylogenet Evol **67**:15-27.

Van der Auwera, G., and B. D O'Connor. 2020. Genomics in the Cloud: Using Docker, GATK, and WDL in Terra. O'Reilly Media, Inc, Sebastopol, Canada.

Van Kleunen, M., and M. Fischer. 2001. Adaptive Evolution of Plastic Foraging Responses in a Clonal Plant. Ecology **82**:3309-3319.

Vangestel, C., A. J. Eckert, J. L. Wegrzyn, J. B. S. Clair, and D. B. Neale. 2018. Linking phenotype, genotype and environment to unravel genetic components underlying cold hardiness in coastal Douglas-fir (Pseudotsuga menziesii var. menziesii). Tree Genetics & Genomes **14**:1-14.

Vasconcellos, M. M., G. R. Colli, J. N. Weber, E. M. Ortiz, M. T. Rodrigues, and D. C. Cannatella. 2019. Isolation by instability: Historical climate change shapes population structure and genomic divergence of treefrogs in the Neotropical Cerrado savanna. Molecular Ecology **28**:1748-1764.

Vigh, L., B. Maresca, and J. L. Harwood. 1998. Does the membrane's physical state control the expression of heat shock and other genes? Trends in Biochemical Sciences **23**:369-374.

Vuilleumier, B. S. 1971. Pleistocene changes in the fauna and flora of South America. Science **173**:771-780.

Wainwright, P. C. 1996. Ecological Explanation through Functional Morphology: The Feeding Biology of Sunfishes. Ecology **77**:1336-1343.

Waldvogel, A.-M., D. Schreiber, M. Pfenninger, and B. Feldmeyer. 2020. Climate Change Genomics Calls for Standardized Data Reporting. Frontiers in Ecology and Evolution **8**.

Wallace, A. R. 1854. On the monkeys of the Amazon. Annals and Magazine of Natural History **14**:451-454.

Wang, Z., M. Gerstein, and M. Snyder. 2009. RNA-Seq: a revolutionary tool for transcriptomics. Nature reviews. Genetics **10**:57-63.

Weber, L. C., J. VanDerWal, S. Schmidt, W. J. McDonald, and L. P. Shoo. 2014. Patterns of rain forest plant endemism in subtropical Australia relate to stable mesic refugia and species dispersal limitations. Journal of Biogeography **41**:222-238.

Weir, J. T., and D. Schluter. 2007. The latitudinal gradient in recent speciation and extinction rates of birds and mammals. Science **315**:1574-1576.

Wellband, K. W., and D. D. Heath. 2017. Plasticity in gene transcription explains the differential performance of two invasive fish species. Evolutionary applications.

Wellenreuther, M., and B. Hansson. 2016. Detecting Polygenic Evolution: Problems, Pitfalls, and Promises. TRENDS in Genetics **32**:155-164.

Whitehead, A. 2012. Comparative genomics in ecological physiology: toward a more nuanced understanding of acclimation and adaptation. Journal of Experimental Biology **215**:884-891.

Whitehead, A., and D. L. Crawford. 2006a. Neutral and adaptive variation in gene expression. Proceedings of the National Academy of Sciences **103**:5425-5430.

Whitehead, A., and D. L. Crawford. 2006b. Variation within and among species in gene expression: raw material for evolution. Molecular Ecology **15**:1197-1211.

Whitlock, R. 2014. Relationships between adaptive and neutral genetic diversity and ecological structure and functioning: A meta-analysis. Journal of Ecology **102**:857-872.

Wilson, K. A., N. A. Auerbach, K. Sam, A. G. Magini, A. S. L. Moss, S. D. Langhans, S. Budiharta, D. Terzano, and E. Meijaard. 2016. Conservation research is not happening where it is most needed. PLoS Biology **14**:e1002413.

Wong, B. B., J. S. Keogh, and D. McGlashan. 2004. Current and historical patterns of drainage connectivity in eastern Australia inferred from population genetic structuring in a widespread freshwater fish Pseudomugil signifer (Pseudomugilidae). Molecular Ecology **13**:391-401.

Woon, J. S., D. Atkinson, S. Adu-Bredu, P. Eggleton, and C. L. Parr. 2021. Termites have developed wider thermal limits to cope with environmental conditions in savannas. bioRxiv.

Wootton, R. J. 2012. Ecology of teleost fishes. Springer Science & Business Media, London, UK.

Wu, M., G. Schurgers, M. Rummukainen, B. Smith, P. Samuelsson, C. Jansson, J. Siltberg, and W. May. 2016. Vegetation–climate feedbacks modulate rainfall patterns in Africa under future climate change. Earth System Dynamics **7**:627-647.

Wund, M. A. 2012. Assessing the impacts of phenotypic plasticity on evolution. Integrative and Comparative Biology **52**:5-15.

Xie, D., C. Chen, Y. Dong, C. You, S. Wang, Ó. Monroig, D. R. Tocher, and Y. Li. 2021. Regulation of long-chain polyunsaturated fatty acid biosynthesis in teleost fish. Progress in Lipid Research **82**:101095.

Xu, Q., C. Zhu, Y. Fan, Z. Song, S. Xing, W. Liu, J. Yan, and T. Sang. 2016. Population transcriptomics uncovers the regulation of gene expression variation in adaptation to changing environment. Scientific Reports **6**:25536.

Yeaman, S., and S. P. Otto. 2011. Establishment and maintenance of adaptive genetic divergence under migration, selection, and drift. Evolution; international journal of organic evolution **65**:2123-2129.

Zelditch, M. L., D. L. Swiderski, and H. D. Sheets. 2012. Geometric morphometrics for biologists: a primer. Elsevier Academic Press, London, UK.

Zhang, J. 2018. Neutral Theory and Phenotypic Evolution. Molecular biology and evolution **35**:1327-1331.

Zhang, W., and Y. Dong. 2021. Membrane lipid metabolism, heat shock response and energy costs mediate the interaction between acclimatization and heat-hardening response in the razor clam Sinonovacula constricta. Journal of Experimental Biology **224**:jeb243031.

Zhen, Y., R. J. Harrigan, K. C. Ruegg, E. C. Anderson, T. C. Ng, S. Lao, K. E. Lohmueller, and T. B. Smith. 2017. Genomic divergence across ecological gradients in the Central African rainforest songbird (Andropadus virens). Molecular Ecology **26**:4966-4977.